STUDIES ON HINDERED SETTLING AND RELATED TOPICS

by

Leslie Davies, B.Sc., A.R.T.C.S., C.Chem., F.R.I.C., F.S.S.

A thesis submitted for the degree of Doctor of Philosophy of the University of Salford

Department of Chemistry and Applied Chemistry

1977

This thesis is dedicated to the memory of the late Professor George Rowntree Ramage, Ph.D., D.Sc., F.R.I.C., F.S.D.C., Head and Chairman of the Department of Chemistry and Applied Chemistry, 1955 - 1972.

My sincere thanks go to Dr. David Dollimore for his ever-ready advice and support during the course of the investigations now reported, and also to Dr. J. H. Sharp and Dr. G. B. McBride for their friendly co-operation in some aspects of the work. I also gratefully acknowledge the encouragement of my wife, Barbara; and that of my colleagues, Dr. M. Spencer and Dr. J. Hill, whose shouldering of administrative duties helped to provide the necessary opportunity for the project.

This is to certify that the whole of

the work in this thesis was carried

out by Mr. L. Davies under my advice

and supervision during the period

October 1972 - July 1977.

D. Dollimore, Ph.D., D.Sc., C.Chem.,
F.R.I.C., J.P.,

Reader in Physical Chemistry,

University of Salford

Contents

		page
Summary		1
Chapter 1	The sedimentation of suspensions - a literature review	3
1.1	Introduction	3
1.2	Experimental observations on the rate of sedimentation of suspensions	9
1.3	Hindered settling equations	14
1.3.1	Hindered settling equations relating interface settling rates to functions of concentration only	15
1.3.2	Sedimentation equations relating interface settling rates to functions of concentration and to other variables	19
1.3.3	Some hindered settling equations studied in detail	33
1.3.4	Particle-particle interactions in dilute suspensions	41
Chapter 2	Experimental procedures and results	46
2.1	Materials	46
2.2	Hindered settling technique and observation of settled sediment volumes	47
2.3	Results	49

		page
Chapter 3	Discussion	50
3.1	Treatment of results for calculation of mean equivalent spherical radii	50
3.2	Detailed studies of the hindered settling of various practical systems	52
3.2.1	The generalised Richardson-Zaki equation	55
3.2.2	The significance of the modified Richardson and Zaki equation	57
3.2.3	New interpretation of some published data	63
3.2.4	The generalised Steinour empirical equation	67
3.2.5	The Dollimore-McBride empirical equation	69
3.2.6	The significance of ε_1, the initial porosity for maximum solids flux	75
3.2.7	The significance of the quantity Q $(1-\varepsilon)$	82
3.2.8	Predicted and observed values of the interface settling rate at maximum solids flux, Q_{ε_1}	86
3.3	The sedimentation behaviour of closely-sized samples of glass spheres in 75% aqueous glycerol	89
3.3.1	The applicability of interface settling rates to the determination of mean equivalent spherical radii of sedimenting particles	90

page

3.3.2 The sigmoidal nature of sedimentation curves in cases of hindered settling 94

3.3.3 Conclusions from observations of the sedimentation of relatively monodisperse samples of ballotini in aqueous glycerol 107

3.4 Analysis of the sedimentation behaviour of calcium carbonate suspensions 109

3.5 Tests of the robustness of interpreting sedimentation behaviour in terms of the parameter a 114

3.6 Factors affecting the dispersion and hindered settling of calcium and other carbonates in a variety of liquids 119

3.7 Consequences of hexagonal models of the sedimenting 'plug' 127

3.8 Studies of settled sediments 136

3.9 Constancy of the structure of the sedimenting 'plug' 147

Chapter 4 Summary of conclusions 149

Appendix 158

References 161

The experiments on glass ballotini were carried out as a part of a collaborative investigation with Mr. J. I. Bhatty. The interpretations placed on the results are those of the present author only.

Tables

Table no.		on or following page
1.1	Maximum equivalent spherical radii for solid particles falling through water at 20°C, so as to give limiting laminar flow (Re = 0.2)	6
1.2	Logarithmic relationship of interface settling rates (Q) and initial porosities (ε) for a variety of suspensions	18
2.1 - 2.15		49
2.1, 2.2	Calibration of measuring cylinders	
2.1	Comparison of nominal and observed cylinder volumes, above the 30 cm^3 mark (cylinders subsequently designated F, G, H, I, J)	
2.2	Height/volume relationships at 20°C for cylinders A - Z, AA - CC	
2.3 - 2.15	Sedimentation and settled volume data for calcium carbonate in various liquids	
2.3	Calcium carbonate in water	
2.4	Calcium carbonate in 0.137 M sodium chloride	
2.5	Calcium carbonate in 0.216 M sodium chloride	
2.6	Calcium carbonate in 0.263 M sodium chloride	

Table no.		on or following page
2.7	Calcium carbonate in 0.458 M sodium chloride	
2.8	Calcium carbonate in 0.756 M sodium chloride	
2.9	Calcium carbonate in 0.915 M sodium chloride	
2.10	Calcium carbonate in dry acetone	
2.11	Calcium carbonate in dry benzene	
2.12	Calcium carbonate in dry chloroform	
2.13	Calcium carbonate in dry diethyl ether	
2.14	Calcium carbonate in dry ethyl acetate	
2.15	Calcium carbonate in dry ethyl acetoacetate	
3.1	Initial porosities (ε_1) at which solids flux has maximum value, and corresponding values of the Richardson-Zaki power index n	56
3.2	Values of n and ε_1 from some experimental systems	59
3.3	Comparative values of A, calculated by Steinour's theory (equation 1.51) and by equations 3.15 and 3.16	72
3.4	Comparative values of ε_1 and n, calculated by log Q - C plot (equations 3.17 and 3.18) and by log Q - log ε plot (equations 3.8 and 1.53)	73

Table no.		on or following page
3.5	Values of Q_{ε_1}/V_s calculated from equation 3.9	87
3.6	Relationship of interface settling rates (Q) to suspension liquid volume fractions (ε) for glass ballotini in 3:1 ($^v/v$) glycerol:water	91
3.7	Particle size distribution of ballotini	91
3.8	Calculated, observed and extrapolated infinite-dilution settling rates (V_s, $cm.s^{-1}$) for glass ballotini in 3:1 ($^v/v$) glycerol:water, and corresponding mean particle radii (r, μ)	91
3.9	Values of n, ε_1 and ε^* for ballotini in aqueous glycerol	97
3.10	Comparison of values of Q_{ε_1}/V_s, interpolated from experimental data, with predictions from theoretical equations, for ballotini in aqueous glycerol	100
3.11	Largest visible radii of calcium carbonate flocs from suspension in acetone (μ)	111
3.12	Sedimentation data for calcium carbonate in acetone	111
3.13	Variation of the porosity ε^* with choice of sedimentation equation, for Steinour's tapioca/oil data	117

Table no.		on or following page
3.14	Sedimentation data for dried laboratory-grade calcium carbonate in 0.137 M sodium chloride (aqueous)	119
3.15	Sedimentation data for dried laboratory-grade calcium carbonate in various liquids	119
3.16	Sedimentation data for dried laboratory-grade calcium carbonate in anhydrous ethyl acetate (repeat runs)	120
3.17	Stability constants for water and ethyl acetoacetate as ligands	122
3.18	Sedimentation rate data ($cm.s^{-1}$) for grades C - G ballotini at $\varepsilon = 0.81$	129
3.19	Values of n for calcium carbonate in various liquids	138
3.20	Compressibility coefficients (x) and one-gram settled volumes (c) for calcium carbonate sediments in various liquids	140
3.21	Comparison of flow unit/sediment ratios (p), liquid volume fractions in flow units (v_i) and hindrance and compressibility data for calcium carbonate suspensions	143
3.22	Mean sediment and flow-unit volumes per gram of solid for calcium carbonate suspensions, and the hindrance parameter n.	145

Figures

Figure no.		following page
1.1, 1.2, 1.3	Interface height-time curves for lower and higher hindered settling concentrations and for compressive settling	10
1.4	Transmission of X-rays through sedimenting kaolinite suspensions as a function of time	12
1.5	Interface height-time curves for sedimenting kaolin suspensions at pH 6	12
1.6	Variation of (interface settling rate/ Stokes' limiting rate) with initial porosity ε	17
1.7	Logarithmic relationship of interface settling rates and initial porosities for aqueous suspensions of calcium carbonate	18
1.8	Logarithmic plot of interface settling rates against initial porosities for a variety of suspensions	18
1.9	Sedimentation of a particle through its diffuse layer of charge	19
1.10	Schematic representation of the electric potential in the double layer of charge round a suspended particle	19
1.11	Variation of the shape factor $\theta(\varepsilon)$ with the empirical parameter A	35

Figure no.		following page
1.12	Dependence of sedimentation rate on liquid volume fraction in uniformly-mixed suspensions of closely-sized spheres	43
2.1 a - d	Representative interface height-time curves for calcium carbonate in various liquids	49
3.1	Plot of log (linear settling rate) versus log (initial porosity) following the theory of Richardson and Zaki	56
3.2	Plot of the function Q $(1-\varepsilon)$ versus initial porosity	56
3.3	Plot of log (sedimentation rate) against concentration for calcium carbonate in 0.915 M sodium chloride solution	69
3.4	Variation of the correction term 2 log $\varepsilon/(1-\varepsilon)$ with initial porosity ε	72
3.5	Variation of the function Q $(1-\varepsilon)/V_s$ with initial porosity ε (from the literature)	82
3.6	Variation of the function Q $(1-\varepsilon)/V_s$ with initial porosity for glass ballotini in aqueous glycerol	82
3.7	Variation of the function Q $(1-\varepsilon)/V_s$ with initial porosity for calcium carbonate in various liquids	82

Figure no.		following page
3.8	Variation of the function $\varepsilon_1^{\varepsilon_1/1-\varepsilon_1} = Q_{\varepsilon_1}/V_s$ with ε_1	87
3.9 a - g	Variation of the power number a with solid volume fraction for glass ballotini in aqueous glycerol	95
3.10	Plot of log (sedimentation rate) versus log (initial porosity) for ballotini in aqueous glycerol	97
3.11	Fit of experimental data for grade D ballotini to theoretical curves	98
3.12	Fit of experimental data for grade E ballotini to theoretical curves	99
3.13	Relationship of 'break' in plot of log Q/ε^2 against ε to variation of $Q(1-\varepsilon)$ with ε, and to inflection in the Q versus ε plot, for ballotini grade D.	106
3.14 a - g	Electron micrographs and stereoscan photograph of calcium carbonate from suspensions in water and acetone	110
3.15 a - n	Variation of the power number a with solid volume fraction for calcium carbonate in various liquids	112
3.15 p, q	The effect on the log log V_s/Q versus log $(1-\varepsilon)$ plot of different values of V_s	114

Figure no.		following page
3.15 r, s	The effect on the parameter a of variants of the log log V_s/Q - log $(1-\varepsilon)$ plot	116
3.15 t	Values of the parameter a for Steinour's glass spheres A in aqueous hexametaphosphate	118
3.16 a	Horizontal cross-section of the Richardson and Zaki 'configuration II'	127
3.16 b	'Configuration II' cross-section corresponding to $\varepsilon = 0.81$, $\varepsilon_{eff} = 0.375$	131
3.16 c	Cross-section of simple-hexagonal configuration corresponding to $\varepsilon = 0.81$, $\varepsilon_{eff} = \exp^{-1}$	133
3.17 a, b	Logarithmic plots of settled sediment volumes (V) against mass (m) of calcium carbonate in various liquids	140

Summary

The stability of some suspensions, and the settling-out of others, both natural and man-made, are of widespread occurrence and importance. Nonetheless, in spite of the efforts of numerous workers, published theories and mathematical representations of sedimentation behaviour are relatively rudimentary. Some of these theories have been developed from model systems which are markedly different from suspensions of practical significance. Other theories, although based on studies of more-realistic mixtures, nonetheless have failed to consider chemical and physical properties which may be thought to influence sedimentation.

This study has been essentially an attempt to improve upon this position, and the work has been carried out in a number of ways. The scope and limitations of some existing theories of sedimentation have been examined, and additional useful interpretation has been proposed. The relationship of sedimentation rates to the concentrations of the suspensions under consideration has been investigated in some detail for a number of systems, and new mathematical models suggested to represent the observed behaviour. It has been concluded that the relationship of sedimentation rate to suspension-concentration is better represented by a combination of sigmoid and exponential curves, rather than by the purely exponential expressions previously used. The experimental evidence has been used to try to identify chemical and physical properties of solids and liquids, which affect sedimentation phenomena. It has also been possible to suggest some improvements in the use of sedimentation data to estimate mean particle sizes for suspended

materials, and some consideration has also been given to the usefulness of observations of settled sediment volumes. It has been concluded that there are two fundamental causes of hindrance to sedimentation; one is flocculation of the sedimenting material, and the other is association of liquid round the sedimenting particles and flocs. Evidence is presented that the second effect is more important that the first.

The suspension concentration necessary for maximum sedimentation mass transfer rate has been identified as the threshold concentration for the onset of the phenomenon known as hindered settling, in which particles sediment together at one rate irrespective of their sizes. The fact that this threshold concentration varies considerably from one experimental system to another has been interpreted in terms of a linear-upflow model of the sedimenting mass.

Chapter 1 The sedimentation of suspensions - a literature review

1.1 Introduction

The rates of sedimentation of solid particles in liquid media and the characteristics of the resultant sediments are of wide applicability in chemical and metallurgical processes. Industries where the phenomena are of importance include ore processing, the manufacture of chemicals, ceramics and paints, the dredging and dewatering of sediments from rivers and canals, and sewage treatment. Hence, to quote Michaels and Bolger (1962), "sedimentation phenomena have been subjects of research for many decades, and much insight has been gained into the hydrodynamics of sedimentation processes." Nevertheless, the present state of development of theories of sedimentation is not very satisfactory from the chemist's point of view. This is because they have largely failed to correlate sedimentation rates with the chemical and physical properties of the components of the suspension, and therefore give no insight into which system parameters should be varied in order to encourage or discourage sedimentation. The initial purpose of the study described herein was to try to improve this state of affairs, and some developments in this respect will be reported. However, it was realised during the work that the purely mathematical form of established sedimentation equations appeared capable of improvement, and considerable attention has been given to this aspect.

The best known sedimentation equation is that of Stokes (1851):

$$V_s = \frac{2r^2(\rho_s - \rho_l)g}{9\eta} \qquad \text{(Stokes' Law)} \qquad (1.1)$$

where V_s = terminal falling velocity of a single spherical particle in an infinite fluid ($cm.s^{-1}$),

r = sphere radius (cm)

ρ_s = sphere density ($g.cm^{-3}$)

ρ_l = fluid density ($g.cm^{-3}$)

η = fluid viscosity ($g.cm^{-1}.s^{-1}$)

g = acceleration due to gravity ($cm.s^{-2}$).

This does relate the sedimentation rate to certain system properties (ρ_s, ρ_l and η), but is by definition restricted to a sphere in a condition of infinite dilution. Stokes derived the equation by equating the viscous resistance (F) of the fluid to the motion of the particle:

$$F = 6\pi\eta V_s r \qquad (1.2)$$

to the effective gravitational force on the particle:

$$6\pi\eta V_s r = \frac{4}{3}\pi r^3 (\rho_s - \rho_l) g \qquad (1.3)$$

which re-arranges to give equation 1.1.

The terminal velocities predicted by Stokes' Law will not be attained unless the flow of fluid round the particle is laminar (otherwise known as streamline or non-turbulent). Flow conditions round particles are defined by the dimensionless group known as the Reynolds number Re:

$$Re = \frac{2V_s \, r \, \rho_l}{\eta} \tag{1.4}$$

According to Heywood (1962), Stokes' Law may be used to calculate terminal velocities if Re does not exceed 0.2, although the values of V_s calculated thereby will be about 5% too great. According to Richardson and Zaki (1954 a), the error in V_s does not exceed 4% at Re = 0.2. An exception to the generally-held view is that of Gaudin (1939) who concluded that Stokes' Law holds for spherical particles up to Re = 0.6. Above Re ≈ 0.2, there is a continuous transition to turbulent liquid flow, and the terminal velocities reached in practice are increasingly different from those predicted by Stokes' Law.

The particle radius corresponding to Re = 0.2 may be calculated by substituting for V_s from equation 1.1 in equation 1.4 to give

$$Re = \frac{8r^3(\rho_s - \rho_l) \, \rho_l \, g}{18 \, \eta^2} \tag{1.5}$$

and therefore, for Re = 0.2,

$$8r^3 = \frac{3.6\ \eta^2}{(\rho_s - \rho_l)\ \rho_l\ g} \qquad (1.6)$$

and thus

$$r = \left(\frac{0.45\ \eta^2}{(\rho_s - \rho_l)\ \rho_l\ g}\right)^{0.33'} \qquad (1.7)$$

If the particle is not spherical, r is the equivalent spherical radius for the observed limiting velocity. The critical radii for some common solids sedimenting under Stokes' conditions in water at 20°C are shown in Table 1.1. Above these sizes, Stokes' Law would be measurably in error in determining terminal velocities and the equivalent spherical radii.

Table 1.1

Maximum equivalent spherical radii for solid particles falling through water at 20°C, so as to give limiting laminar flow (Re = 0.2)

Solid	ρ_s (g.cm^{-3})	Maximum equivalent radius (μ)
Sulphur	2.03	35.5
Calcium carbonate	2.71	30.0
Glass ballotini	2.94	28.7
Basic copper carbonate	3.66	25.8

ρ_l = 1.0 g.cm^{-3}; η = 0.01 g.cm^{-1} s^{-1}

In many technological systems, the mean particle sizes will be greater than those in table 1.1, indicating that many problems concerning particle motion through fluids will be beyond the range of validity of Stokes' equation. For a given liquid, any increase of particle radius or solid density above the values appropriate for Re = 0.2 in equation 1.5 will give rise to sufficiently high sedimentation velocities of isolated particles for some turbulence of flow to occur. Additionally, the very great majority of suspensions of industrial importance are composed of non-spherical particles. Also, natural and industrial sediments are not commonly of uniformly-sized particles (i.e. are not 'monodisperse'), although flocs do tend to become uniform in size under shear (Reich and Vold, 1957). It is also the case that practically-important dispersions are not infinitely dilute. On the other hand, any reduction of settling rate below V_s, due to the presence of other particles, will allow for the possibility of laminar flow with larger (and/or denser) particles than equation 1.5 would suggest. However, according to Richardson and Zaki (1954 b), no satisfactory (theoretical) treatment has been developed for particles of any shape other than spherical, or for high relative velocities, or for systems in which there is interference between particles. Instead, the problem has been studied experimentally.

The settling under gravity of technologically important dispersions usually differs markedly from the behaviour predicted by Stokes' Law. Instead of the free fall of individual

particles, liquid flow round any one particle is hindered by other particles in the suspension. Burgers (1941 a, b; 1942) suggested that the motion of a typical particle in a slurry would be influenced by both the motion and the presence of the other particles. The main effect of the motion would be to produce a return flow of liquid, whilst the presence of the other particles would cause an effect analogous to an increase in the viscosity of the liquid. At relatively low concentrations of solid (with the concentration magnitudes varying from system to system), there may be different settling rates for different sizes of particles (Stokes-type settling), but the settling rates will be less than those expected from the Law. At relatively higher concentrations, most or all of the particles fall together, at one rate, irrespective of size. This frequently results in the formation of a clear suspension/supernatant interface, which for some part of the sedimentation time settles down at a constant rate, with in some cases a quite clear supernatant liquor. This phenomenon is known as hindered settling (Steinour, 1944) or mass subsidence (Orr and Dalla Valle, 1959).

The experimental investigations referred to by Richardson and Zaki, and those carried out since, have dealt primarily with the study of this hindered settling condition, and for good reasons. It corresponds to a circumstance which not only occurs naturally but also is often sought in industrial operations, and the measurement of most interest is that of the settling rate (Q) of the interface. In some practical cases, there is need to

increase this rate (as in separation procedures in the chemical industry) while in others, the aim is to arrest the sedimentation as completely as possible (as in the manufacture of paints and inks and the preparation of cement slurries). Factors influencing the magnitude of this settling rate are clearly of scientific and technological importance.

In the absence of a satisfactory theory of sedimentation derived from first principles for circumstances outside Stokes' limiting conditions, numerous workers have attempted to relate the interface settling rate Q to Stokes' limiting velocity V_s by introducing some multiplying proportionality term. If this term be designated for the moment as p, then we may write simply

$$Q = V_s.p \tag{1.8}$$

to indicate the general nature of the relationships, a number of which are discussed in Section 1.3. Such equations, which relate Q with the conditions of the experiment, are called hindered settling equations.

1.2 Experimental observations on the rate of sedimentation of suspensions

If a sufficiently-concentrated suspension is allowed to settle, it will do so with a clear interface between the settling

particles and the supernatant suspension liquid. This interface first appears at some threshold solids concentration, the threshold value being different in different suspensions. Below this critical concentration, an indistinct suspension-supernatant interface may appear, but close observation will show that particles of different sizes are falling at different rates. These rates will be less than would be expected from Stokes' equation, but the existence of size-dependent differential rates leads to this type of sedimentation being called Stokes-type settling.

At any given concentration equal to or greater than the threshold value, many or all of the particles settle at one rate, irrespective of size, which corresponds to the condition of hindered settling. The position of the falling interface is recorded at appropriate times, and a graph of interface height against time gives the rate of fall of the interface. At relatively low concentrations, the curve will be of the type shown in figure 1.1, with a linear portion, the gradient of which is designated Q. At somewhat higher concentrations, the curve will be as shown in figure 1.2, but again there will be a linear portion, the slope of which is Q. It is these magnitudes Q which appear in hindered settling equations. Q is normally plotted against the liquid volume fraction of uniformly-mixed suspension ('initial porosity' or, simply, 'porosity', ϵ) to give graphs known as sedimentation curves.

At still greater concentrations, the height-time curve will

Figures 1·1, 1·2, 1·3

Interface height — time curves

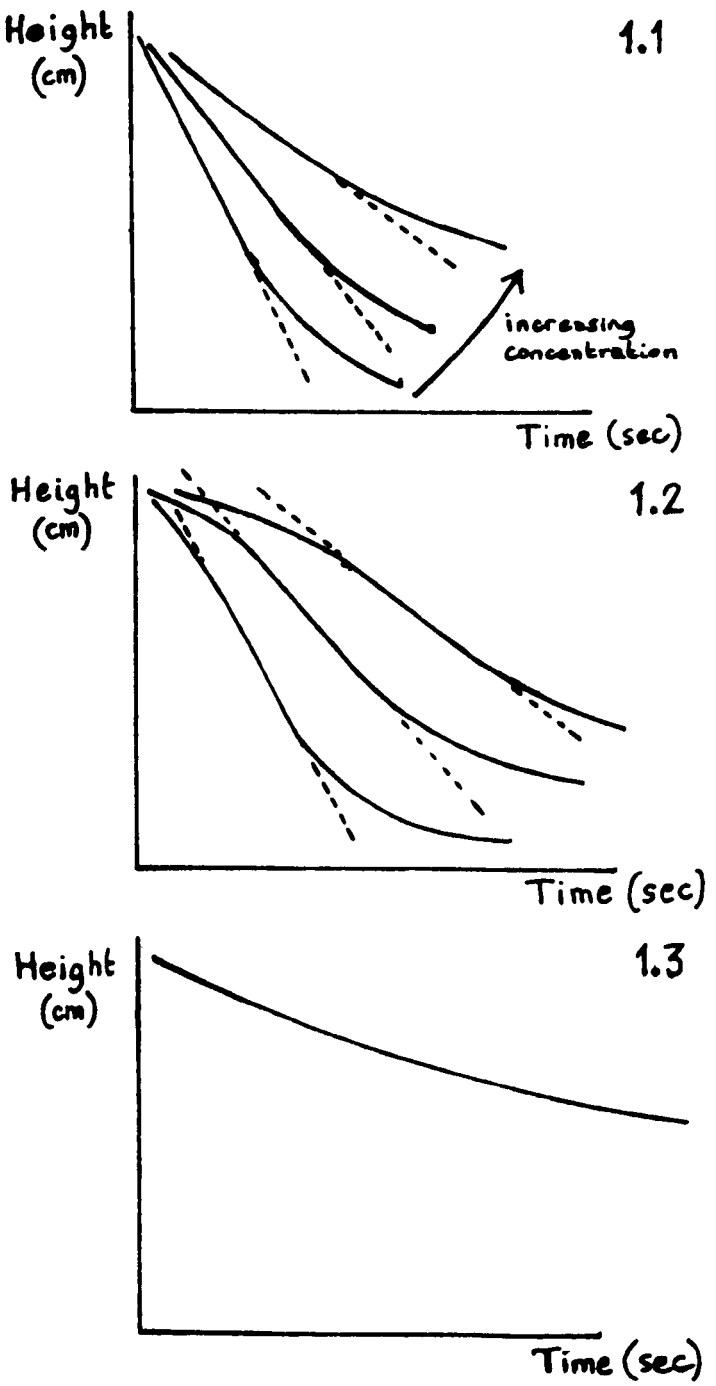

1.1 LOWER HINDERED - SETTLING CONCENTRATIONS

1.2 HIGHER HINDERED - SETTLING CONCENTRATIONS

1.3 COMPRESSIVE SETTLING

– – – – – – – – linear settling rates Q

exhibit no measurable linear portion, being as shown in figure 1.3. This kind of behaviour is said by Dixon (1977) to arise when the particles in the suspension are sufficiently in contact that the upward reaction of the bottom of the container, against the downward gravitational force of the sedimenting particles, is felt throughout the suspension from the earliest instant the interface can be identified. Such behaviour is known as compressive settling.

If this interpretation is correct, then it follows that below the threshold concentration for compressive settling (but within the hindered settling region), the compressive upward reaction is operative through only that part of the sediment which has settled out, and the remainder of the sediment will settle without being affected by this retarding force. This 'plug' of sediment will settle at a steady rate (Q), determined by a balance between gravity acting in the one direction and fluid friction and buoyancy forces acting in the other (Michaels and Bolger, 1962).

Experimental evidence leading to this conclusion was obtained by Gaudin and his co-workers (1958, 1959, 1960), who used X-ray absorption techniques to measure local concentrations in settling beds of kaolin as a function of time and position. Working with 1.9% $^{w}/_{w}$ kaolin in 0.013% aqueous calcium hydroxide, they found that, in the first hour of sedimentation, there was a region extending from the interface downward, whose density was constant and equal to that of the original suspension at time t = 0.

The density profiles obtained (reproduced in figure 1.4) indicate that the displaced supernatant liquid leaves the sediment through pores of comparatively large diameter during the hindered settling stage, being expelled through much smaller tubules during compressive settling. Coe and Clavenger (1916) had observed much earlier that the upward flow of supernatant through flocculated suspensions is a special case of pore flow. Very recently, Werther (1977) has studied the related phenomenon of the passage of gas bubbles through fluidized beds (i.e. arrays of particles maintained in equilibrium positions by upward fluid flow). His results clearly indicate that the bubbles do not rise randomly distributed in space, but rather in the form of bubble chains - another example of pore flow.

Michaels and Bolger observed interface height - time plots of figure 1.1 type for aqueous suspensions of kaolin which were 0.22 - 0.7 $^{o}/_{o}$ $^{v}/_{v}$ in kaolin, and of figure 1.2 type for the range 0.8 - 3.8 $^{o}/_{o}$ $^{v}/_{v}$. In the lower concentration range, microscopic observation showed that the kaolin aggregates settled as roughly spherical, individual units, with horizontal diameters ranging from about 5 to 40 microns. Their paper does not specifically state that these differently sized particles all fell at a given rate, but their graphed data (reproduced as figure 1.5) show long linear portions, suggesting a well-formed sharp interface, which would arise in well-developed hindered settling. The authors suggested that the aggregates formed into a coherent network in the higher-concentration region (and equated this to Gaudin's 'plug') but

Figure 1.4

Transmission of X-rays through sedimenting kaolinite suspensions as a function of time (from Gaudin et al., 1958, 1959, 1960)

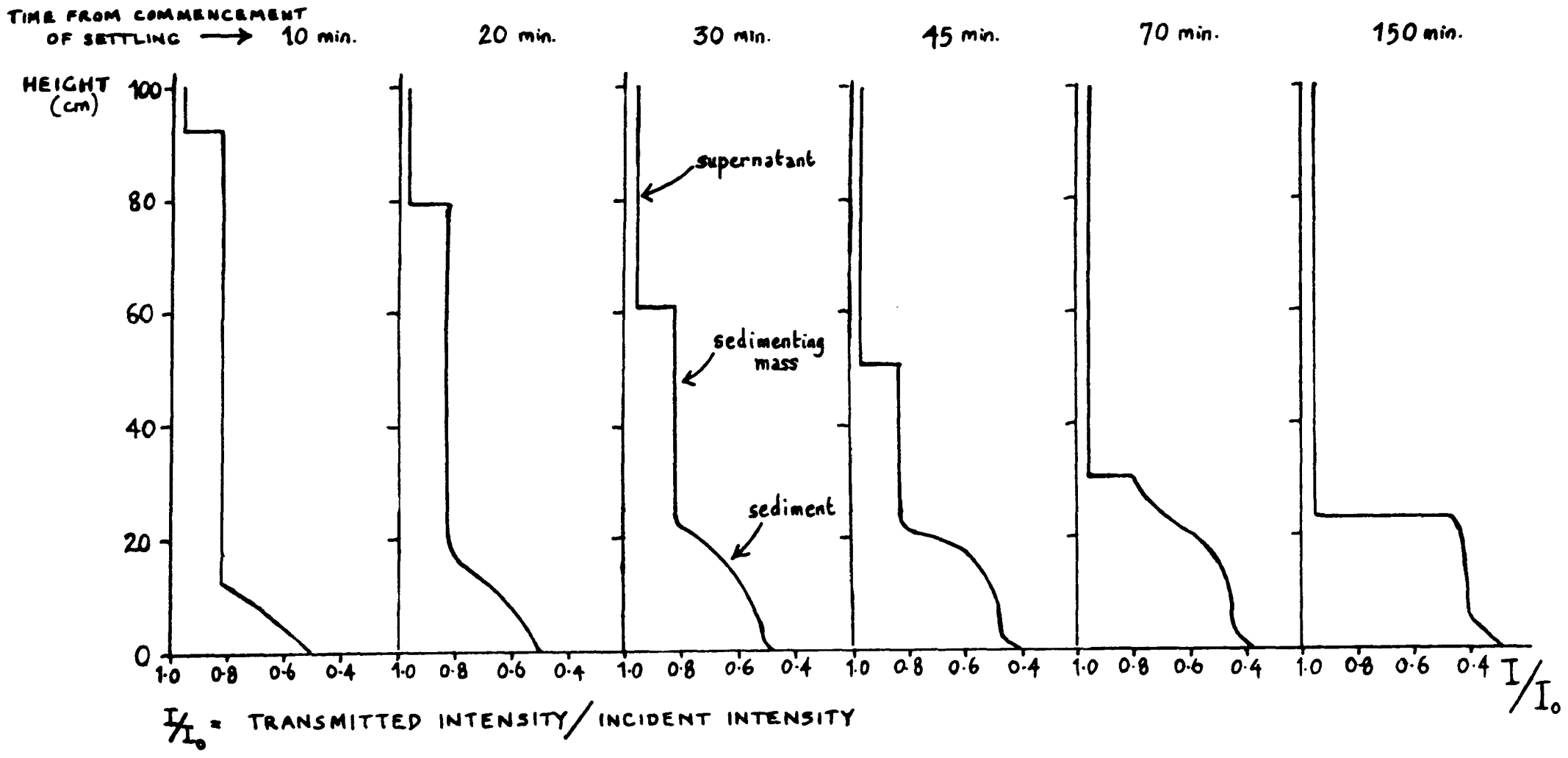

Figure 1·5

Interface height — time curves for sedimenting kaolin suspensions at pH 6

(from Michaels and Bolger, 1962)

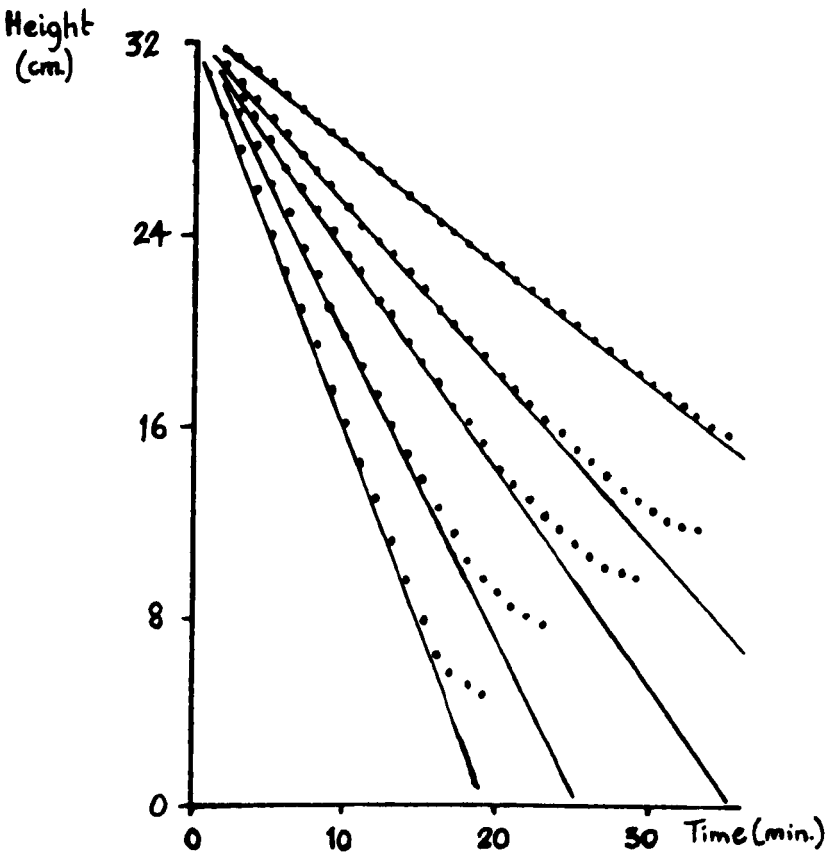

$\epsilon = 0.9937 - 0.9978$

do not appear to have given any experimental evidence for this.

McBride (1974) suggested that the difference between more-dilute and less-dilute behaviour (i.e. between figures 1.1 and 1.2) is that the upper 'shoulder' of figure 1.2 is due to flocs, which have been broken up during mixing of the suspension and which then re-assemble in the early part of the sedimentation time. Michaels and Bolger observed both types of behaviour with a flocculated system, but floc size does increase with increase of concentration and with decrease of shear rate. It follows that the behaviour represented by figure 1.2 would be more likely at higher concentrations, as is commonly observed. Also, because a heavily-flocculated system has less free flow space (for given solids concentration) than a lightly-flocculated one, a given mixing procedure will cause less shear on the flocs in the more-flocculated case. This also would increase the chance of figure 1.2 behaviour, in line with McBride's suggestion. An important practical point also follows: it is necessary to have a standardised mixing procedure.

Michaels and Bolger interpreted the linear portion of figure 1.2-type curves as corresponding to supernatant liquid flowing through the sedimenting plug in paths approaching the configuration of smooth, vertical tubes, which implies that the suggested coherent network of aggregates has assumed a considerable degree of geometrical regularity. However, their observations in the dilute concentration range may be of even greater interest, namely that particles of solid, of different sizes

and separated from one another by liquid, settle at a common velocity. This suggests that some relatively ordered regime of flow, and/or array of particles has been set up, without direct coherence between particles.

1.3 Hindered settling equations

Numerous investigators have measured the concentration-dependence of interface settling rates Q. One application of such relationships is to determine mean particle sizes, since, if the dependence is established, extrapolation to infinite dilution would transform Q into the Stokes' limiting velocity V_s, and Stokes' Law (equation 1.1) would give the corresponding radius r. (It is of course necessary to assume that the extrapolation is valid; this assumption is examined in section 3.3.1 below). Such work has naturally often caused the proportionality term p of equation 1.8 to be a function of concentration only, so that we may re-write equation 1.8 as

$$Q = V_s . f(c) \qquad (1.9)$$

where f(c) is some function of suspension concentration. Such expressions are discussed in section 1.3.1.

In other hindered settling equations, suspension concentration and some other variable appear in the correction term; such expressions are discussed in section 1.3.2. Numerous expressions have also been derived for viscous flow through multiparticle systems in slow sedimentation or in the fluidised bed condition,

and here again both 'concentration-only' and 'concentration plus other variable' expressions are represented. The additional variables may be identifiable system properties, or numerical variables which future work may relate to identifiable properties, or both.

In the equations, suspension concentration is commonly expressed in terms of the liquid volume fraction (ϵ) of the uniformly-mixed suspension, and the corresponding solid volume fraction ($1-\epsilon$), or the quantity γ. The value of ϵ is obtained experimentally from the mass of solid, solid density and total suspension volume. γ is derived from theoretical models which assume, for instance, that a solid sphere (radius a) is surrounded by a concentric liquid sheath (radius b), and that $\gamma = {}^{a}/_{b}$. If it assumed that the particle - sheath volume ratio is the same as the relative volumes of particles to fluid in the entire suspension, as has been done by Happel (1958), then $\gamma = (1 - \epsilon)^{0.33}$, where ϵ is the 'initial porosity' defined earlier. For consistency below, all expressions are expressed in terms of ϵ.

1.3.1 Sedimentation equations relating interface settling rates to functions of concentration only

These equations include the following:

Powers (1939)

$$Q = V_s \left[0.10 \, \frac{(\epsilon - W_i)^3}{1-\epsilon} \right] \qquad (1.10)$$

where W_i = an experimentally-determined quantity related to the volume of liquid carried down immobile on the sedimenting particles.

Burgers (1941-2)

$$Q = V_s \left(1 + 6.88 \left(1-\varepsilon\right)\right)^{-1} \tag{1.11}$$

Steinour (1944 a,b)

$$Q = V_s \left(\varepsilon^2 . \; 10^{-1.82(1-\varepsilon)}\right) \tag{1.12}$$

$$Q = V_s \left(0.123 \; \frac{\varepsilon^3}{1-\varepsilon}\right) \tag{1.13}$$

$$Q = V_s \left[0.176 \; \frac{(\varepsilon-0.168)^3}{1-\varepsilon}\right] \tag{1.14}$$

Brinkman (1947-8-9)

$$Q = V_s \left(1 + 0.75 \left(1-\varepsilon\right) \left\{ 1 - \left(\frac{8}{1-\varepsilon} - 3\right)^{0.5} \right\}\right) \tag{1.15}$$

Uchida (1949)

$$Q = V_s \left(1 + 2.1(1-\varepsilon)^{0.33^*}\right)^{-1} \tag{1.16}$$

Hawksley (1951)

$$Q = V_s \left[\frac{\varepsilon^2}{\exp\left(\frac{2.5 \left(1-\varepsilon\right)}{1 - \frac{39}{64} \left(1-\varepsilon\right)}\right)} \right] \tag{1.17}$$

McNown and Lin (1952)

$$Q = V_s \left(1 + 1.6 \left(1-\varepsilon\right)^{0.33^*}\right)^{-1} \tag{1.18}$$

Richardson and Zaki (1954)

$$Q = V_s \ (\varepsilon^{4.65}) \tag{1.19}$$

Dalla Valle et al (1958)

$$Q = V_s \ (\frac{1}{9.4} \ \frac{\varepsilon^3}{1-\varepsilon}) \tag{1.20}$$

Happel (1958)

$$Q = V_s \left[\frac{3 - 4.5 \ (1-\varepsilon)^{0.33^\bullet} + 4.5 \ (1-\varepsilon)^{1.66^\bullet} - 3 \ (1-\varepsilon)^2}{3 + 2 \ (1-\varepsilon)^{1.66^\bullet}}\right] \tag{1.21}$$

and, for $\varepsilon > 0.999$,

$$Q = V_s \ (1 - 1.5 \ (1-\varepsilon)^{0.33^\bullet}) \tag{1.22}$$

The variation of Q/V_s with ε according to these equations is shown in figure 1.6, with the exception of equation (1.10), in which W_i can be assigned a value only by experiment. The curve for equation (1.10) must be similar to that for equation (1.14).

If an equation is to apply up to infinite dilution (i.e. to ε=1), it must reduce to $Q = V_s$ at $\varepsilon = 1$. This is the case for the equations listed above, except for equations 1.10, 1.13, 1.14 and 1.20. These four involve a term of the $\varepsilon^3/1-\varepsilon$ type, and must therefore give indefinitely large values for the settling rate when $\varepsilon = 1$, with $Q = V_s$ at some value $\varepsilon < 1$. Although there is evidence of settling rates $Q > V_s$ at $\varepsilon < 1$ (Kaye and Boardman, 1962; Johne, 1966; Koglin, 1971) due to clustering of

Figure 1·6

Variation of (interface settling rate/Stokes' limiting rate) with initial porosity ϵ

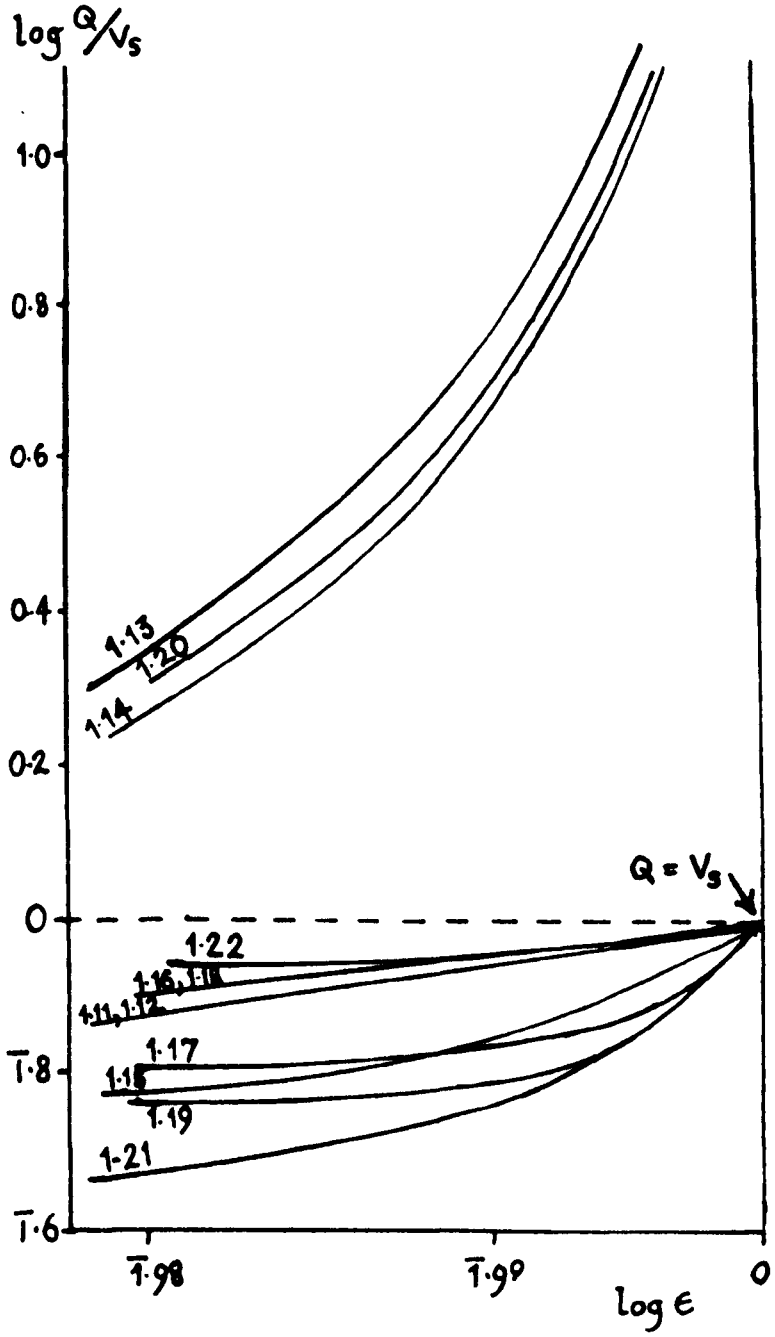

particles, and Faxen (1927) concluded that particle doublets at very high dilution would fall at 1.55 times the V_s for single particles, equations 1.10, 1.13, 1.14 and 1.20 clearly should not be used to calculate the limiting velocity of an isolated particle. The accuracy of values of V_s calculated by substituting observed values of Q into the other equations will depend on how closely the equations represent the actual behaviour right up to $\varepsilon = 1$.

One limitation of all the equations 1.10 - 1.22 is that the correction terms are functions of concentration only, which implies that Q/V_s has a fixed value at given initial porosity ε, irrespective of the nature of the components of the suspension. In other words, the variation of Q with ε, $^{dQ}/_{d\varepsilon}$, is said to be independent of the chemical and physical nature of the system. But this is not the case. Even closely-similar suspensions show different curves when Q is plotted against ε (figure 1.7), and there are wide discrepancies between $^{dQ}/_{d\varepsilon}$ values when more-disparate suspensions are compared. This last point is evident from the literature data summarised in table 1.2, in which the values n give the magnitudes of (d log Q / d log ε) for various suspensions in closely-similar ranges of porosity.

Figure 1·7

Logarithmic relationship of interface settling rates (Q) and initial porosities (ϵ) for calcium carbonate suspensions

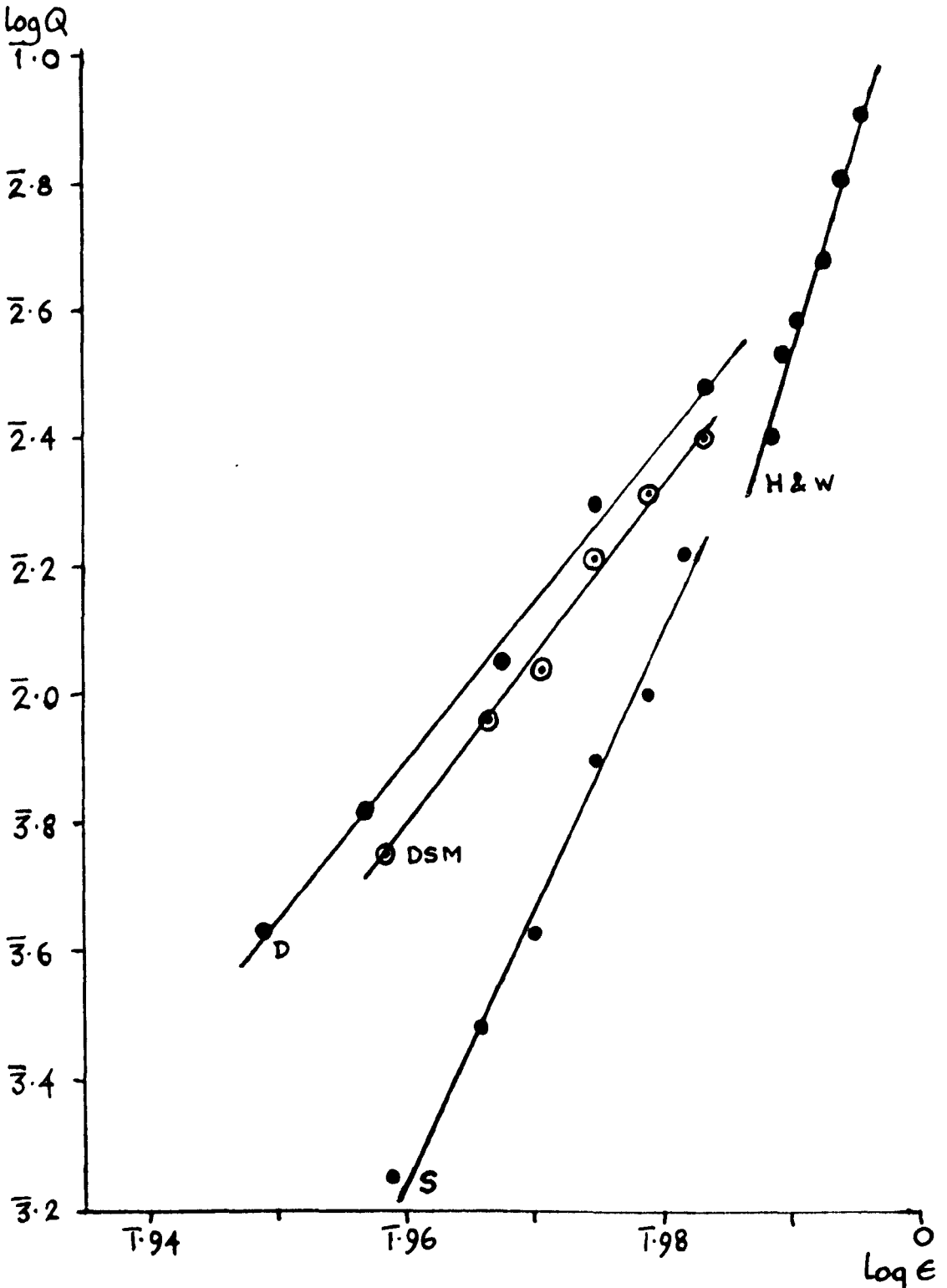

The initials indicate the origins of the samples:

H&W : Hopkin and Williams
S : Sturge
DSM : Derbyshire Stone Mine
D : Dista Products

Table 1.2

Logarithmic relationship of interface settling rates (Q) and initial porosities (ε) for a variety of suspensions

System	Reference	Range of initial porosity ε	$n = \frac{d \log Q}{d \log \varepsilon}$
Flocculated kaolinite/water, pH 4.9 ± 0.5[a]	Dollimore and Horridge (1971)	0.947 - 0.973	45.4
Flocculated kaolinite/water, pH 4.9 ± 0.5[b]	Dollimore and Horridge (1971)	0.947 - 0.973	46.1
Flocculated kaolinite/water, pH 4.9 ± 0.5[c]	Dollimore and Horridge (1971)	0.947 - 0.973	48.3
Basic copper carbonate/water	Dollimore and McBride (1968)	0.936 - 0.982	54.2
PbO + $PbSO_4$/dilute sulphuric acid	Christian and Dollimore (1971)	0.963 - 0.984	80.7
Pyrogenic silica/water	Dollimore and Owens (1972)	0.981 - 0.992	287.5
Kaolinite/aqueous, pH 6	Michaels and Bolger (1962)	0.994 - 0.998	296.0
Pyrogenic silica/dry heptane	Dollimore and Owens (1972)	0.989 - 0.994	466.7

a = anionic polyacrylamide flocculant
b = cationic polyacrylamide flocculant
c = neutral polyacrylamide flocculant

The data of table 1.2 are shown in figure 1.8

Figure 1·8

Logarithmic plot of interface settling rates (Q) against initial porosities (ε) for a variety of suspensions

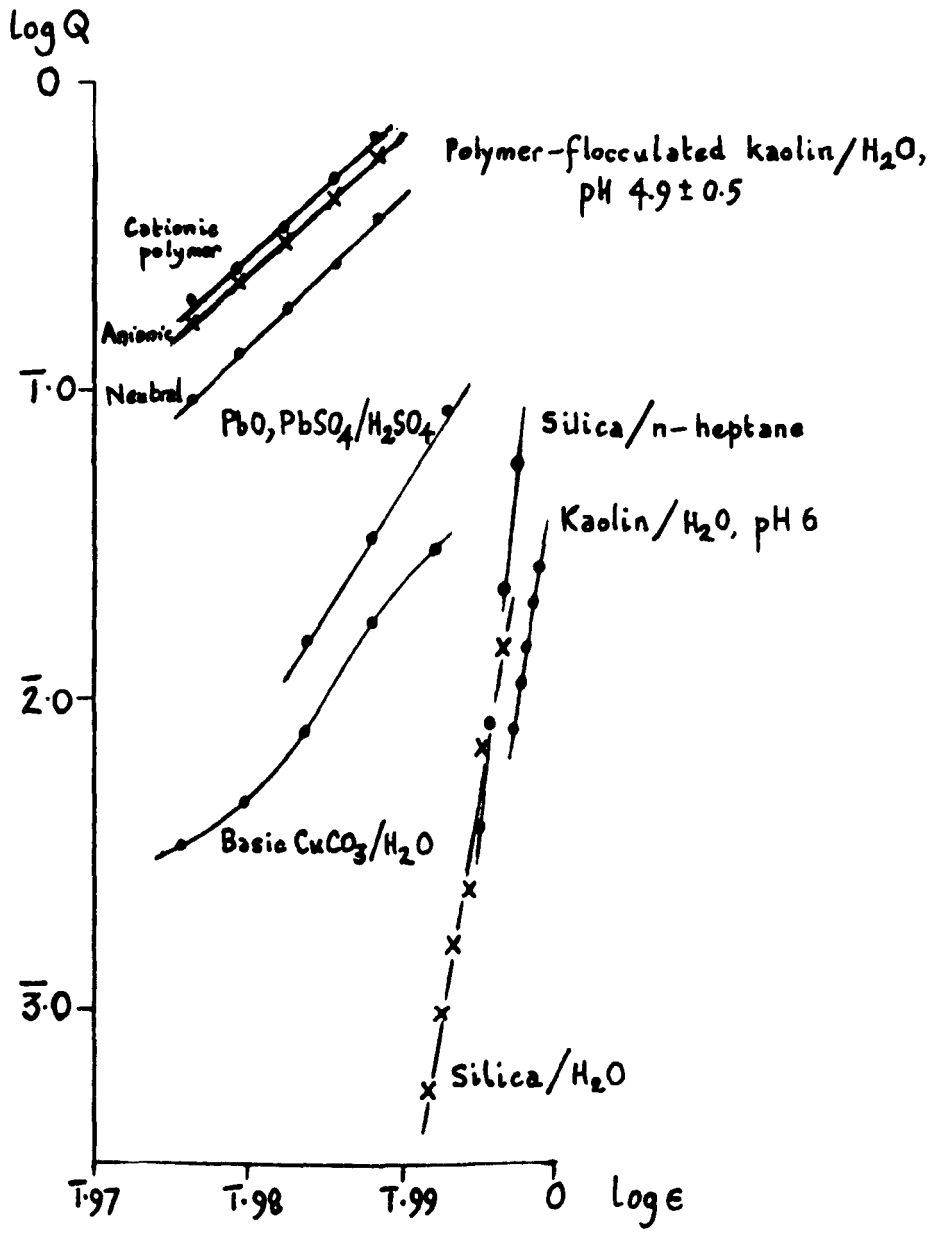

From the practical point of view, since the correction terms include no physical or chemical properties, they can give no insight as to how sedimentation behaviour may be modified and controlled by the manipulation of such variables.

1.3.2. Sedimentation equations relating interface settling rates to functions of concentration and to other variables

Various authors have proposed equations which introduce system variables, in addition to or in place of suspension porosity, into the correction term relating Q to V_s. Attention has been given, by workers such as Smoluchowski (1921), Booth (1950, 1954), Sengupta (1968), Pavlik and Sansone (1973) and Sansone and Civic (1975), to the electroviscous effect, which arises when a sedimenting particle has a surface electric charge. This charge attracts a layer of opposite charge to near the surface, and that layer causes the formation, farther out in the solution, of another more-diffuse layer of ions, again of opposite charge. Only this diffuse layer of ions is free to move. A sedimenting particle will tend to fall through its diffuse layer, leading to a polarization of charge distribution (figure 1.9) with a consequent diminution in the sedimentation rate. Therefore, the equations proposed on this basis deduct from V_s a term, which may or may not be a function of V_s. Booth (1954) derived an expression

$$Q = V_s \left(1 - \alpha \beta \left(\frac{e\zeta}{kT}\right)^2\right) \qquad (1.23)$$

Figure 1·9

Sedimentation of a particle through its diffuse layer of charge (schematic)

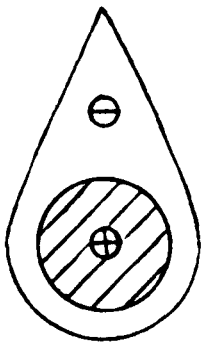

Figure 1·10

Schematic representation of the electric potential in the double layer of charge round a suspended particle

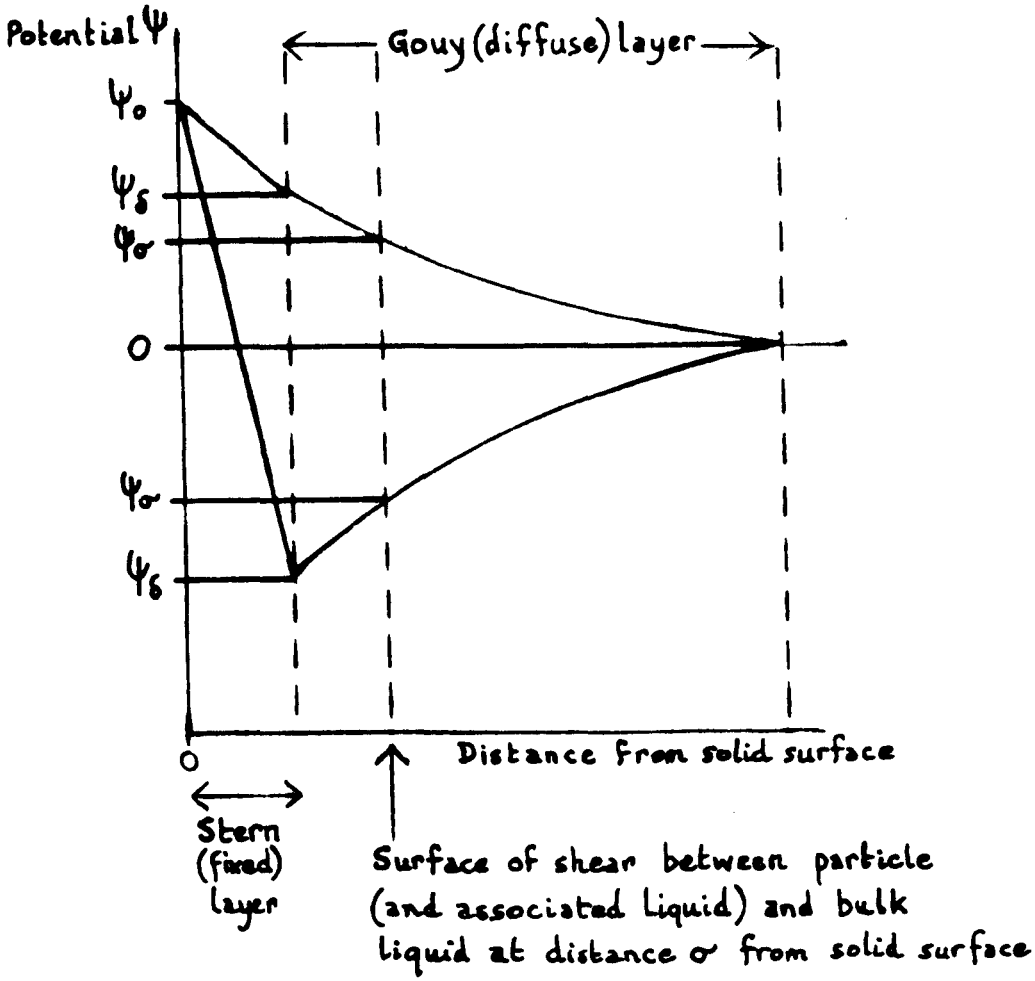

for an isolated sphere, radius r, where

α = a dimensionless parameter depending on ionic mobilities and concentrations in solution,

β = a function of Kr, in which

K = the inverse of the Debye-Hückel thickness of the charge double layer round the particles in solution,

e = the electronic charge,

ζ = the zeta-potential for the particles,

k = the Boltzmann constant,

T = absolute temperature.

For very large particles, and assuming all ionic mobilities are equal, this reduces to the equation of Smoluchowski (1921).

The electric potential gradients on and near a solid/liquid interface are represented schematically in figure 1.10, which is based on the work of Stern (1924). The Stern layer is a layer of specifically adsorbed ions and of ions located within a distance δ from the solid surface. Following Kruyt (1952),

it is assumed in sedimentation studies that the Stern layer is immovably attached to the particle, moving with it during sedimentation. It is also assumed that the zeta-potential measures the electric potential at the effective slipping plane between the particle (and associated fluid) and bulk fluid - i.e., $\zeta = \psi_\sigma$. ψ_σ may be of the same or opposite sign, compared to ψ_o, the potential on the solid surface, or may be zero even though ψ_o is not.

Analysis of the electroviscous problem for suspensions is much more complex than for single particles, because the effects of electrostatic interactions between the particles, and of flow round the particles, must be taken into account. Sengupta (1968) has indicated that equation (1.23) is applicable if the double layer thickness is much greater than the mean separation between particles and there is laminar flow. These two conditions restrict the applicability of equation 1.23 to the special case of highly concentrated suspensions of extremely fine particles in almost electrolyte-free solutions. In effect, this means that the suspension may be regarded as an ordinary electrolyte, the particles being merely exceptionally large and highly charged ions. Sengupta's argument suggests that Booth's equation might be applicable to suspensions in liquids of low dielectric constant, provided that flocculation of the particles in such a liquid is not sufficient to make the sedimenting units of solid other than fine.

For the case where the double layer thickness is small compared

with the mean separation, and again with laminar flow, the potential near any given particle would be undisturbed by electrical effects from other particles. However, the retardation field of the particle, arising from the polarization of the otherwise symmetrical field by the fluid flow, will be supplemented by an additional term representing the effect of other particles on that flow. As an example, for the special case where the double layer thickness equals the particle radius, Sengupta quotes an expression which converts to

$$Q = V_s \left[1 - \alpha(0.0037 + 0.23\ fv\ (1-\varepsilon)\ )\ \ (\frac{e\zeta}{kT})^2 \right] \qquad (1.24)$$

where f = a factor depending on the geometrical shapes of the surfaces bounding the suspension,

v = total suspension volume,

whereas equation 1.23 gives

$$Q = V_s\ (1 - 0.0037\ \alpha(\frac{e\zeta}{kT})^2). \qquad (1.25)$$

Sengupta points out that the additional correction term, $0.23\ fv\ (1-\varepsilon)\alpha$, may be of comparable or greater importance than the first part, 0.0037α.

The additional term arises from consideration of the interactions between electrostatic fields and the effect of the fluid flows round the particles. In principle, Sengupta's equation (and

related equations for other double layer thickness/particle radius ratios) may be used in studying the dependence of Q/V_s upon ε, whereas equations such as Booth's may not.

Kermack, McKendrick and Ponder (1928) derived the expression

$$Q = V_s \left(1 - c \left(1-\varepsilon\right)\right) \tag{1.26}$$

for the sedimentation of mammalian red-blood cells, where c = a constant, with values varying from 4.74 to 6.91 according to the type of mammal. For a suspension of many small rigid spheres, theory indicated that c should have a value about 7.1, while thin rigid discs should give $5.5 < c < 7.1$. Experiments on the blood cells (which are discoidal) gave a mean value $c = 5.8 \pm 0.3$.

The results of Kermack et al. indicate that for given solids volume fraction, $1-\varepsilon$, a change from spherical to discoidal shape results in an increase of Q/V_s. This observation would be unexpected if hindrance to settling is caused fundamentally by liquid turbulence, since discs settle in a direction parallel to their smallest axis, and a sedimenting disc will have a more turbulent 'tail' of liquid behind it than a sphere will. But if hindered settling is essentially a phenomenon of non-turbulent flow, the results of Kermack et al. are understandable on the basis that discs can pack vertically into smoother-sided arrays than spheres can. Conversely, the results suggest that hindered settling arises under streamline flow conditions, in agreement with the conclusion of Michaels and Bolger.

Kozeny (1927), Fair and Hatch (1933) and Carman (1937-8-9), working independently, developed an equation which for sedimentation takes the form

$$Q = V_s \left(\frac{1}{2k} \cdot \frac{\varepsilon^3}{1-\varepsilon}\right) \tag{1.27}$$

where k is an experimentally-determined constant.

The assumption underlying their work was that the flow space is equivalent to a bundle of parallel capillaries with a common hydraulic radius (i.e. each capillary has the same flow volume per unit area of wetted particle surface). Carman's experimental data for packed beds of uniform spheres when $0.26 < \varepsilon < 0.48$ gave a best correlation with $k = 4.8$, the experimental uncertainty giving a range $4.5 < k < 5.1$. Experiments with variously-shaped particles gave $k \simeq 5.0$ for $0.26 < \varepsilon < 0.80$, providing the particles were in relatively fixed positions. Particles undergoing hindered settling are in relatively fixed positions with respect to one another. It follows from these observations that Q/V_s at given porosity is not very sensitive to particle shape, and sedimentation behaviour is well interpreted by models of relatively high symmetry allowing for streamline flow. The similarity of these conclusions to those of Kermack et al and of Michaels and Bolger lend them further credence. Indeed, it has been recognised since the time of Poiseuille (1842) and D'Arcy (1856) that the flow of water through sand is governed by essentially the same factors as the streamline flow of water

through pipes.

Richardson and Zaki (1954 a) similarly found relatively little sensitivity of the $Q/V_s - \varepsilon$ relationship to particle shape. Working on a larger scale with steel and glass spheres, cylinders, hexagonal prisms, and square plates, they found that d log Q / d log ε varied with shape from 2.01 to 2.55 overall (i.e. about 27%). These experiments were done under conditions of turbulent flow, and therefore it seems that whatever the flow regime, the shape of the particle is not a major factor in varying its sedimentation behaviour from that predicted or observed for spheres. Particle shape has therefore not been one of the experimental variables studied in the present work.

However, a number of theories of sedimentation have involved correction terms named 'shape factors'. In Steinour's (1944) theory, the shape factor is a function of pore space, which itself must be related to particle shape, while in that of Fair and Hatch (1933) it is explicitly a function of particle shape. In some experimental cases, this correction term makes a marked difference to the interface settling rate which would otherwise be predicted. In view of the evidence summarised in the last three paragraphs, it seems unlikely that such a major factor is predominantly connected with particle shape, and Steinour's shape factor has therefore been studied in the work now reported.

Hawksley (1951) developed equation 1.17 by utilising a part of

Vand's (1948) theory of suspension viscosities, from which the hydrodynamic interaction of particles in a suspension should lead to

$$\frac{\eta e}{\eta} = \exp \frac{\frac{2.5\ (1-\varepsilon)}{1 - \frac{39}{64}\ (1-\varepsilon)}}{} \qquad (1.28)$$

where ηe = effective local viscosity within a suspension.

It is therefore possible to re-write equation 1.17 as

$$Q = V_s\ (\varepsilon^2\ \frac{\eta}{\eta e}), \qquad (1.29)$$

so that an expression is obtained for the influence of suspension viscosity on the settling rate. Richardson and Zaki (1954 a) took the view that suspension viscosity is not validly used in theories for systems of monodisperse particles, since in such a case the particles would settle through liquid. This comment, which would apply to well-developed hindered settling, involves the assumption that there is no particle-liquid interaction, and that therefore the suspension viscosity would be that of the liquid. This is not true in many more-realistic suspensions than Richardson and Zaki used. A more serious difficulty is that effective viscosities in the neighbourhood of a particle, ηe, cannot be measured, so that the validity of equation 1.29 cannot be checked. It has also been said that experimental data do not unequivocally support Vand's equations for suspension viscosities (Happel, 1958). Nonetheless, the

present work has included a theoretical study of the influence of suspension and liquid viscosities on hindrance to settling.

Michaels and Bolger's (1962) interpretation of their studies of flocculated and deflocculated kaolin suspensions was based on the premise that in a flocculated suspension, the basic flow units are small clusters of particles (flocs) which at low sedimentation rates may group into aggregates, which in turn may join to form extended networks throughout the suspension. They concluded that settling rates (and settled sediment volume and aggregate size) are a function of just two variables: the volume fraction occupied in the suspension by flocs, and the strength of the attractive forces between flocs. They represented any variation of Q/V_s values from those predicted by Richardson and Zaki's equation 1.19 as being due to the sedimentation of flocs, and therefore wrote

$$Q = V_s \left(1 - k \left(1-\varepsilon\right)\right)^{4.65} \qquad (1.30)$$

where k = volume of each floc per unit volume of solid contained in it.

The assumption here is that any deviation from dependence of Q/V_s upon ε expected for individual, uniformly-sized spheres, is due to flocculation. Dixon (1977) has supported Michaels and Bolger's view that there is no need to invoke any other cause.

Steinour (1944), following upon work by Powers (1939), developed an equation in which the multiplicative correction term is a function of suspension concentration and of a shape factor $\theta(\varepsilon)$. Steinour modified Stokes' expression for the total viscous resistance experienced by an isolated sphere sedimenting in laminar flow

$$F = 6\ \pi\eta\ V_s\ r \tag{1.2}$$

to account for the presence of other particles by writing

$$F = \frac{6\ \pi\eta\ V\ r}{\phi(\varepsilon)} \tag{1.31}$$

where V = settling velocity of sphere relative to fluid,

$\phi(\varepsilon)$ = a factor dependent upon the size and shape of the flow space.

For a sphere sedimenting at a steady rate, this force must be balanced by the nett gravitational attraction force. This was defined by Stokes as $\frac{4}{3}\pi r^3\ (\rho_s - \rho_l)\ g$, but Steinour modified this to $\frac{4}{3}\pi r^3\ (\rho_s - \rho_{sus})\ g$, where ρ_{sus} = density of suspension, on the grounds that the buoyancy of the particle is due to its having displaced an equal volume of suspension, rather than of liquid. Steinour also assumed a linear relationship between ρ_s, ρ_l and ρ_{sus} and volume fractions of solid and liquid:

$$\rho_{sus} = \varepsilon\rho_l + (1-\varepsilon)\,\rho_s \tag{1.32}$$

so that

$$\rho_s - \rho_{sus} = \rho_s - \left(\varepsilon\rho_l + (1-\varepsilon)\,\rho_s\right) = (\rho_s - \rho_l)\,\varepsilon \tag{1.33}$$

and therefore Steinour wrote

$$\frac{6\,\pi\eta\,Vr}{\phi(\varepsilon)} = \frac{4}{3}\,\pi r^3 g\,(\rho_s - \rho_l)\,\varepsilon \tag{1.34}$$

leading to

$$V = \frac{2\,r^2 g\,(\rho_s - \rho_l)\,\varepsilon.\,\phi(\varepsilon)}{9\eta} \tag{1.35}$$

as the expression for the average relative velocity between spheres and fluid.

In order to express equation 1.35 in terms of the measured velocity relative to a fixed horizontal plane (i.e. the interface settling rate Q), one proceeds as follows. The volumes of solid and fluid that move in opposite directions through a unit of horizontal cross-section in unit time must be equal; hence, for solid volume fraction $(1-\varepsilon)$,

$$(1-\varepsilon)V_{solid} = \varepsilon\,V_{liquid} \tag{1.36}$$

where V_{solid}, V_{liquid} = absolute solid and liquid flow rates.

But the absolute solid flow rate = Q, and so

$$(1-\varepsilon)\ Q = \varepsilon V_{liquid} \tag{1.37}$$

Now the relative velocity $V = Q + V_{liquid}$, so

$$(1-\varepsilon)\ Q = \varepsilon\ (V - Q) \tag{1.38}$$

and therefore

$$Q = V\ \varepsilon \tag{1.39}$$

Modifying equation 1.35 then yields

$$Q = \frac{2\ r^2 g\ (\rho_s - \rho_l)\ \varepsilon^2 .\ \phi(\varepsilon)}{9\eta} \tag{1.40}$$

$$= V_s\ .\ \varepsilon^2 .\ \phi(\varepsilon) \tag{1.41}$$

The correction term is therefore $\varepsilon^2 .\ \phi(\varepsilon)$. Of this, Steinour took the effect of size and part of the effect of shape of flow space to be evaluated by use of the hydraulic radius. For a suspension,

$$\text{hydraulic radius} = \frac{\varepsilon}{(1-\varepsilon)\sigma} \tag{1.42}$$

where σ = specific surface of solid ($cm^2 . cm^{-3}$).

For spheres, $\sigma = {}^3/r$, and hence

$$\text{hydraulic radius for spheres} = \frac{r\ \varepsilon}{3\ (1-\varepsilon)} \tag{1.43}$$

Having demonstrated this concentration dependence of the hydraulic radius, Steinour wrote the whole correction factor as

$$\phi(\varepsilon) = \frac{\varepsilon}{1-\varepsilon} \cdot \theta(\varepsilon) \tag{1.44}$$

where the shape factor $\theta(\varepsilon)$, according to Steinour, represents those effects of shape which are not evaluated by the hydraulic radius. Equation 1.41 then becomes

$$Q = V_s \cdot \frac{\varepsilon^3}{1-\varepsilon} \cdot \theta(\varepsilon) \tag{1.45}$$

Steinour concluded that all his data (on the sedimentation of uniformly-sized unflocculated spherical particles of tapioca and glass, in hydrocarbon oil and 0.1% aqueous sodium hexametaphosphate respectively) could be correlated by an empirical equation

$$Q = V_s\ \varepsilon^2 .\ 10^{-1.82\ (1-\varepsilon)}, \tag{1.12}$$

and therefore, from equation 1.45,

$$\theta(\varepsilon) = \frac{1-\varepsilon}{\varepsilon} .\ 10^{-1.82\ (1-\varepsilon)}. \tag{1.46}$$

His experiments were conducted in the porosity ranges $0.502 \leqslant \varepsilon \leqslant 0.949$ for tapioca, and $0.50 \leqslant \varepsilon \leqslant 0.85$ for glass. Over the range $0.3 < \varepsilon < 0.7$, $\theta(\varepsilon)$ is approximately constant at about 0.12, and Steinour wrote

$$Q = 0.123\, V_s \cdot \frac{\varepsilon^3}{1-\varepsilon} \tag{1.13}$$

However, to use this value of the shape factor to correlate data for angular particles such as emery powder, Steinour had to introduce an experimentally-determined modification to the porosity term:

$$Q = \frac{V_s\, \theta(\varepsilon)\, (\varepsilon - W_i)^3}{(1-W_i)^2(1-\varepsilon)} = \frac{0.123\, V_s\, (\varepsilon - W_i)^3}{(1-W_i)^2(1-\varepsilon)}, \tag{1.47}$$

which is reminiscent of a correction Powers (1939) had found necessary for flocculated pastes of Portland cement and water. Kozeny (1932) and Carman (1938 b, 1939 b) also found that a term equivalent to W_i was necessary in accurately representing the water permeability of clays. W_i was taken to represent that portion of the liquid volume which is not free to flow, and Powers, Kozeny and Carman all concluded that this liquid is bound in some way to the particles. Steinour followed Fair and Hatch (1933) in concluding that the liquid is not bound, but simply 'stagnant', i.e. carried down immobile in the angularities of the particles. Steinour found that equation 1.47 applied to a variety of flocculated and non-flocculated systems, although W_i varied from zero for non-flocculated glass spheres and about

0.10 for flocculated glass spheres, to 0.350 for flocculated fine particles of emery powder.

1.3.3 Some hindered settling equations studied in detail

The published hindered settling equations chosen for particular study in the work now reported are that of Richardson and Zaki (1954), the associated Michaels and Bolger (1962) expression, Happel's (1958) equation, an empirical equation derived from the work of Dollimore and McBride (1968), and the equations of Steinour (1944). The last-named equations, although partly empirical, have more theoretical basis than some others, and were based on a large amount of experimental work reported in detail. Happel's theoretical treatment, although supported by only a limited amount of data, did give best agreement with experiment in dilute suspensions ($\varepsilon \geq 0.98$) and particularly in extremely dilute cases ($\varepsilon = 0.999$). Since some of the systems to be examined could be expected to show hindrance at very high dilutions, this equation seemed likely to have particular relevance to the work proposed. The Richardson and Zaki equation was chosen as a simple expression which nonetheless gave a good fit to the authors' experimental data, while tests of the Michaels and Bolger variant would assess the validity of their assumption that abnormally low values of Q/V_s for given values of ε - i.e. abnormally high hindrance to settling - can be adequately explained by flocculation only.

The equations of Steinour have found considerable application in

the estimation of Stokes' limiting rate V_s and the equivalent spherical radius r. A typical use of equation 1.47 is that of Dollimore and Heal (1962) for the estimation of the particle size of silica gels under conditions of hindered settling. Re-arrangement of the equation gives

$$Q\ (1-\varepsilon) = \frac{V_s\ \theta(\varepsilon)}{(1-W_i)^2} .\ \ (\varepsilon - W_i)^3 \qquad (1.48)$$

from which

$$(Q(1-\varepsilon)\ )^{0.33'} = f\ \varepsilon - f\ W_i \qquad (1.49)$$

where $f = \left(\frac{V_s\ \theta(\varepsilon)}{(1-W_i)^2}\right)^{0.33'}$

Therefore, a plot of $(\ Q(1-\varepsilon)\ )^{0.33'}$ against ε should be linear, with slope = f and intercept on the ε-axis = W_i. It follows from equation 1.49 that

$$V_s = \frac{f^3\ (1-W_i)^2}{\theta(\varepsilon)} \qquad (1.50)$$

The average equivalent spherical radius was then calculated by substituting for V_s in Stokes' equation. The plot of $(Q(1-\varepsilon)\ )^{0.33'}$ against ε gave a good straight-line fit, with one or two 'kinks' which could be taken as within experimental error. However, one of the weaknesses of this method is that the extrapolation from the experimental points to the intercept

$\varepsilon = W_i$ is often long. In Dollimore and Heal's case, it was equivalent in ε to about the experimental range over which the measurements were taken; in Steinour's case, the extrapolation was often considerably longer.

Ramakrishna and Rao (1965) criticised this approach of Steinour's, as a result of observations of the sedimentation of non-porous silica in benzene and xylene in the region $0.80 < \varepsilon < 0.97$. They found two values for the positive slope in each case, and extrapolating from the slopes gave values for V_s which differed by a factor of about eight for any one liquid.

In fact, on purely mathematical grounds, a single slope for the plot is not to be expected. If W_i is a constant, and since V_s has a fixed value, it follows from equation 1.48 that the curve of $(Q\ (1-\varepsilon)\ )^{0.33^\circ}$ against ε is governed by the variation of $\theta(\varepsilon)$ with ε (equation 1.46).

If $\theta(\varepsilon)$ is constant in a set of observations (e.g. $\theta(\varepsilon) = 0.123$), the plot should indeed be linear, as found by Steinour and by Dollimore and Heal. However $\theta(\varepsilon)$ as defined by equation 1.46 declines rapidly in magnitude above $\varepsilon = 0.70$, to $\theta(\varepsilon) = 0$ at $\varepsilon = 1$. Furthermore, if the constant of the power index in equation 1.46 is other than 1.82, the variation of $\theta(\varepsilon)$ with ε changes markedly, as shown in Figure 1.11. In general, the plot of $(Q\ (1-\varepsilon)\ )^{0.33^\circ}$ against ε will have a shape similar to those in figure 1.11; various values of the slope f can be expected, dependent upon the range of porosity examined, and linear

Figure 1·11

Variation of the shape factor $\theta(\epsilon)$ with the empirical parameter A

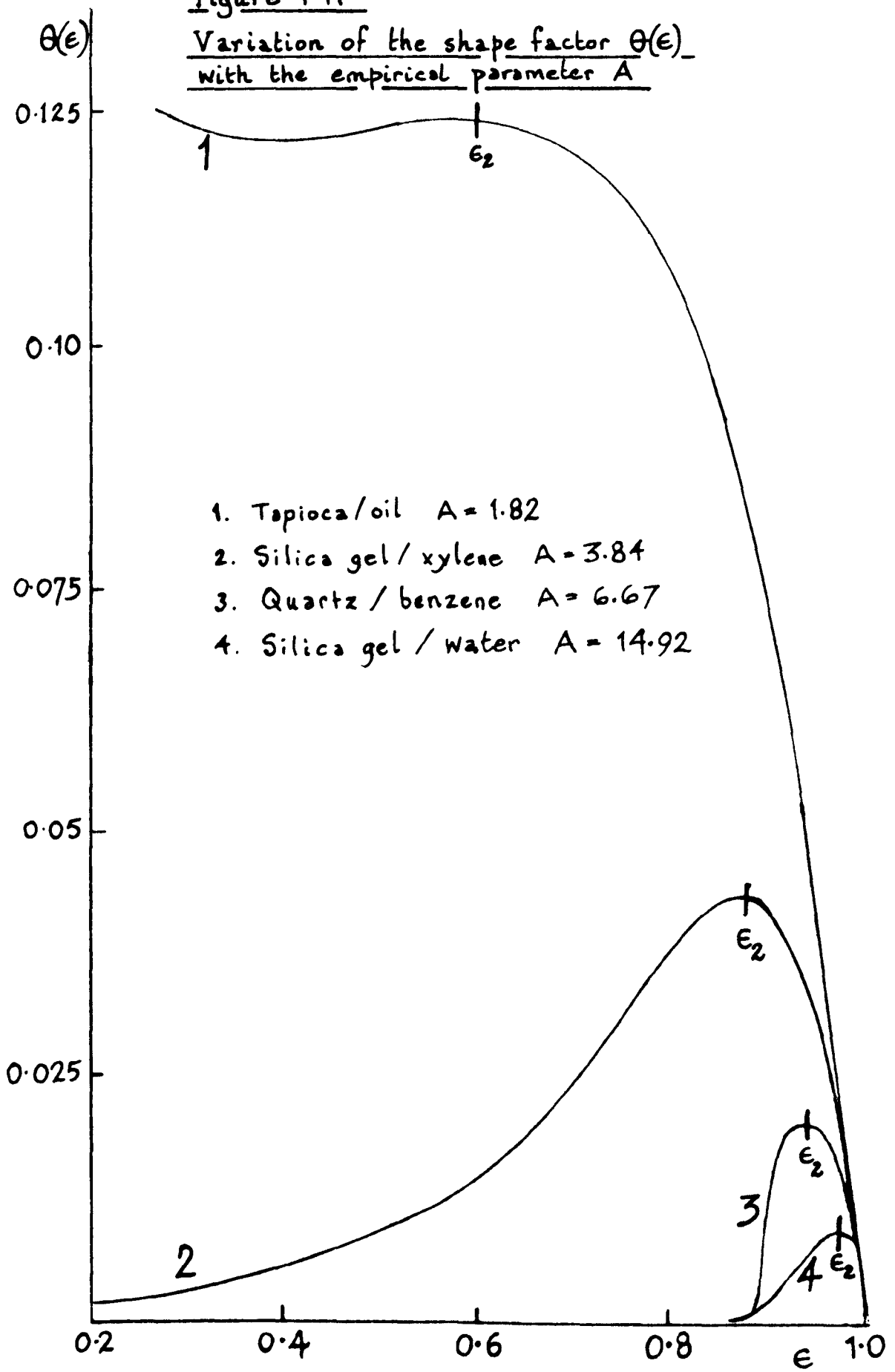

extrapolation to give W_i is unlikely to be sound. This type of calculation has therefore not been used in the study now reported.

Ramakrishna and Rao recommended the use of another of Steinour's plots, which derives from the empirical equation

$$Q = V_s \ \varepsilon^2 . \ 10^{-1.82 \ (1-\varepsilon)} \qquad (1.12)$$

If this is generalised to allow for values other than 1.82, one may write

$$Q = V_s \ \varepsilon^2 . \ 10^{-A \ (1-\varepsilon)} \qquad (1.51)$$

where A = slope of the plot of log Q/ε^2 against ε, and, by extrapolating to infinite dilution (ε=1),

$$\log Q/\varepsilon^2 = \log V_s$$

According to equation 1.51, the plot should again have a single slope. Ramakrishna and Rao nonetheless obtained two distinctly-different slopes for silica, both in benzene and in xylene, with the break point occurring at about ε = 0.90. This, they suggested, was the region of concentration in which the edge-to-edge distance between neighbouring particles became equal to the diameter of the particles. They further suggested that at lower concentrations (i.e. $\varepsilon > 0.90$), differential rates of settling might occur for particles of different sizes, even though

hindrance would still be present, and it would only be at porosities $\varepsilon < 0.90$ that true hindered settling would occur, with particles of different sizes settling at one uniform rate. These ideas were examined in the work now reported, since other published data also show what appear to be clear variations of slope, even though they were not so regarded previously (see e.g. Richardson and Zaki's (1954 b) figure 1 interpreting data by Lewis, Gilliland and Bauer (1949), and Steinour's (1944 a) figure 8).

It has become clear that the value $A = 1.82$ (or $\theta(\varepsilon) = 0.123$) does not apply to all systems. Dollimore and Horridge (1971) have obtained $A = 20.2$ for a series of aqueous suspensions of clays, Thompson (1972) has found values ranging from 24.3 to 36.6 for a series of freshly-precipitated calcium carbonates in aqueous sodium chloride, and Dollimore and Owens (1972) have obtained $A = 81$ and $A = 206$ for non-porous silica in water and n-heptane respectively. Steinour's theory has therefore been studied in the present work in an attempt to identify factors which determine the magnitudes of $\theta(\varepsilon)$ and A under various conditions.

Richardson and Zaki (1954 a) developed a cell-type model for sedimenting spherical particles, in which the particles were assumed to be spaced in a hexagonal-type pattern in the horizontal plane, and the liquid upflow was assumed to be vertical and laminar. Particles were assumed to be settling in such a way that they were all lined up vertically above each other, but for the

distance between adjacent horizontal layers, two cases were worked out. The specification of this distance which gave better agreement with their own data in the porosity range $0.4 < \varepsilon < 0.9$ was one which assumed that the horizontal layers actually touch. This arrangement offers the minimum resistance to the fluid flow through horizontal hexagonal arrays (Burgers, 1941 a). It gives the largest free cross-sectional area, and hence the maximum rate of settling for given concentration, and corresponds to a situation in which adhesion (and/or lack of repulsion) between particles allows them to make contact vertically, while being held apart horizontally by liquid flow through parallel vertical pores. This model was correlated by Richardson and Zaki with the expression

$$Q = V_s . \varepsilon^{4.65} \tag{1.19}$$

although their experimental values for the power number varied from 3.5 to 5.2 for glass ballotini, dependent on particle size and nature of fluid.

Richardson and Zaki's other model configuration assumed that the spheres are the same distance apart from one another, vertically and horizontally. This model gave better agreement with experimental data in the porosity range $0.9 < \varepsilon < 0.95$. (Both models are unreliable in the region $\varepsilon > 0.95$, leading to expectations of infinitely-high sedimentation rates.) Compared with the previous model, the expansion in the vertical direction

must involve a constriction in the flow spaces, for given concentration. This would give lower values of Q/V_s - i.e. a more-hindered condition - for given ε. On such a basis, values of the power number greater than 4.65 would be interpreted as due to opening-up of the suspension 'lattice' vertically. This could be taken as due to increased association of 'stagnant' fluid round the particles, or to constriction of flow space due to floc formation, or both. Values of the power number less than those obtained by Richardson and Zaki would not be expected. Davies, Dollimore and Sharp (1976) have generalised Richardson and Zaki's equation to

$$Q = V_s \varepsilon^n, \tag{1.53}$$

from which plotting log Q against log ε should give a straight line, slope = n, and the intercept at log ε = 0 will be equal to log V_s.

Richardson and Zaki showed that, for the first-named configuration, the relationship between the particle radius r and the horizontal distance 2R between neighbouring particle centres is

$$\frac{r}{R} = 1.225\ (1-\varepsilon)^{0.5} \tag{1.54}$$

while for the second configuration the relationship is

$$\frac{r}{R} = 1.126\ (1-\varepsilon)^{0.5} \tag{1.55}$$

To equate these with Ramakrishna and Rao's suggestion that the break they observed in plots of log Q/ε^2 against ε corresponds to the distance of nearest approach equalling their diameter, one writes $2r = R$. This would then predict the break (for spherical particles in hexagonal horizontal arrays and vertical columns, and interacting only hydrodynamically) at $\varepsilon = 0.832$ and $\varepsilon = 0.803$ respectively. These predictions have been compared with data obtained for glass spheres in viscous media, and for calcium carbonate suspensions, in the present study (section 3.6). It is notable that Steinour's (1944 a, figure 8) data for glass spheres show a break at about $\varepsilon = 0.8$.

Happel's (1958) model for the sedimenting suspension was that uniformly-sized, smooth, solid spheres move in random assemblage through the fluid, without any fluid inertia, that the entire fluid is divided up into 'cells' round the individual particles, and that there is no disturbance by any particle outside its own shell (which is assumed to have a frictionless surface). That is to say, there is no interaction between particles, except that the range of fluid disturbance by any one particle is restricted by the presence of the other particles. This gave agreement to within 2 - 15% with McNown and Lin's (1952) data in the porosity range $\varepsilon \gtrsim 0.98$, with best agreement at $\varepsilon = 0.999$, but the theoretical values of Q/V_s were stated to be 25 - 100% below experimental values for the region $0.6 < \varepsilon < 0.95$, indicating that Q/V_s is not uniquely characterised by the porosity ε. It is of particular interest that values of Q(experimental) were in general greater than those of Q(theoretical),

since this may imply the existence of interactions which increase the settling rate above that expected for a no-interaction model. Particle-particle and particle-liquid interactions of a physicochemical kind may be presumed to have a role in determining the sedimentation behaviour, because the properties of interfacial surfaces are commonly different from those of bulk matter. If the sedimenting particles are small, the system will have a relatively large interfacial area per unit mass, and consequently will be expected to show a relatively high degree of these interactions. For larger particles, the interactions will be reduced and the sedimentation will be more in accord with a purely fluid-dynamic model. In a similar way, the interactions will be expected to vary directly with the surface activity of the interfacial areas.

1.3.4 Particle-particle interactions in dilute suspensions

Smoluchowski (1912) showed theoretically that a pair of equally-sized spheres sedimenting through a fluid and separated by only a few diameters will attain a terminal velocity which is greater than V_s for such a particle, and Faxen (1927) that such a doublet at very high dilution would fall at 1.55 V_s.
Hall (1956) showed experimentally that the limiting velocity of two equal spheres, spaced at 2.6 diameters between centres, was 1.2 times V_s for a single sphere. This separation, if it were repeated in three dimensions in a suspension, would correspond to a porosity $\varepsilon \approx 0.98$.

Kaye and Boardman (1962), using different sizes of glass spheres in liquid paraffin, found that at $\varepsilon > 0.9995$, the particles settled essentially as expected from Stokes' Law. However, in the region $0.97 \lesssim \varepsilon < 0.9995$, the terminal velocity of marker spheres increased with increase of concentration. This was explained by the formation of clusters. Below $\varepsilon = 0.97$, increase of concentration decreased the terminal velocities. At $\varepsilon = 0.97$, a diffuse supernatant/sediment interface was forming, and the subsequent reduction of velocity towards V_s was interpreted as due to return flow counteracting cluster formation. The maximum value of Q/V_s in a closely-sized sample was about 1.5 in the region $0.97 < \varepsilon < 0.997$. At about $\varepsilon = 0.98$, the sedimentation rates of the markers varied by up to a factor of four in repeat runs, indicating a porosity region of variable cluster formation and irregular upward flow of fluid. At $\varepsilon = 0.90$, there was well-established hindered settling. Kaye and Boardman's observations have been confirmed by studies by Johne (1966) and by Koglin (1971). Kaye and Boardman concluded that sedimentation behaviour is not related to the suspension concentration by a single relationship, but can be divided into four fundamental concentration ranges:

(i) free settling at very high porosities;

(ii) a region of viscous interaction in which the particles fall faster than their Stokes' terminal velocity;

(iii) a range of instability where clusters form and

the return flow is irregular and localised;

(iv) a well-defined range of higher concentrations of solid, where hindered settling occurs under conditions of uniformly diffuse return flow through the evenly dispersed cloud of particles.

This analysis leads to a general form of sedimentation curve of the type shown in figure 1.12, which may be compared to those in figure 1.6. In contrast to the exponential nature of the latter, the positive slope of figure 1.12 is of sigmoid type, and Kaye and Boardman's analysis indicates that the observed curve will be compound, rather than simple. This last point is reminiscent of Ramakrishna and Rao's observation of two slopes in the plot of log Q/ϵ^2 against ϵ. It is important to have a test equation for the best fit of experimental settling rates to porosities, and such an equation has been developed in the study now reported.

A striking observation was made by Slack (1962) during work with small particles in castor oil, in the region of Reynolds' number $0.001 < Re < 10$. He found that three, four, five or six spheres formed a horizontal polygon, which increased in size as settling progressed, with each sphere rotating downwards and inwards through the centre of the polygon; seven or more spheres formed a roughly spherical cluster. The behaviour of the polygons is consistent with greater fluid flow rate outside the polygon, compared with within. Hindered settling modelled on

Figure 1·12

Dependence of sedimentation rate on liquid volume fraction in uniformly-mixed suspensions of closely-sized spheres

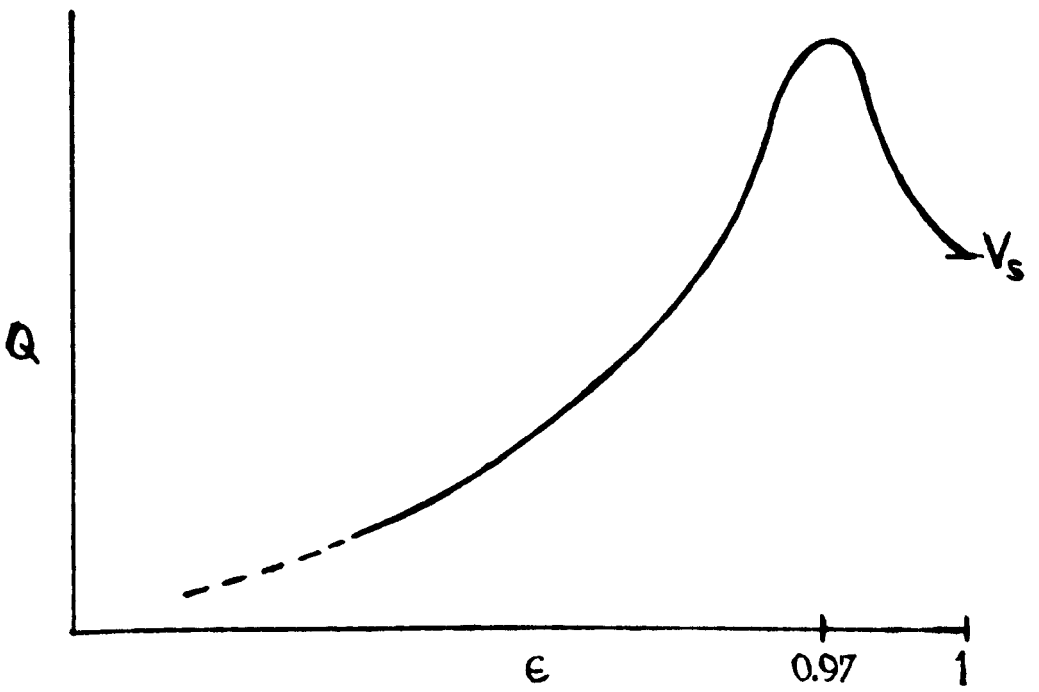

(schematic; based on observations of Kaye and Boardman (1962); Johne (1966) and Koglin (1971))

fused hexagons, as in Richardson and Zaki's theory, cannot be reconciled with spheres rotating about horizontal axes, since spheres are shared between hexagons. Perhaps the threshold porosity for hindered settling is that porosity at which polygons of particles approach sufficiently closely for fusion to occur, and particle rotation stops. Absence of rotation about the horizontal axis implies equal vertical shear within and without the hexagon. With fused hexagons, flow outside one hexagon is flow inside another. This leads to a theoretical model of the 'plug' during hindered settling as being of horizontal arrays of fused hexagons, each corner being occupied by a particle, with a parallel upward liquid flow through each hexagon. In this model, the particle at the centre of any hexagon in the Richardson and Zaki model is replaced by a fluid flow. The mathematical consequences of a simplified form of this simple-hexagon model has been investigated in the present work, and compared with corresponding ones from the Richardson and Zaki model. Experimental data have been used to give an assessment of the degree to which the structure of an actual sedimenting mass might correspond to such models.

One limitation of the Richardson-Zaki model is that - apart from a relatively small vertical compression - the only compression possible in the 'plug', on decrease of porosity, is the compression of the established (but expanded) close-packed-type hexagonal layers. The relationship of flow space (and thus sedimentation rate) to porosity is therefore a single smooth curve. The introduction of a simple-hexagonal model at the

threshold porosity for hindered settling allows for the possibility of a transition, at some lower porosity, to the close-packed regime. If this occurs, it would give a change in shape of the sedimentation curve at that lower porosity. The shapes of some hindered-settling sedimentation curves have therefore been examined in detail.

Chapter 2 Experimental procedures and results

2.1 Materials

Since it was intended to conduct sedimentations in organic liquids, and in view of evidence (Kruyt and van Selms, 1943; McGown and Parfitt (1966), Micale, Lui and Zettlemoyer (1966), Romo, 1966) that dispersion in non-aqueous media of low dielectric constant can be strongly affected by trace amounts of water, the materials used in this study were dried as thoroughly as possible. The solids used to make suspensions were therefore dried at 150°C for one hour and cooled and stored in vacuo over indicator silica gel. More-rigorous outgassing was not possible in view of the considerable bulk of material required. Except where otherwise indicated, the calcium carbonate experiments were carried out with a single batch of Hopkin and Williams laboratory grade material, density $\rho_s = 2.71$ g.cm^{-3}, with surface area (as measured by nitrogen adsorption) of 4.0 m^2. g^{-1}. Organic liquids were dried over silica gel, and distilled and stored in glass over excess of the gel. The water used was either distilled in glass or deionised with commercial ion-exchange resins, but in all cases was stored in polythene. Sodium chloride solutions were prepared using distilled water and analytical reagent grade solid. The measuring cylinders used were dried by washing with dry acetone and dry ether, and blowing with compressed air, immediately before use.

2.2 Hindered settling technique and observation of settled sediment volumes

The use of a hindered settling technique for particle size measurement has been used by Steinour (1944), Richardson and Zaki (1954), Dollimore and Griffiths (1960), Dollimore and Heal (1962), and others. In the present case, the sedimentation tubes were 250 cm^3 sedimentation cylinders. Twenty-nine such cylinders, designated A - Z and AA - CC, were used in the investigation. The uniformity of cross-section of the cylinders was assessed as satisfactory by a detailed calibration, with water at 20°C, of five cylinders chosen at random. The results are shown in table 2.1. The vertical heights in all the cylinders, for 100, 150 and 200 cm^3 contained volume, were then measured, and the results appear in table 2.2. The mean height for 200 cm^3 was 18.36 cm, with a range of 17.0 - 19.50 cm, corresponding to a mean diameter of 3.73 cm, with a range of 3.614 - 3.87 cm. Interface heights were measured as volume (cm^3) occupied up to the interface, and then converted to heights (cm) by use of the conversion factors shown in table 2.2. There is some doubt as to true heights above the cylinder internal base, due to lack of uniform shape near the base, but this is not a problem in interface settling rate measurements, since the relevant parameter is the height difference from the meniscus, and all height measurements are therefore relative.

The technique of preparing a suspension, unless otherwise stated was as follows: 100 cm^3 liquid was placed in a cylinder,

a weighed amount of solid added, and the whole gently mixed before making up to 200 cm^3 with that liquid. A sample was prepared for observation by inverting the cylinder, end over end, thirty times, at one inversion per second, and then setting it down in front of a fluorescent (i.e. cold source) light box on the laboratory bench. The experiments were carried out either in a constant-temperature room, thermostatted to within very narrow limits to 20°C, except where otherwise stated, or - when this was not possible - the tubes were stood in a thermostat bath (20 ± 0.5°C) until required. Measurements of interface height were made at appropriate regular time intervals, as shown in the tables of results below, taking zero time as the instant when any initial turbulence ceased on setting down. In more-dilute suspensions, the plot of interface height h (cm) against time t (sec) gave an initial sedimentation rate dh/dt in accordance with figure 1.1, while in more-concentrated suspensions, the sedimentation behaviour was as figure 1.2. In all cases recorded, there was a substantial linear portion of the plot, the slope of this portion being designated Q. Readings were continued until the rate decreased considerably below that value. The experiment was repeated two to four times for each tube, in quick succession, and the mean results plotted, h against t, to give the best-fit values of Q ($cm.s^{-1}$).

When all sedimentation had ceased, the volume of settled sediment was observed and recorded. Since 250 cm^3 cylinders are not calibrated below 30 cm^3 by the manufacturers, those used

in this investigation were calibrated below that level by the addition of 5 cm^3 volumes of water at 20^oC. Intermediate values were marked by interpolation between the observed levels.

2.3 Results

The quantitative results obtained in this investigation refer to the sedimentation of calcium carbonate and of glass ballotini. Those for the ballotini are discussed specifically in section 3.3 and are reproduced there for convenience. The data for calcium carbonate (calcium carbonate masses (g), interface heights (cm) at corresponding times (seconds), the linear settling rates (Q, $cm.s^{-1}$) obtained therefrom, and settled sediment volumes (cm^3)) are given in tables 2.3 - 2.15, with illustrative graphs of interface height h plotted against time t, since they are discussed in various sections of what follows.

Tables 2.1, 2.2

Calibration of measuring cylinders

Table 2.1: comparison of nominal and observed cylinder volumes, above the 30 cm^3 mark (cylinders subsequently designated F, G, H, I, J)

Nominal volume (cm^3)	Observed volume (cm^3)				
	F	G	H	I	J
30	30	30	30	30	30
55	55.5	56	56	56	56
80	80	80	80	80	81
105	106	106	106	104	106
130	131	130.5	131	129	131
155	154.5	156	156	153	156
180	181	180	181	179	181
205	206	206	205	204	206
230	231	231	231	230	231.5
250	251	251	251	251	252

The observed volumes were those read off from the cylinder calibrations when eight 25 cm^3 pipetted aliquots, and one 20 cm^3 aliquot, of water at 20°C were added to water initially present to the 30 cm^3 mark.

Table 2.2: Height/volume relationships at 20°C for cylinders A - Z, AA - CC

Cylinder	Heights for given volumes (cm)			Mean height/volume ratio (cm^{-2})
	100 cm^3	150 cm^3	200 cm^3	
A	9.0	13.45	18.1	0.0901
B	9.1	13.65	18.2	0.0910
C	9.2	13.8	18.4	0.0920
D	8.8	13.3	17.6	0.0883
E	8.85	13.55	18.5	0.0904
F	9.05	13.55	18.0	0.0903
G	9.1	13.6	17.9	0.0904
H	8.9	13.35	17.7	0.0888
I	8.8	13.2	17.6	0.0870
J	8.9	13.4	17.95	0.0894
K	8.3	12.6	17.0	0.0840
L	8.6	12.8	17.2	0.0857
M	9.1	13.4	17.8	0.0894
N	8.8	13.4	18.1	0.0893
O	9.4	13.4	18.5	0.0919
P	8.8	13.35	18.0	0.0889
Q	9.25	13.95	18.5	0.0927
R	9.05	13.45	18.2	0.0904
S	-	-	18.4	0.0920
T	-	-	19.1	0.0955
U	-	-	19.5	0.0975
V	-	-	18.8	0.0940
W	-	-	19.05	0.0953
X	-	-	19.05	0.0953
Y	-	-	19.2	0.0960
Z	-	-	19.5	0.0975
AA	-	-	18.7	0.0935
BB	-	-	19.0	0.0950
CC	-	-	19.0	0.0950

Tables 2.3 - 2.15

Sedimentation and settled volume data for calcium carbonate in various liquids

Initial interface level (i.e. at time = zero) 200 cm^3 in all cases

Table 2.3: calcium carbonate in water

Cylinder Solid mass (g) Initial porosity, ϵ	F 5.068 0.9907	G 6.920 0.9873	H 9.129 0.9832	I 11.253 0.9793	P 12.778 0.9764	Q 14.856 0.9726
Time (min.)	Interface levels (cm^3)					
0.5	177	182	186.5	186	188	190
1.0	150	159	168	170	177	182
1.5	123	137	151	156	167	174
2.0	97	116.5	134.5	143	155	166
2.5	72	95.5	118	131	144	
3.0	47	76.5	103.5	119	135	152
3.5	39		90	109	127	144
4.0	30	50	78	100	119	139
5	25	42	64.5	87	107	128
6		37	52	78		118
7			48.5	71		
8				66	84	
10					75	
12				50		
13						77
14	16.7					
17			32			
18		22				
20						56
26	16.5					
Linear settling rate Q ($cm.s^{-1}$)	0.0818	0.0640	0.0478	0.0386	0.0342	0.0253
Settled sediment volume (cm^3), 20 hr.	16	22	25	29	33	37

Other settled sediment volumes:
cylinder B mass 11.12 g volume 30 cm^3
" D " 19.14 g " 47 "

Table 2.4: calcium carbonate in 0.137 M sodium chloride

Cylinder	A	C	E	F	K	I
Solid mass (g)	5.038	6.868	9.045	11.096	13.012	14.980
Initial porosity, ε	0.9907	0.9874	0.9833	0.9795	0.9760	0.9724
Time (min.)	Interface levels (cm^3)					
0.5	182	183	184.5	189	189	192
0.75	161	171	174.5	182	183.5	188
1	150	158	165	175	178.5	183.5
1.25	132	146.5	155.5	168	172	179.5
1.5	117	134.5	146.5	161.5	167	175
1.75	103	125	138.5	155	161.5	171
2	89.5	113.5	130.25	148.5	157	167
2.25	75	102.5	123	142.5	152	164
2.5	62	92.5	115.25	136	147	160
2.75	48	83	108.5	130	142.5	156
3	38.5	73	101.25	-	138	153
3.25	35	64.5	95.25	-	134	149.5
3.5	32	57.5	90.25	114	130	146
3.75		53.75	85.5	109	126.5	143
4		51	81.5	104.5	123	140.5
4.25		48.25		100.5	119.5	137.5
4.5		46.25		96.5		135
4.75				93		132
5				90		130
Linear settling rate Q ($cm.s^{-1}$)	0.0892	0.0691	0.0539	0.0395	0.0292	0.0229
Settled sediment volume (cm^3), 20 hr.	14.2	19	26	31	36.5	40.5

Table 2.5: calcium carbonate in 0.216 M sodium chloride

Cylinder Solid mass (g) Initial porosity, ε	R 4.974 0.9908	Q 7.140 0.9868	M 8.929 0.9836	N 11.296 0.9792	O 12.762 0.9765	P 15.139 0.9721
Time (min.)	Interface levels (cm^3)					
0.5	183	189	188	190	191	194.5
0.75	167	176	179	184	186	191
1	150	166	170.5	177.75	181	187
1.25	134.5	153.5	162.5	170.75	176	183.5
1.5	123.5	145	154.5	164.75	171	180
1.75	111	135	145.5	156.75	166	176.5
2	96	126.5	137.5	154	162	173
2.25	84	117	130	147.75	158	170
2.5	72.5	107.5	123	142	153.5	167
2.75	61	97.5	115	137.5	149.5	164
3	50	89	109	132	144	161
3.25	43.5	80	102	127.5	141.5	157.5
3.5	40	72	96	122.5	138	155
3.75	37.5	64.5	90.25	118.25	135.5	152
4		59.25	86	114.5	131	149.5
4.25		55.5	82	110	128	146.5
4.5		52.5	78.5	106	125	144
4.75				103	122	
5				100	119.5	
Interface settling rate Q ($cm.s^{-1}$)	0.0815	0.0591	0.0469	0.0356	0.0281	0.0212
Settled sediment volume (cm^3), 24 hr.	15.5	20	20.5	32	36	41.5

Table 2.6: calcium carbonate in 0.263 M sodium chloride

Cylinder Solid mass (g) Initial porosity, ε	M 5.220 0.9904	N 6.973 0.9872	O 9.227 0.9830	P 10.987 0.9797	Q 13.154 0.9758	R 14.958 0.9724
Time (min.)	Interface levels (cm^3)					
0.5	177	182	190	190	194	194
0.75	164	170.5	182	183	189	189.5
1	154	159	172	176	184.5	186
1.25	134.5	146	164	169.5	180	182
1.5	121	134	156	163	175.5	178.5
1.75	109	125.5	148	156	171	175
2	95.5	113.5	140	150	166.5	171.5
2.25	83	105.5	133	144	162	169
2.5	72	95	126	138.5	158	165.5
2.75	61	86.5	119	133	154	162
3	51	77.5	113	127.5	150	159
3.25	44	69.5	106	123	146	156
3.5	40	63.5	100	118	142	153.5
3.75	37.25	58.5	95.5	114	138.5	150
4	35.25	54.75	90.5	110	135	147.5
4.25	33.5	52	86.5	106	131	145
4.5	32	50	82.5	103	128	142
4.75	31	48	79.5	100	125	140
5	30	46	76	96.5	122	137.5
Linear settling rate Q ($cm.s^{-1}$)	0.0772	0.0640	0.0495	0.0387	0.0277	0.0220
Settled sediment volume (cm^3), 20 hr.	16.2	20.5	26.5	31	36	41

Table 2.7: calcium carbonate in 0.458 M sodium chloride

Cylinder Solid mass (g) Initial porosity, ε	A 5.100 0.9906	C 6.969 0.9872	E 9.057 0.9833	F 10.929 0.9799	K 12.973 0.9761	I 15.123 0.9721
Time (min.)	Interface levels (cm^3)					
0.5	182	187.5	190	193	193.5	194
0.75	-	-	181	187	188	190.5
1.0	161	168	172.5	180.5	183	187.5
1.25	-	-	165	174	177.5	183.5
1.5	136	148	156	169	173.5	180
1.75	-	-	149	163	168	176
2	112	129.5	141.5	156	164	173
2.25	-	-	134	151.5	159.5	170
2.5	88.5	110	126.5	146	155	167
2.75	-	-	120	140	151	163.5
3	65.5	92.5	114	135	147	160
3.25	-	-	107	130	143	157
3.5	42	75	102	125	139	154
3.75	-	-	96	120	135.5	151.5
4	34	61	91.5	115.5	132	148
4.25	-	-	87	111	129	146
4.5	30.5	53	83.5	106.5	126	143
5	28	48.5	77.75	101	121	139.5
5.5	-	-	-	93	114	134
6	-	-	69.5	88	110	129
6.5	-	-	-	83.5	105	125
7	-	-	63	80	101.5	122
9	20	-				
18		24				
Linear settling rate Q ($cm.s^{-1}$)	0.0715	0.0570	0.0447	0.0353	0.0268	0.0197
Settled sediment volume (cm^3), 44 hr.	14.7	18.5	24	29	34	39

Table 2.8: calcium carbonate in 0.756 M sodium chloride

Cylinder Solid mass (g) Initial porosity, ε	C 7.086 0.9852	E 9.069 0.9833	F 10.894 0.9799	K 13.016 0.9760	I 14.988 0.9724
Time (min.)	Interface levels (cm^3)				
0.5	187.5	189	-	194	196
0.75	176	179	187	189	192
1	168	171	180	185	188
1.25	158	164	175	180	185
1.5	149	156	169	175	181
1.75	139	149	163	170	177.5
2	131	142	157.5	166	174
2.25	123	135	151.5	161	171
2.5	114	128	146	157	168
2.75	105	121.5	141	153.5	164.5
3	97	116	135.5	149	161.5
3.25	89	110	130.5	145	158.5
3.5	81	104	125.5	141	156
3.75	73	99	121	138	152.5
4	66.5	94	116	134	150
4.25	60	89.5	111.5	131	147
4.5	56	86	107	127.5	145
4.75	53		103	125	142
5	51		99.5	122	140
5.25			96		137.5
5.5			93		135
Linear settling rate Q ($cm.s^{-1}$)	0.0546	0.0437	0.0342	0.0259	0.0210
Settled sediment volume (cm^3), 3 days	20	26	30	36	39

Table 2.9: calcium carbonate in 0.915 M sodium chloride

Cylinder Solid mass (g) Initial porosity, ε	A 5.036 0.9907	B 7.115 0.9869	C 8.963 0.9835	D 10.941 0.9798	E 13.128 0.9758	F 15.006 0.9723
Time (min.)	Interface levels (cm^3)					
0.5	-	-	190	194	193	195
1	166	174	178	182	185	189.5
1.5	142	156	163	-	177	183
1.75	-	-	-	166	-	-
2	118	139	151	161	169.5	178
2.5	98	113	138	150	162	172
3	77	106	126	141	155	167
3.5	56	-	113	130	148	162
3.75	-	83	-	-	-	-
4	36	75	103	-	142	157
4.5	31.5	62	92	113	135.5	152
5	28.5	54	83	105.5	130	148
5.5	-	-	-	-	125	-
6	24.5	46.5	-	92.5	120	139
7	22	42	-	83	112	
8	-	38	57.5	76	105	
9	-	34	53	-	99	
10	19	32	49	66	94	
11			-	-	89.5	
12			-	-	-	
13			-	54	81	
15			-			
20			30.5			
Linear settling rate Q ($cm.s^{-1}$)	0.0659	0.0488	0.0386	0.0300	0.0223	0.0160
Settled sediment volume (cm^3), 20 hr.	13.5	20	25.5	31	36	39.5

Table 2.10: calcium carbonate in dry acetone

Cylinder	F	G	H	I	J
Solid mass (g)	5.274	9.983	15.104	19.964	24.934
Initial porosity, ε	0.9903	0.9816	0.9722	0.9632	0.9540
Time (sec.)	Interface level (cm^3)				
10	-	-	178	193	196
20	154	154	150	183	189
30	104	120	120	160	183
40	61	89	99	136	179
50	40	71	93	126	175
60	36	67	89	122	171
70	34	64	86	118	168
80	32	60.5	84	115	164
90	31	59.5	82.5	112	160
100	30	57.5	81	110	158
110	29.5	56	79.5	108	155
120	28.5	54.5	78	106	152
130	28	54	77	104	150
140	27.5	53	76	103	145
150	27	52	75	102	144
160	27	51.5	74	100	142
170	-	-	-	-	-
180	26.5	50	72	98	138
190	-	-	72	-	136
200	26	49.5	71.5	96	133
210	-	-	-	-	132
220	26	48	70	95	130
230	-	-	-	-	129
240	26	48	70	93	126
250					125
260					123
270					122
280					121
290					120
300					120
Linear settling rate Q ($cm.s^{-1}$)	0.421	0.291	0.255	0.209	virtually no linear settling
Settled sediment volume (cm^3), 19 hr.	23	44	62	78	94

Table 2.11: calcium carbonate in dry benzene

Cylinder Solid mass (g) Initial porosity, ε	S 7.449 0.9863	T 9.756 0.9819	U 12.368 0.9772	V 15.327 0.9716	W 17.365 0.9681	X 20.107 0.9629
Time (sec.)	Interface level (cm^3)					
10	154	166	177	190	190.7	189
12	101	121	142	170.7	178	171.7
20	74	94	116	144.3	164.3	158.3
30	65	86	106	133.3	155.3	151
40	64	81.75	102	127.7	148	146.3
50	59.5	78	97.5	123.3	141.7	141.3
60	57	75.5	94	119	137.3	137.3
70	55	73.5	92	116	133	135.3
80		72	90	113.7	129.3	132.3
90						130
100						
Linear settling rate Q ($cm.s^{-1}$)	0.470	0.431	0.347	0.218	0.125	almost no linear settling
Settled sediment volume (cm^3), 2 days	39	50	62	76	85	96

Table 2.12: calcium carbonate in dry chloroform

Cylinder Solid mass (g) Initial porosity, ε	Y 7.135 0.9868	Z 9.391 0.9827	AA 12.774 0.9764	BB 15.752 0.9709	CC 17.962 0.9669
Time (sec.)	Interface levels (cm^3)				
10	188.5	189.5	193.5	196.5	197
20	168	173.5	178.75	190.2	194.5
30	147	156.5	164	180	190.7
40	127	139.5	147	169.2	187.5
50	105.5	121.5	130	156.2	183
60	85	104	114	141.3	179.5
70	68.5	89.5	102	127.7	175.5
80	62	79	95.5	120.8	172
90	59	74.5	93.25	117.2	167.8
100	57	72	90.25	114	164.3
110		70	88.75	112.2	161.5
120				111.5	159
130					156.7
140					155
150					151.2
160					149.3
170					147.7
180					145.8
Linear settling rate Q ($cm.s^{-1}$)	0.198	0.167	0.150	0.133	0.032
Settled sediment volume (cm^3), 5 days	36	46	60	72	81

Table 2.13: calcium carbonate in dry diethyl ether

Cylinder Solid mass (g) Initial porosity, ε	G 4.949 0.9909	H 6.929 0.9872	I 8.919 0.9836	J 10.976 0.9798	K 12.954 0.9761	L 15.062 0.9722
Time (sec.)	Interface levels (cm^3)					
5	166	165	164	174	170	175
10	100	100	114	130	122	140
15	51	66.5	79.3	98	101	115
20	44	59	72	86	93.5	105
25	40.5	54.5	67.3	80	90	100
30	38.5	51.5	65	76.5	86	96.5
35	36	49.5	62	74	84	93.5
40	35	48	59.7	72	82	91.5
45	34	46.5	59	69.5	80	90
50	33.5	45.5	57.3	68	78	88
55	33	44.5	56.3	66.5	77	86
60	32	44	55.7	66	76	85.5
Interface settling rate Q ($cm.s^{-1}$)	1.069	0.939	0.802	0.712	0.651	0.520
Settled sediment volume (cm^3), 4 hr.	28	38	47	54	64	70

Table 2.14: calcium carbonate in dry ethyl acetate

The first settling was carried out on the day of mixing all samples. The 2nd - 5th settlings were carried out on the next day, and the 8th, 52nd and 64th day after mixing, respectively.

Cylinder	M	N	O	P	Q
solid mass (g)	8.077	11.058	14.029	16.959	19.991
Initial porosity, ε	0.9851	0.9796	0.9741	0.9687	0.9631
1st settling Time (min.)	Interface levels (cm^3)				
0.25	188.5	191	192.5	195.5	197.5
0.5	174	181	185	190	194
0.75	161	170.5	177.3	185.2	190
1	149	161	170.8	180	186.5
1.25	134.5	151.5	163.7	175.5	183
1.5	123	142	158	170.7	179.5
1.75	111	133	151.8	166.5	176
2	99	124	145.7	162	172
2.25	85	115.5	139.7	157.3	168
2.5	75	107.5	134.2	152.7	164
2.75	65	100	129	148.2	160
3	55	92.25	123.8	143.7	156
3.25	47.5	85	119	139.2	152
3.5	43.5	79.25	114	135	148
3.75	40.75	73.5	109.5	130.7	144
4	38	69.25	104.8	126.3	140.5
4.25			100.5	121.8	136.5
4.5			96.5	117.8	132.5
4.75			93	113.8	129
5			89	110	124.5
5.25			85.5	105.7	120.5
5.5			82	101.8	116.5
5.75			78.25	98.3	113
6			75	94.5	108
Linear settling rate Q ($cm.s^{-1}$)	0.0745	0.0547	0.0401	0.0265	0.0244
Settled sediment volume (cm^3), 24 hr.	25.5	36	42	53	61.5

(Table 2.14 continued)

2nd settling

Time (min.)	Interface levels (cm^3)				
0.25	-	191	192	194	197
0.5	-	181	184	188	193
0.75	164	170	176	182	189
1	150	160	168	176	184.5
1.25	136	150	160	170	180.5
1.5	123	140	153	164.5	176.5
1.75	113	130	146	159	173
2	100	121	139	153	169
2.25	88	112	132	148.5	165.5
2.5	76	103	125.5	142	162
2.75	65	94	119.5	137	158
3	55	86	113	132	154.5
3.25	46	78	107	127	151
3.5	41	70	101	122	147.5
3.75	38	64	96	118	144
4	36	60	91	114	140.5
4.25				109.5	137
4.5				106	133.5
4.75				102.5	130
5				99.5	126.5
5.25					123
5.5					120
5.75					117
6.0					114
Linear settling rate Q ($cm.s^{-1}$)	0.0732	0.0571	0.0449	0.0342	0.0242
Settled sediment volume (cm^3), 3 days	20.2	26	33.5	42	48

(Table 2.14 continued)

3rd settling

Time (min.)	Interface levels (cm^3)				
0.25	-	-	194	194.5	196.5
0.5	-	180	186	188	192
0.75	165	171	178	182	187.5
1	152	161	171	176	183
1.25	142	152	163	170	179
1.5	129	142	156	164	175
1.75	118	133	149	158	171
2	107	124	142	152	167
2.25	95	115	135	146	162.5
2.5	84	106	128	140.5	158.5
2.75	73	98	122	135	154.5
3	63	90	116	129.5	151
3.25	53	81.5	110	124	146.5
3.5	44	74	104	119.5	143
3.75	39	67	98	114.5	139
4	36	61	93.5	110	135
4.25	34	56.5	88	106	131.5
4.5		53	84	102	127.5
4.75			80	99	124
5			76	95	120
5.25			73.5		117
5.5			71		113.5
5.75			68		110.5
6			66		107.5
6.25					104.5
6.5					102
6.75					99
7					96.5
Linear settling rate Q ($cm.s^{-1}$)	0.0668	0.0551	0.0438	0.0350	0.0257
Settled sediment volume (cm^3)	18.5	26	33.5	41	48

(Table 2.14 continued)

4th settling

Cylinder	E	I	K	C	H	AA
Solid mass (g)	8.746	11.594	13.851	15.835	18.440	20.520
Initial porosity, ϵ	0.9839	0.9786	0.9745	0.9708	0.9660	0.9621
Time (min.)	Interface levels (cm^3)					
0.25	-	191	192	194	195	197
0.5	183	182	184	188	190	193
0.75	173	174	177.75	182.5	185.5	188.5
1	163.3	165	169	176	180	184
1.25	153	156	161.5	170.25	175.5	180
1.5	143.7	147	154	164.25	170	176
1.75	133.7	139	146.75	158.5	165.5	172
2	124.7	130.5	139	152.75	160.5	167.5
2.25	115.3	123	131.75	147	156	163.5
2.5	106.3	115	125	141.5	151	159.5
2.75	97.3	106.75	117.5	136	146.5	155.5
3	88	99	111.5	130.25	142	151.5
3.25	79.3	91.25	105	125.5	137.5	147.5
3.5	71.7	84.75	98.5	120.25	133	143.5
3.75	63.7	77.5	92.5	115.25	129	140
4	56.5	70.5	86.75	110	124.5	136
4.25	49.5	64.5	81.75	105.75	120.5	132
4.5	44	59.5	76.75	102	117	128.5
4.75	40.7	56.25	72.75	98	113.5	125
5	38.7	53.5	69.75	94	109.5	121.5
5.25	-		66	90	106.5	118
5.5	36.25			86.5	103.5	115
5.75				84	100.5	112
6				81.5	98	109
Linear settling rate Q ($cm.s^{-1}$)	0.0563	0.0495	0.0427	0.0355	0.0286	0.0250
Settled sediment volume (cm^3), 4 days	17.9	22	25.5	31.5	35	39.5

(Table 2.14 continued)

5th settling

Time (min.)	Interface levels (cm^3)					
0.5	187	-	186	188	191.5	192.5
1	172	171	175	179	184	186
1.5	156	158	164	170	176	179.5
2	141	146	152	161.5	168	173
2.5	126	133	142	153	160	167
3	112	121	132	144.5	153	160.5
3.5	97	109	120.5	136	145	154
4	84	96	110	127.5	138	148
4.5	70	85	100.5	119.5	130.5	141.5
5	58	73.5	90	112	123.5	136
5.5	47	63	81.5	104.5	116.5	130
6	36.5	53	72.5	97	110	124
6.5	33	47	65	91	104	118
7			60	84.5	98	112.5
7.5				79	93.5	107.5
8						102.5
8.5						98
Linear settling rate Q ($cm.s^{-1}$)	0.0451	0.0352	0.0300	0.0266	0.0228	0.0196
Settled sediment volume (cm^3), 1 day	17.5	21.9	25.5	30.5	34.5	38

Table 2.15: calcium carbonate in dry ethyl acetoacetate (duplicate runs)

Run 1

Cylinder	A	B	C	D	E	F
Solid mass (g)	4.915	6.988	9.144	10.926	12.984	15.094
Initial porosity, ε	0.9910	0.9871	0.9832	0.9799	0.9761	0.9722
Time (min.)	Interface levels (cm^3)					
1	-	-	190	195	196	197
2	-	-	-	188	190	192
3	-	180	-	182	185	187.5
4	168	-	172	175	179	183
5	162	164	166	169	174	179
6	150	155	158	163	168	174
7	140	148	152	-	163	170
8	132	140	146	151	157	166
9	123	132	-	145	152	161
10	116	124	131	139	146	157
11	-	-	-	133	142	152
12	95	-	-	127	136	148
13	-	-	-	121	131	144
14	-	-	-	115	126	140
15	-	78	95	-	-	136
16	-	-	-	104	116	-
17	-	-	-	-	-	127
18	-	-	-	-	107	-
19	-	-	-	86	-	119
20	-	-	-	80	98	
21	-	-	-	-	-	
22	14	30	54	-	89	
23				64		
Linear settling rate Q ($cm.s^{-1}$)	0.0138	0.0126	0.0108	0.0089	0.0079	0.0067
Settled sediment volume (cm^3), 4 days	9.5	14	18	23	26.5	31

(Table 2.15 continued)

2nd Run

Cylinder Solid mass (g) Initial porosity, ε	J 5.985 0.9886	A 7.977 0.9853	R 12.042 0.9778	L 14.002 0.9742
Time (min.)	Interface levels (cm^3)			
1	-	192	194	195
2	187	184	188	189
3	177	177	182	184
4	168	170	176	178
5	158	161	170	173.5
6	148	154	164	168
7	140	146	158	162.5
8	130	138	152	157.5
9	121	131	146	152
10	113	123	-	147
11	104	117	135	-
12	-	110	129.5	137
13	86	103	124	132
14	78	95	119	127
15		87	113	122.5
16		80	108	117.5
17		73	103	113
18			98	108
19			94.5	104
20				99
Linear settling rate Q ($cm.s^{-1}$)	0.0136	0.0111	0.0091	0.0075
Settled sediment volume (cm^3), 5 days	10.9	13.6	22	27.5

Figures 2·1 a–d
Representative interface height – time curves for calcium carbonate in various liquids

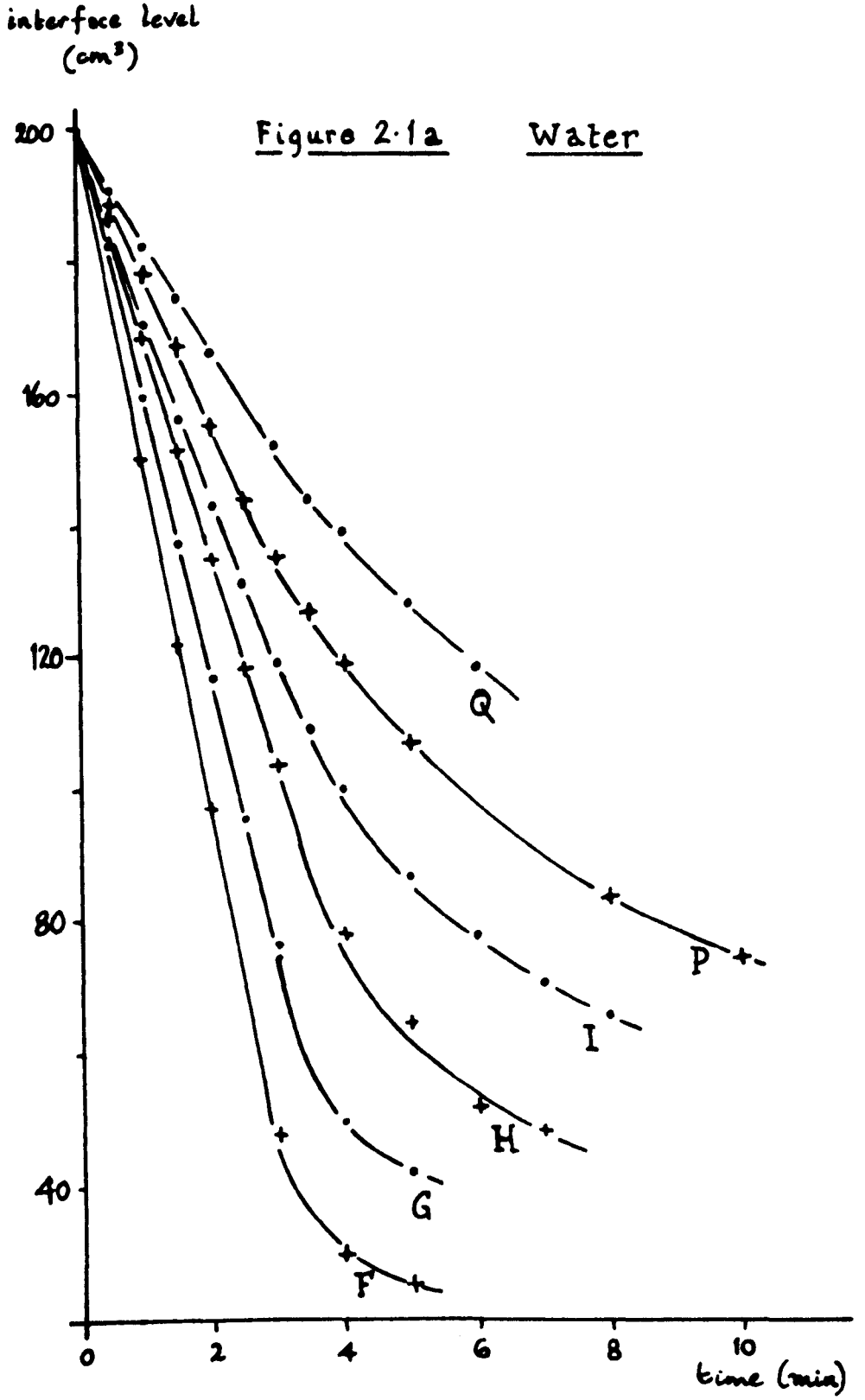

Figure 2·1a Water

Figure 2·1 b 0·137 M sodium chloride

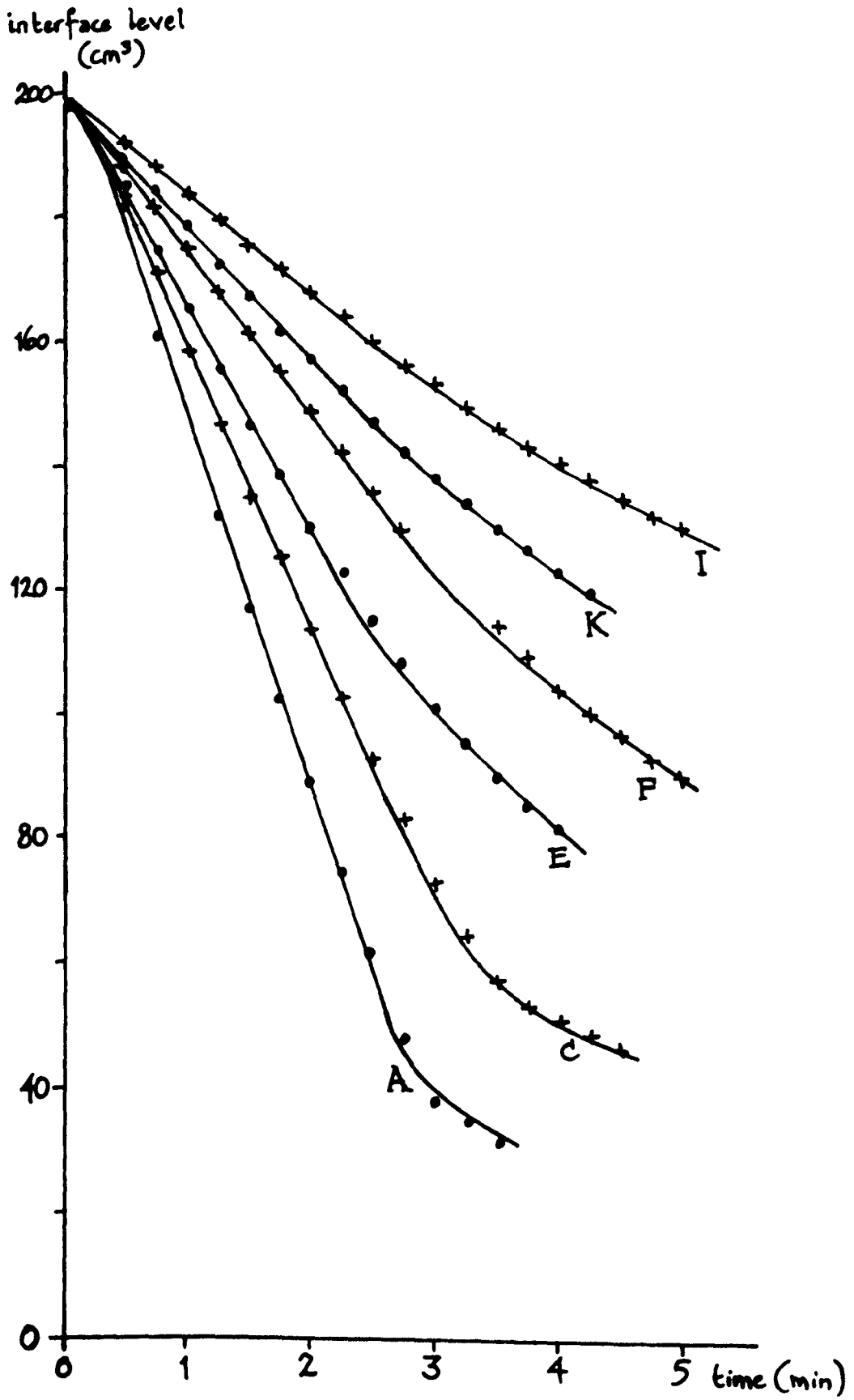

Figure 2·1c Benzene

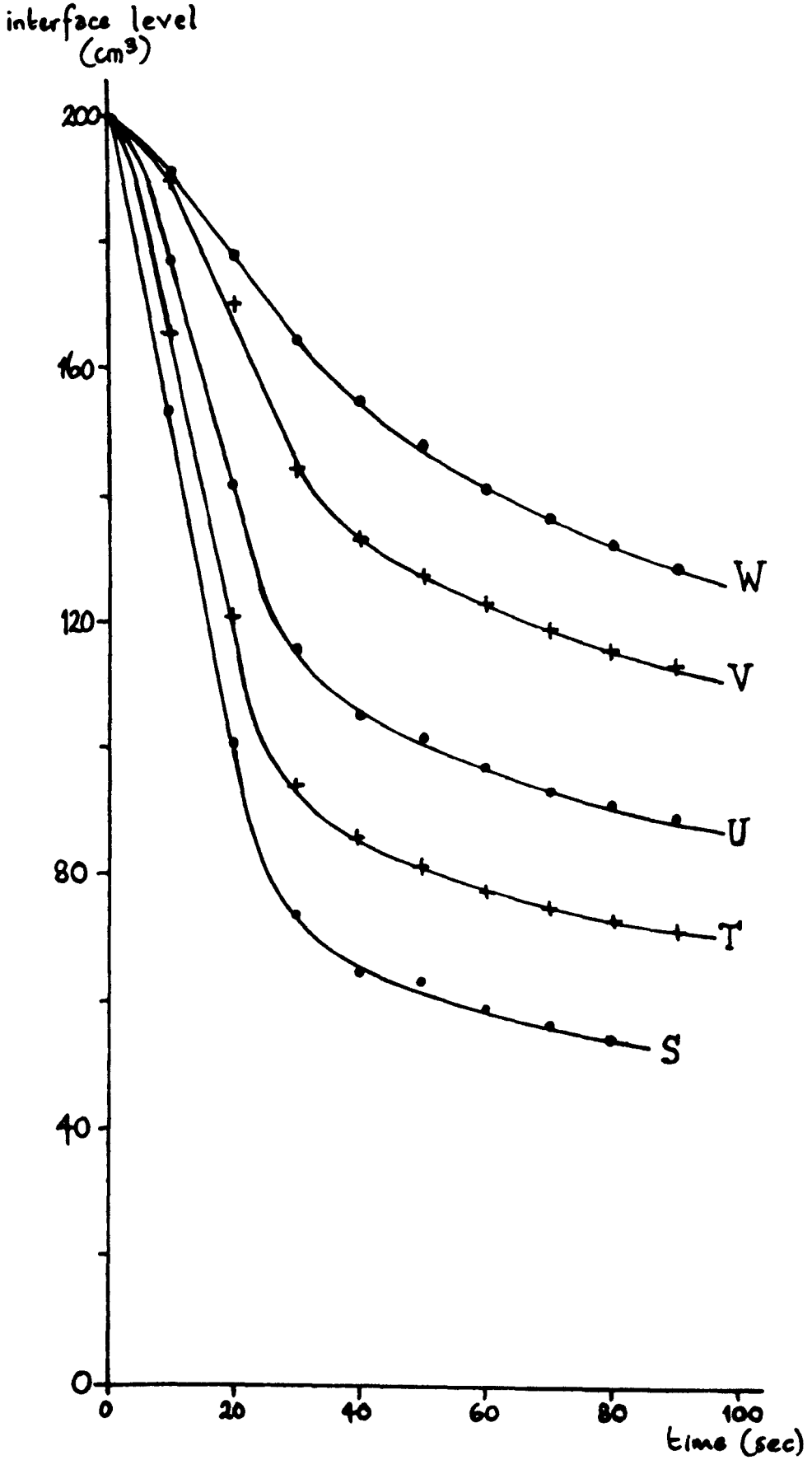

Figure 2·1 d Ethyl acetoacetate

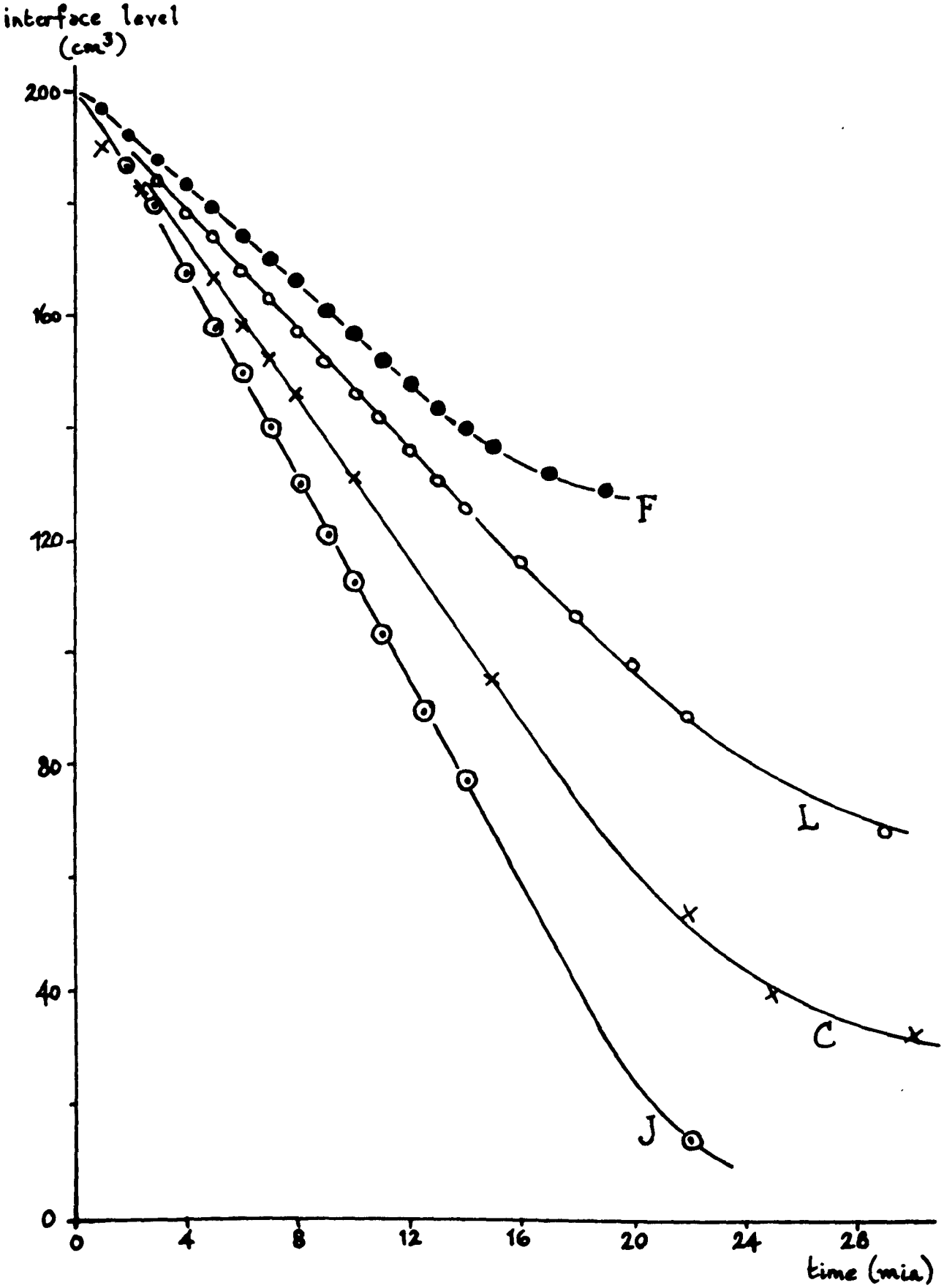

Chapter 3 Discussion

3.1 Treatment of results for calculation of mean equivalent spherical radii

The constant rate Q is often used to calculate the mean particle radius $\bar{r}$ for the uniform or variously-sized particles which all sediment together during hindered settling. This has usually been done by extrapolating hindered settling results to infinite dilution ($\varepsilon = 1$) to yield an estimate of the limiting rate V_s, and then using Stokes' Law. There are several possible methods of calculation, as follows.

(i) Use of the generalised Richardson and Zaki equation

$$Q = V_s \varepsilon^n \qquad (1.53)$$

leads to an estimate of V_s by plotting log Q against log ε (or equivalent least-squares calculation) and extrapolating to log Q = log V_s at log ε = 0. V_s is then substituted in Stokes' equation to yield $\bar{r}$.

(ii) Use of Dollimore and McBride's plot of log Q against weight of solid (W,g) leads to log Q = log V_s at W = 0. V_s is then substituted as under (i).

(iii) Use of Steinour's equation

$$Q = \frac{V_s \cdot \theta(\varepsilon)\ (\varepsilon - W_i)^3}{(1 - W_i)^2(1 - \varepsilon)} \qquad (1.47)$$

allows for the calculation of V_s if $\theta(\varepsilon)$ is known. This method was not used in the present work, for reasons explained in section 1.3.3.

(iv) Use of the modified Steinour empirical equation

$$Q = V_s\ \varepsilon^2 .\ 10^{-A\ (1-\varepsilon)} \qquad (1.51)$$

allows for plotting $\log Q/\varepsilon^2$ against ε, either to $\log Q/\varepsilon^2 = \log V_s$ at $\varepsilon = 1$, or to obtain a value for the slope A, which may then be substituted in the equation

$$\bar{r} = \left\{\frac{9Q\eta\ 10^{A\ (1-\varepsilon)}}{2g\ (\rho_s - \rho_l)\varepsilon^2}\right\}^{0.5} \qquad (3.1)$$

to obtain a value for $\bar{r}$.

This last-named method has an advantage over the others, namely that each value of ε_l and the corresponding value of Q may be used to give an estimate of $\bar{r}$. A set of n determinations thus yields n estimates of $\bar{r}$, and hence a mean of these estimates

(mean $\bar{r}$), together with a standard deviation $SD_{\bar{r}}$ if desired. Any of the methods (i) - (iii) yields only a single estimate of $\bar{r}$ from n determinations (Davies and Dollimore, 1977 b). The calculation using equation 3.1 was therefore commonly used in the study now reported. Values of A were obtained by the method of least squares, and values of log V_s, when required, by calculation using the appropriate values of A, mean ε and mean log Q/ε^2. It should be noted that method (iv) does not require extrapolation to give a value of V_s (a procedure which has been criticised by Dixon (1977)). What the method measures is the effective mean particle radius over the range of porosities examined, without necessarily implying that this radius would be maintained at infinite dilution. Radii calculated from equation 3.1 have been compared with directly-observed values of $\bar{r}$ and V_s in section 3.3.1 below.

A simpler method of calculating A was developed (Davies, Dollimore and McBride, 1977) after the mean radii calculations had been completed in the present study, and was used in specimen re-calculations, as described in section 3.2.5 below.

3.2 Detailed studies of the hindered settling of various practical systems

In addition to using hindered settling data to calculate mean equivalent radii and extrapolated Stokes' limiting velocities, observed rates of settling of the suspension/supernatant

interface have been used in accordance with nine sedimentation equations, to develop a variety of derived data and theoretical postulates. The nine equations were

(i) the generalised Richardson and Zaki equation 1.53,

(ii) the generalised Steinour empirical equation, 1.51,

(iii) the Dollimore and McBride empirical equation

$$Q = V_s . 10^{-bC} \tag{3.2}$$

where $-b$ = slope of the plot of log Q against C,

and C = concentration of solid in uniformly-mixed suspension ($g. cm^{-3}$),

(iv) an equation

$$Q = V_s \exp -\left(\frac{1-\varepsilon}{1-\varepsilon_1}\right) \tag{3.3}$$

which is equivalent to the Dollimore-McBride expression, and in which ε_1 is that initial

porosity which corresponds to maximum sedimentation mass transfer rate,

(v) Michaels and Bolger's equation 1.30,

(vi) Happel's equation 1.21,

& (vii) an equation

$$Q = V_s \exp - \frac{(1-\varepsilon)^a}{1-\varepsilon_1} \tag{3.4}$$

and two related equations

$$Q = V_s \exp - \frac{(1-\varepsilon)^a}{1-\varepsilon^*} \tag{3.5}$$

and

$$Q = V_s \exp - \left(\frac{1-\varepsilon}{1-\varepsilon^*}\right)^a \tag{3.6}$$

which were developed in the course of the present work, and in which a is a variable, with magnitude dependent upon the initial porosity ε and with the value $a = 1$ when $\varepsilon = \varepsilon^*$. It will be shown from experimental data (sections 3.3.2 and 3.5) that the magnitude of a at $\varepsilon < \varepsilon_1$ is notably different from that at $\varepsilon > \varepsilon_1$, and that this difference has fundamental importance. In addition, ε_1 has other significant aspects (sections 3.2.1, 3.2.7 and 3.6), and it will be concluded that ε_1 is indeed an important parameter affecting sedimentation behaviour.

3.2.1 The generalised Richardson-Zaki equation

The linear rate of settling (Q) of the interface will increase with increasing initial liquid volume fraction (ε) of the mixed suspension.

If a system obeys

$$Q = V_s . \varepsilon^n, \tag{1.53}$$

the data will give a linear plot of log Q against log ε, with slope = n, and log Q = log V_s at log ε = 0. Figure 3.1 illustrates this with data from the present study. Additionally, since $(1-\varepsilon)$ decreases to zero as ε increases, a plot of the function Q $(1-\varepsilon)$ against ε will pass through a maximum at some initial porosity ε_1, as shown in figure 3.2 using the same data.

The quantity Q $(1-\varepsilon)\rho_s$, known as solids flux (Kynch, 1952), indicates the mass transfer of solid per unit cross-section per unit time down the sedimentation column. The initial porosity ε_1 would yield maximum solids flux, and the importance of having an expression for ε_1 was recognised. It was derived by Davies, Dollimore and Sharp (1976) as follows.

If the system obeys equation 1.53, then the slope in figure 3.2 may be represented by

$$\frac{d\,(Q\,(1-\varepsilon)\,)}{d\varepsilon} = \frac{d\,(V_s\,\varepsilon^n\,(1-\varepsilon)\,)}{d\varepsilon}$$

$$= -V_s\,\varepsilon^n + n\,V_s\,\varepsilon^{n-1}\,(1-\varepsilon)$$

The maximum value of $Q\,(1-\varepsilon)$ occurs when $d\,(Q\,(1-\varepsilon)\,)/d\varepsilon = 0$. Defining the initial porosity at this point as ε_1 gives

$$V_s\,\varepsilon_1^{\,n} = V_s\,\varepsilon_1^{\,n}.\;n\,\varepsilon_1^{\,-1}\,(1-\varepsilon_1)$$

from which

$$n = \frac{\varepsilon_1}{1-\varepsilon_1} \tag{3.7}$$

and

$$\varepsilon_1 = \frac{n}{n+1} \tag{3.8}$$

The generalised equation may thus be written in the modified form

$$Q = V_s.\boldsymbol{\epsilon}^{\frac{\varepsilon_1}{1-\varepsilon_1}} \tag{3.9}$$

Since ε_1 is the condition of maximum mass sedimentation rate, it is an important parameter in describing the settling rates of suspensions. Table 3.1 gives values of ε_1 for various magnitudes of n.

Figure 3·1

Plot of log (linear settling rate) vs. log (initial porosity) following the theory of Richardson and Zaki

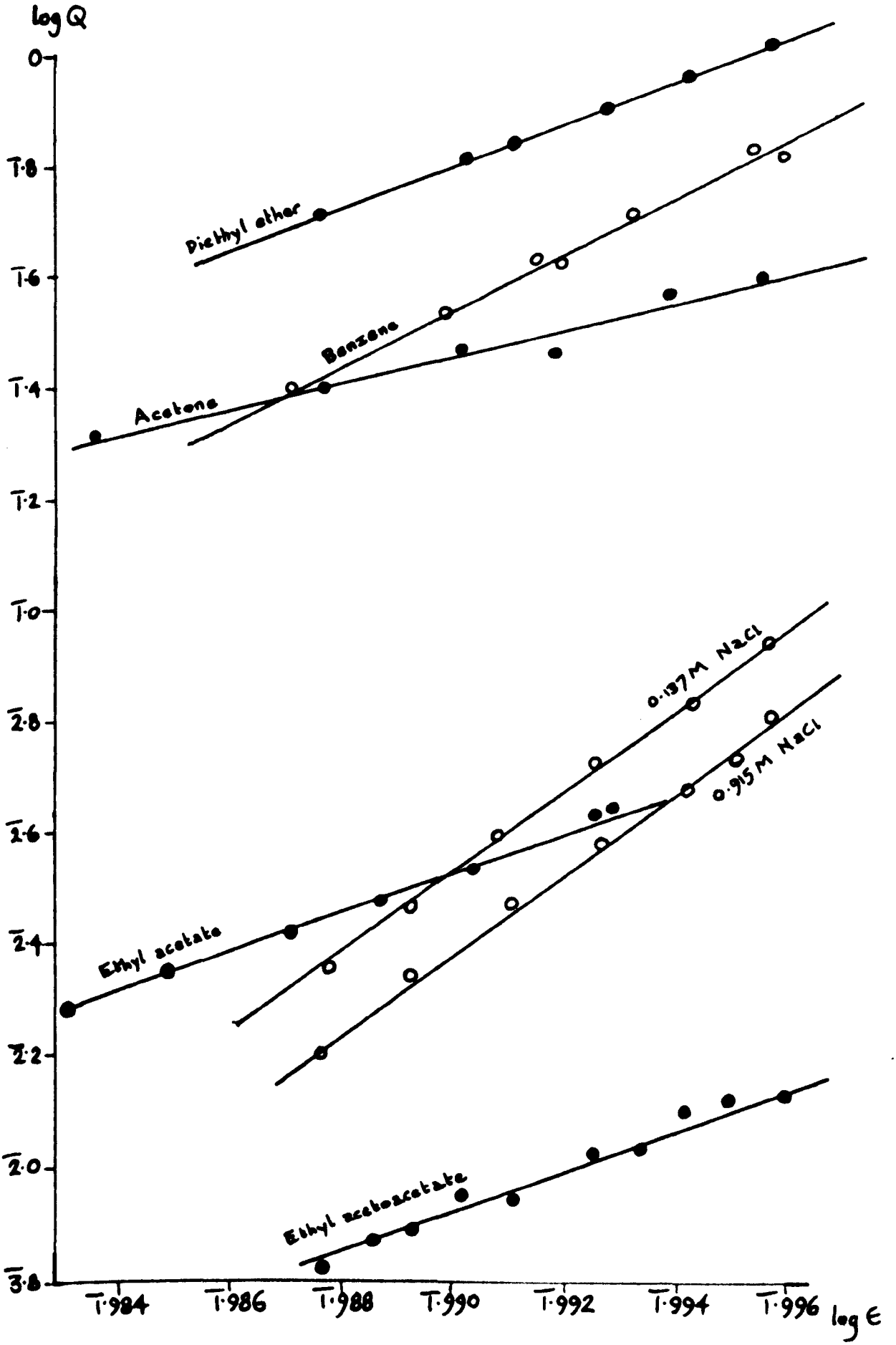

Figure 3·2

Plot of the function $Q(1-\epsilon)$ vs. initial porosity ϵ

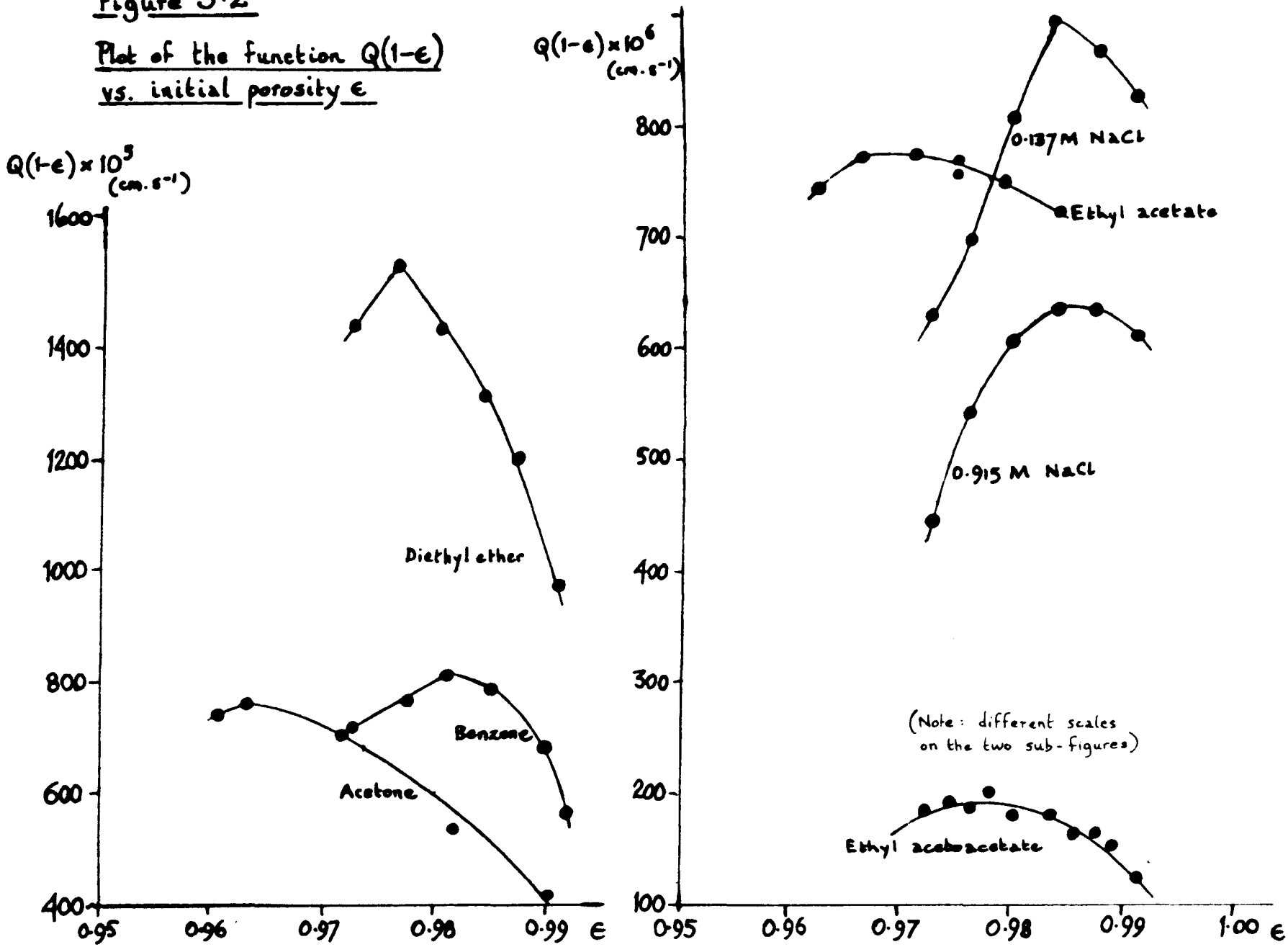

Table 3.1

Initial porosities (ε_1) at which solids flux has maximum value, and corresponding values of the Richardson-Zaki power index n

ε_1	n
0.50	1.00
0.55	1.22
0.60	1.50
0.65	1.86
0.70	2.33
0.75	3.00
0.80	4.00
0.85	5.67
0.90	9.00
0.95	19.00
0.96	24.00
0.97	32.33
0.98	49.00
0.99	99.00

3.2.2 The significance of the modified Richardson and Zaki equation

The fact that experimental data fit equation 3.9, with ε_1 varying from system to system, implies the presence of an intensive factor (related in some way to the chemical nature of the system, and determining ε_1) in addition to the extensive property of suspension porosity ε.

It is to be expected that settling rate will decrease with decrease of ε. If the settling rate of any particular particle were reduced by the presence of other particles because they reduced the flow space by an amount equal to their solid volume (and had no other effect), one would expect $Q = V_s \varepsilon$. The experimental relationship $Q/V_s \propto \varepsilon$ is therefore expected. It is more significant that the influence of porosity is raised to a power which has the form

$$\frac{\varepsilon_1}{1-\varepsilon_1} = \frac{\text{liquid volume fraction}}{\text{solid volume fraction}}$$

If the hindrance to settling were merely an effect of solid concentration, expressible as a multiple power law because any one particle interacts with more than one other, the solid volume fraction would be expected to appear in the numerator, not the denominator, of the power term.

If equation 3.9 is obeyed, then the nearer ε_1 is to unity, the

more rapid is the decrease of interface settling rate Q with initial porosity ε. The higher the value of ε_1, the more the sedimentation may be said to be hindered. The most hindered systems show hindrance at very low concentrations ($\varepsilon \not\ll 1$), which means that the forces causing hindrance must be effective at relatively long range in such systems. If the forces are electrostatic in origin, they must arise from relatively high potentials and the liquid medium must transmit them effectively. Such hindrance is not simply a function of particle concentration; it is also related to the range and intensity of forces acting in the system. Theories which treat Q/V_s entirely in terms of concentration must therefore be incomplete.

Particles of solid in suspension commonly have a residual electrostatic charge (the magnitude of which is related to surface area and surface charge density) and the interactions between such particles may be interpreted in terms of the electrical double layers which exist around them. The simplest expression for the charge interaction is given by the Poisson equation

$$\nabla^2\psi = -\frac{4\pi d_c}{D}$$

where ∇^2 = the Laplace operator $\frac{d^2}{dx^2} + \frac{d^2}{dy^2} + \frac{d^2}{dz^2}$

ψ = electrical potential

d_c = charge density in the double layer

D = liquid dielectric constant

The rate of decrease of ψ with distance from the particle surface is thus inversely related to the liquid dielectric constant, and (other things being equal) the range of effect of the electrostatic charge will be greater in liquids of higher D. Thus electrostatic hindrance is expected at a maximum with charged or polar particles of large surface areas per gramme in polar solvents, and at a minimum with uncharged or non-polar solids of small specific surface in non-polar solvents. (This treatment will apply to non-flocculated solids; the occurrence of flocculation due to ions in solution, to the predominance of van der Waals - London attractive forces over electrostatic repulsions, or to the clustering effect on particles of traces of water in organic media will complicate the situation. Traces of water in organic liquids have also been shown to have marked effects on the sign and magnitude of zeta-potentials, as mentioned earlier. Additionally, some organic liquids give degrees of hindrance (and particle sizes) which are unexpected from their dielectric constants; this aspect is discussed in section 3.5.)

Values of ε_1 (table 3.2) have been calculated from data in the literature (Davies, Dollimore and Sharp, 1976). It is in general agreement with the hypothesis just put forward that high values of n and ε_1 are given by systems such as silica, china clay and metal carbonates in water and aqueous electrolyte solutions, while Steinour's low values for A (equivalent to $n = 5 \rightarrow 6$) were obtained with tapioca in hydrocarbon oil and glass spheres in aqueous medium.

Table 3.2

Values of n and ε_1 from some experimental systems

System	Reference	Range of ε	$n = \varepsilon_1/(1-\varepsilon_1)$	ε_1	$\varepsilon_1^{\varepsilon_1/(1-\varepsilon_1)}$
Glass spheres/dry glycol[1]	A	0.514 - 0.792	2.30	0.6970	0.4361
Glass spheres/dry glycol[2]	A	0.480 - 0.760	3.35	0.7701	0.4172
Glass spheres/dry glycol[3]	A	0.440 - 0.760	3.73	0.7886	0.4122
Tapioca/hydrocarbon oil	B	0.508 - 0.926	5.10	0.8361	0.4015
Ground glass/0.25% $ZnSO_4$	C	0.525 - 0.650	5.55	0.8473	0.3990
Emery/diethyl phthalate	D	0.625 - 0.750	6.75	0.8709	0.3930
Silica gel/dry xylene[4]	E	0.676 - 0.871	9.33	0.9032	0.3868
$CaCO_3$/aqueous	F	0.914 - 0.963	23.33	0.9589	0.3761
Polymer-flocculated kaolinite/H_2O pH 4.9 ± 0.5[5]	G	0.947 - 0.973	45.36	0.9784	0.3724
Polymer-flocculated kaolinite/H_2O pH 4.9 ± 0.5[6]	G	0.947 - 0.973	46.05	0.9787	0.3719
Polymer-flocculated kaolinite/H_2O pH 4.9 ± 0.5[7]	G	0.947 - 0.973	48.33	0.9797	0.3715
Basic Cu carbonate/H_2O	F	0.936 - 0.982	54.16	0.9819	0.3712
PbO + $PbSO_4$/dil. H_2SO_4	H	0.963 - 0.984	80.67	0.9878	0.3703
Pyrogenic SiO_2/H_2O[8a]	I	0.981 - 0.992	287.5	0.9965	0.3679
Kaolinite/aqueous, pH 6[9]	J	0.994 - 0.998	296.0	0.9966	0.3679
Pyrogenic SiO_2/dry n-heptane[8b]	I	0.989 - 0.994	466.7	0.9979	0.3679

Key to references and superscript numbers: see overleaf

Notes to Table 3.2

SUPERSCRIPTS

1 Mean radius (calculated from eqn. (1.51) and Stokes' Law) 172 μm; $\rho_s = 2.88$

2 Mean radius (by microscopy) 106 μm; $\rho_s = 2.50$

3 Mean radius (by microscopy) 184 μm; $\rho_s = 2.50$

4 Data for sample soaked at pH 7; surface area about 600 $m^2\ g^{-1}$

5 Anionic polyacrylamide flocculant

6 Cationic polyacrylamide flocculant

7 Neutral polyacrylamide flocculant

8ab Surface area 390 $m^2\ g^{-1}$

8a Mean radius (calculated from eqn. (1.51) and Stokes' Law) 40.15 μm

8b Mean radius (calculated as for 8a) 35.56 μm

9 Kaolinite flocculated at this pH by particle–particle attractions

REFERENCES

A Goddard and Monecelli, 1973

B Steinour, 1944a

C Steinour, 1944c

D Steinour, 1944b

E Dollimore and Heal, 1962

F Dollimore and McBride, 1968

G Dollimore and Horridge, 1971

H Christian and Dollimore, 1971

I Dollimore and Owens, 1972

J Michaels and Bolger, 1962

It seems possible to suggest that hindrance to settling be interpreted as partly due to particle-liquid interactions (including the concept of liquid bound to or 'stagnant' on the particles). The concept of electrostatic interactions outlined above involved the notion of particle-particle repulsions only, as a cause of hindrance, whereas the modified model would involve particle-liquid attractions also. The former idea implies that electrostatic repulsion prevents or reduces particle-particle cohesion, and thus causes relatively slow settling. The latter notion would ascribe it not only to solvated particle-solvated particle repulsion, but also to particle-liquid cohesion (reducing the effective density of the solid and reducing the free flow space), and possibly also to the setting up of relatively extensive arrays of solid particles and liquid molecules.

The idea of bound or stagnant fluid has been familiar since the work of Kozeny (1932), Fair and Hatch (1933), Eirich and Mark (1937), Carman (1938-9) and Steinour (1944). Eirich and Mark concluded that the effect of a particle having slots or crevices is mainly given by its outermost extremities, so that the liquid filling all the holes or indentations could be regarded as immobilised. Vand (1948) concluded that a touching pair of equal-sized spheres, holding fluid between them but not otherwise solvated, would thereby be increased in effective volume by about 27%. Kusik and Happel (1962), using Happel's sedimentation theory, derived the expression

$$\varepsilon_b = 0.75\ (1-\varepsilon)\ (\varepsilon - 0.2)$$

for spheres, where ε_b is that fraction of the initial porosity which represents the stagnant regions of fluid. Galloway and Sage (1970) and Gauvin and Katta (1973) have calculated values of ε_b for non-spherical particles in turbulent flow, where the stagnant volume was assumed to consist of part of the wakes of the particles. In the hindered settling of particles under laminar flow, these wakes would be replaced by stagnant interconnecting volumes of fluid analogous to the tori which form between touching spheres (Kruyer, 1958). Kruyer stated that the tori form after complete covering of the solid surface by liquid; hence sedimenting particles will be completely covered by stagnant fluid. If the particles are in fact flocs, there will also be stagnant fluid in the spaces within the flocs.

Harris (1977) has reviewed evidence to assess the validity of the immobile liquid model in interpreting deviations from theoretical behaviour in the flow of liquids through porous media. He has concluded that the balance of evidence "supports a position more in favour of limited acceptance of the model, rather than outright rejection." He has also concluded that the volume of immobile liquid is proportional to solid volume, irrespective of porosity. On the other hand, the ratio of this associated liquid volume to the solid volume can apparently vary widely from system to system. For instance, Harris's own data on ground coals gave values ranging from 4% to 16%, while his results for the sedimentation of quartz sand in water gave a value of 23%. Data by Keyes (1946) on pulverised quartz gave 9%,

while sedimentation and viscosity data on irregularly-shaped particles of polymethylmethacrylate in solutions of glycerol and lead nitrate give a value of 26% for particles of mean solid radius 44.5 μ (Ward and Whitmore, 1950). In contrast, McKay (1976 a, b) has carried out hindered settling and rheological studies of dispersions of copper phthalocyanine pigments in hydrocarbons, and has concluded that they behave as essentially porous solids, with associated immobile liquid forming between about 60% and over 97% of the sedimenting flow units, the percentage increasing with increasing flocculation. McKay has pointed out that his findings should not be surprising since aqueous presscakes of the pigments, after industrial filter pressing, contain 79 - 87% water by volume.

These arguments predict that the total stagnant fluid will reduce the free flow space, and thus increase hindrance to settling, by two mechanisms:

(i) a solid-liquid effect, causing the formation of stagnant liquid on or between particles;

and (ii) a solid-solid effect - i.e. the formation of flocs - with consequent occlusion of fluid.

For a given ionic solid, one predicts that mechanism (i) will be more noticeable in liquids of high dielectric constant D, while (ii) should be more important in liquids of relatively low D. Evidence will be presented in section 3.5 that these

two mechanisms of hindrance do exist in the sedimentation of metal carbonates in a variety of liquids. Michaels and Bolger interpreted the sedimentation of kaolinite suspensions in terms of flocculation only, but it seems difficult to omit solid-liquid interactions in view of the occurrence of high hindrance at high liquid volume fractions.

3.2.3 New interpretation of some published data

Numerous systems have been reported upon hitherto, and data corresponding to these are summarised in table 3.2. Values of n were calculated, wherever original data were available, by the method of least squares on log - log data. In a few cases, the slopes of published graphs had to be taken. Values of ε_1 were calculated from equation 3.8.

The data indicate a general increase of n and ε_1 with increase of polar nature of solid surface and of liquid. That is to say, with increase of polar nature of the system, a given increment of solids concentration has an increased effect in reducing settling rate, and hindrance to settling is observed at progressively higher porosities. To summarise, the greater the system polarity, the greater the hindrance.

The fact that ionic solids are flocculated (and thus sedimented) by addition of soluble electrolyte (i.e. by increasing the ionic character of the liquid) does not necessarily contradict this. The flocculation is associated with a reduction in the

solid surface density of charge, and this is the dominant effect. It follows that a reduction of charge on the solid surface is a major effect to seek in endeavouring to secure sedimentation. If this reduction is sufficient for van der Waals attractive forces to overcome electrostatic repulsions, particle-particle cohesion will occur, and (because the effective particles of solid are now greater in mass) gravitational effects will enhance the reduced polar character in promoting sedimentation.

The data in table 3.2 include two examples which appear to be in disagreement with the hypothesis that hindrance to settling varies directly with system polarity. The obvious example is that of pyrogenic silica, which has been reported as more hindered in dry n-heptane than in water. The mean particle radius was reported as smaller in n-heptane, and this too is surprising. Owens (1971) found that there was marked flocculation in both liquids, but extra flocculation would normally have been expected in the non-polar solvent. However, it is known that the variation of ionic concentration in hydrocarbons from zero to only about 10^{-13} M can make a marked difference to the flocculation/dispersion behaviour of suspended solids (van der Minne and Hermanie, 1953), due to variation of the zeta-potentials on the particles, and that traces of water also can have profound effects on the electrical behaviour (McGown and Parfitt, 1966). Such trace contaminants may have been responsible for the unexpected behaviour in n-heptane. An alternative possible cause of the slower settling rate in the

heptane is lack of effective wetting in the organic liquid, with air bubbles trapped in the flocs giving unexpected buoyancy. The other example is the greater hindrance reported for emery powder in diethyl phthalate as compared with ground glass in dilute zinc sulphate solution. In this instance also, it is not possible to reach any conclusion,due to lack of information about the surface properties of the solids, but in any case the difference reported between the systems is small.

The data for polymer-flocculated and pH-flocculated kaolinites are worthy of study, since Michaels and Bolger (1962) concluded that flocculation alone is the cause of hindered settling. The degree and mode of flocculation of kaolin platelets in aqueous suspension is markedly dependent on pH and the presence of neutral electrolytes, and one cannot make detailed comparisons between the kaolinites mentioned in table 3.2 without precise knowledge of the experimental circumstances. However, at pH 6 (Michaels and Bolger) and at pH 4.9 ± 0.5 (Dollimore and Horridge), both samples should have been in the form of open 'card-house' flocs caused by the electrostatic attraction of opposite charges on the faces and edges of the platelets.

One may now note that Dixon (1977) has used Michaels and Bolger's pH 6 data to give an extrapolated limiting velocity corresponding to a mean equivalent particle radius of about 10μ. Similar treatment of Dollimore and Horridge's data for polymer-flocculated kaolinite gives average radii of 58 - 77 μ,

dependent on the nature of the polyacrylamide used.

If the extrapolation is valid (an assumption which is discussed in section 3.3.1 below), the fact that the larger radii are associated with markedly lower values of n is an indication that floc size is not dominant in determining hindrance in kaolinite suspensions. This is in marked contrast to Michaels and Bolger's conclusion.

Polymer flocculants act by adhering to active sites on the particle surfaces, giving polymer bridging between particles (Ruehrwein and Ward, 1952) and also suppression of charge double layer effects (Linke and Booth, 1959; Kitchener, 1972). In so far as the organic polymer covered the ionic kaolinite surfaces, so their affinity for the aqueous medium would be lessened. This effect, reducing hindrance to settling, appears to have been dominant over the increase of floc size by polymer addition, which would increase the hindrance. The conclusion is that there are two factors causing hindrance, namely floc size and system polarity, and that, when both are operative, the latter is the more important.

Relatively-slow sedimentation due to hindrance is related to the topic of the long-term stability of dispersions of particles. For such dispersions in non-aqueous media, Koelmans and Overbeek (1954) and McGown, Parfitt and Willis (1965) showed that dispersion stability in hydrocarbon media can be qualitatively accounted for by the repulsion of

overlapping electrical double layers on neighbouring particles. McGown and Parfitt (1967) showed that such stability, if due solely to an electrical mechanism, may be predicted from a knowledge of particle sizes and surface potentials. McGown and Parfitt were also able to show that electrical repulsion between particles would reach a maximum before steric hindrance due to the adsorption of large molecules on the particle surfaces could be felt. This conclusion - that electrostatic interactions are more important than space-filling effects - is in agreement with that reached in the last paragraph.

The data for silica in table 3.2 indicate that surface areas as measured by nitrogen absorption are not simply related to the degree of hindrance, since the material of greater specific surface showed substantially less hindrance to settling. It may be that the greater part of the measured surface of porous solids is not involved in the interactions which cause hindrance, and that the determining property is the density of charge on that fraction of surface which is fundamentally exposed to other particles and the bulk liquid. This can be expected to be the case if the indentations and cavities of the particles are filled with associated liquid, which acts to reduce the specific surface area and to increase the effective volume fraction of the solid (Harris, 1977).

3.2.4 The generalised Steinour empirical equation

According to Steinour (1944 a), the equation

$$Q = V_s \, \varepsilon^2 . \, 10^{-A(1-\varepsilon)} \qquad (1.51)$$

fitted all his data with A = 1.82. The correction term $10^{-A(1-\varepsilon)}$ was related to his shape factor by the expression

$$\theta(\varepsilon) = \frac{1-\varepsilon}{\varepsilon} \cdot 10^{-A(1-\varepsilon)} \tag{1.52}$$

Let the value of ε at which $\theta(\varepsilon)$ has maximum value be designated ε_2.

Equation 1.52 is in logarithmic form

$$\log \theta(\varepsilon) = \log \frac{1-\varepsilon}{\varepsilon} - A(1-\varepsilon)$$

and so $$\frac{d \log \theta(\varepsilon)}{d\varepsilon} = \frac{d \log (^{1-\varepsilon}/\varepsilon)}{d\varepsilon} - \frac{d (A (1-\varepsilon))}{d\varepsilon}$$

$$= - 0.4343 \frac{\varepsilon^{-2}}{\varepsilon^{-1} - 1} + A$$

$$= \frac{0.4343}{\varepsilon(\varepsilon-1)} + A$$

Therefore, when $\varepsilon = \varepsilon_2$,

$$A = \frac{0.4343}{\varepsilon_2(1-\varepsilon_2)} \tag{3.10}$$

It follows from equations 1.52 and 3.10 that the shape factor may be expressed as

$$\theta(\varepsilon) = \frac{1-\varepsilon}{\varepsilon} \cdot 10^{-0.4343\ (1-\varepsilon)/\varepsilon_2\ (1-\varepsilon_2)} \qquad (3.11)$$

and $\theta(\varepsilon)$ at ε_2 is given by

$$\theta(\varepsilon)_{max} = \frac{1-\varepsilon_2}{\varepsilon_2} \cdot 10^{-0.4343/\varepsilon_2} = \frac{1-\varepsilon_2}{\varepsilon_2} \cdot \exp^{-(\frac{1}{\varepsilon_2})} \qquad (3.12)$$

Thus, from equation 3.11, the magnitude of $\theta(\varepsilon)$ at any value of ε depends on whatever factors determine ε_2. It is misleading to call it a 'shape factor', unless for some reason deviation of particle shape from the spherical is the dominant variable affecting ε_2. As mentioned in section 1.3.2, experimental results indicate that such deviation is not an important factor in varying sedimentation behaviour. It is concluded that it is misleading to call correction terms in sedimentation equations 'shape factors'.

3.2.5 The Dollimore-McBride empirical equation

Dollimore and McBride (1968) showed that a plot of log Q against C (the concentration of solid in the uniformly-mixed suspension, $g.cm^{-3}$) may be sensibly linear. An example using data from the present study is shown in figure 3.3.

If there is linearity, then

$$\log Q = a - bC$$

Figure 3.3 Plot of log(sedimentation rate) against concentration for calcium carbonate in 0.915 M sodium chloride solution

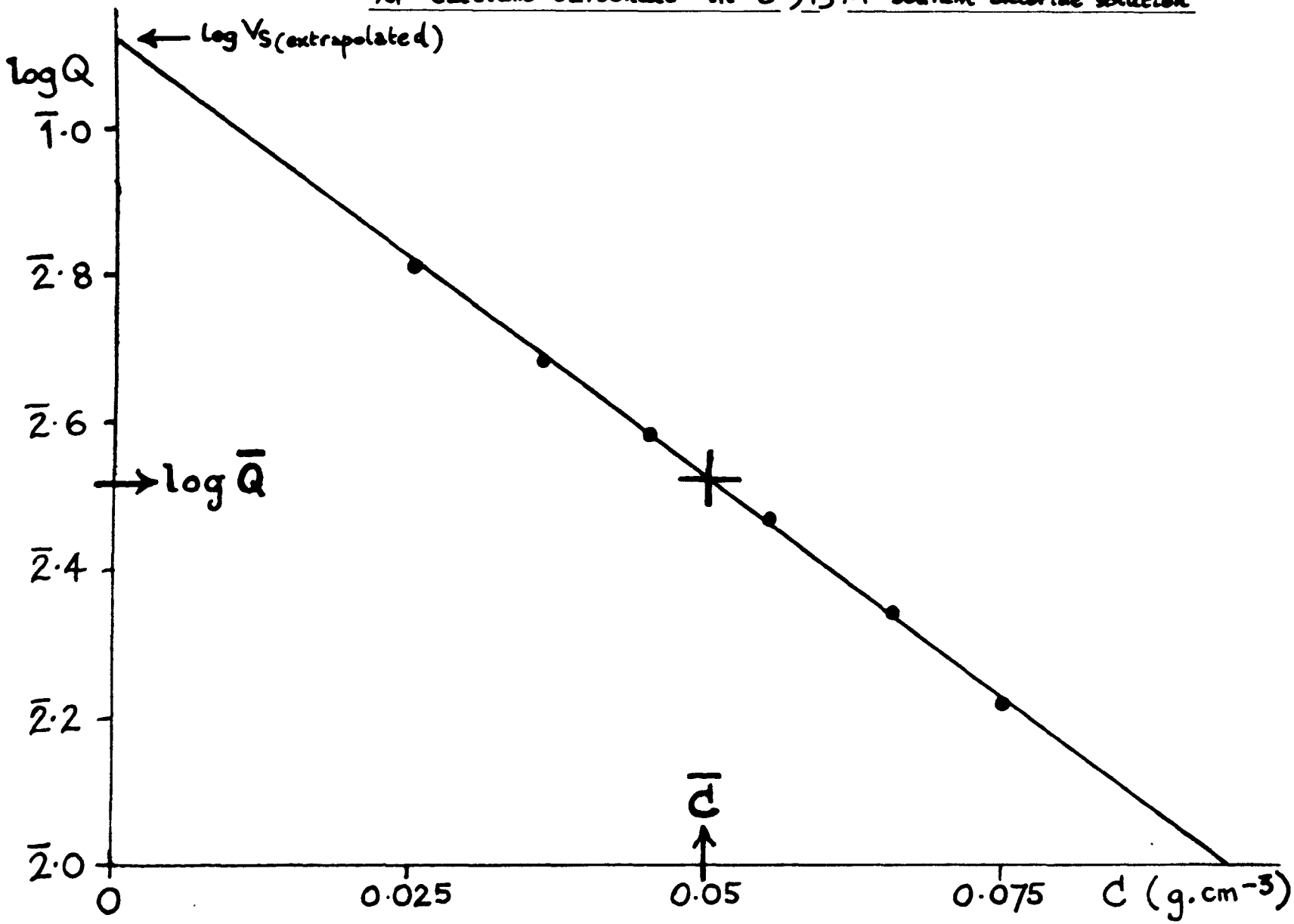

so that $Q = 10^{a} . 10^{-bC}$

Now, at infinite dilution, $a = \log Q$ and $Q = V_s$; whence

$$10^{a} = 10^{\log V_s} = V_s$$

and therefore

$$Q = V_s . 10^{-bC} \qquad (3.12)$$

Now, the initial porosity ε of a suspension is given by

$$\varepsilon = \frac{V_{sn} - V_{sd}}{V_{sn}}$$

where V_{sn} = volume of suspension

V_{sd} = volume of solid

But $V_{sd} = \frac{\text{mass of solid}}{\text{density of solid}} = \frac{m_s}{\rho_s}$

$$\text{whence } \varepsilon = \frac{V_{sn} - m_s/\rho_s}{V_{sn}} = 1 - \frac{m_s}{\rho_s V_{sn}}$$

However, since $\frac{m_s}{V_{sn}} = C$, it follows that

$$\varepsilon = 1 - \frac{C}{\rho_s}, \quad \text{or } C = \rho_s (1-\varepsilon) \qquad (3.13)$$

and one may write

$$Q = V_s \cdot 10^{-b\rho_s (1-\varepsilon)} \qquad (3.14)$$

This is somewhat similar in form to Steinour's empirical equation

$$Q = V_s \varepsilon^2 \cdot 10^{-A (1-\varepsilon)} \qquad (1.51)$$

Thus, for a highly-hindered system, in which hindered settling occurs when ε is very close to unity, and no linear settling rate occurs at much below that value, comparison of equations 3.14 and 1.51 gives

$$A \simeq b \rho_s \qquad (3.15)$$

The precise relationship between A and b was derived (Davies, Dollimore and McBride, 1977) as follows.

From equations 3.14 and 1.51 in logarithmic form,

$$\log V_s - b \rho_s (1-\varepsilon) = \log V_s + 2 \log \varepsilon - A (1-\varepsilon)$$

whence $b \rho_s (1-\varepsilon) = A (1-\varepsilon) - 2 \log \varepsilon$

and therefore $A = b \rho_s + \frac{2 \log \varepsilon}{1-\varepsilon}$. (3.16)

At infinite dilution, $\log \varepsilon = 0$, and $A = b \rho_s$.

Comparative values of A, derived from equations 1.51, 3.15 and 3.16 are given in table 3.3, columns 2, 3 and 4 respectively. The values, all obtained by least squares method from experimental data, show that in general the more-precise equation 3.16 gives better agreement with those from equation 1.51, as would be expected. However, the simpler equation 3.15 does not give bad estimates for the systems studied. Figure 3.4 shows values for the correction term 2 log $\varepsilon/1-\varepsilon$, from which it is seen that in the region $0.97 \lesssim \varepsilon \lesssim 0.995$, the value of A may be taken as $b\ \rho_s - 0.88$.

Steinour's method of calculating A was to plot log Q/ε^2 against ε. It is considerably simpler to use the plot of log Q against C, obtain the negative of the slope, and multiply by ρ_s. In addition, for highly-hindered systems, Steinour's method requires frequent use of logarithms of values close to unity, where (unless an electronic calculator is used) rounding-up errors are not small compared with the difference between successive values. The method just outlined avoids this. It is recommended, provided that the semi-log plot used is acceptably linear.

McBride (1974) used the present writer's differential $d(Q\ (1-\varepsilon)\ )/d\varepsilon$, but based on equation 3.14, to show that

$$\varepsilon_1 = 1 - \frac{1}{2.303\ b\ \rho_s}\ , \qquad (3.17)$$

where ε_1 is again the initial porosity for maximum solids flux.

Table 3.3

Comparative values of A, calculated by Steinour's theory (equation 1.51) and by equations 3.15 and 3.16

System	Porosity range	A			$\frac{A(eqn.\ 3.15)}{A(eqn.\ 1.51)}$	$\frac{A(eqn.\ 3.16)}{A(eqn.\ 1.51)}$
		Eqn. 1.51	Eqn. 3.15	Eqn. 3.16		
$CaCO_3/H_2O$	0.9726 - 0.9907	26.40	27.38	26.50	1.037	1.004
$CaCO_3$/ethyl acetoacetate	0.9722 - 0.9910	16.40	17.31	16.43	1.055	1.002
$CaCO_3$/0.915M NaCl	0.9723 - 0.9907	31.80	32.11	31.23	1.010	0.982
$CaCO_3$/ethyl acetate	0.9631 - 0.9851	23.0	23.39	22.51	1.017	0.979
Basic $CuCO_3/H_2O$	0.9272 - 0.9818	17.19	18.16	17.27	1.056	1.005
Basic $NiCO_3/H_2O$	0.9307 - 0.9743	15.99	16.98	16.09	1.062	1.006

Figure 3·4

Variation of the correction term $\left(\frac{2\log\epsilon}{1-\epsilon}\right)$ with initial porosity ϵ

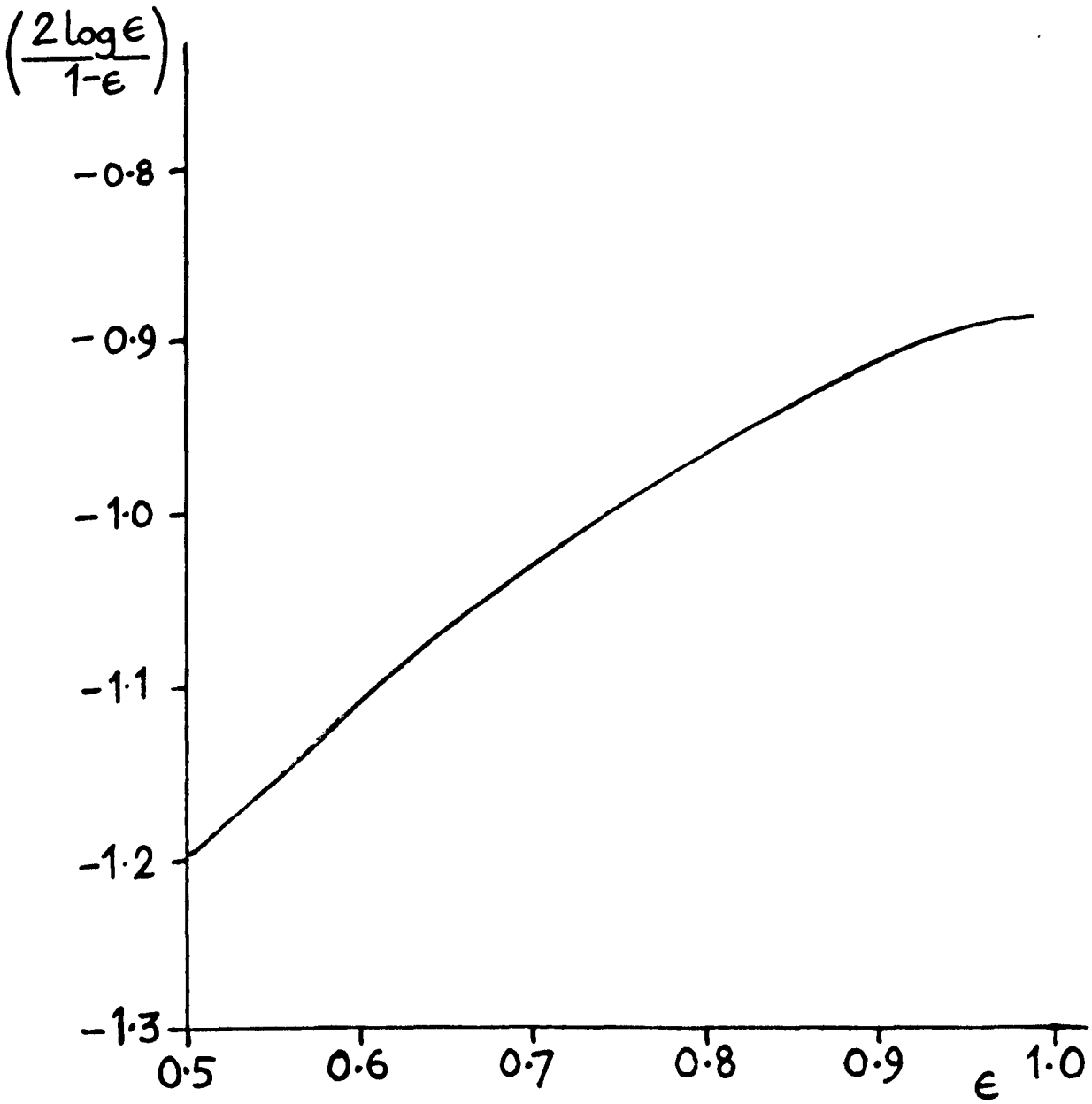

Values of ε_1 obtained from equation 3.17 are shown in table 3.4, column 3, allowing comparison with those from the earlier method (equation 3.8). In addition, for any system which obeys equations 3.7 and 3.17, we may write

$$n = \frac{\varepsilon_1}{1-\varepsilon_1} = \frac{1 - \frac{1}{2.303\ b\ \rho_s}}{\frac{1}{2.303\ b\ \rho_s}}$$

$$= (2.303\ b\ \rho_s) - 1 \qquad (3.18)$$

and values of n calculated from the slope -b are shown in column 4. They may be compared with the values of n obtained by the Richardson and Zaki method (column 5). It is seen that the simple Dollimore-McBride plot yields results in close agreement with those by the Richardson and Zaki method, over the range of porosities examined. Once again, the use of logarithms of values close to unity are not required by the former method (Davies, Dollimore and McBride, 1977).

Dixon, Buchanan and Souter (1977) have criticised the use of the Dollimore-McBride plot, claiming that data for 1 mm ballotini in bromoform in the range $0.63 < \varepsilon < 0.89$ (Richardson and Zaki, 1954 b, run 1) are 'much better' fitted by the Richardson-Zaki equation (1.53) than by equation 3.1. It is true that calculation of mean equivalent radius by the two methods would lead to a difference between the results of 6.7%,

Table 3.4

Comparative values of ε_1 and n, calculated by log Q - C plot (equations 3.17 and 3.18) and by log Q - log ε plot (equations 3.8 and 1.53)

System	ε_1 (eqn. 3.8)	ε_1 (eqn. 3.17)	n (eqn. 3.18)	n (eqn. 1.53)
$CaCO_3/H_2O$	0.9842	0.9841	61.9	62.2
$CaCO_3$/ethyl acetoacetate	0.9749	0.9753	38.9	39.5
$CaCO_3$/0.915M NaCl	0.9867	0.9865	73.0	74.2
$CaCO_3$/ethyl acetate	0.9817	0.9814	52.9	53.7
Basic $CuCO_3/H_2O$	0.9755	0.9761	40.8	39.7
Basic $NiCO_3/H_2O$	0.9738	0.9744	38.1	37.2
	Calculated by method of Davies, Dollimore and Sharp (1976)	Calculated by methods proposed in this section		Calculated by method of Richardson and Zaki (1954)

for the ballotini, but neither method yields a valid estimate of the radius in this case, giving radii about 40% lower than the true value. This is because the data were obtained in turbulent flow conditions (Re = 38.3), and extrapolation to infinite dilution is not valid if the interface settling rates have been obtained under turbulent conditions. The agreement between extrapolated and calculated limiting velocities is much better when there is laminar flow - i.e. Re < 0.2 (Richardson and Zaki's table 1). In the systems listed in table 3.4, the flow was laminar (Re 0.0024 - 0.093) and the Richardson-Zaki and Dollimore-McBride methods of calculating mean radius would give an average difference of result of only about 1%. This is closely similar to the difference between Richardson and Zaki's extrapolated values and those calculated by Stokes' Law. It was also shown that, even for the ballotini, the two methods yield estimates of ε_1 which differ by only about 0.9% and that the data do not allow a decision as to which is better. For the data of table 3.4, the difference between the estimates of ε_1 is in no case greater than 0.06%. It is concluded that the Dollimore-McBride method is a perfectly acceptable substitute for the Richardson-Zaki procedure, if Re < 0.2 and the semi-log plot used is acceptably linear (Davies and Dollimore, 1977 c). It is also simpler, and - as explained below - has certain additional applications.

The Dollimore-McBride plot may be used simply to calculate the weight-to-volume solids concentration (in uniformly-mixed suspension) for maximum solids flux. Re-arranging equation 3.17

and substituting for ρ_s from equation 3.13 gives

$$2.303\ bC\ (1-\varepsilon_1) = 1-\varepsilon$$

Now, when $\varepsilon = \varepsilon_1$, $C = C_{\varepsilon_1}$, and then

$$C_{\varepsilon_1} = \frac{1}{2.303\ b} \qquad (3.19)$$

The solids concentration C_{ε_1} ($g.cm^{-3}$) for maximum solids flux may therefore be estimated simply by plotting log Q against C, obtaining the slope -b, and using equation 3.19.

3.2.6 The significance of ε_1, the initial porosity for maximum solids flux

The parameter ε_1 has advantage over Richardson and Zaki's n from which it is derived (and similarly ε_2 has advantage over Steinour's A). Although all are dimensionless, ε_1 and ε_2 have the advantage of being volume fractions, which have simple physical meaning. In addition, ε_1 and ε_2 have upper bounds of unity, whereas n and A diverge rapidly to indefinitely large values. Thus, for instance, describing a system as having $\varepsilon_2 = 0.90$ is immediately meaningful, whereas A = 4.83 is not. ε_1 is preferred over ε_2 for purposes of further discussion, since the former is related to the product Q $(1-\varepsilon)$ of directly observable quantities, whereas ε_2 is a function of $\theta(\varepsilon)$, a

quantity which cannot be directly observed or interpreted with certainty. Additionally, the practical relevance of $Q\ (1-\varepsilon)\rho_s$ has been mentioned earlier; the parameters which determine ε_1 are by definition those which fix the initial porosity at which solids transport is maximum for a given suspension.

Equation 3.2 may be re-written as

$$Q = V_s . \exp^{-2.303\ bC}$$

but $C_{\varepsilon_1} = 1/2.303\ b$, so that

$$Q = \exp^{-C/C_{\varepsilon_1}}$$

and, from equation 3.13, $C = \rho_s\ (1-\varepsilon)$ and $C_{\varepsilon_1} = \rho_s\ (1-\varepsilon_1)$,

so that

$$Q = V_s \exp^{-\left(\frac{1-\varepsilon}{1-\varepsilon_1}\right)} \qquad (3.20)$$

This modified Dollimore-McBride equation, and the modified Richardson-Zaki equation

$$Q = V_s\ \varepsilon^{\varepsilon_1/1-\varepsilon_1} \qquad (3.9)$$

both show that the larger ε_1 is, the smaller Q/V_s is for given ε. That is to say, ε_1 is a direct measure of the hindrance to settling which reduces Q below V_s. ε_1 is also the initial

porosity for maximum sedimentation mass transfer.

Additionally, Davies and Dollimore (1977 a) have derived a relationship between the solid density ρ_s, and the viscosities of the suspension and pure liquid (η_s and η_l, respectively), commencing with the equation

$$\epsilon_l = 1 - \frac{1}{2.303\ b\ \rho_s} \qquad (3.17)$$

This equation indicates that hindrance to settling will, for given slope b, be more likely for relatively-dense solids. Particles of such solids will have relatively large gravitational attraction, and will therefore be more likely to move directly downwards, against the disturbance of thermal motions, than will similarly sized particles of lower density. The fact that denser particles are more likely to show hindered settling suggests that hindrance is associated with systems which tend to show smooth sedimentation, and corresponding smooth vertical upflow of fluid. This is in qualitative agreement with the evidence of streamline flow discussed in sections 1.2 and 1.3.2. Now, it is to be expected that such relatively non-turbulent movement will be more likely in more-viscous systems. The influence of the viscosities of the sedimenting suspension and of the bulk free liquid was therefore considered.

Einstein (1906, 1911, 1920) proposed a relationship which may be written as

$$\eta_s = \eta_l \ (1 + 2.5 \ (1-\epsilon) \ ) \qquad (3.21)$$

where η_s = suspension viscosity

η_l = liquid viscosity,

for a suspension of many small rigid spherical particles at a concentration low enough to avoid interaction between particles under laminar flow conditions. Kermack et al (1928) and Happel (1958) suggested that the effective viscosity experienced by any particle in the slurry is intermediate between η_s and η_l. It is difficult to know how to measure this effective viscosity, and if Gaudin et al (1958, 1959, 1960) are correct in saying that the sedimenting plug has the same viscosity as the uniformly-mixed suspension, the effective viscosity will not differ from η_s. This assumption was made in the present study.

Equations 3.21 and 3.13 lead to

$$\eta_s = \eta_l \ (1 + 2.5 \ \frac{C}{\rho_s} \ ) \qquad (3.22)$$

where C = concentration of solid, density ρ_s, in uniformly-mixed suspension.

Einstein's assumptions mean that the equation will not apply well in perhaps many experimental systems. Guth, Gold and Simha (1936) suggested the relationship

$$\eta_s = \eta_1 \left(1 + 2.5\ (1-\varepsilon) + 14.1\ (1-\varepsilon)^2 + \ldots\right) \qquad (3.23)$$

for moderate concentrations of rigid spheres, and Hatschek (1928) suggested an expression equivalent to

$$\eta_s = \eta_1 \left[1 + \frac{(\ (1-\varepsilon)\ K)^{0.33^\cdot}}{1 - (\ (1-\varepsilon)\ K)^{0.33^\cdot}} \right] \qquad (3.24)$$

for very concentrated suspensions; K was termed a 'voluminosity factor'. Ward (1955) reviewed many investigations, and concluded that the data of seven sets of workers, using spheres, could be represented by

$$\eta_s = \eta_1\ (1 + k\ (1-\varepsilon) + k^2\ (1-\varepsilon)^2 + k^3\ (1-\varepsilon)^3 + \ldots) \qquad (3.25)$$

with $k = 2.34 - 2.77$ (mean = 2.49).

Such an expression may be simplified to

$$\eta_s = \eta_1\ (1 + f\ (1-\varepsilon)\ ) = \eta_1\ (1 + f\ \frac{C}{\rho_s}\ ) \qquad (3.26)$$

where f is related to k but is porosity-dependent. For instance (for $k = 2.5$), $f = 2.63$ at $\varepsilon = 0.98$, $f = 4.38$ at $\varepsilon = 0.80$. Davies and Dollimore therefore assumed the validity of equation 3.26, where the function f relates the suspension viscosity ρ_s to the concentration C of a solid, density ρ_s,

in a liquid of viscosity ρ_l, the whole making up the sedimenting plug.

Equation 3.26 indicates that, for given concentration dependence fC, a more dense solid will have less effect in increasing η_s above η_l than a less dense one will. (This is in agreement with the results of Oliver (1954), who found k = 2.06 for $\rho_s - \rho_l = 1.82$ and k = 2.45 for $\rho_s - \rho_l = 0$.) This, taken with the conclusion from equation 3.17 that hindered settling is more likely with denser solids, leads to the view that more-hindered solids (in a given liquid) are those for which $\eta_s - \eta_l$ is relatively small. Mathematically, we may substitute for ρ_s from equation 3.17 into equation 3.26 to give

$$\eta_s = \eta_l \ (1 + 2.303 \ b \ (1-\varepsilon_l) \ fC) \tag{3.27}$$

which re-arranges to

$$\varepsilon_l = 1 - \left[\frac{\Delta\eta}{\eta_l} \quad \frac{1}{2.303 \ b \ fC} \right] \tag{3.28}$$

where $\Delta\eta = \eta_s - \eta_l$, the enhancement of suspension viscosity over liquid viscosity.

Thus, for given b and fC, high values of ε_l will be associated with high values for η_l and/or relatively small values for the

viscosity enhancement $\Delta\eta$. The role of viscosity in affecting hindered settling now seems clear. Firstly, hindrance to settling is more likely in relatively viscous liquids. Secondly, hindered settling is not caused by enhancement of suspension viscosity by solid particles. The converse is true: the most hindered systems are those for which the suspension viscosity is relatively closest to the liquid viscosity. This last point suggests that the slip surface on the particle, as it sediments through free liquid, will be most like that liquid in most-hindered systems. This in turn suggests a relatively large amount of liquid associated with the particle, with the outermost layer of such liquid under relatively little influence from the solid surface. It seems clear that hindrance to settling involves solid-liquid interactions, as has been suggested previously.

ε_1 is also important in considering the influence of shear on suspension viscosities. For ideal suspensions, viscosity will be linearly dependent on concentration, as in equation 3.21, and independent of shear rate. For non-ideal systems, however, neither will hold, and ε_1 should be considered. Since ε_1 is the initial porosity for maximum sedimentation mass transfer rate, it must also correspond to maximum supernatant upward mass transfer rate. It follows that at ε_1 there is maximum shear at the particle/fluid interface. If a series of suspensions is examined, each at its own ε_1, they can be said to be in corresponding states, and direct comparisons are possible. At ε_1, a dilatant suspension will show maximum shear-enhancement of

viscosity, and a thixotropic suspension will show a corresponding maximum reduction of viscosity, due to the same shear forces.

3.2.7 The significance of the quantity Q (1-ε)

It has been shown in section 3.2.1 that the plot of Q (1-ε) against ε must go through a maximum at some porosity ε_1. It follows that a sedimentation equation should be able to represent this maximum. Such an equation should also be able to reflect the experimental fact that ε_1 varies from one suspension to another (table 3.2). The dependence of Q (1-ε)/V_s upon ε has been calculated for each of the equations 1.11 - 1.21 inclusive (section 1.3.1), together with the equations for the two theoretical models of Richardson and Zaki (1954 a), and the results are shown in figure 3.5. For comparison, a variety of experimental data are presented in figures 3.6 and 3.7.

The ballotini used to produce the data summarised in figure 3.6 closely resemble the individual spherical particles for which most equations have been derived (theoretically or empirically). They produce a maximum on the plot of Q (1-ε) against ε at $\varepsilon_1 \simeq 0.80$, and as far as can be ascertained this porosity value is independent of particle diameter over the range of sizes studied. Any general equation for the sedimentation of spherical particles should therefore yield a maximum in figure 3.5 at $\varepsilon \simeq 0.80$.

It is immediately apparent from figure 3.5 that the equations

Figure 3.5

Variation of the function $Q(1-\epsilon)/V_s$ with initial porosity ϵ (from the literature)

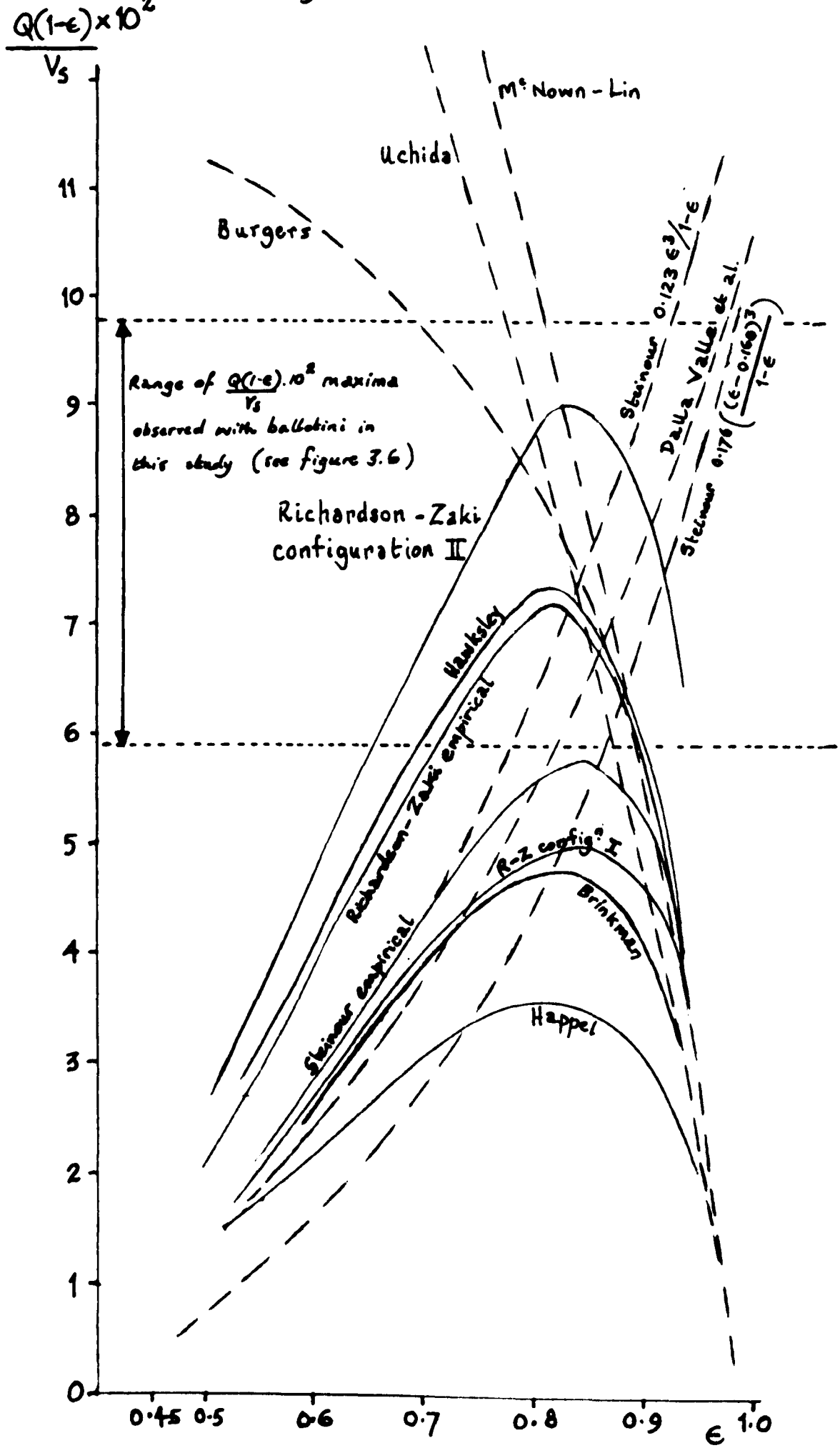

Figure 3·6

Variation of the function $Q(1-\epsilon)/V_s$ with initial porosity ϵ for glass ballotini in aqueous glycerol

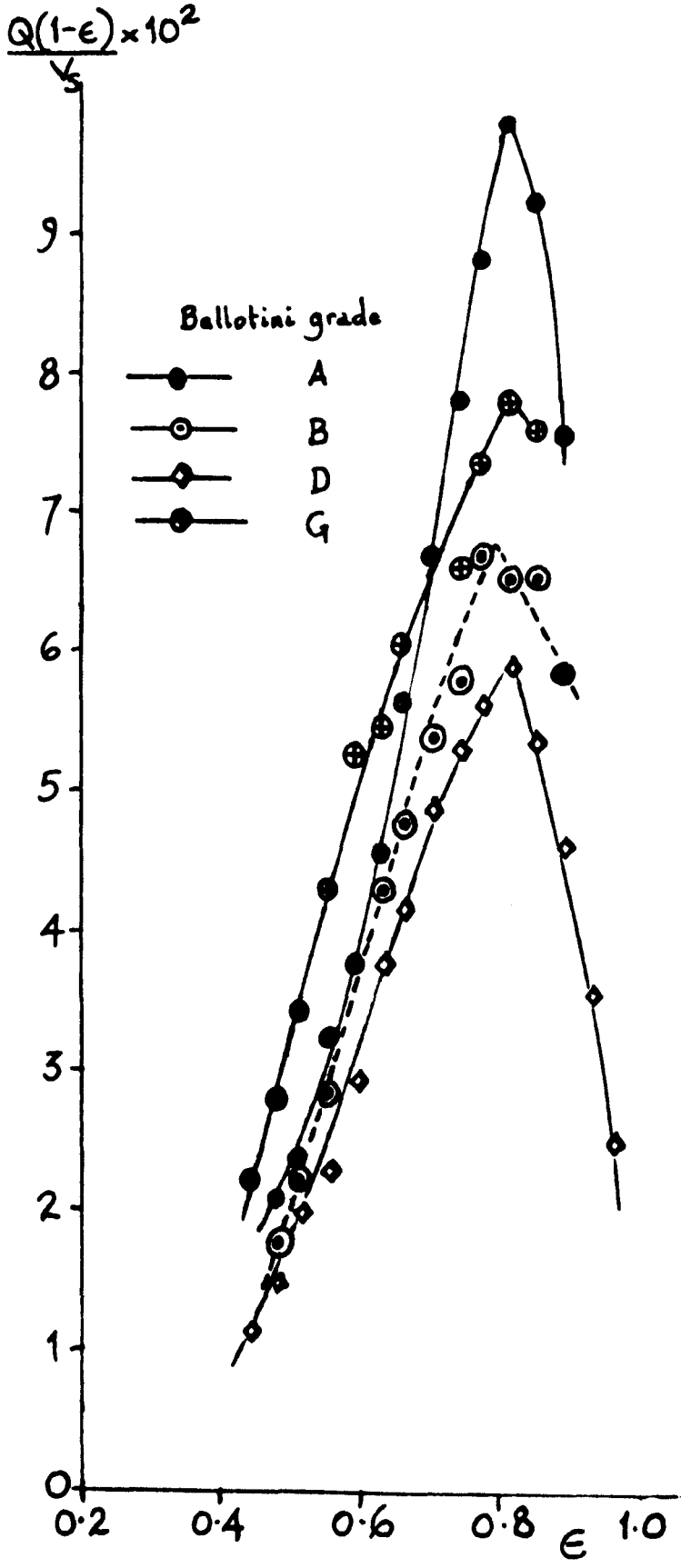

Figure 3·7

Variation of the function $Q(1-\epsilon)/V_s$ with initial porosity ϵ for calcium carbonate in various liquids

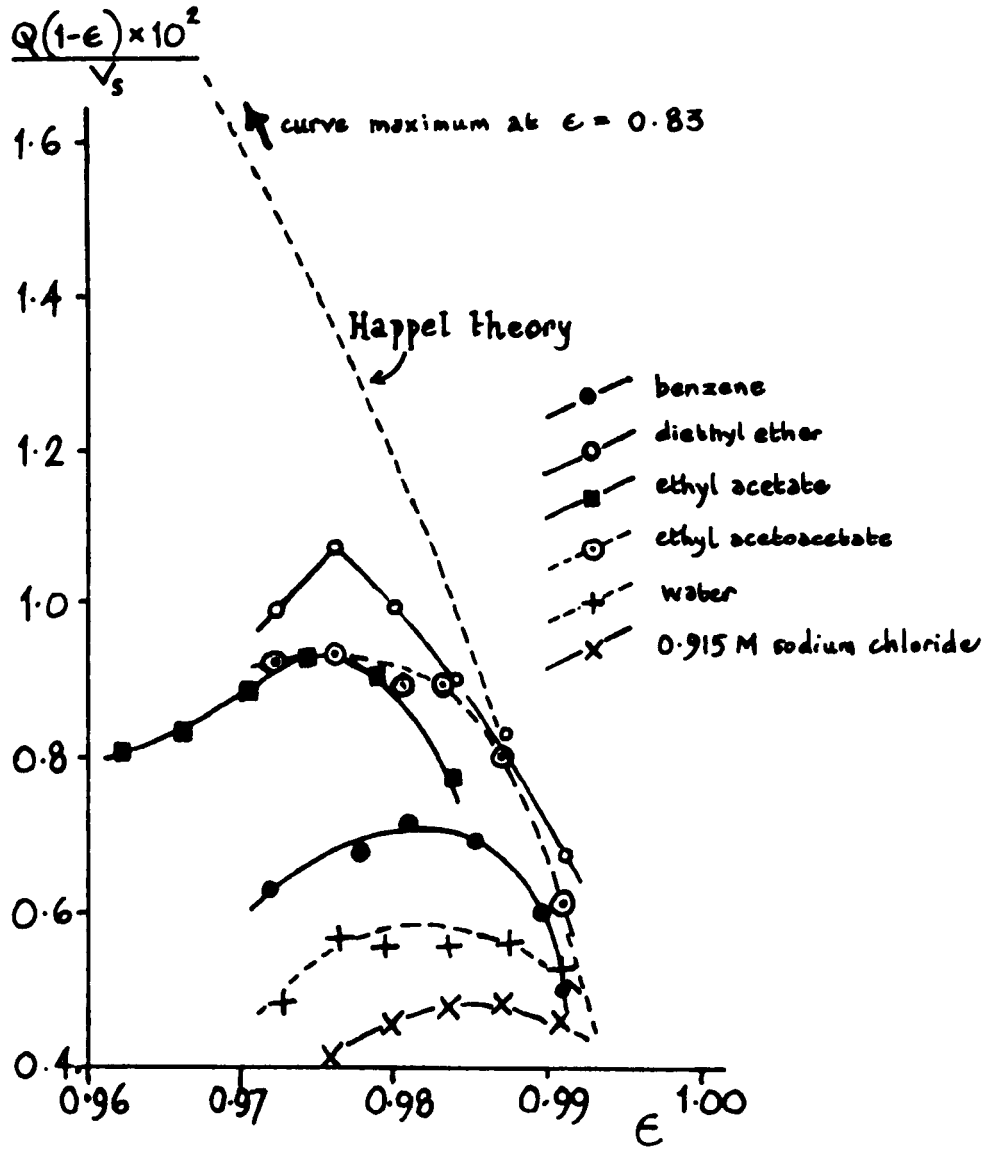

of Burgers, Uchida, McNown and Lin, Steinour (equations 1.13 and 1.14) and Dalla Valle et al fail to meet this criterion. Since experimentally every suspension must show a maximum of $Q(1-\varepsilon)$ at some porosity ε_1, these equations were excluded from further consideration in this study. Powers' equation 1.10 has been discarded in the same way. (It was also concluded in section 1.3.1 that the two Steinour equations, and those of Powers and Dalla Valle et al, should not be used for the calculation of Stokes' limiting velocity, for what is in fact the same reason). The Kozeny-Carman equation 1.27 also has been omitted, as it is of the form of Dalla Valle's expression, although it could be retained if its parameter k is allowed to assume increasing values as $\varepsilon \to 1$ above ε_1. In particular, it is clear that correction terms including the expression $\varepsilon^3/1-\varepsilon$ should be used with care. The expression has been familiar since the work of Kozeny (1927) and Fair and Hatch (1933), but it may lead to failure to produce a maximum on the $Q(1-\varepsilon)$ plot.

The remaining expressions include two empirical equations (Steinour's equation 1.12, and Richardson and Zaki's equation 1.19), two theoretical equations based on models of random assemblages of spheres (Brinkman's equation 1.15 and Happel's equation 1.21) and three theoretical equations based on models of geometrically regular arrays of spheres (Hawksley's equation 1.17, and the two model equations of Richardson and Zaki (1954 a), which are not reproduced here). In the last-named theories, the particles were assumed to be spaced in an expanded form of

hexagonal close-packing in the horizontal plane, and settling in such a way as to be lined up vertically above each other. Figure 3.5 shows that Richardson and Zaki's data agreed closely with Hawksley's equation and relatively well with their own 'configuration II' equation, which in fact was based on Hawksley's model. In both of these models, the horizontal layers were assumed to touch one another. The data agreed less well with the Richardson and Zaki 'configuration I', in which the particle separation was assumed the same, horizontally and vertically. The last-named model predicts sedimentation rates similar to those of Brinkman's theory of random swarms of spheres - an indication that observed rates may be equally interpretable in terms of quite conflicting theories. Happel's random-assemblage theory (which assumes that each particle is surrounded by a fluid envelope, and that no particle exerts any influence outside its own fluid) predicts the lowest Q/V_s of the theories here considered.

The sedimentation of seven grades of glass ballotini in 3 : 1 ($^v/v$) glycerol : water gave a surprising range of $Q\,(1-\varepsilon)/V_s$ curves, but at least some of the variation may have been due to difficulty in knowing the correct V_s values. The curves A and D on figure 3.6 encompass the whole range. The experiments are discussed in detail in section 3.3. However, the observed rates Q were roughly twice those predicted by Happel's random assemblage theory (e.g. 1.68 - 2.76 times, at $\varepsilon = 0.81$, according to particle size). The other random theory, namely that of Brinkman, gave somewhat better estimates,

the experimental/theoretical rates ratio being about 1.6 on average. Successively better estimates of the observed rates were given by the Richardson and Zaki configuration I and the Steinour empirical equation. In general, however, the observed rates bracketed the curves for the Richardson and Zaki empirical equation and the Hawksley and Richardson and Zaki configuration II theoretical equations based on hexagonally-arranged columns of sedimenting spheres. The experimental data obtained in this investigation therefore favour a model of the sedimenting 'plug' in which there is a high degree of symmetry, with linear upflow of supernatant liquid.

Two theoretical models have been proposed to account for the variation of practical suspensions from the behaviour given by assemblies of smooth, uniformly-sized spheres. One is that the flow channels through the sedimenting mass are tortuous, and that increasing deviation from theoretical behaviour is due to increasing tortuosity; a recent treatment is that of Wasan, Whek, Davies, Jackson and Kaye (1976). The other assumes that the values assumed for the porosity ε and the specific surface S of the solid may not be correct for the actual conditions in the sedimenting suspension (Harris, 1977). This second model can be interpreted by the concept that 'immobile' or 'stagnant' liquid is associated with the sedimenting particles, decreasing ε and decreasing S. Tortuosity of flow would be expected to occur among random assemblies of particles, and the data reviewed appear not to support such a model. Therefore, the assumption has been made in the work now reported that the

upflow through the sedimenting mass can be taken as through linear vertical pores, with increasing hindrance to sedimentation being due to increasing proportions of associated fluid on the particles.

Hawksley's equation and the empirical and 'configuration II' equations of Richardson and Zaki give values of about 0.82 - 0.83 for ε_l, in good agreement with the observed values of about 0.80 - 0.81 for ballotini. However, they (and all the other equations discussed in this section) are incapable of showing values for ε_l much different from 0.80 (see figure 3.5), whereas figure 3.7 shows that suspensions of calcium carbonate in a variety of fluids have ε_l values in the region 0.973 - 0.987. In addition, the $Q(1-\varepsilon)/V_s$ values obtained for the carbonate suspensions are low to very low, even when compared with the underestimates of the Happel theory. One way out of this difficulty might be to assume that the <u>effective</u> porosity at maximum solids flux is 0.80 or thereabouts, for any suspension, irrespective of the actual solids volume fraction $(1-\varepsilon_l)$ at that condition. The consequences of this hypothesis are explored in section 3.7.

3.2.8 Predicted and observed values of the interface settling rate at maximum solids flux, Q_{ε_l}.

For the special case where a suspension has initial porosity ε_l, one may write the modified Richardson-Zaki equation

$$Q = V_s \cdot \varepsilon^{\varepsilon_l/1-\varepsilon_l} \qquad (3.9)$$

or the modified Dollimore-McBride equation

$$Q = V_s \cdot \exp - \left(\frac{1-\varepsilon}{1-\varepsilon_1}\right) \qquad (3.20)$$

The ratio Q_{ε_1}/V_s of the settling rate at porosity ε_1 to the corresponding Stokes' Law velocity has been calculated from equation 3.9 for various values of ε_1, and the data are shown in table 3.5 and figure 3.8.

Table 3.5

Values of $Q\varepsilon_1/V_s$ calculated from equation 3.9

ε_1	$\varepsilon_1^{\varepsilon_1/(1-\varepsilon_1)} = Q_{\varepsilon_1}/V_s$
0.5	0.500
0.6	0.465
0.7	0.435
0.8	0.410
0.82	0.405
0.84	0.400
0.86	0.396
0.88	0.392
0.90	0.387
0.92	0.383
0.94	0.379
0.96	0.375
0.98	0.372
0.99	0.370
0.995	0.369
0.999	0.368
1.000	0.3679 ($= \exp^{-1}$)

Figure 3·8

Variation of the function $Q\epsilon_1/V_s$ ($= \epsilon_1^{\left(\frac{\epsilon_1}{1-\epsilon_1}\right)}$) with initial porosity ϵ_1 according to the generalised Richardson - Zaki equation

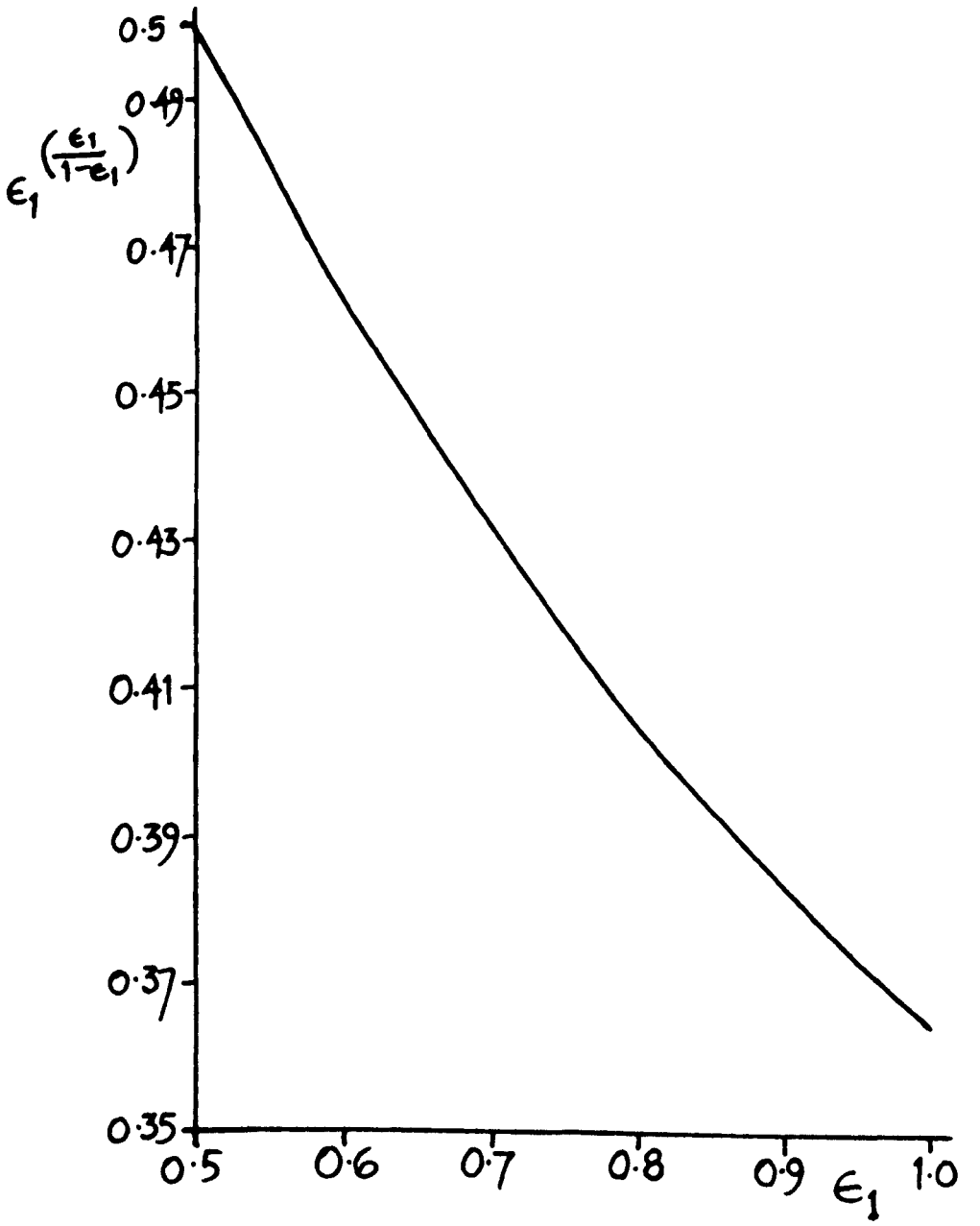

Figure 3.8 shows that, in systems which obey the generalised Richardson-Zaki equation at very high porosities, only a relatively slight addition of solid to pure liquid causes a marked fall from the Stokes' limiting velocity; there is, for instance, a fall to about 0.37 V_s simply by moving from infinite dilution ($\varepsilon = 1$) to $\varepsilon = \varepsilon_l = 0.990$. If equation 3.9 is obeyed, the minimum value of Q_{ε_l}/V_s equals $\exp^{-1}$, and this occurs when ε_l approaches unity: substituting for $\varepsilon = \varepsilon_l$ in equation 1.53 from equation 3.8 yields

$$Q_{\varepsilon_l} = V_s \left(\frac{n}{n+1}\right)^n = V_s \left(1 + \frac{1}{n}\right)^{-n} \qquad (3.29)$$

As ε_l approaches unity, n becomes indefinitely large, and when this is so, by the binomial theorem, $(1 + \frac{1}{n})^{-n}$ approaches to value $\exp^{-1}$; hence

$$Q\varepsilon_l/V_s \rightarrow \exp^{-1} \quad \text{as} \quad \varepsilon_l \rightarrow \text{unity.}$$

A somewhat different result is obtained from the modified Dollimore-McBride expression 3.20, since this yields $Q_{\varepsilon_l}/V_s = \exp^{-1}$ for <u>any</u> value of ε_l. The two expressions are approximately the same for highly-hindered systems, since then $\varepsilon_l \simeq$ unity. A comparison can be made between the equations by experimental determination of Q_{ε_l}/V_s ratios, and this has been done for several closely-sized samples of glass spheres (ballotini) in 75% $^v/_v$ aqueous glycerol (see section 3.3.3).

3.3 The sedimentation behaviour of closely-sized samples of glass spheres in 75% aqueous glycerol

The biggest single difficulty in testing the validity of hindered settling equations by observations on practical suspensions is that the Stokes limiting velocity V_s cannot be directly determined, because there are distributions of particle sizes and shapes present and representative individual particles cannot be isolated and observed. It has therefore been customary to carry out validation investigations by using dispersions of closely-sized (ideally monodisperse) spheres, of sufficient diameter to be observable when taken singly. Observed values of V_s can be obtained from the sedimentation of single particles using the same equipment as is used for the examination of suspensions. In addition, V_s can be calculated from Stokes' Law, knowing the solid density and the density and viscosity of the liquid and having measured the particle diameter by optical means. Finally, extrapolated values of V_s can be obtained from hindered settling data by various methods. The three limiting velocities $V_{s\ (obs)}$, $V_{s\ (calc)}$, and $V_{s\ (extrap)}$, can then be compared. The observed values $V_{s\ (obs)}$ may be measurably smaller than the theoretical values $V_{s\ (calc)}$, due to wall effects; that is to say, the particle does not fall through infinite fluid but is somewhat constrained by the presence of the container. The observed velocities in this section were corrected by the method of Francis (1933).

3.3.1 The applicability of interface settling rates to the determination of mean equivalent spherical radii of sedimenting particles

Measurements of the interface settling rate may be used to determine mean particle size (Allen, 1976), either by methods which explicitly extrapolate the observed rates to infinite dilution, so that Stokes' Law may be applied directly to the extrapolated rate (Ramakrishna and Rao, 1965) or by equations which assume the validity of such extrapolation even though the extrapolated rate is not calculated. The use of equation 3.1 involves this assumption. Nonetheless, there appear to be two *a priori* reasons to doubt the reliability of such extrapolations. Firstly, Ramakrishna and Rao drew attention to distinct 'breaks' in what previous work (Steinour, 1944) had suggested should be straight-line plots. Secondly, the observations of Kaye and Boardman, Johne, and Koglin (summarised in section 1.3.4) suggest that the dependence of interface settling rate on concentration might correspond more closely to a sigmoid sedimentation curve, rather than to the exponential-type functions commonly proposed previously, on some of which the radii determinations have been based. In any case, since only some portion of the left-hand side of the curve in figure 1.12 can be observed in hindered settling experiments, extrapolation to infinite dilution might be along a significantly erroneous line.

However, detailed studies by Richardson and Zaki (1954), of uniformly-sized spherical particles of divinylbenzene and of

glass in various liquids, gave close agreement between extrapolated sedimentation rates at infinite dilution ($V_{s\ (extrap)}$) and those calculated from Stokes' Law ($V_{s\ (calc)}$), provided the Reynolds' number was less than 0.2. For Re > 0.2, extrapolation gave increasingly low estimates of $V_{s\ (calc)}$, and Bell and Crowl (1969) concluded that particle sizes may be studied by sedimentation methods only when Re < 0.2. Previously, however, Gaudin (1939) reported a number of investigations indicating that Stokes' Law holds (for spherical particles) up to Re = 0.6. Wilhelm and Kwauk (1948) calculated a modified Reynolds' number, Re_m, using the interface settling rates in place of the limiting rate in an otherwise normal Reynolds calculation. Table 3.6 cites the values of Re and Re_m in the investigation described below (Bhatty, Davies and Dollimore, 1977).

Experimental

The materials used were seven grades, A - G, of glass ballotini, of nominal radii 65, 45, 35, 32.5, 27.5, 23.75 and 13.75 x 10^{-3} cm. respectively, and of density ρ_s = 2.938 $g.cm^{-3}$, and 3:1 ($^v/v$) glycerol: water, of viscosity η = 0.403 $g.cm^{-1}\ s^{-1}$ and density ρ_l = 1.202 $g.cm^{-3}$ (both at 24°C). In the hindered settling experiments, weighed samples of single grades of ballotini were mixed with the aqueous glycerol to give 180 cm^3 total volume per sample, in 250 cm^3 measuring cylinders, and the interface sedimentation rate observed in a constant-temperature room thermostatted within very close limits to 24°C. A sample was prepared for observation by inverting the cylinder slowly, end over end, twenty times, and then setting it down in front of a fluorescent

(i.e. cold source) light box. Measurements of interface height were made at appropriate time intervals, taking zero time as the instant when any initial turbulence ceased on setting down. Initially, the settling rate in any cylinder was constant, and the readings were continued until the rate decreased significantly below the initial value. The linear settling rates (Q, $cm.s^{-1}$) were calculated. The suspension concentrations were converted into liquid volume fractions, ϵ , and the relationship of Q to ϵ for the seven grades of ballotini are shown in table 3.6. The data were linearized as far as possible by calculating log Q and log ϵ (Richardson and Zaki, 1954) and V_s (extrapolated) calculated by the method of least squares on the logarithmic data.

Sedimentation rates for single particles $V_{s\ (obs)}$ were measured in the same fluid and laboratory conditions; each rate used for calculation was the mean of at least twenty-five separate observations. A sample of each grade of ballotini was examined microscopically, the number of particles observed varying from 1030 to 2310 according to grade. The diameters were subdivided into ranges, and the data (table 3.7) used to estimate the number weighted mean radius for each grade.

Limiting settling rates were calculated from the nominal radii and weighted mean radii, and compared with the corrected observed rates and the limiting rates extrapolated from the hindered settling data. The results are summarised in table 3.8, together with a corresponding comparison of mean radii.

Table 3.6

RELATIONSHIP OF INTERFACE SETTLING RATES (Q) TO SUSPENSION LIQUID VOLUME FRACTIONS (ε) FOR GLASS BALLOTINI IN 3:1 ($^{v}/_{v}$) GLYCEROL:WATER

ε	Q						
	Grade A	Grade B	Grade C	Grade D	Grade E	Grade F	Grade G
1.00							
0.96			0.90	0.61	0.453		
0.93			0.763	0.50	0.418	0.333	
0.89	2.40	1.10	0.633	0.41	0.35		
0.85	2.15	0.90	0.507	0.35	0.30	0.25	0.095
0.81	1.80	0.71	0.420	0.307	0.25	0.212	0.077
0.77	1.34	0.60	0.333	0.24	0.204	0.1765	0.06
0.74	1.05	0.46	0.27	0.20	0.176	0.15	0.048
0.70	0.78	0.37	0.23	0.16	0.14	0.12	
0.66	0.58	0.29	0.18	0.12	0.11	0.091	0.0334
0.63	0.43	0.24	0.14	0.10	0.092	0.0726	0.0285
0.59	0.32	0.19	0.104	0.07	0.063	0.054	0.024
0.55	0.25	0.13	0.07	0.05	0.045	0.04	0.0178
0.51	0.17	0.094	0.05	0.04	0.033	0.0267	0.013
0.48	0.14	0.070	0.037	0.028	0.026	0.02	0.010
0.44		0.041	0.026	0.02	0.019		0.0074
Re	1.54	0.51	0.24	0.19	0.12	0.075	0.015
Re_m	0.05-0.93	0.01-0.30	0.005-0.19	0.004-0.12	0.003-0.08	0.003-0.05	0.0006-0.008

Table 3.7

PARTICLE SIZE DISTRIBUTION OF BALLOTINI

GRADE	DIAMETER ($cm.10^3$)							
	160-180	140-160	120-140	100-120	80-100	60-80	40-60	20-40
A	36	54	806	248	56	14	-	-
B	-	-	29	789	1123	319	55	-
C	-	-	-	27	164	672	160	67
	70-80	60-70	50-60	40-50	30-40			
D	342	982	183	4	-			
E	-	73	1686	203	44			
	55-60	50-55	45-50	40-45				
F	77	500	1003	99				
	30-35	25-30	20-25	15-20				
G	62	646	259	64				

Table 3.8

CALCULATED, OBSERVED AND EXTRAPOLATED INFINITE-DILUTION SETTLING RATES (V_s.cm.s^{-1}) FOR GLASS BALLOTINI IN 3:1 ($^v/_v$) GLYCEROL:WATER, AND CORRESPONDING MEAN PARTICLE RADII (r, μ)

GRADE		A	B	C	D	E	F	G
V_s CALCULATED	from nominal radius	3.97	1.90	1.15	0.99	0.71	0.53	0.18
	from weighted mean radius	3.80	2.07	1.10	1.02	0.68	0.57	0.16
V_s EXTRAPOLATED		4.61	1.91	1.10	0.73	0.59	0.53	0.17
V_s OBSERVED	(corrected for wall effect)	3.78	2.18	1.05	1.02	0.74	0.59	0.19
MEAN RADIUS $\bar{r}$ (microns, μ)	nominal	650	450	350	325	275	237.5	137.5
	weighted from microscopy	636.5	468	343	330	269.5	246	130
	from V_s observed (corrected)	635	482	334	330	281	251	142
	from V_s extrapolated	701	451	342	279	251	238	135
RATIO $\bar{r}$ extrapolated /	average of other values	1.094	0.966	0.999	0.850	0.912	0.972	0.989

Discussion

Table 3.8 shows that the ratios of the extrapolated radii to the averages of the other values varied from 0.85 to 1.094, with no simple relationship to Reynolds' number, over the range $0.015 < Re < 1.54$. The mean value of the ratio was 0.969. The standard deviation of the ratios (= 0.07) indicates probability = 0.954 that any individual radius, obtained by extrapolation, would lie within ± 14% of the mean value expected from the other methods, over the given range of Re. The difference between mean radii (extrapolation: other methods, 0.969:1.000) is not significant by t-test (Davies and Goldsmith, 1972); $t = 1.17$, and for six degrees of freedom, $p > 0.20$. That is to say, there was over 20% chance of the results obtained being observed without there being any true difference between the means. Therefore, the overall result by extrapolation is not significantly different from the overall mean result by the other methods, at least for the materials and size of investigation now reported.

In the experiments with grades C - G inclusive, each determination of settling rate could be assumed to be under laminar flow, as indicated by $Re_m \lesssim 0.2$. For these grades, the ratio ($\bar{r}_{extrapolated}$/mean of other values) was 0.93, with standard error = 0.0255. This leads to $t = 2.75$, and for four degrees of freedom, $0.05 < p \ll 0.10$. These results are perhaps best described as 'possibly significant'. There is some possibility that hindered settling experiments in the region $0.015 < Re < 0.24$ may yield significantly low estimates of mean radius when

compared with the other methods of this study. On the other hand, there is more than 5% chance that the results obtained could be observed without there being any true difference between the methods.

The most obvious differences between the extrapolated and calculated mean radii in the laminar flow region (grades D and E) appear to be due to unexpectedly low settling rates at high porosities, similar to those reported by Ramakrishna and Rao (1965). The low rates were associated with relatively-diffuse interfaces, as compared with the behaviour at lower porosities, and it was considered that their appearance might correspond to a change of the actual mode of sedimentation.

3.3.2 The sigmoidal nature of sedimentation curves in cases of hindered settling

The possibility that interface settling rates might bear a sigmoidal relationship to porosity was investigated by submitting the data to a test equation developed as follows. It has been shown (section 3.2.6) that the empirical equation

$$Q = V_s \cdot 10^{-bC} \tag{3.1}$$

may be transformed into

$$Q = V_s \exp - \left(\frac{1-\varepsilon}{1-\varepsilon_1}\right) \tag{3.2}$$

This exponential equation may be transformed into a sigmoidal expression by writing

$$Q = V_s \exp^{-\frac{(1-\varepsilon)^a}{1-\varepsilon_1}} \qquad (3.30)$$

In fact, if a $<$ unity, the expression is of exponential form, while if a $>$ unity, it is sigmoidal (Lumer, 1937). This variation is shown graphically in the Appendix, with a derivation of equation 3.30 by analogy from the expression for the normal distribution curve.

It follows from equation 3.30 that a plot of $\log_{10} \log_{10} V_s/Q$ against $\log_{10} (1-\varepsilon)$ has slope = a. If the experimental data yield a $<$ 1, the best fit of Q against ε is an exponential curve; if a $>$ 1, the best fit is a sigmoidal curve. Figures 3.9 a - g, corresponding to ballotini grades A to G respectively, show the plots obtained in this investigation. Predominantly, the slope a varied from less than unity at high porosity to more than unity in more-concentrated suspensions. The value a = 1 tends to occur in the region of porosity including ε_1. It therefore seems that the shape of the Q $(1-\varepsilon)$ versus ε curve, which goes through a maximum at ε_1, corresponds to a change in sedimentation behaviour from an exponential dependence on concentration (when $\varepsilon > \varepsilon_1$) to a sigmoidal dependence (when $\varepsilon < \varepsilon_1$).

The experimental data do not allow the firm conclusion that a = 1 precisely at $\varepsilon = \varepsilon_1$. For that reason, equation 3.30 was

Figures 3·9 a-g

Variation of the power number 'a'
with solid volume fraction
for glass ballotini in aqueous glycerol

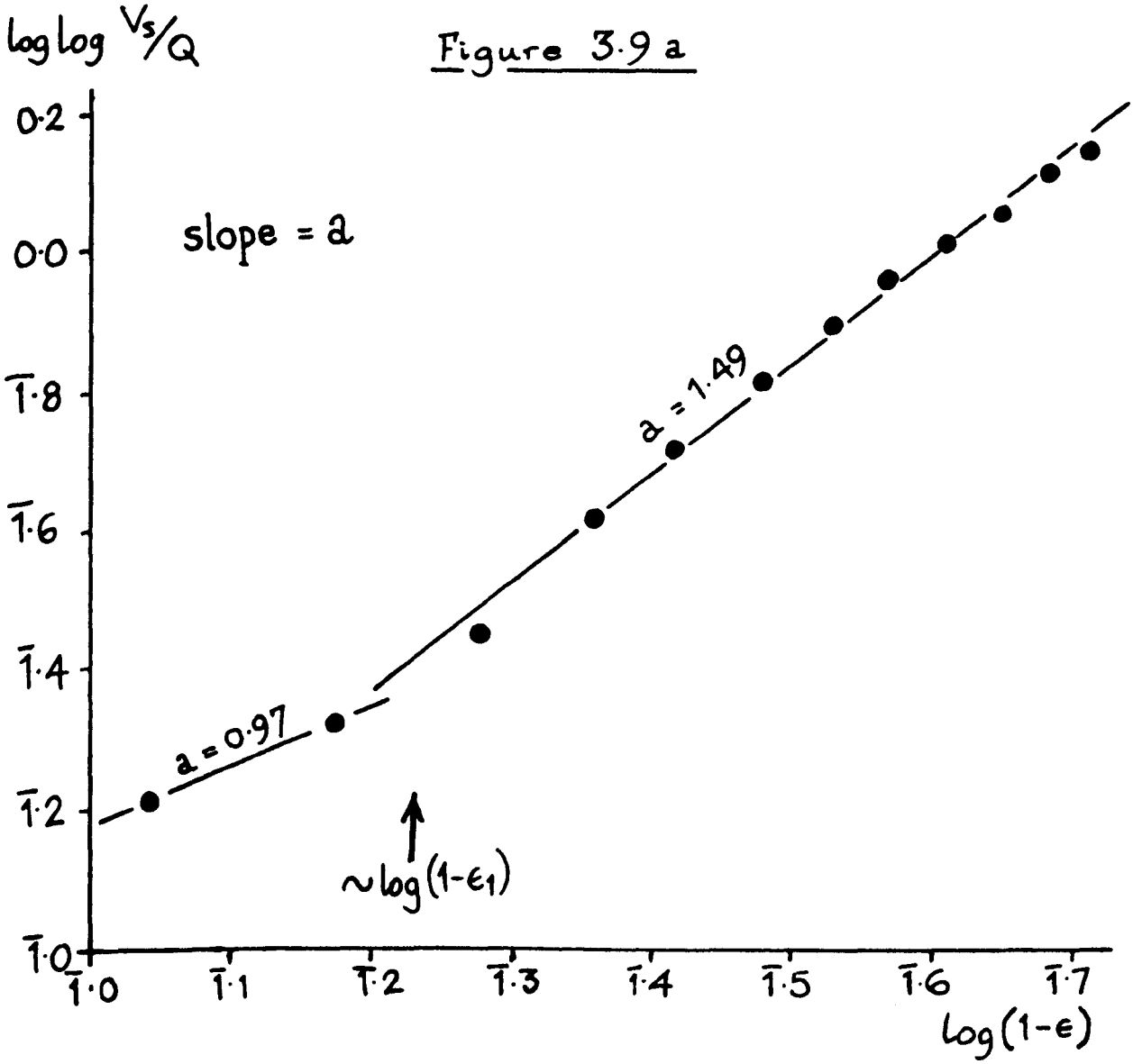

Figure 3·9 a

Figure 3.9b

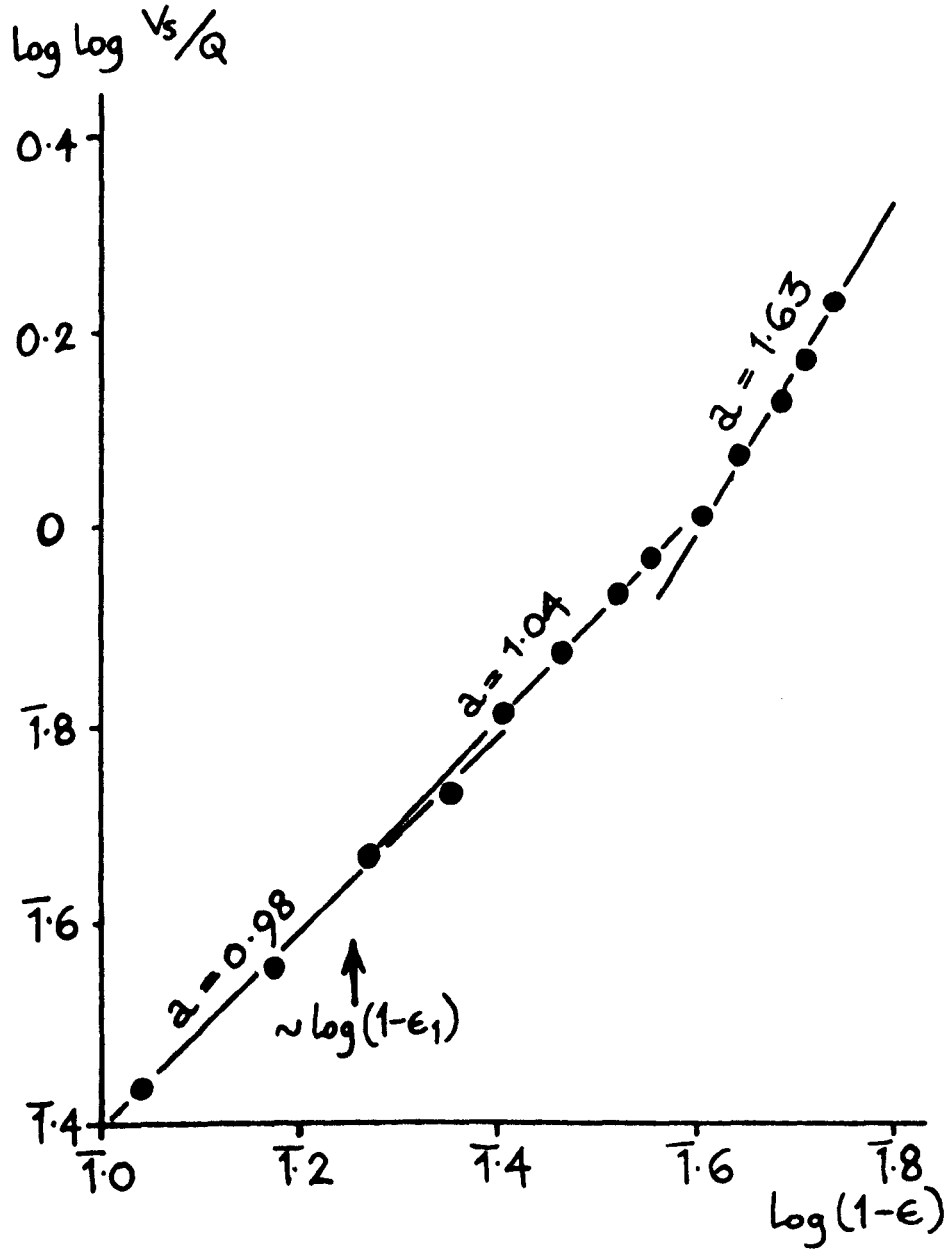
log log Vs/Q
0·4
0·2
0
$\bar{1}$·8
$\bar{1}$·6
$\bar{1}$·4
$\bar{1}$·0
$\bar{1}$·2
$\bar{1}$·4
$\bar{1}$·6
$\bar{1}$·8
log (1-ϵ)
a = 0.98
a = 1.04
a = 1.63
≈ log (1-ϵ1)

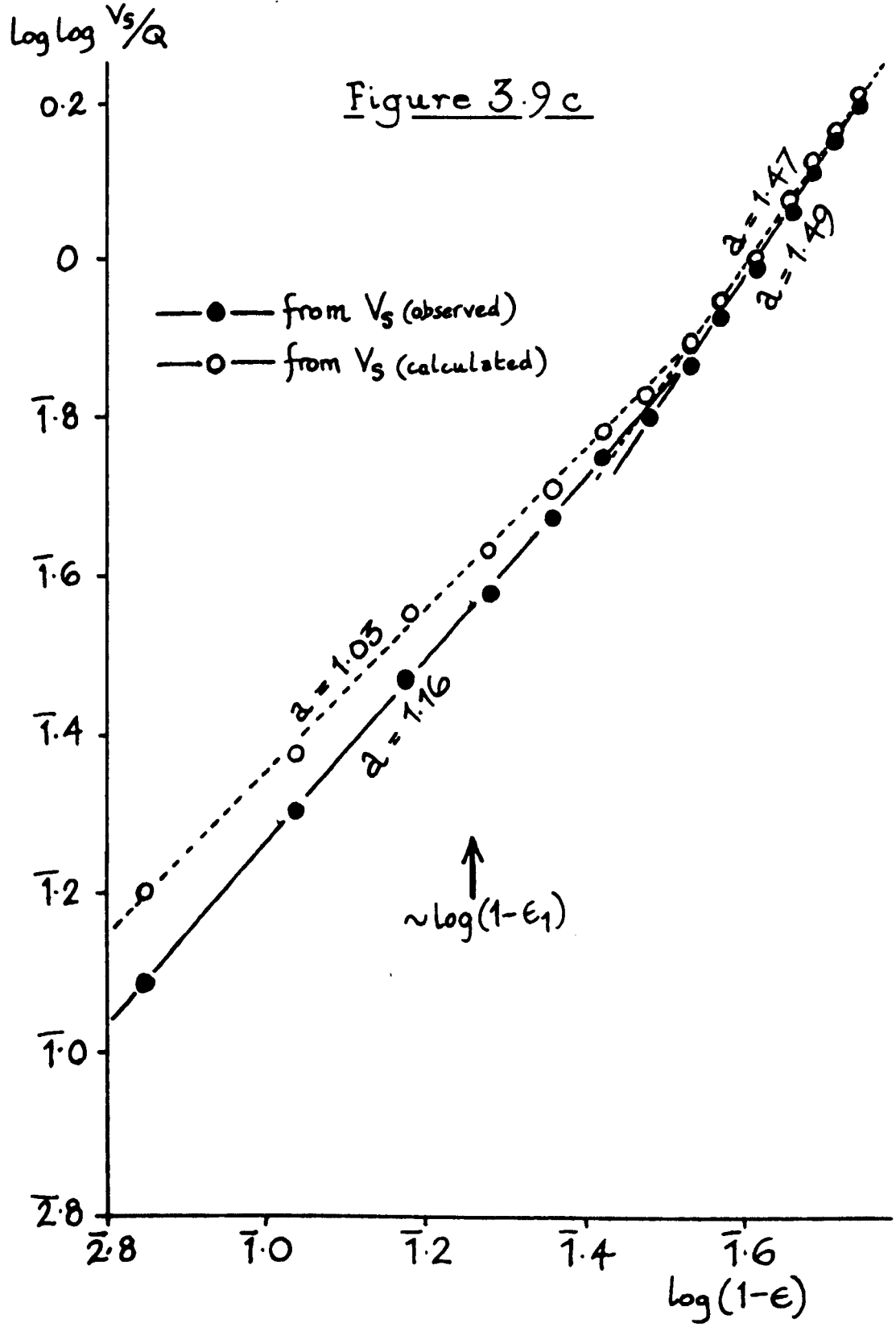
log log Vs/Q
Figure 3.9c
0·2
0
$\bar{1}$·8
$\bar{1}$·6
$\bar{1}$·4
$\bar{1}$·2
$\bar{1}$·0
$\bar{2}$·8
—●— from Vs (observed)
—o— from Vs (calculated)
a = 1.03
a = 1.16
a = 1.47
a = 1.49
~log(1-ε1)
$\bar{2}$·8
$\bar{1}$·0
$\bar{1}$·2
$\bar{1}$·4
$\bar{1}$·6
log(1-ε)

Figure 3.9d

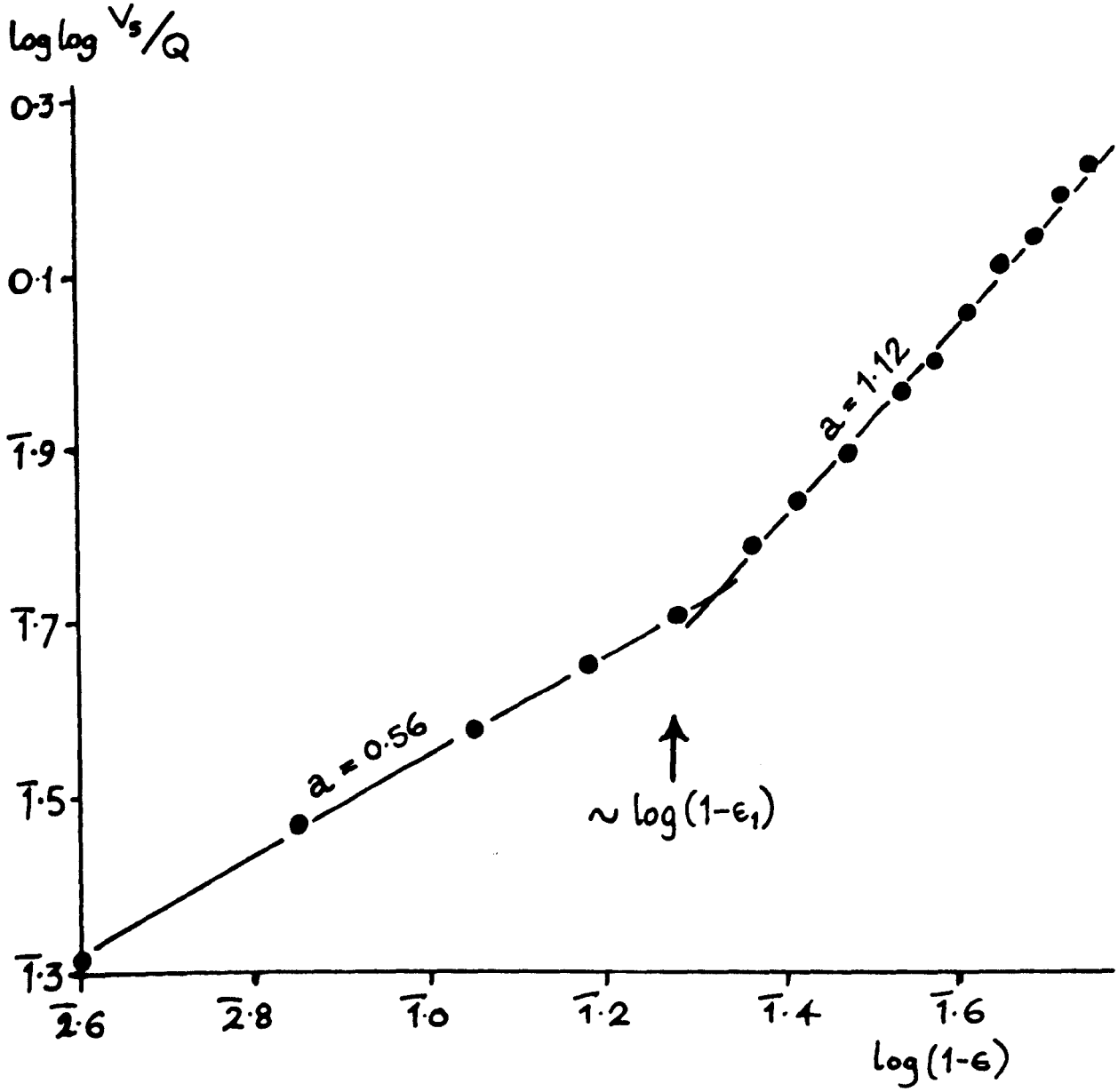
log log Vs/Q
0·3
0·1
$\bar{1}$·9
$\bar{1}$·7
$\bar{1}$·5
$\bar{1}$·3
$\bar{2}$·6
$\bar{2}$·8
$\bar{1}$·0
$\bar{1}$·2
$\bar{1}$·4
$\bar{1}$·6
log(1-ε)
a = 0.56
a = 1.12
~ log(1-ε1)

Figure 3.9e

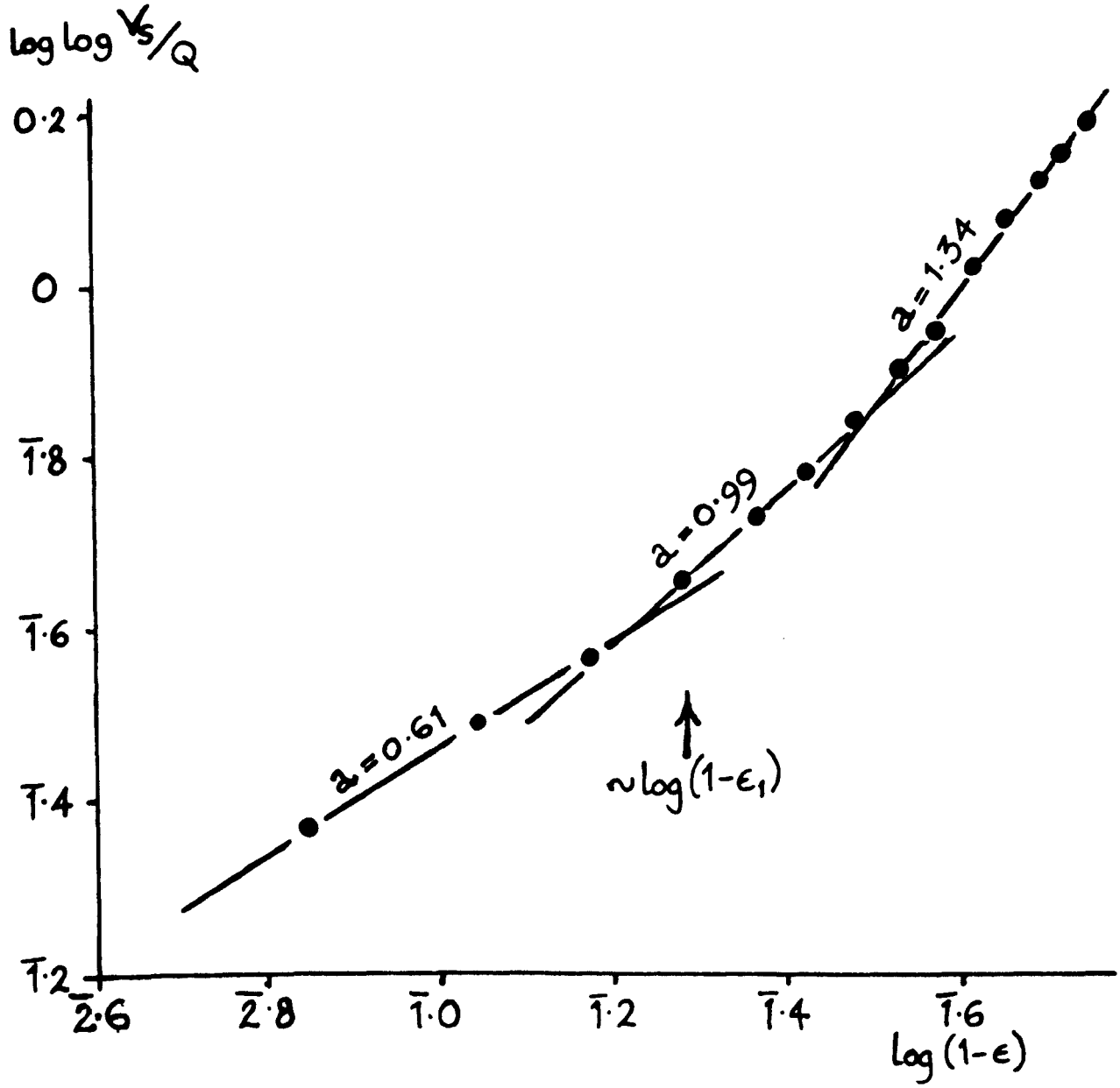
log log Vs/Q
0·2
0
$\bar{1}$·8
$\bar{1}$·6
$\bar{1}$·4
$\bar{1}$·2
$\bar{2}$·6
$\bar{2}$·8
$\bar{1}$·0
$\bar{1}$·2
$\bar{1}$·4
$\bar{1}$·6
log (1-ε)
a=0.61
a=0.99
a=1.34
≈log(1-ε1)

Figure 3.9 f

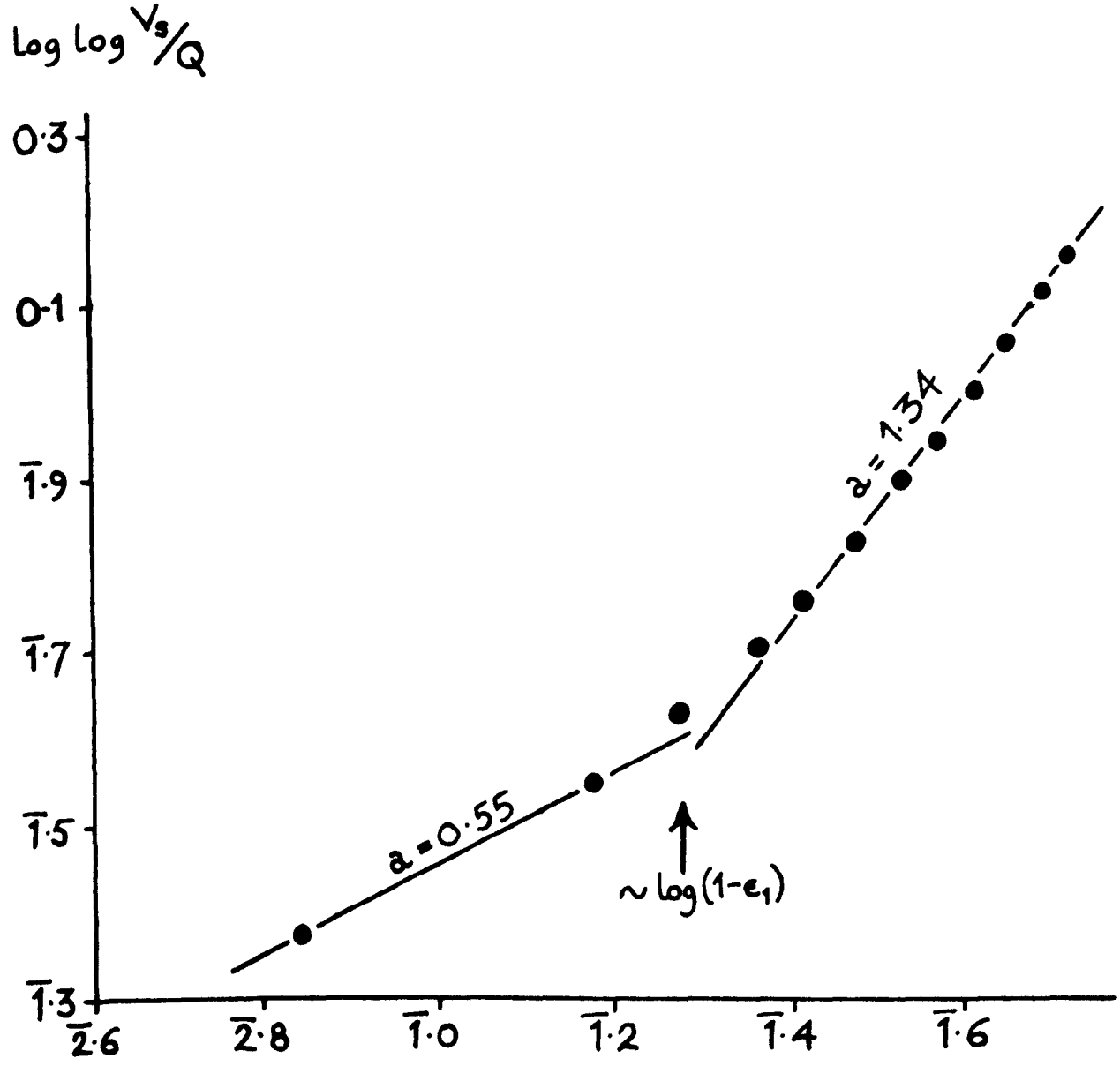
log log V_s/Q
0·3
0·1
$\bar{1}$·9
$\bar{1}$·7
$\bar{1}$·5
$\bar{1}$·3
$\bar{2}$·6
$\bar{2}$·8
$\bar{1}$·0
$\bar{1}$·2
$\bar{1}$·4
$\bar{1}$·6
a = 0·55
a = 1·34
~ log(1-e_1)

Figure 3.9g.

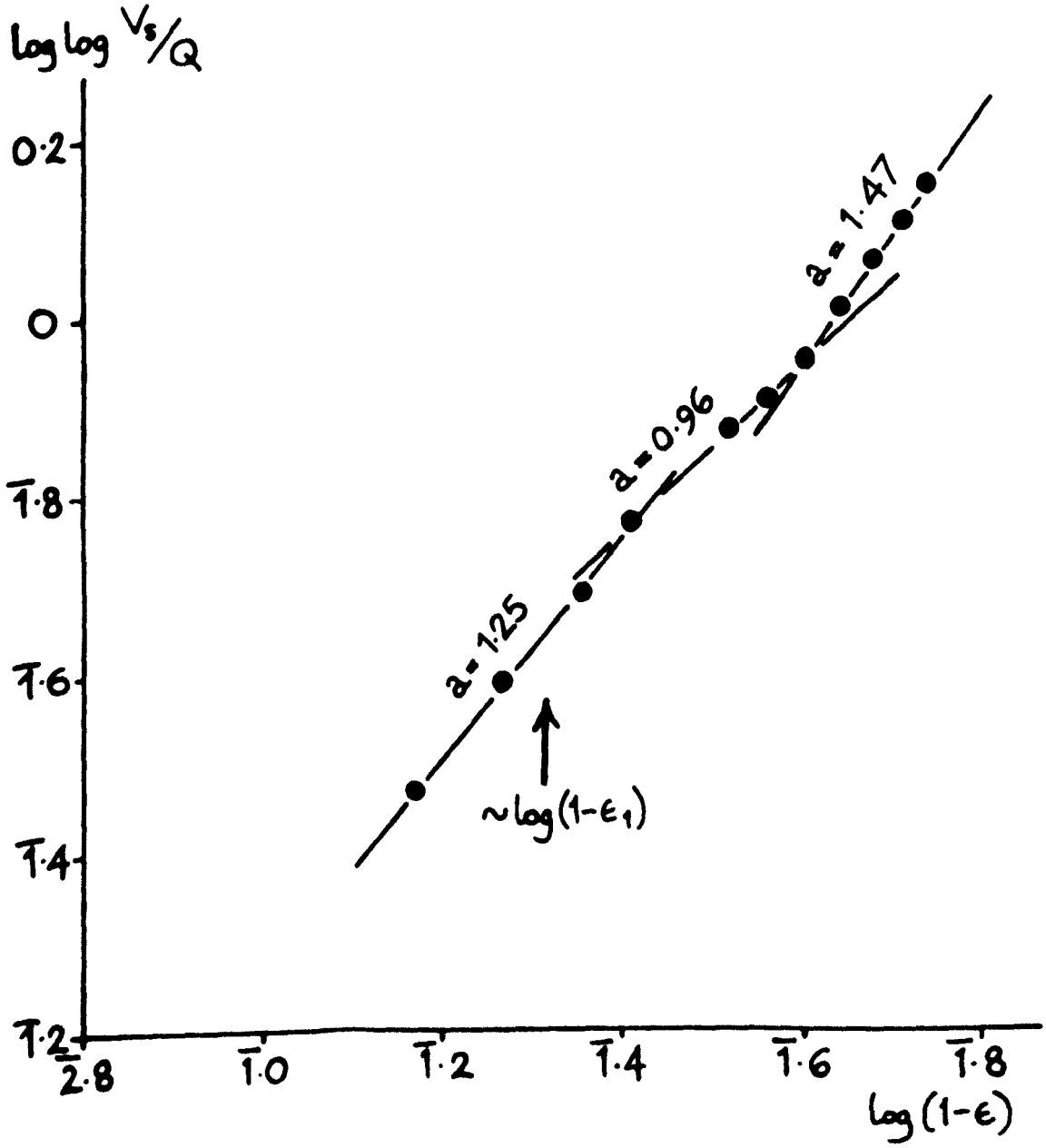
log log Vs/Q
0·2
0
T·8
T·6
T·4
T·2
2·8
T·0
T·2
T·4
T·6
T·8
log (1-ε)
a = 1·25
a = 0·96
a = 1·47
~log(1-ε1)

modified to

$$Q = V_s \exp^{-\frac{(1-\varepsilon)^a}{1-\varepsilon^*}} \tag{3.31}$$

where ε^* is that porosity at which $a = 1$ precisely.

When $\varepsilon = \varepsilon^*$, equation 3.31 becomes

$$Q_{\varepsilon^*} = V_s \exp^{-1} \tag{3.32}$$

At porosities $\varepsilon^* \leq \varepsilon < 1$, $a \leq 1$, and equation 3.31 then yields an exponential curve, which may be compared with the Richardson-Zaki equation in its exponential form. From

$$Q = V_s \varepsilon^n \tag{1.53}$$

by taking logarithms, we obtain

$$\ln Q = \ln V_s + n \ln \varepsilon$$

and taking antilogarithms then gives

$$Q = V_s \exp^{2.303\, n \log_{10} \varepsilon} \tag{3.33}$$

whence, from equations 3.31 and 3.33, for $a \leq 1$,

$$-\frac{(1-\varepsilon)^a}{1-\varepsilon^*} = 2.303 \log_{10} \varepsilon$$

It follows that, when

$$\varepsilon = \varepsilon^*, \quad a = 1,$$

$$-\frac{1}{2.303\ n} = \log_{10} \varepsilon^* \qquad (3.34)$$

The least-squares values of n from figure 3.10 are given in table 3.9. ε^* values calculated from equation 3.34 are also given, together with ε_1 values calculated from equation 3.5.

Table 3.9

VALUES OF n, ε_1 AND ε^* FOR BALLOTINI IN AQUEOUS GLYCEROL

GRADE	A	B	C	D	E	F	G
n	4.89	4.54	4.55	4.38	4.20	4.34	3.81
ε_1	0.830	0.819	0.820	0.814	0.808	0.813	0.792
ε^* from eqn. 3.34	0.815	0.802	0.803	0.796	0.788	0.794	0.769
ε^* (interpolated)	0.78	0.72	0.81	0.86	0.81	0.80	0.78

Alternatively, if V_s is known, $Q_{\varepsilon^*} = V_s \exp^{-1}$ may be calculated, and ε^* determined by direct observation of the settling rates Q.

Figure 3·10

Plot of log(sedimentation rate) versus log(initial porosity) for ballotini in aqueous glycerol

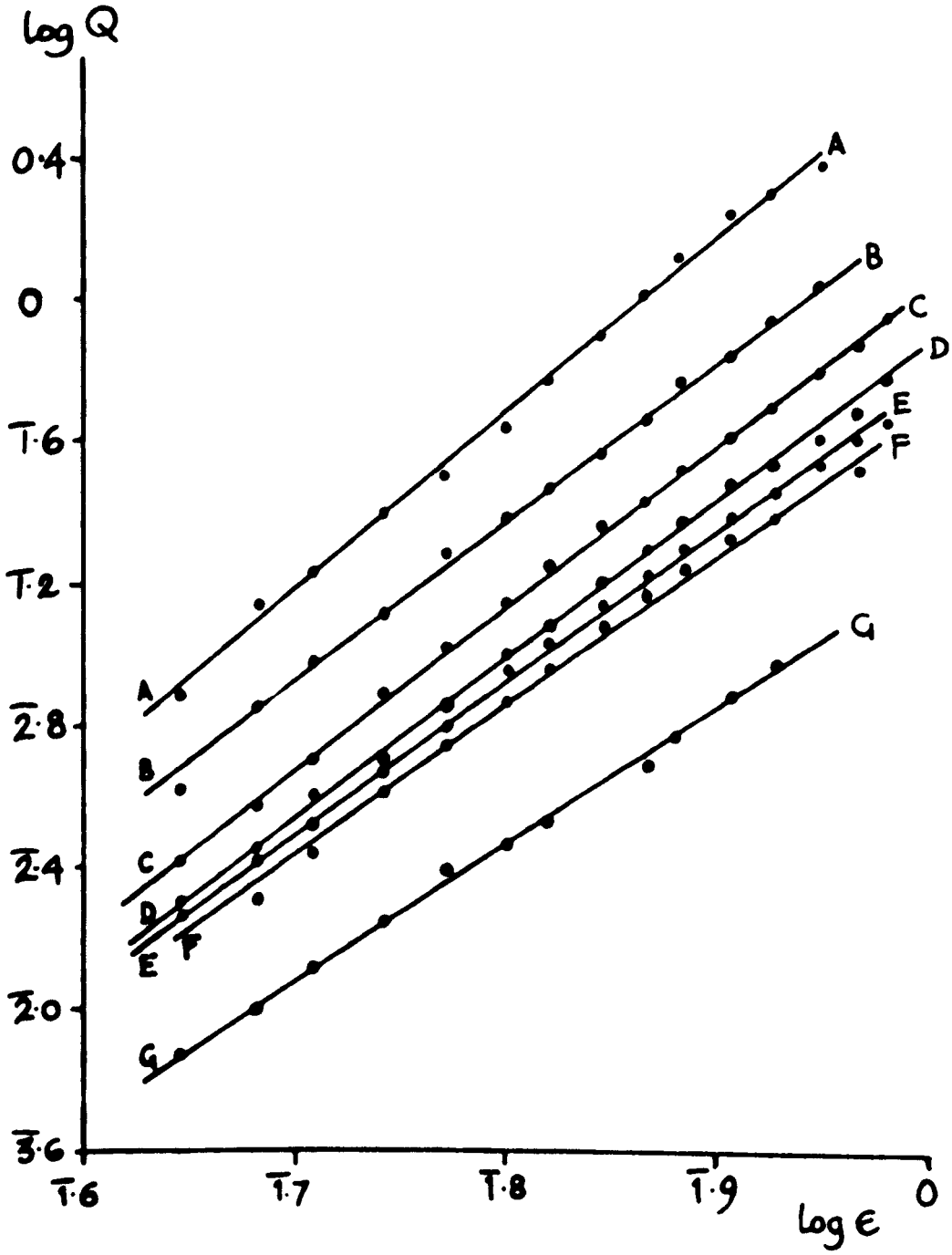

A further alternative is to estimate ε^* by interpolation among existing data for Q and ε. In the present case, the last-named method gave the values of ε^* (interpolated) given in table 3.9. The value of V_s used was the mean of the calculated values (table 3.8). Agreement between the two estimates of ε^* was not good if $Re_m > 0.2$ (grades A and B) or if there was a pronounced 'break' in the Q versus ε plot (grades D and E). These are the cases in which the observed values of Q did not extrapolate by the generalised Richardson-Zaki equation to give very good estimates of the calculated V_s (table 3.8). That is to say, the values of n obtained do not properly relate Q and V_s. It follows that these values of n, substituted in equation 3.34, do not give very good values for ε^*, since they will not properly relate Q_{ε^*} and $V_s \exp^{-1}$. In such cases, the interpolated value of ε^* is to be preferred. With the other three grades of ballotini, the calculation of ε^* by the two methods agreed to within 1%, and the interpolated values were intermediate between ε^* calculated from equation 3.34, and ε_1.

Figure 3.11 shows the fit of the experimental data for grade D to the theoretical curves for $\varepsilon^* = 0.86$ (the interpolated value), with $a = 0.56$ when $\varepsilon > \varepsilon_1$, and $a = 1.12$ when $\varepsilon < \varepsilon_1$. The theoretical values for $a = 1.12$ were derived from equation 3.31:

$$Q = V_s \exp - \frac{(1-\varepsilon)^{1.12}}{1-\varepsilon^*}$$

and this expression fits at $\varepsilon < \varepsilon_1$. However, the experimental curve for $\varepsilon > \varepsilon_1$ was reproduced by a modified equation

Figure 3·11

Fit of experimental data for grade 'D' ballotini to theoretical curves

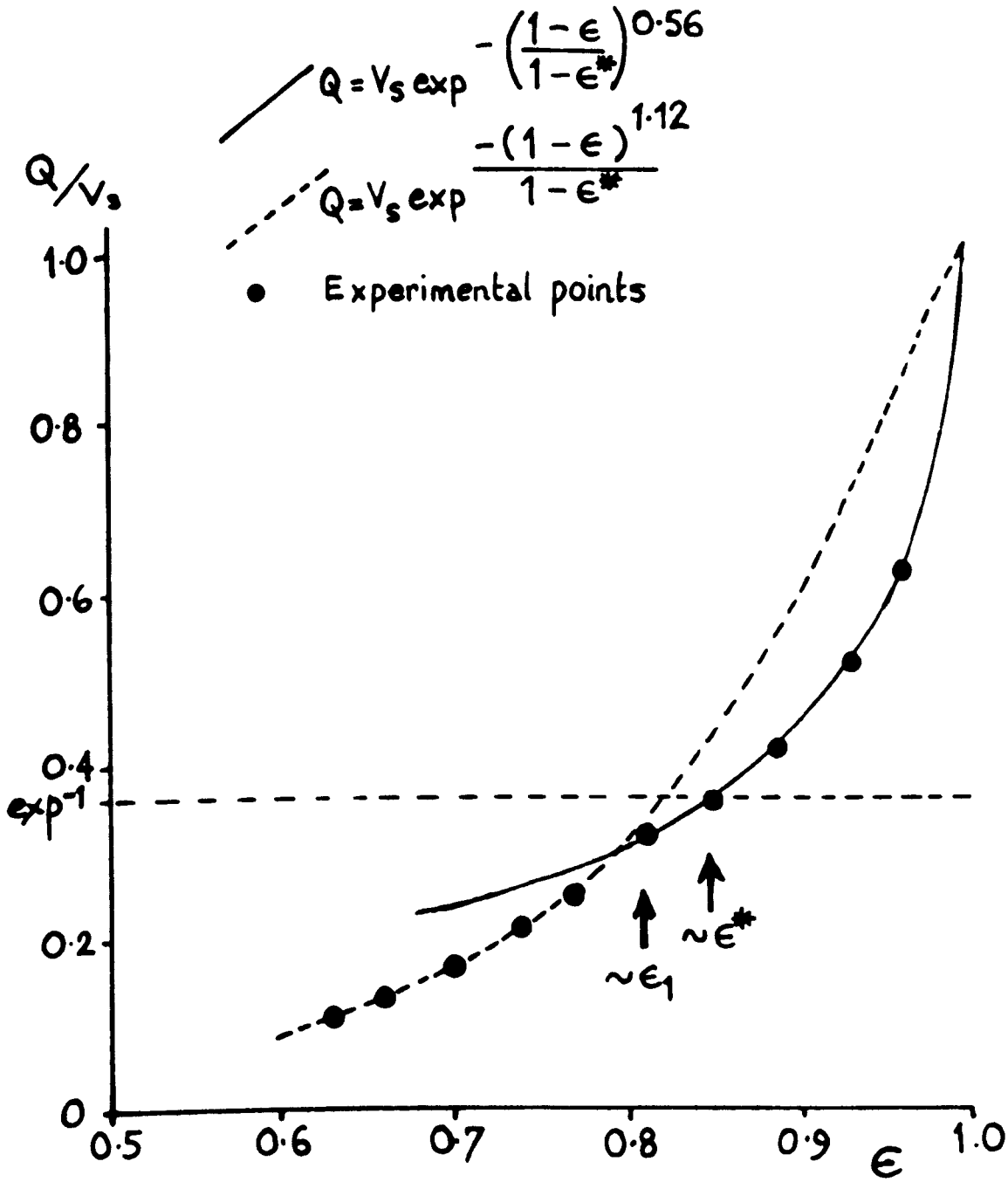

$$Q = V_s \exp - \left(\frac{1-\varepsilon}{1-\varepsilon^*}\right)^a \qquad (3.35)$$

with a = 0.56.

These results mean that the dependence of interface settling rate Q upon suspension porosity ε changes, at or near ε_1, from a sigmoidal dependence (at $\varepsilon < \varepsilon_1$) to an exponential dependence (at $\varepsilon > \varepsilon_1$).

Similar behaviour was also clearly apparent with grade E ballotini. Figure 3.12 shows the fit of equations 3.31:

$$Q = V_s \exp - \frac{(1-\varepsilon)^{1.34}}{1-\varepsilon^*}$$

and 3.35:

$$Q = V_s \exp - \left(\frac{1-\varepsilon}{1-\varepsilon^*}\right)^{0.61}$$

for this grade, using $\varepsilon^* = 0.81$. Mean calculated V_s values were taken in these calculations.

It appears that at or about $\varepsilon = \varepsilon_1$, when $Q \simeq V_s \exp^{-1}$, there is a change of sedimentation behaviour. The most clearly-defined hindered settling occurs in the region $\varepsilon < \varepsilon_1$, and this is associated with a sigmoidal dependence of interface sedimentation

Figure 3·12

Fit of experimental data for grade 'E' ballotini to theoretical curves

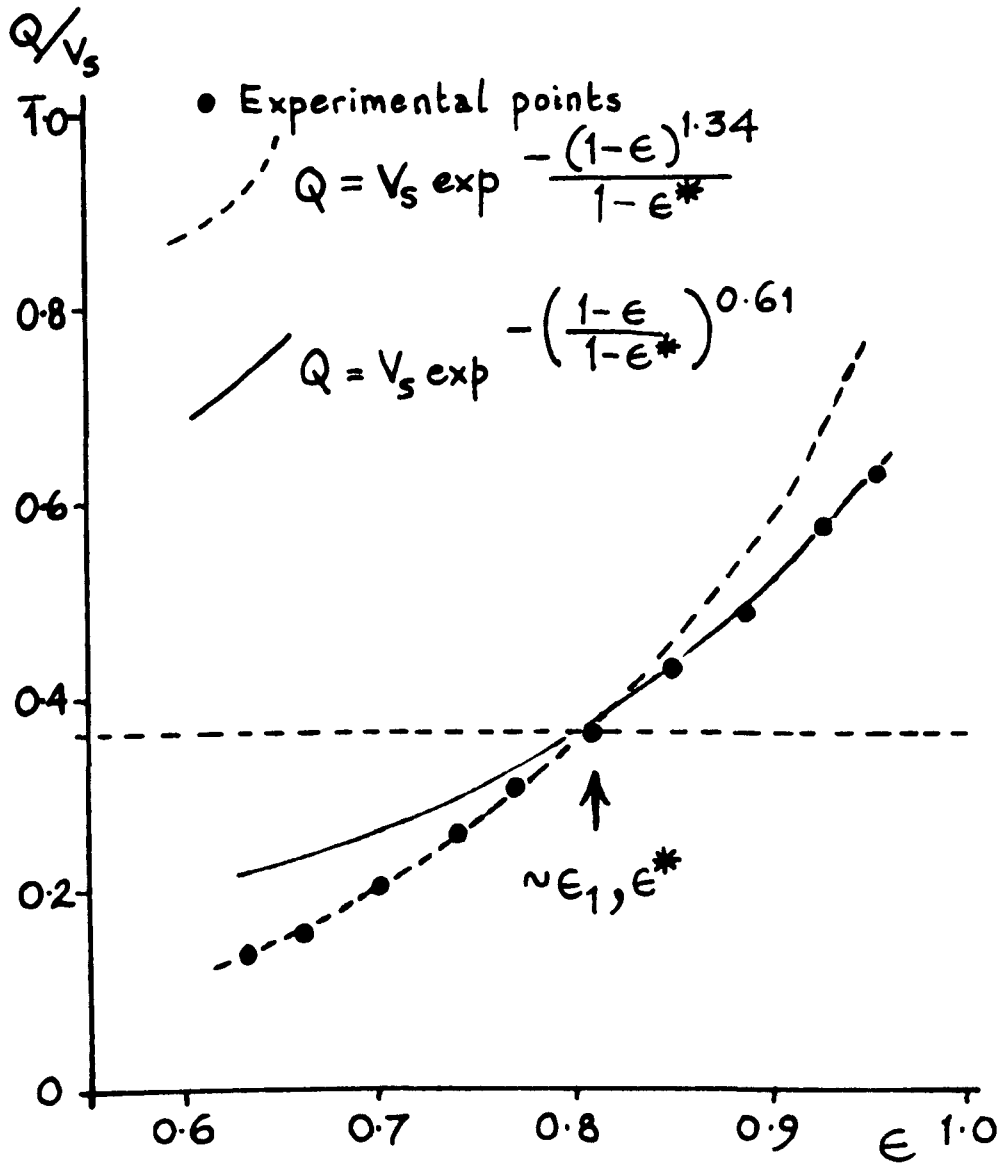

rate on concentration. The true points of inflexion in the sedimentation curves shown by Ramakrishna and Rao are difficult to identify precisely, but they appear to correspond to $Q/V_s \simeq 0.35$ and $Q/V_s \simeq 0.42$, in fair agreement with the prediction of a transition at $V_s \exp^{-1}$ ($= 0.368\ V_s$). The data for grades D and E ballotini, given above, correspond to $Q\varepsilon_1/V_s \simeq 0.305$ and 0.370 respectively, using the mean calculated values for V_s, and are thus in reasonable to very good agreement with the prediction.

Taking interpolated values of $Q\varepsilon_1$ from table 3.6, for the values of ε_1 in table 3.9, allows them to be compared with the prediction of the modified Richardson-Zaki equation 3.9:

$$Q_{\varepsilon_1/V_s} = \varepsilon_1^{\varepsilon_1/1-\varepsilon_1}$$

and that of the modified Dollimore-McBride equation (i.e. that $Q\varepsilon_1/V_s = \exp^{-1}$ at any value of ε_1). The values of V_s used in calculating from the equations was the mean of the calculated values (table 3.8). Table 3.10 shows the values obtained. The conclusion from the modified Dollimore-McBride equation, that $Q\varepsilon_1/V_s = \exp^{-1}$, was not substantiated.

Ramakrishna and Rao concluded that the 'breaks' in sedimentation curves occur when the distance between neighbouring particles becomes equal to the particle diameter. It is now concluded that this also corresponds to a change in sedimentation behaviour, with the onset of a sigmoidal dependence of settling rate on

Table 3.10

Comparison of values of $Q\varepsilon_1/V_s$, interpolated from experimental data, with predictions from theoretical equations, for ballotini in aqueous glycerol

GRADE		A	B	C	D	E	F	G
ε_1		0.830	0.819	0.820	0.814	0.808	0.813	0.792
$\frac{Q\varepsilon_1}{V_s}$	experimental	0.508	0.379	0.393	0.310	0.357	0.391	0.406
	modified Richardson-Zaki equation	0.403	0.406	0.404	0.406	0.408	0.406	0.411
	modified Dollimore-McBride equation	0.368 irrespective of ε_1						

The grades C, F and G, where the behaviour was not complicated by turbulent flow or by 'breaks' in the settling curves, gave better agreement with the Richardson-Zaki expression, but overall the two theoretical expressions were similar in their ability to predict $Q\varepsilon_1/V_s$.

porosity. The clearly-defined interfaces of well-developed hindered settling cannot be observed at porosities much higher than that of the 'break'. It is therefore suggested that the onset is that of true hindered settling.

Since it is obviously more satisfactory to measure the settling rate of well-defined interfaces, it would seem that the best method of determining mean equivalent particle radii from hindered settling data will be to measure them in the well-defined condition, and extrapolate them to infinite dilution by the sigmoidal expression 3.31, using the appropriate value of a. Unfortunately, no method has been found of determining a independently of V_s; and in any case such functions are not easy to fit satisfactorily to actual data (Vieira and Hoffmann, 1977). If an independent value of a were available, the method of Stevens (1951) would be available for data-fitting, but it requires more data than would normally be obtained in a sedimentation investigation. Hence it is recommended that a simpler (exponential) expression be used for the determination of mean radii by what is after all a convenient but unsophisticated method.

Equation 3.31 is a special case of a Gompertz function, which in general form is

$$y = \exp^{p - qx^{r}} \qquad (3.36)$$

where p, q and ✖ are parameters, with $q > 0$ and $0 < ✖ < 1$

(Vieira and Hoffmann, 1977).

If $y = Q/V_s$, $p = 0$, $q = {}^{1}/1-\varepsilon^*$, $x = 1-\varepsilon$ and $r = a$, we have

$$Q = V_s \exp^{-\frac{(1-\varepsilon)^a}{1-\varepsilon^*}} \qquad (3.31)$$

The characteristics of the Gompertz function are such that they must lie between two asymptotes, 0 and $\exp^p$ (here 1). These are appropriate for sedimentation, corresponding as they do to $Q = 0$ and $Q = V_s$. The function has a point of inflexion which, in terms of equation 3.31, is at $a = \log (1-\varepsilon^*)/\log (1-\varepsilon)$ and $Q/V_s = \exp^{-1}$. This fits the definition of ε^* as that value of ε for which $a = 1$ and $Q/V_s = \exp^{-1}$. It follows that ε^* is the point of inflexion of equation 3.31. The S-shaped Gompertz function is asymmetric, with the point of inflexion relatively nearer the lower asymptote; for instance, if V_s = unity, the asymptotes are $Q = 0$ and 1, and the inflexion is at $Q = 0.3679$. The curve therefore resembles a letter S with the upper half larger than the lower. A suspension obeying such a function will have $Q/V_s = \exp^{-1}$ at ε^*, and will have $Q_{\varepsilon_1}/V_s = \exp^{-1}$ only if $\varepsilon_1 = \varepsilon^*$.

If one considers the increase of Q with ε according to this function, then at the inflexion (i.e. at $\varepsilon = \varepsilon^*$) Q is increasing with ε as rapidly as is possible. It has been seen from figures 3.9 a - g, 3.11 and 3.12 that a 'break' in sedimentation behaviour is often observed at or about porosity ε_1, which is itself approximately equal to ε^*. Above ε^*, according to the function, $dQ/d\varepsilon$ would decrease with increase of ε, and increasingly

rapidly. But the 'break' shows the Gompertz-type dependence of Q on ε cannot be maintained above $\varepsilon = \varepsilon_1$ or ε^*. Instead, there is a transition to another behaviour in which, as ε increases further, there is initially a lower $dQ/d\varepsilon$ than would be expected from the Gompertz function, but where, as $\varepsilon \to 1$, $dQ/d\varepsilon$ is greater than that function would predict (figures 3.11 and 3.12).

Hindered settling has been interpreted in section 3.2.7 in terms of the sedimenting mass of particles having a high degree of symmetry, with linear upflow of supernatant liquid. Now, intuitively, the compound curves seen in figures 3.11 and 3.12 may be interpreted as follows. The increasing value of $dQ/d\varepsilon$ up to porosities in the region of ε_1 and ε^*, in accordance with the Gompertz function, may be due to 'opening-up' of this relatively symmetrical array. At some sufficiently high porosity, however, the particles would be so far apart that no symmetry could be maintained, and the ordered structure would collapse. It is presumably at $\varepsilon \simeq \varepsilon_1$, ε^* that this occurs, and for smooth, relatively uniformly-sized spheres, this porosity appears to be about 0.80. Above such a porosity, one expects a disordered mass, with non-linear upflows and correspondingly less-efficient sedimentation. It is in agreement with this that the observed Q/V_s values at $\varepsilon > \varepsilon_1$, ε^* are less than the sigmoidal function would predict (figures 3.11 and 3.12).

The porosity ε_1 was defined by Davies, Dollimore and Sharp (1976), following Kynch (1952), as that porosity for which sedimentation is at its most efficient (in terms of mass deposition rate) for a

given solid-liquid system. In terms of the present model, it represents the maximum porosity (i.e. minimum solids concentration) at which a linear-upflow, symmetrical array of particles can maintain itself. In terms of adding solid to pure liquid, it represents the threshold concentration for the onset of true hindered settling. It is reasonable to suppose that the transition between marked disorder and marked order will occur over some range of porosity, and not at some specific value of ε, particularly for systems with a range of particle sizes. The transition between sigmoidal and exponential dependence of Q upon ε will therefore also take place over a range of ε. This may account for the small difference which frequently occurs between values of ε_1 and ε^*.

This qualitative analysis appears reasonable so far, but it would predict that Q/V_s values in ordered systems should always exceed those in disordered systems, for given ε. However, figures 3.11 and 3.12 show that this is apparently not the case when $\varepsilon < \varepsilon_1$. For such porosities - i.e. where hindered settling is well developed and a highly ordered 'plug' of sedimenting material is postulated - the observed Q/V_s values are <u>less</u> than those predicted by extrapolation from the region $\varepsilon > \varepsilon_1$ (for which a disordered system is postulated).

One way out of this difficulty is to assume that, although the fluid upflow is more efficient in the ordered case, there is in fact less fluid available for upflow (compared with a disordered suspension at the same porosity) and that the second effect is

dominant over the first. It then follows that ε_1 is the threshold for a new structure of the sedimenting mass, in which more liquid is associated with the solid particles than was the case at higher porosities. This is compatible with the notion of the hindered-settling 'plug' as consisting of particles in fixed positions relative to one another, and interconnected by lenses of immobile liquid analogous to the tori of Kruyer (1958). A theory of 'capillary bonds', formed by such lenses, was developed by Ford and White (1957) to account for the fact that up to about 4% $^{v}/_{v}$ of liquid increases the strength of compacts of rounded sand grains. It seems reasonable to suspect that under appropriate conditions such bonds can form between sedimenting particles. In the case of Stokes-type settling, in which there is some movement of particles relative to one another, the interconnecting 'stagnant' volumes would be fewer or absent. For given ε, the presence of interconnecting volumes would give decreased free fluid volume for upflow, and a decreased effective density of particle, and both would contribute to a decrease of sedimentation rate under such circumstances. The 'breaks' observed by Ramakrishna and Rao (1965) and in the present study may therefore be interpreted as due to the onset of hindered settling, itself due to the formation of extended arrays of sedimenting particles (which may be individual crystals or flocs) interconnected by volumes of 'stagnant' or associated liquid. In the case of flocs, some of the associated liquid may of course be within the flocs.

The break in the log Q/ε^2 versus ε plot, and the maximum in the

plot of Q (1-ε) against ε, are shown compared with the Q versus ε curve in figure 3.13, where the data refer to grade D ballotini. It is seen that the inflexions and maximum occur at ε_1. The log Q/ε^2 and Q (1-ε) curves emphasise the change in behaviour at ε_1, compared with the impression given by the Q versus ε curve, in which the points at and near ε_1 might have been thought of as random experimental errors from a smooth curve. That they are not so, but in fact are indicative of a systematic change of behaviour, is shown by the analysis using the test equation 3.30 and exemplified by figures 3.9 d and e, 3.11 and 3.12.

It is of course true that almost any curve can be approximated if sufficient free parameters are permitted - i.e. so-called constants which cannot be verified by independent experiments - and that approximation of experimental data (such as has been done here) is not a verification of particular mathematical expressions used (von Bertalanffy, 1968). The criteria of verification and of equations representing a theory are that (i) the parameters occurring can be confirmed by independent experiment; and (ii) predictions of as yet unobserved facts can be derived from the theory. Equation 3.30 lacks rigour because, although Q, V_s and ε^* can be obtained by independent experiments, a is derived from them, and no independent method of deriving it has yet been found. For this reason, the ideas just put forward as to the nature of hindered settling are described only as a 'model'. On the other hand, the conclusions reached with ballotini would predict that other suspensions also should show a variation of the magnitude of a with ε, with $a < 1$ at $\varepsilon > \varepsilon_1$

Figure 3·13

Relationship of 'break' in plot of $\log Q/\epsilon^2$ vs. ϵ to the inflection in the Q vs. ϵ plot, and to the variation of $Q(1-\epsilon)$ with ϵ, for ballotini grade D

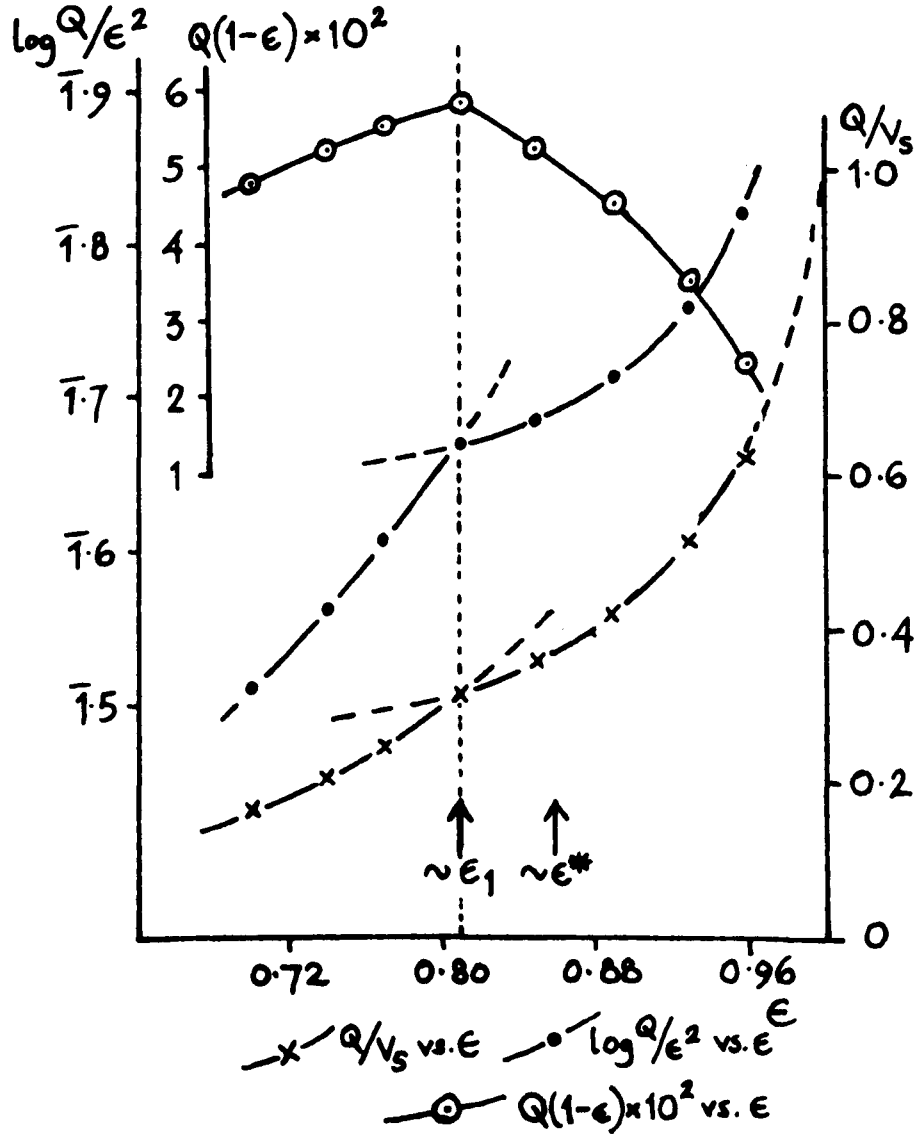

and $a > 1$ at $\epsilon < \epsilon_1$, if the model has general applicability. This possibility is discussed in section 3.4.

3.3.3 Conclusions from observations of the sedimentation of relatively monodisperse samples of ballotini in aqueous glycerol

It may be helpful briefly to summarise the conclusions reached in sections 3.3.1 and 3.3.2:

(i) The extrapolation of interface settling rates to infinite dilution is a simple method of determining mean equivalent spherical radii. For sedimentations under laminar flow (as indicated by the modified Reynolds' number $Re_m < 0.2$), it may yield somewhat low estimates, but the magnitude of error is probably not serious. Some variation of sedimentation behaviour may occur across the range of concentration studied, leading to relatively-diffuse interfaces in more-dilute samples, but the error introduced by observing these is not very important, at least in samples of relatively narrow size distribution.

(ii) The recommended method for the determination of mean equivalent spherical radius $\bar{r}$ is to plot log Q/ϵ^2 against ϵ to obtain a value for Steinour's A, and

then calculate $\bar{r}$ from the equation

$$\bar{r} = \left(\frac{9\ Q.\ 10^{A(1-\varepsilon)}}{2g\ (\rho_s - \rho_l)\varepsilon^2} \right)^{\frac{1}{2}} \qquad (3.1)$$

(iii) The change of sedimentation behaviour with concentration, reported as 'breaks' in plots of experimental data by Ramakrishna and Rao (1965), is due to a fundamental change in the concentration dependence of the sedimentation rate. At porosity values above ε_1 (the liquid volume fraction of uniformly-mixed suspension for maximum mass sedimentation rate), the change of interface settling rate Q with porosity ε is exponentially related to Q:

$$dQ/d\varepsilon = fQ \qquad (3.37)$$

whereas at porosities below ε_1, the relationship is sigmoidal:

$$dQ/d\varepsilon = f_1 Q - f_2 Q^2 \qquad (3.38)$$

(iv) Sedimentation equations representing hindered settling should be of sigmoidal type, rather than the exponential form used previously. The sedi-

mentation rate Q for a clearly-developed interface may be represented by the expression

$$Q = V_s \exp - \frac{(1-\varepsilon)^a}{1-\varepsilon^*} \qquad (3.31)$$

where $a > 1$,

ε^* = that porosity for which a = unity.

For a given suspension, the magnitude of ε^* is similar to (but apparently not the same as) that of the parameter ε_1.

3.4 Analysis of the sedimentation behaviour of calcium carbonate suspensions

The data discussed in section 3.3.2 indicate that relatively monosized samples of approximately spherical glass particles show hindered settling in which, above a certain concentration, there is a sigmoidal dependence of settling rate on concentration. Below that concentration, the dependence is exponential. The transition from one type of behaviour to the other (shown by an inflexion in the Q versus ε curve) corresponds to the 'break' in the plots of log Q/ε^2 against ε, reported by Ramakrishna and Rao (1965). However, since they also used material of relatively uniform particle size, it might be that the behaviour represented by the equations

$$Q = V_s \exp\left(-\frac{(1-\varepsilon)^a}{1-\varepsilon^*}\right) \qquad (3.31)$$

and $$Q = V_s \exp\left(-\left(\frac{1-\varepsilon}{1-\varepsilon^*}\right)^a\right) \qquad (3.35)$$

is less apparent, or not present, with suspensions of marked size distribution. The test procedure of plotting log log V_s/Q against log $(1-\varepsilon)$ has therefore been carried out on the data for a number of calcium carbonate suspensions.

In order to gain an idea of the polydispersity of the suspensions, electron micrographs of the carbonate were taken using suspensions in water and in acetone, with and without deflocculation by ultrasonic frequencies; representative photographs are shown in figures 3.14 a - f. After ultrasonic treatment, it was apparent that the individual crystals had a variety of crudely needle-like shapes, and a range of sizes up to about 6μ longest diameter. It was difficult to identify and photograph a representative range of flocs, but specimens up to about 50μ longest diameter were observed. Many of the flocs were markedly non-spherical, and in some cases were visibly porous, as the photographs show. The non-spherical nature of the flocs is also illustrated by figure 3.14 g, which is a stereoscan photograph of a floc from a suspension in acetone, photographed at a magnification of x 1625. The biggest observable radius here is 25.5μ.

The largest visible diameters of a number of flocs (from acetone

Figures 3·14a–g. Electron micrographs and stereoscan photograph of calcium carbonate from suspensions in water and acetone

a

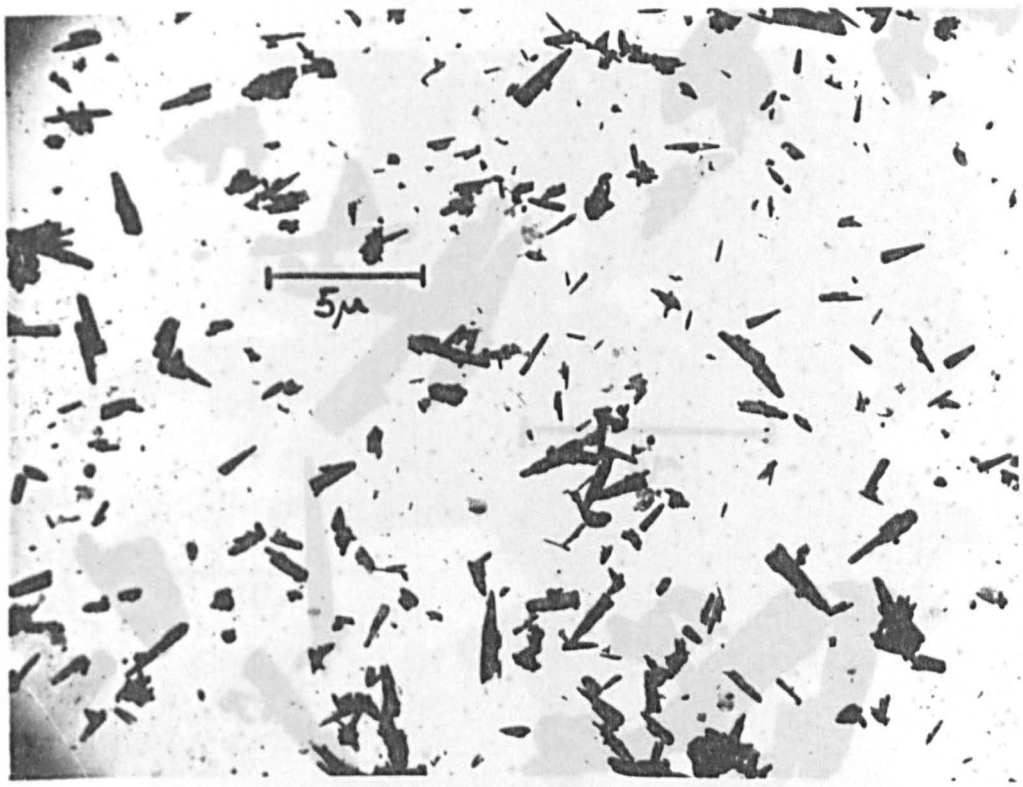

b

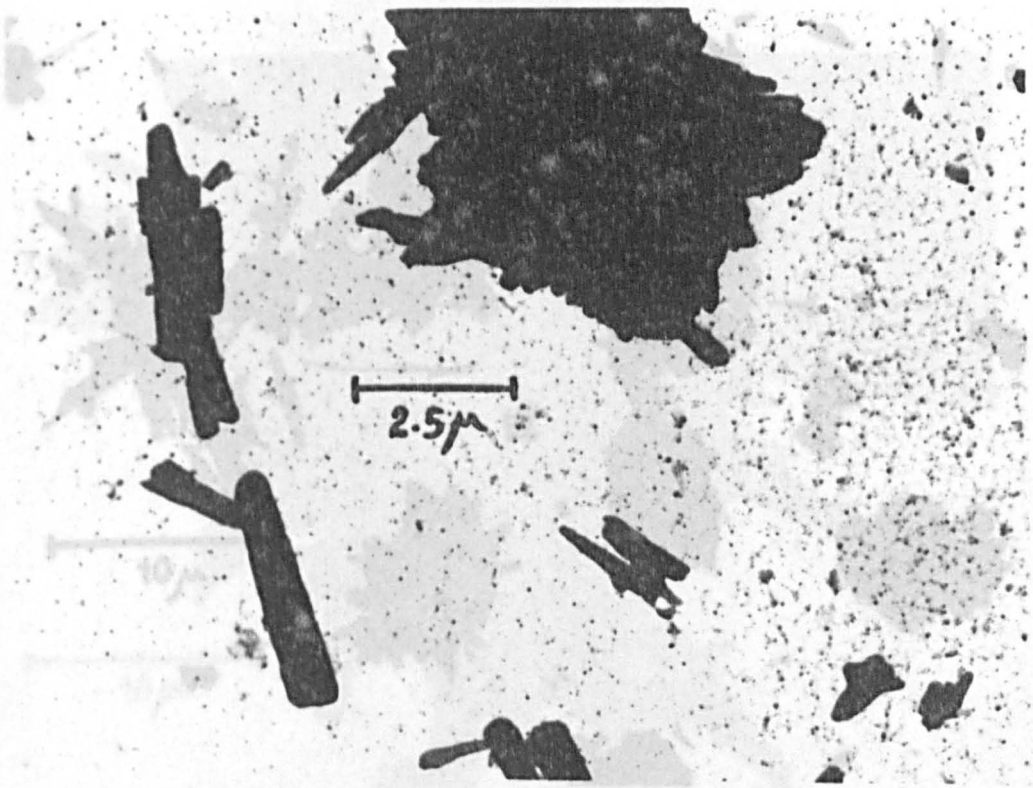

c

d

e

f

suspension) were measured visually by electron microscopy at a magnification of x 4000, and the results (table 3.11) compared with those from the sedimentation of the same suspension (table 3.12).

Table 3.11

Largest visible radii of calcium carbonate

g

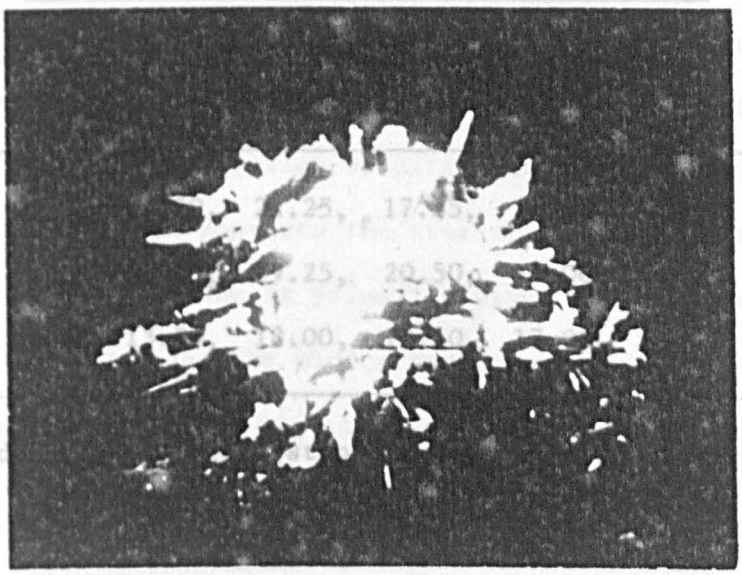

19.75,	[illegible]	[illegible]	[illegible]	15.75,
22.00,	[illegible]	[illegible]	[illegible]	
18.25,	[illegible]	[illegible]	[illegible]	

Mean rad[illegible]adius,

$SD_{\bar{r}}$ = ±

Table 3.12

Sedimentation data for calcium carbonate in acetone

e	0.9903	0.9816	0.9722	0.9632
Q ($cm.s^{-1}$)	0.4205	0.2913	0.2550	0.2085
r (μ)	20.70	19.50	20.80	21.30

Mean radius, $\bar{r}$ = 20.6μ; standard deviation of this radius, $SD_{\bar{r}}$ = ± 0.67μ.

suspension) were measured visually by electron microscopy at a magnification of x 4000, and the results (table 3.11) compared with those from the sedimentation of the same suspension (table 3.12).

Table 3.11

Largest visible radii of calcium carbonate flocs from suspension in acetone (μ)

19.75,	18.00,	17.50,	22.25,	17.25,	18.00,	18.25,	15.75,
22.00,	12.00,	16.25,	19.25,	20.50,	16.00,	20.75,	
18.25,	22.75,	13.75,	18.00,	13.50,	17.00,	22.75	

Mean radius, $\bar{r}$ = 18.1μ; standard deviation of this radius, $SD_{\bar{r}}$ = ± 3.1μ.

Table 3.12

Sedimentation data for calcium carbonate in acetone

ε	0.9903	0.9816	0.9722	0.9632
Q ($cm.s^{-1}$)	0.4205	0.2913	0.2550	0.2085
r (μ)	20.70	19.50	20.80	21.30

Mean radius, $\bar{r}$ = 20.6μ; standard deviation of this radius, $SD_{\bar{r}}$ = ± 0.67μ.

Although the difference between these means is statistically significant ($t = 3.55$, $p < 0.01$), it must be remembered that the techniques used for measurement were very different from one another, and that it is difficult to know how much confidence to place in the accuracy of the mean values. Probably of more interest is the suggestion, based on the reasonable agreement of the mean values, that the sedimentation behaviour appears to be governed by the mean longest diameter of the flocs, even in the presence of a large variety of particle sizes and shapes. This is reminiscent of a conclusion by Eirich and Mark (1937), namely that the factor which converts the true volume of a particle into its effective volume is primarily given by its 'outer outline'. In any case, the micrographic examination showed that the carbonate suspensions were markedly polydisperse, and they therefore afford a test of the sigmoidal equation for such systems.

Figures 3.15 a - n show the results of analysing sets of Q and ε data, taken from section 2.3, by plotting $\log_{10} \log_{10} V_s/Q$ against $\log (1-\varepsilon)$ to obtain the slope a. The values of V_s taken are those derived by extrapolating the Richardson-Zaki plots of $\log Q$ and $\log \varepsilon$ to $\log \varepsilon = 0$. The curves show a general tendency for a to have a value of unity in the region about ε_1, as found for relatively monodisperse samples of ballotini. Apart from that, however, the interpretation is not as simple as it was for ballotini. For instance, suspensions of calcium carbonate in water and sodium chloride solutions (figures 3.15 i, j, k, m, n) show little tendency to variation

Figures 3·15 a-n

Variation of the power number a with solid volume fraction

for calcium carbonate in various liquids

Figure 3·15 a Calcium carbonate / benzene

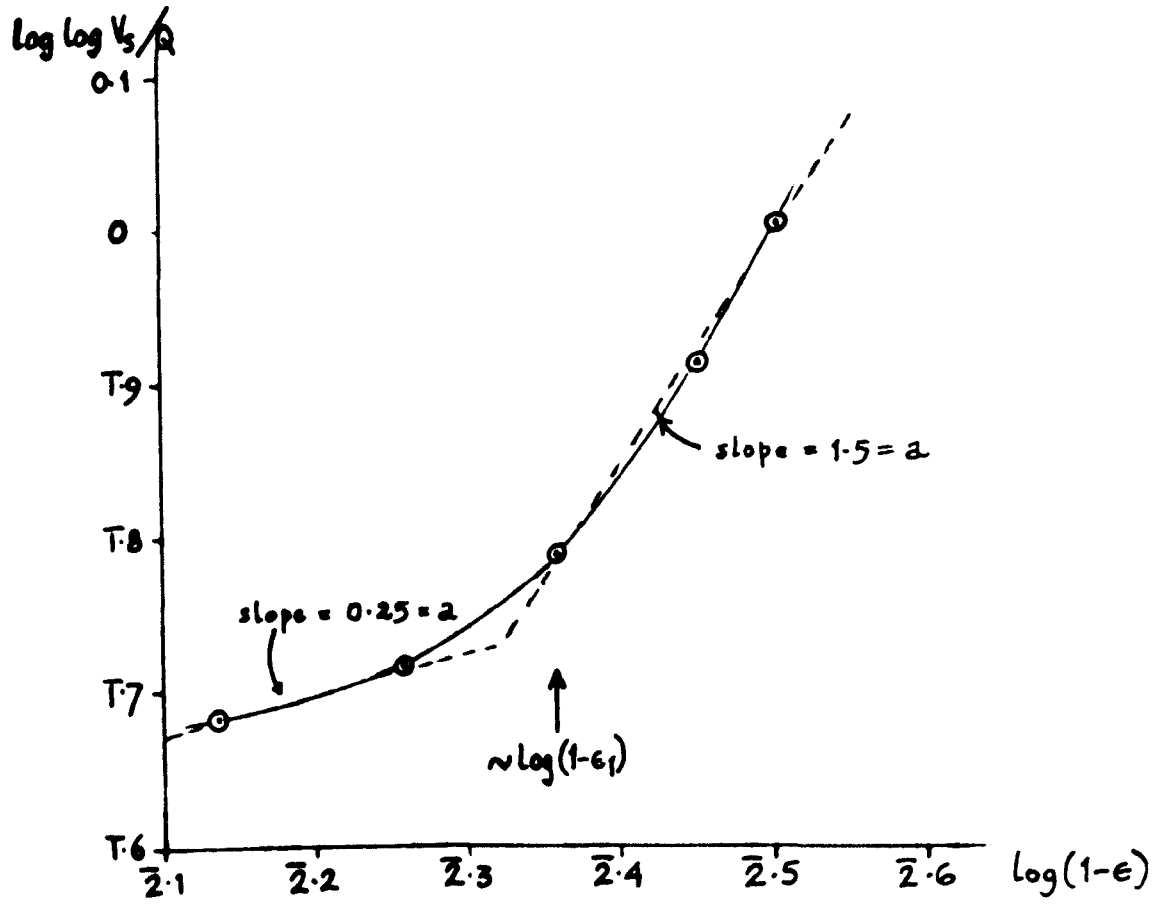

Figure 3·15 b Calcium carbonate/diethyl ether

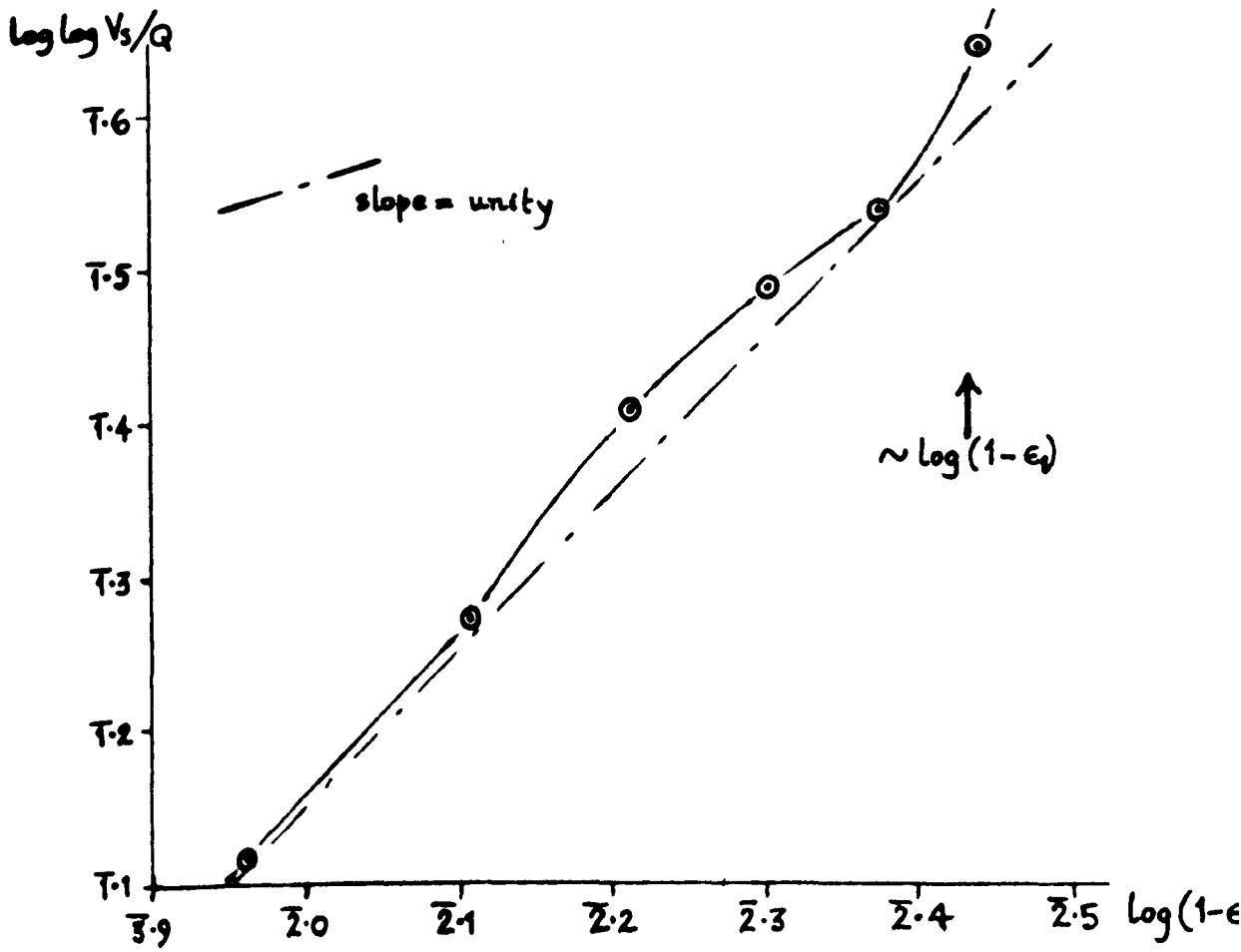

Figures 3·15 c-g.

Calcium carbonate/ethyl acetate

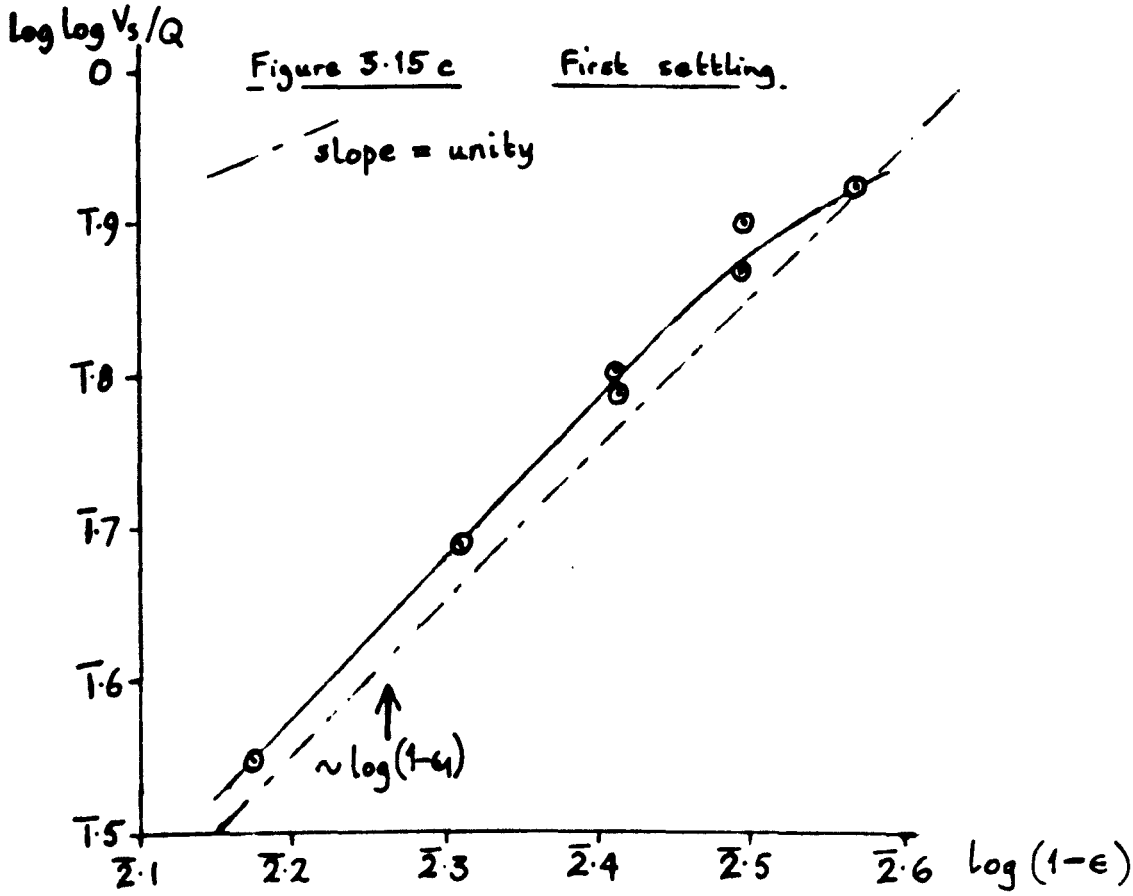

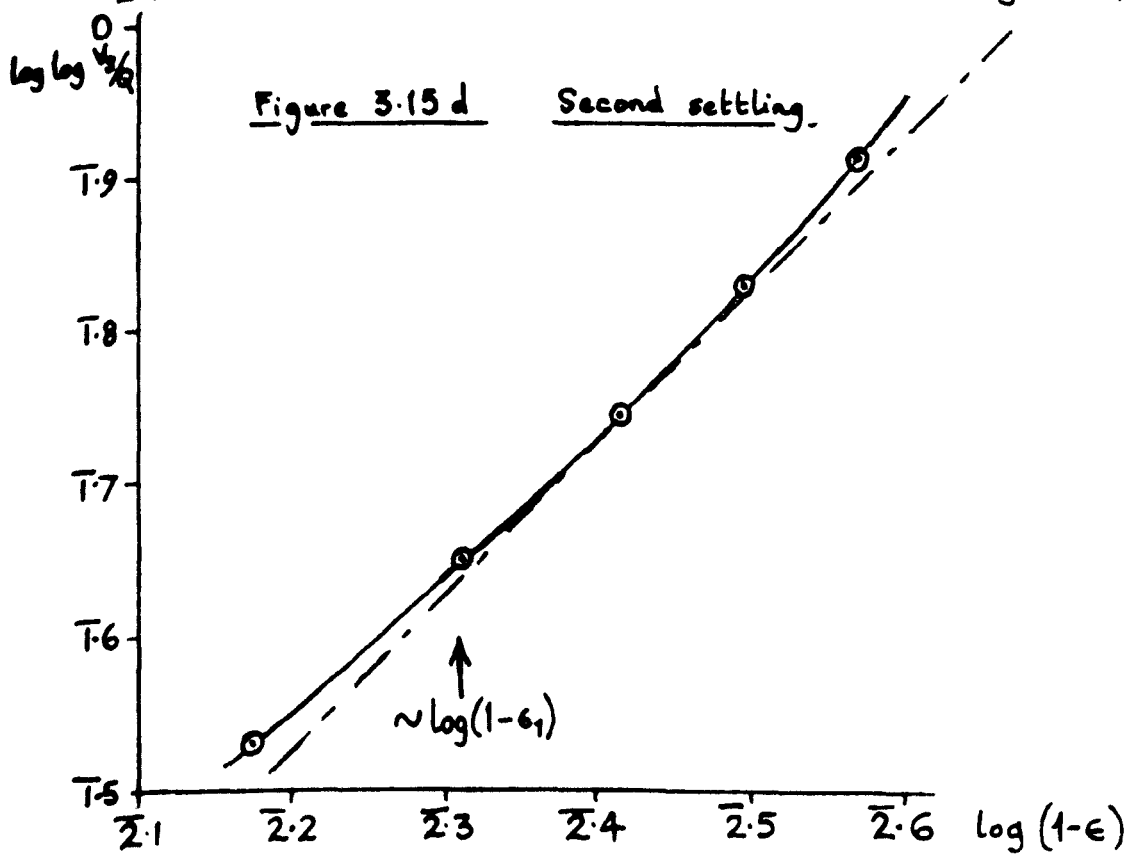

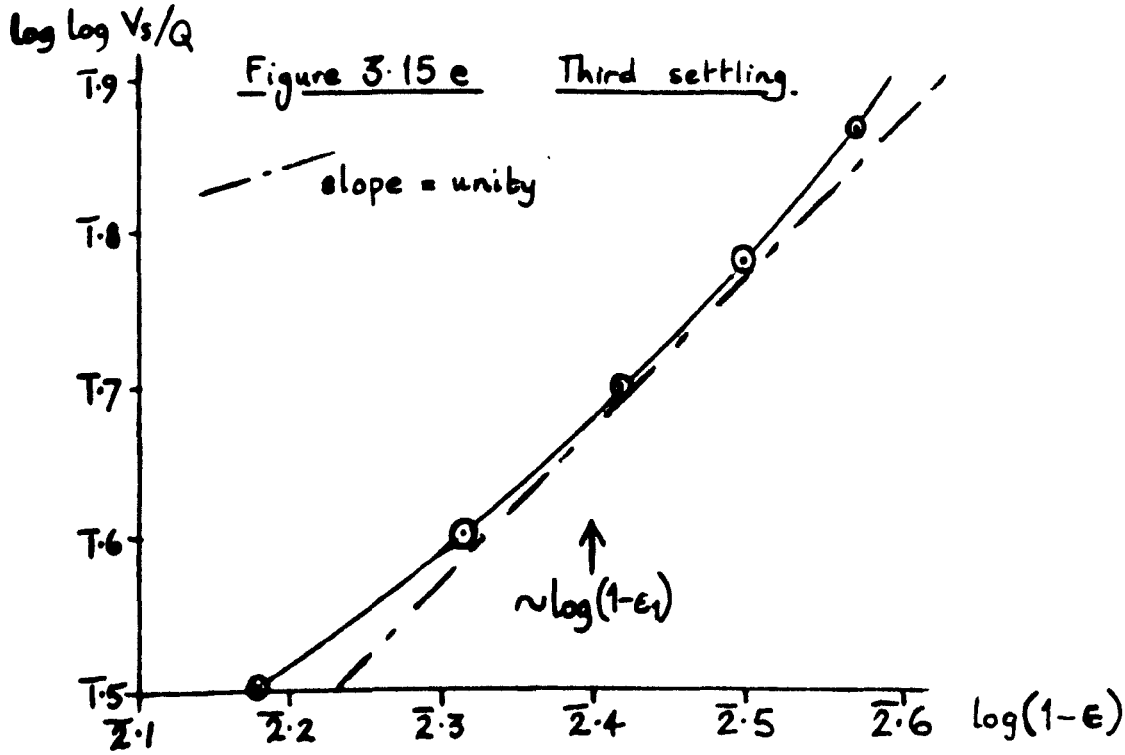
log log Vs/Q
Figure 3·15 e
Third settling.
slope = unity
T·9
T·8
T·7
T·6
T·5
∝log(1-ε)
2·1
2·2
2·3
2·4
2·5
2·6
log(1-ε)

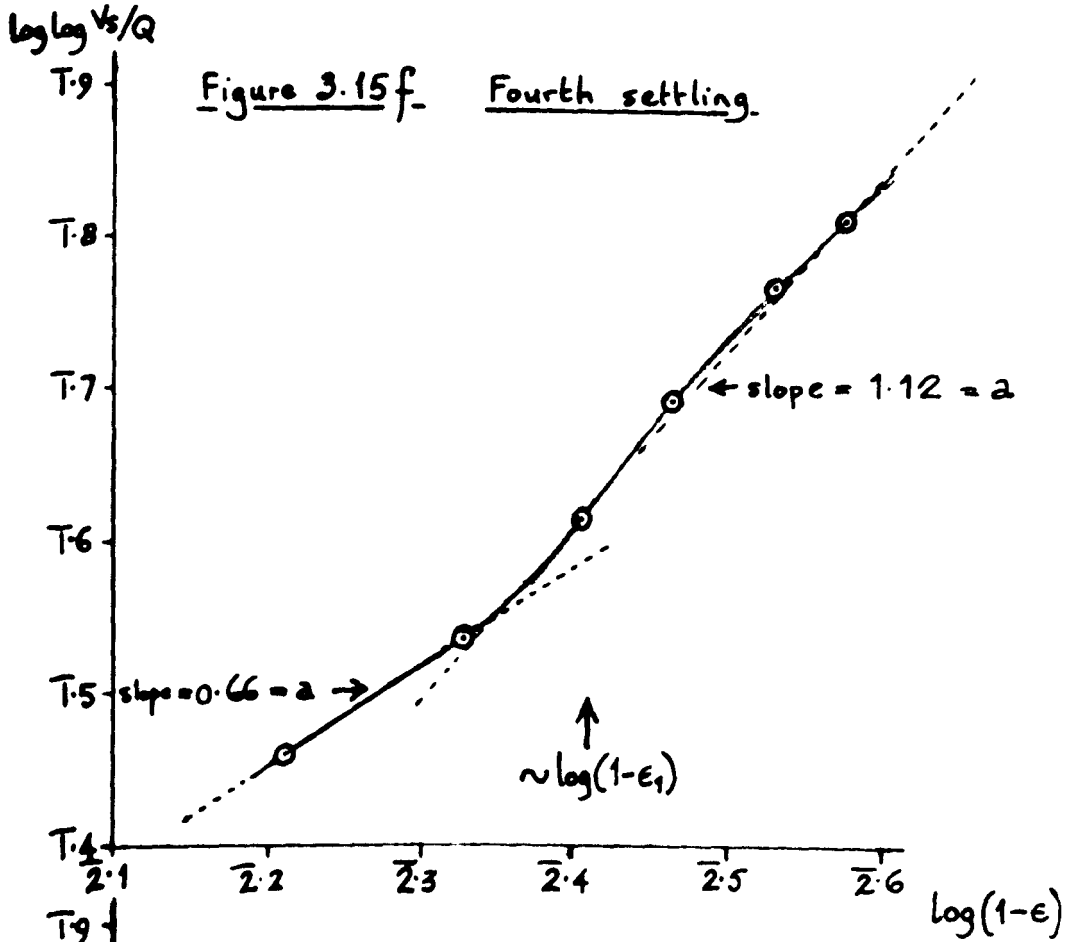

Figure 3.15 f. Fourth settling.

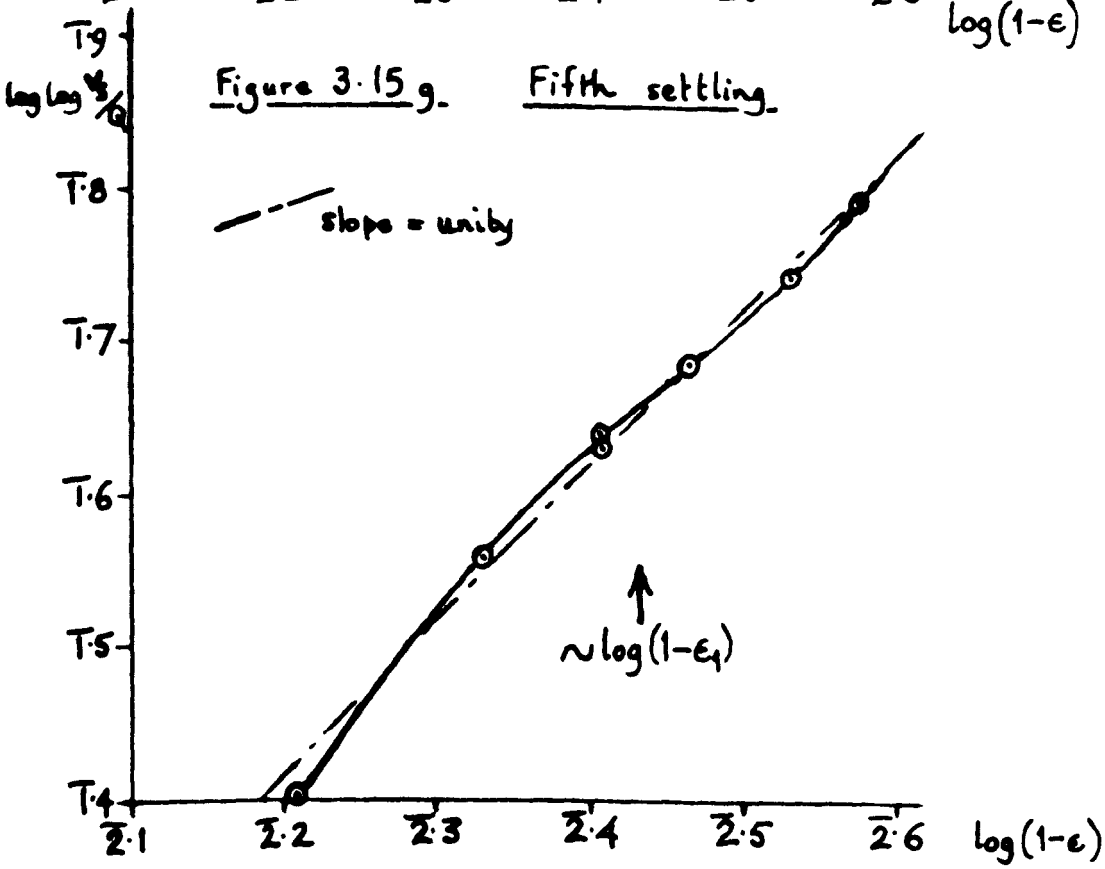

Figure 3.15 g. Fifth settling.

Figure 3·15 h Calcium carbonate/ethyl acetoacetate

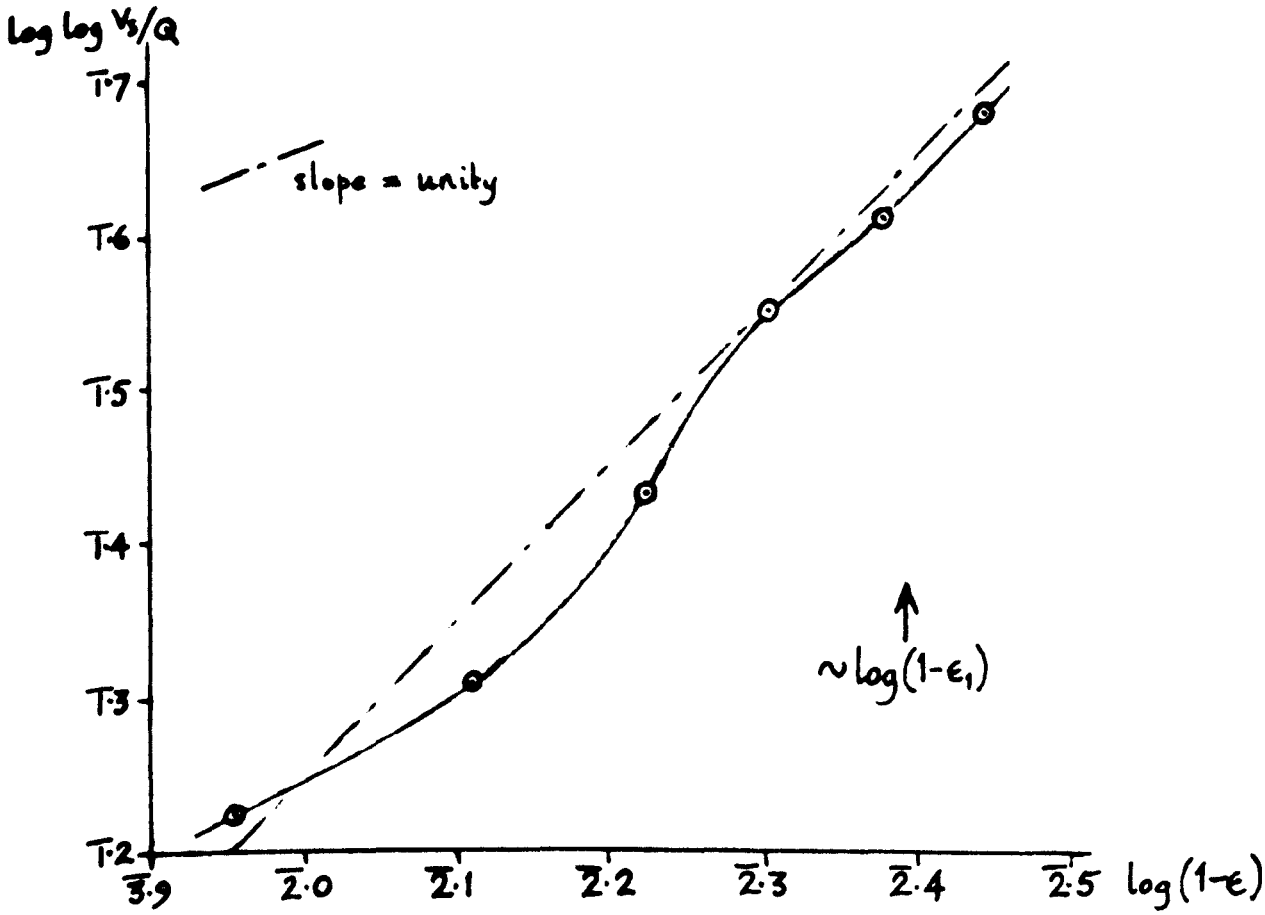

Figure 3·15 i Calcium carbonate / 0·137 M NaCl

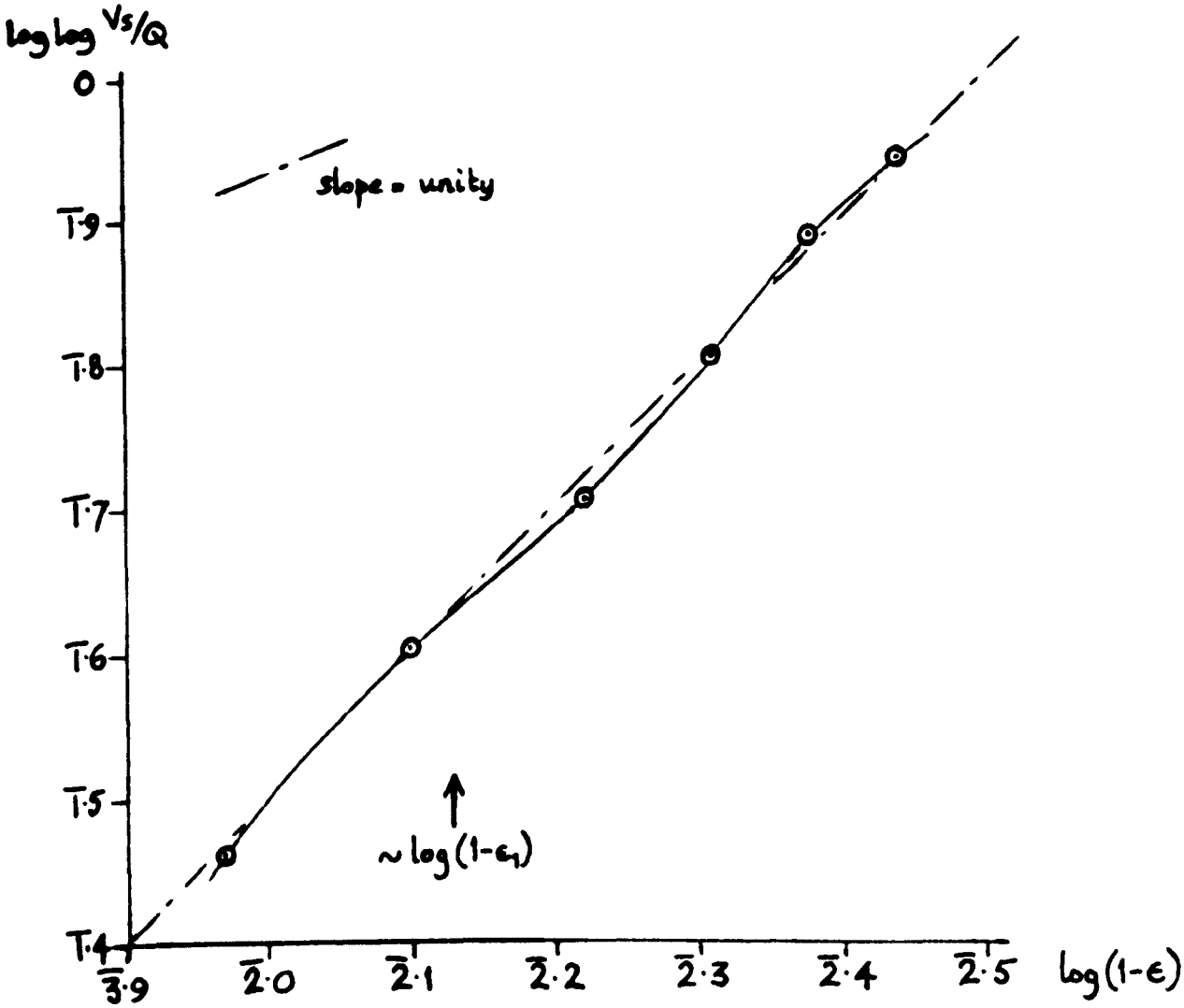

Figure 3·15 j Calcium carbonate / 0·458 M NaCl

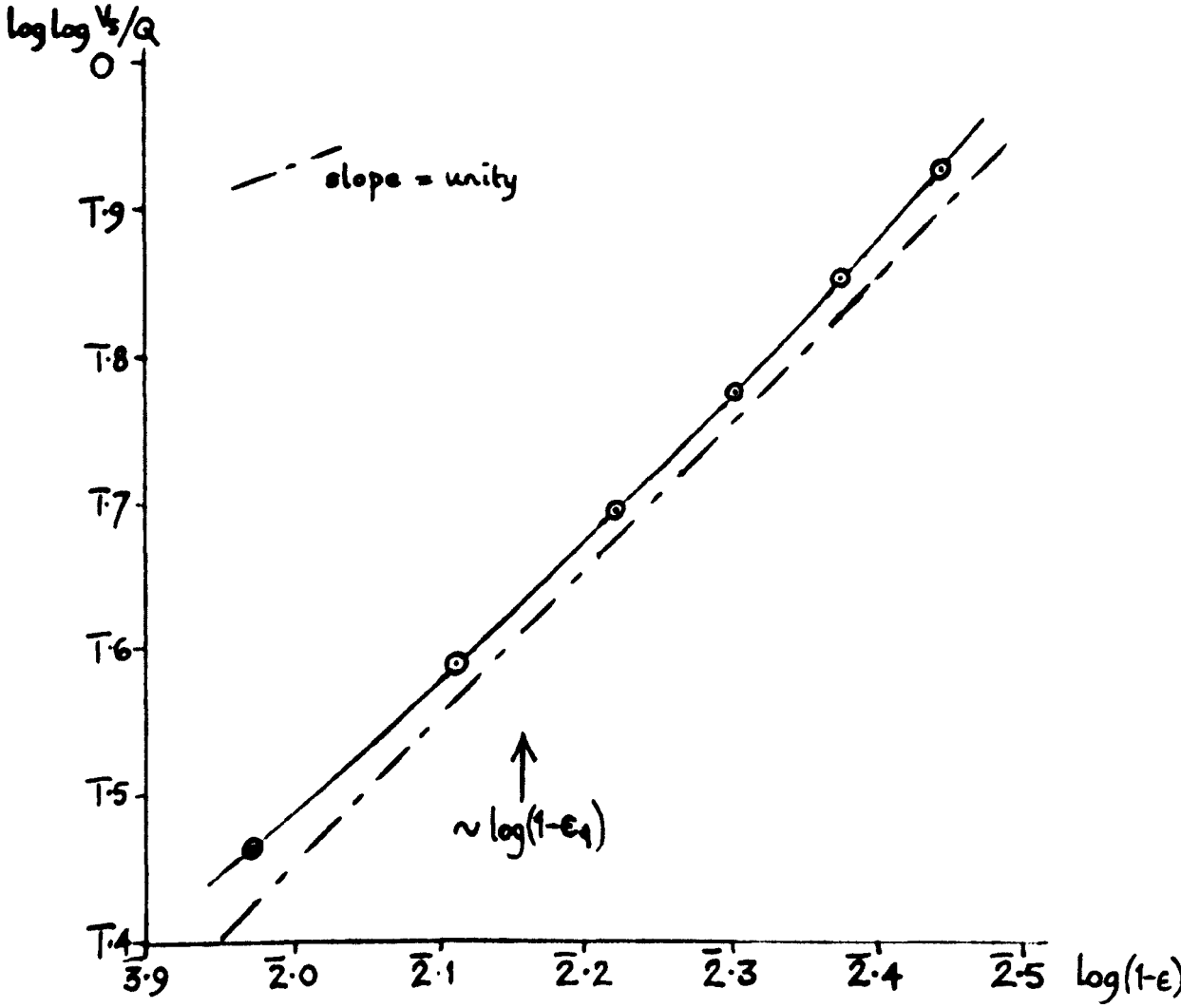

Figure 3·15 k Calcium carbonate / 0·915 M NaCl

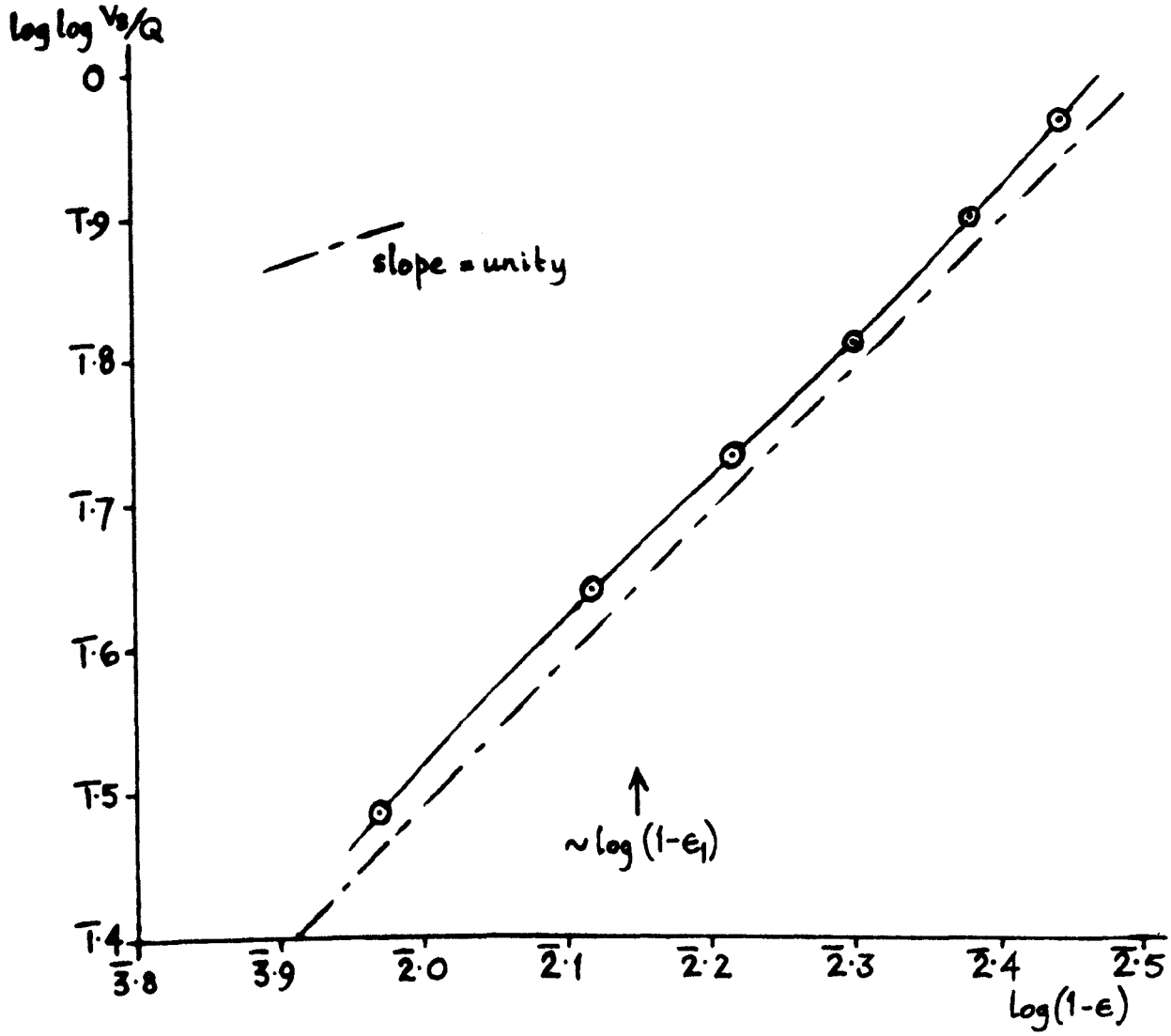

Figure 3·15 m Calcium carbonate/sodium chloride solutions

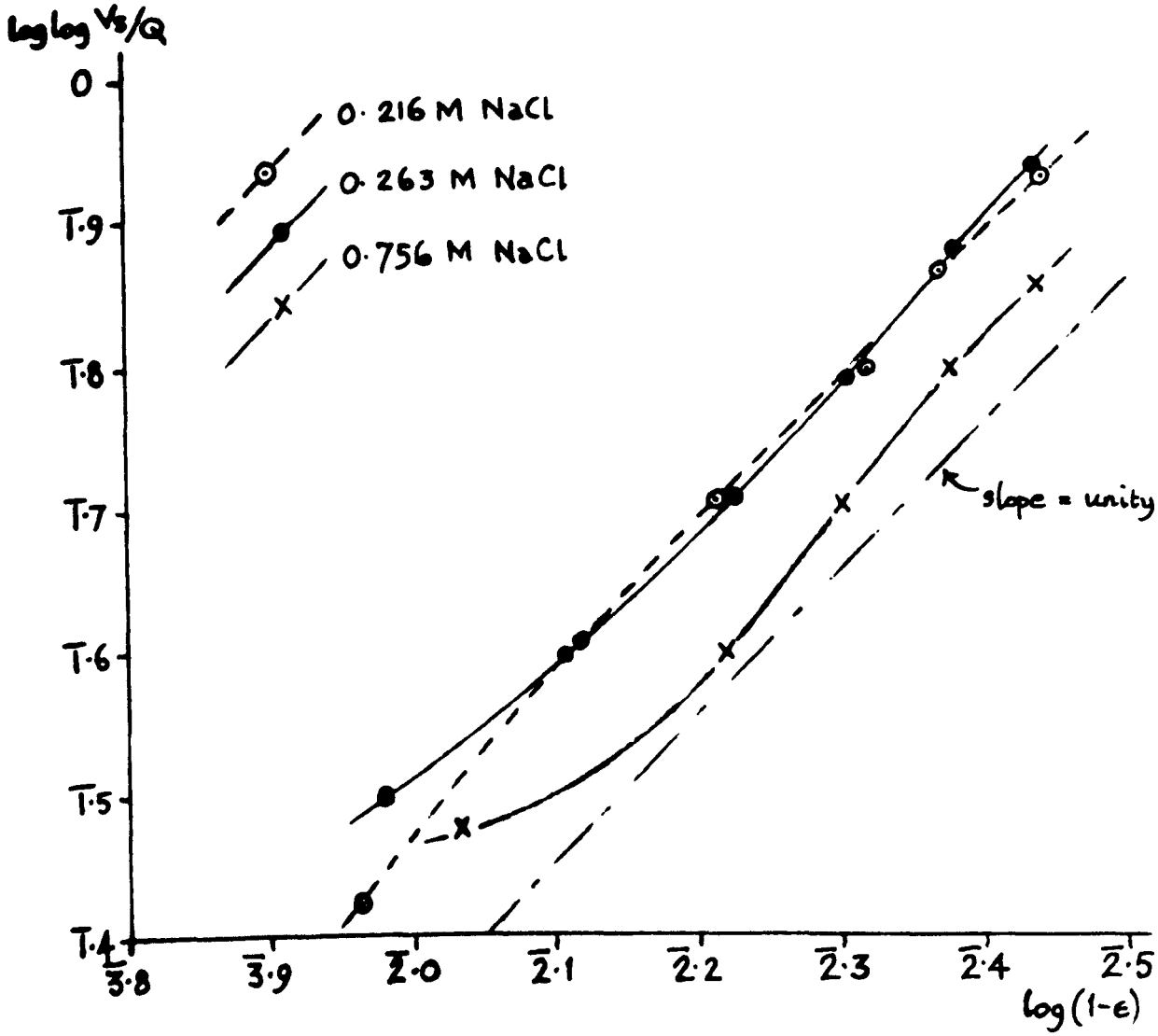

Figure 3·15 n Calcium carbonate / water

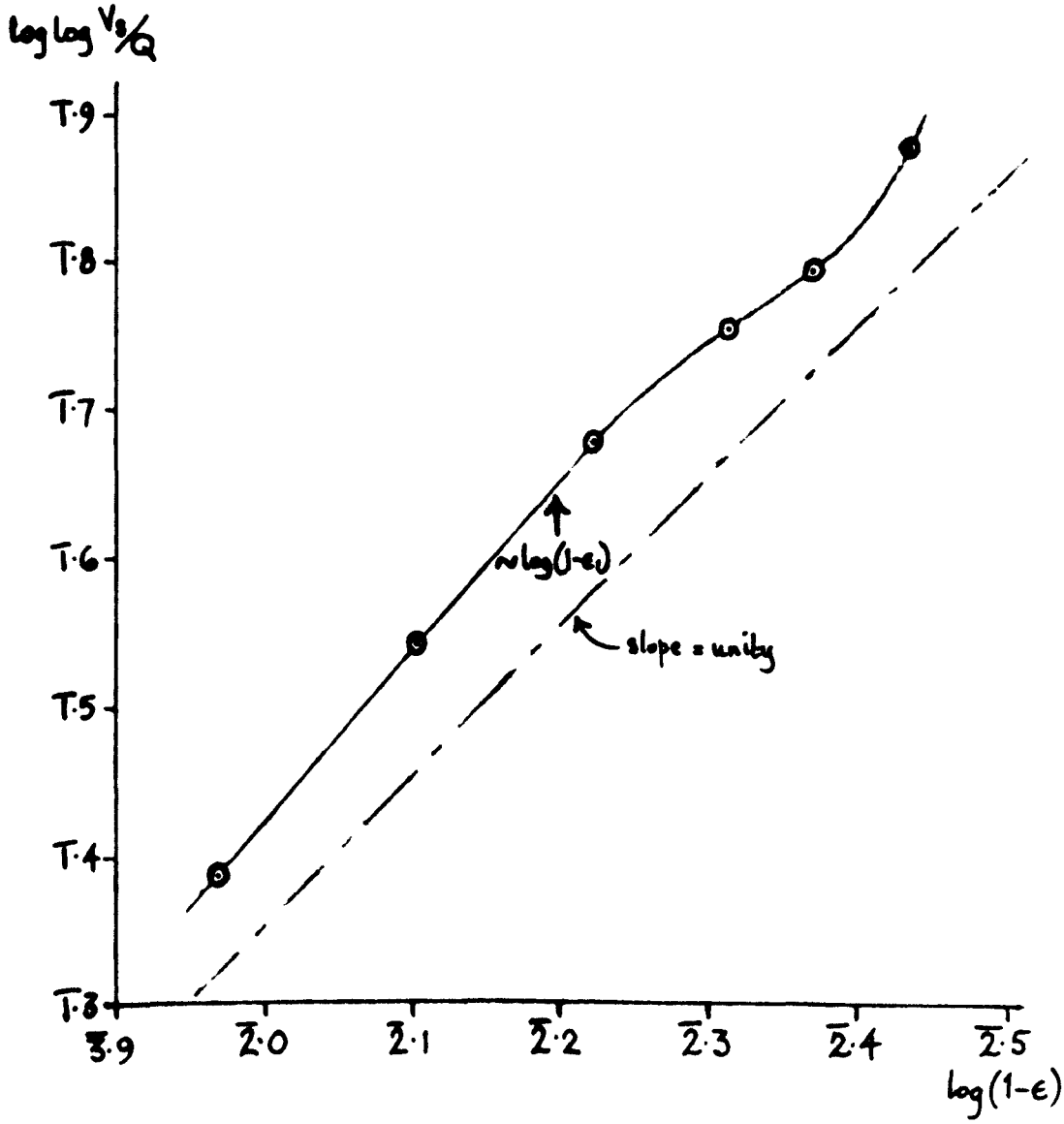

from a = 1, which means that the data would be adequately fitted by an exponential-type equation over the range of porosities examined. On the other hand, dry benzene (figure 3.15 a) gave clear evidence of a change from exponential to sigmoidal dependence of settling rate on porosity, with decreasing porosity, as did some of the repeated settlings in dry ethyl acetate (figures 3.15 d, e, f). The data for suspensions in diethyl ether and ethyl acetoacetate yielded complex curves (figures 3.15 b, h), although the acetoacetate curve could be regarded as showing an increase of the slope, from $a < 1$ to $a > 1$, with decreasing porosity. On balance, analysis of the behaviour of polydisperse suspensions of calcium carbonate supports the conclusion reached in section 3.3.2, namely that an exponential dependence of interface settling rate on porosity is only a partial representation of the true rate/porosity relationship, and that above a certain porosity, a sigmoidal dependence occurs. In general, however, the behaviour is less clearly developed than with relatively monodisperse samples. In particular, it has not been demonstrated that calcium carbonate suspensions in water and 0.137 - 0.915 M sodium chloride solutions show the transition from exponential to sigmoidal behaviour observed with the carbonate in some organic liquids and with ballotini in aqueous glycerol. It may be that there are two different mechanisms of hindrance being exhibited, as all the systems do exhibit clear interfaces at about their respective ϵ_1's, even though the sedimentation rate/porosity dependence varies from one set of experiments to the other.

3.5 Tests of the robustness of interpreting sedimentation behaviour in terms of the parameter a

An uncertainty arises in the plot of log log V_s/Q against log $(1-\varepsilon)$, when polydisperse suspensions are concerned, since the true value of V_s is not known. Any error in V_s, for given Q and ε, will result in a miscalculation of a. It was concluded in section 3.3.1 that extrapolated mean particle radii might be in error by several per cent on average. Since (from Stokes' Law) $V_s \propto r^2$, the error in V_s would be larger, perhaps up to 15% or 20%. It was therefore necessary to check what effect an erroreous value of V_s has on the value calculated for a.

Figures 3.15 p and q show the variations in the plot of log log V_s/Q against log $(1-\varepsilon)$ caused by a variation of ± 20% in the value chosen for V_s. This variation is not sufficient to cause confusion in a case where there is a clear transition from exponential to sigmoidal behaviour (figure 3.15 p), except if the curve were used to try to identify ε^* (i.e. the porosity for which the slope a = 1). In contrast, with calcium carbonate in 0.458 M sodium chloride solution, where no such transition was observed, a ± 20% variation in V_s can change the slope of the curve from a = 0.86 (all-exponential behaviour) to a = 1.22 (all-sigmoidal behaviour), since the originally-chosen V_s gave a = unity (figure 3.15 q). However, such relatively-linear plots arise from data where the plot of e.g. log Q against log ε is itself relatively linear. Extrapolation to obtain log V_s should then not be the cause of much uncertainty, and therefore

Figures 3·15 p,q.

The effect on the log log V_s/Q vs. log $(1-\epsilon)$ plot of different values of V_s.

Figure 3·15 p Calcium carbonate/benzene

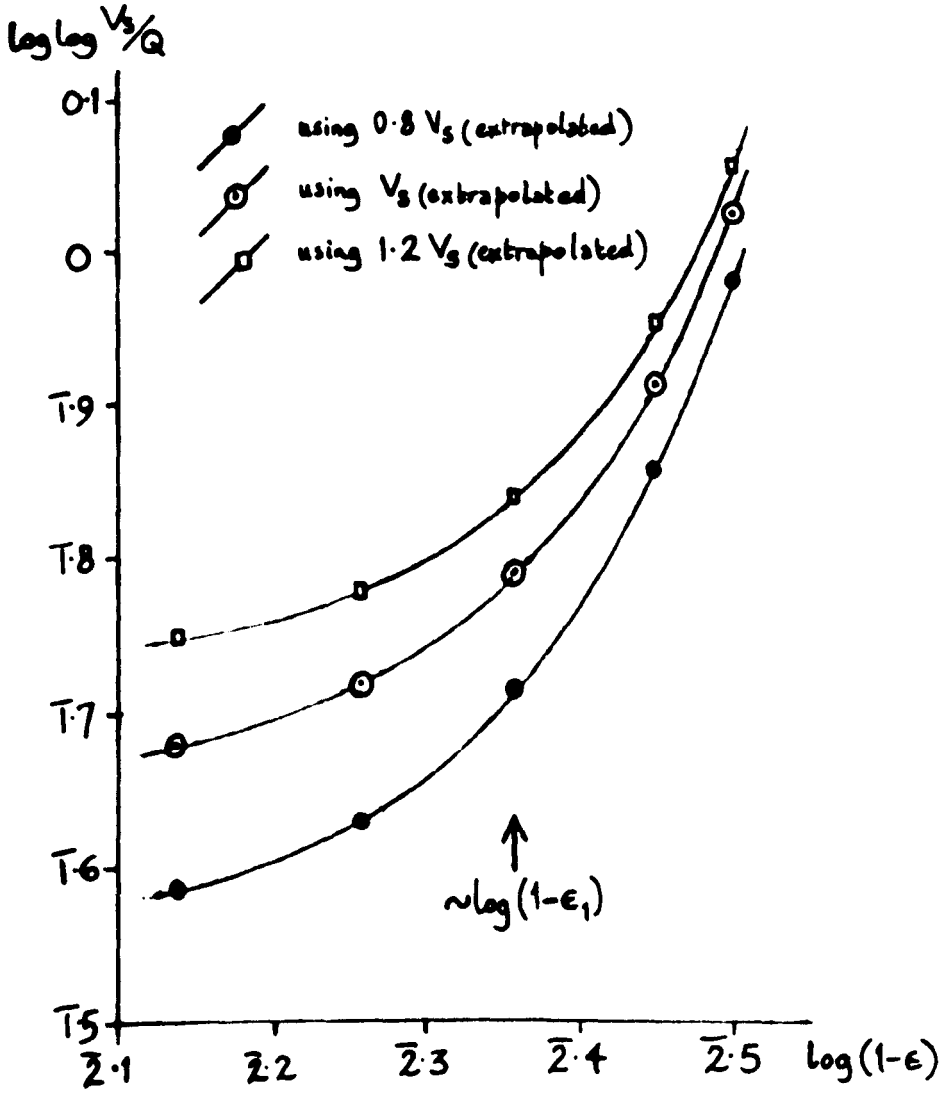

Figure 3·15 q - Calcium carbonate/0·458 M NaCl

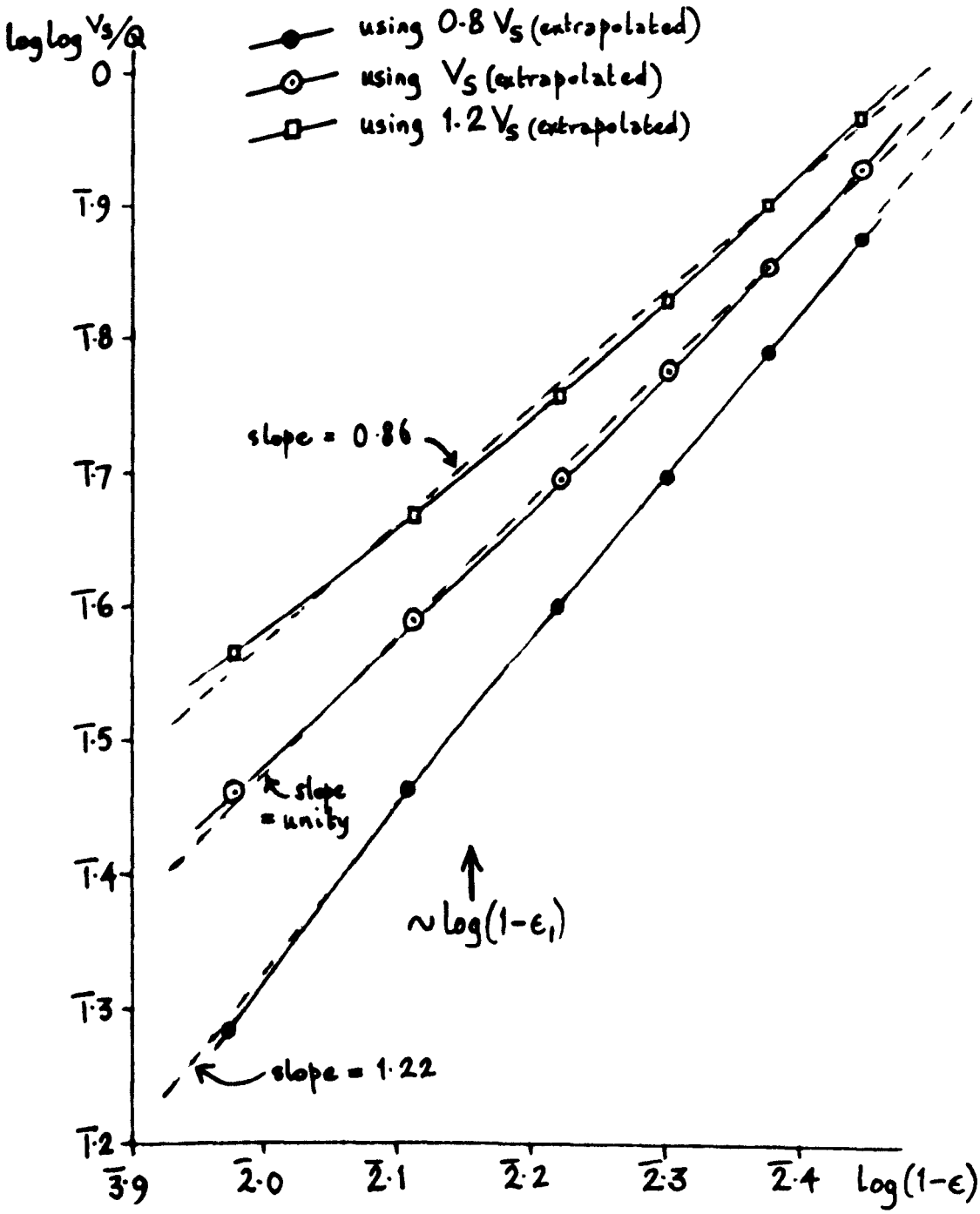

the true value of a should not be far from the calculated value. This is particularly the case since the range of porosities examined spanned ε_1. Any 'break' in the sedimentation curve would have been expected to occur in that region, and - as none was observed - the extrapolation to log ε = 0 should be valid. It is concluded that uncertainties in V_s are unlikely to cause large errors in the magnitude of a.

Another doubt arises when comparing the equation

$$Q = V_s . \exp - \frac{(1-\varepsilon)^a}{1-\varepsilon^*} \qquad (3.31)$$

with the generalised Steinour empirical equation

$$Q = V_s \varepsilon^2 10^{-A(1-\varepsilon)} = V_s \varepsilon^2 \exp^{-2.303 A (1-\varepsilon)} \qquad (1.51)$$

since the latter has the term ε^2, which arose from Steinour's assumption that the effective density difference in a suspension is $(\rho_s - \rho_l)\ \varepsilon$, rather than simply $(\rho_s - \rho_l)$, and from the relationship between the interface settling rate Q and the relative velocity between particles and fluid, V : $Q = V\varepsilon$ (Steinour, 1944 a). Richardson and Zaki's (1954 b) suggestion that the density difference is truly $(\rho_s - \rho_l)$ in hindered settling, because the particle settles through liquid, and not through suspension, would modify equation 1.51 to

$$Q = V_s \varepsilon . 10^{-A(1-\varepsilon)} \qquad (3.39)$$

These considerations would modify equation 3.31 to

$$Q = V_s\, \varepsilon .\, \exp - \frac{(1-\varepsilon)^a}{1-\varepsilon^*} \qquad (3.40)$$

and

$$Q = V_s\, \varepsilon^2 .\, \exp - \frac{(1-\varepsilon)^a}{1-\varepsilon^*} \qquad (3.41)$$

Figures 3.15 r, s show that adopting these equations in place of equation 3.31 makes no meaningful difference to the magnitude of a, and the interpretation of sedimentation behaviour in terms of a is thus not affected by the choice of equation.

It is concluded that the parameter a is not susceptible to serious error because of uncertainties in V_s or in precise choice of sedimentation equation; i.e. it is 'robust' against these uncertainties. The remaining terms of the sedimentation equations (Q and ε) can be determined with accuracy and precision. Therefore, there is robustness of interpretation of sedimentation behaviour in terms of a.

The parameter ε^*, in contrast, is varied by the choice of equation. For Steinour's (1944 a) tapioca/oil data, ε^* has the values shown in Table 3.13.

Figures 3·15 r, s

The effect on the parameter a of variants of the log log V_s/Q – log (1-ε) plot

Figure 3·15 r Calcium carbonate / 0·458 M NaCl

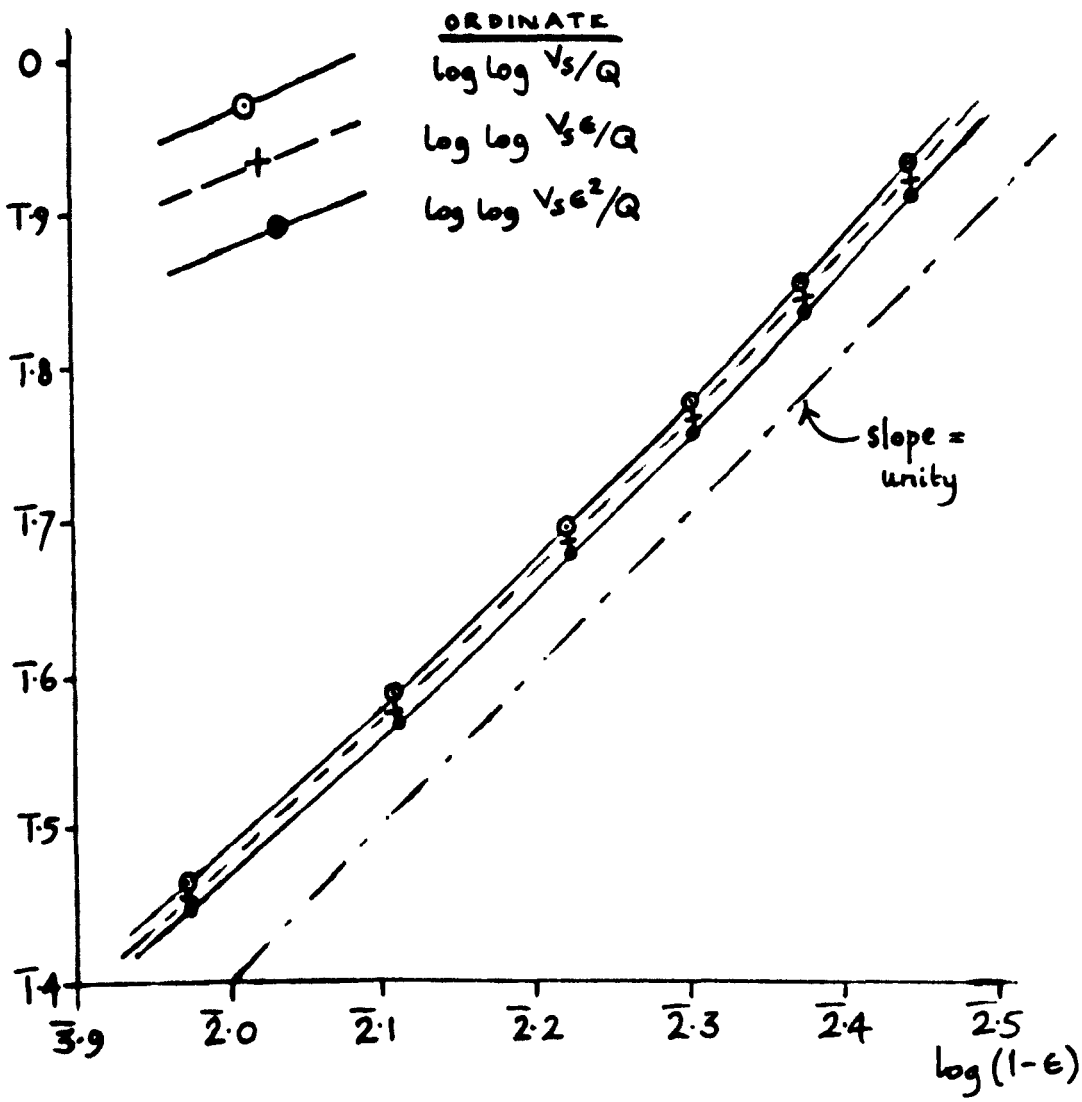

Figure 3·15 s Steinour's tapioca/oil suspensions

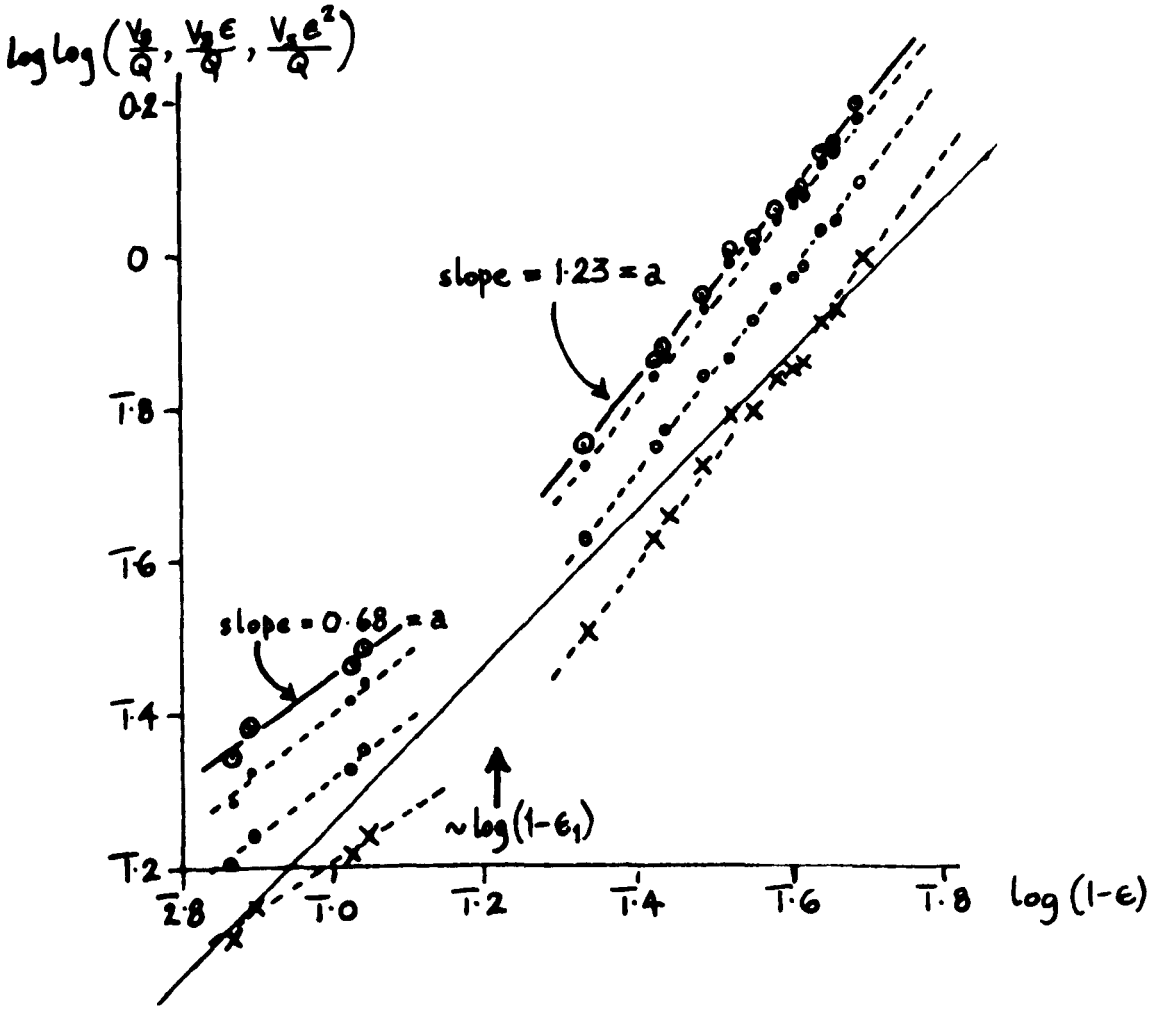

log log V_s/Q, using V_s corrected for wall effect

log log V_s/Q, using V_s observed

log log $V_s\epsilon/Q$, using V_s observed

log log $V_s\epsilon^2/Q$, using V_s observed

linear plot, slope = unity, expected from Steinour empirical equation – contrast the twin slopes of the experimental data

Table 3.13

Variation of the porosity ε^* with choice of sedimentation equation, for Steinour's tapioca/oil data

Equation		Value of ε^*
$Q = V_s \exp\left(-\frac{(1-\varepsilon)^a}{1-\varepsilon^*}\right)$	(3.31)	0.845
$Q = V_s\, \varepsilon . \exp\left(-\frac{(1-\varepsilon)^a}{1-\varepsilon^*}\right)$	(3.40)	0.812
$Q = V_s\, \varepsilon^2 . \exp\left(-\frac{(1-\varepsilon)^a}{1-\varepsilon^*}\right)$	(3.41)	0.761

There is a gap in Steinour's data between $\varepsilon = 0.785$ and $\varepsilon = 0.890$, but the values show that $Q/V_s = \exp^{-1}$ must lie in this region. The equation 3.41, modelled on that of Steinour, therefore gives too low an estimate of ε^*. The lack of data prevents a choice between $\varepsilon^* = 0.845$ and $\varepsilon^* = 0.812$ (i.e. between equations 3.31 and 3.40) and careful experimental determination of ε^* would be required, on systems of very accurately known V_s, to finally decide between the equations. Equation 3.40 has the attractive feature that it relates two relative liquid/solid velocities, Q/ε and V_s, whereas equation 3.31 uses V_s and Q, which is only one component of such a velocity.

In the present work, the simpler equation 3.31 has been used, as a has proved of more interest than ϵ^*.

Figure 3.15 s also shows that Steinour's tapioca/oil data clearly support the hypothesis developed in the present study, namely that the interface settling rates above ϵ_1 have an exponential dependence on porosity, and a sigmoidal dependence on porosity below ϵ_1. The line of unit slope across the graph is the plot of log log $V_s \epsilon^2/Q$ against log $(1-\epsilon)$ to be expected from Steinour's empirical equation, since from

$$Q = V_s \epsilon^2 . 10^{-1.82(1-\epsilon)} \qquad (1.12)$$

$$\log \log \frac{V_s \epsilon^2}{Q} = \log 1.82 + \log (1-\epsilon)$$

and a plot of log log $\frac{V_s \epsilon^2}{Q}$ against log $(1-\epsilon)$ should therefore have unit slope.

The analysis of the data afforded by the plot shows clearly that the equation is an over-simplification of the experimental behaviour. Steinour's data for glass spheres in 0.1% sodium hexametaphosphate also show a sigmoidal dependence below ϵ_1 (figure 3.15 t). In this case, the data do not allow an analysis above ϵ_1, but once again, a decreases towards unity as ϵ increases towards ϵ_1.

Figure 3·15 b

Values of the parameter a for Steinour's glass spheres A in aqueous hexametaphosphate

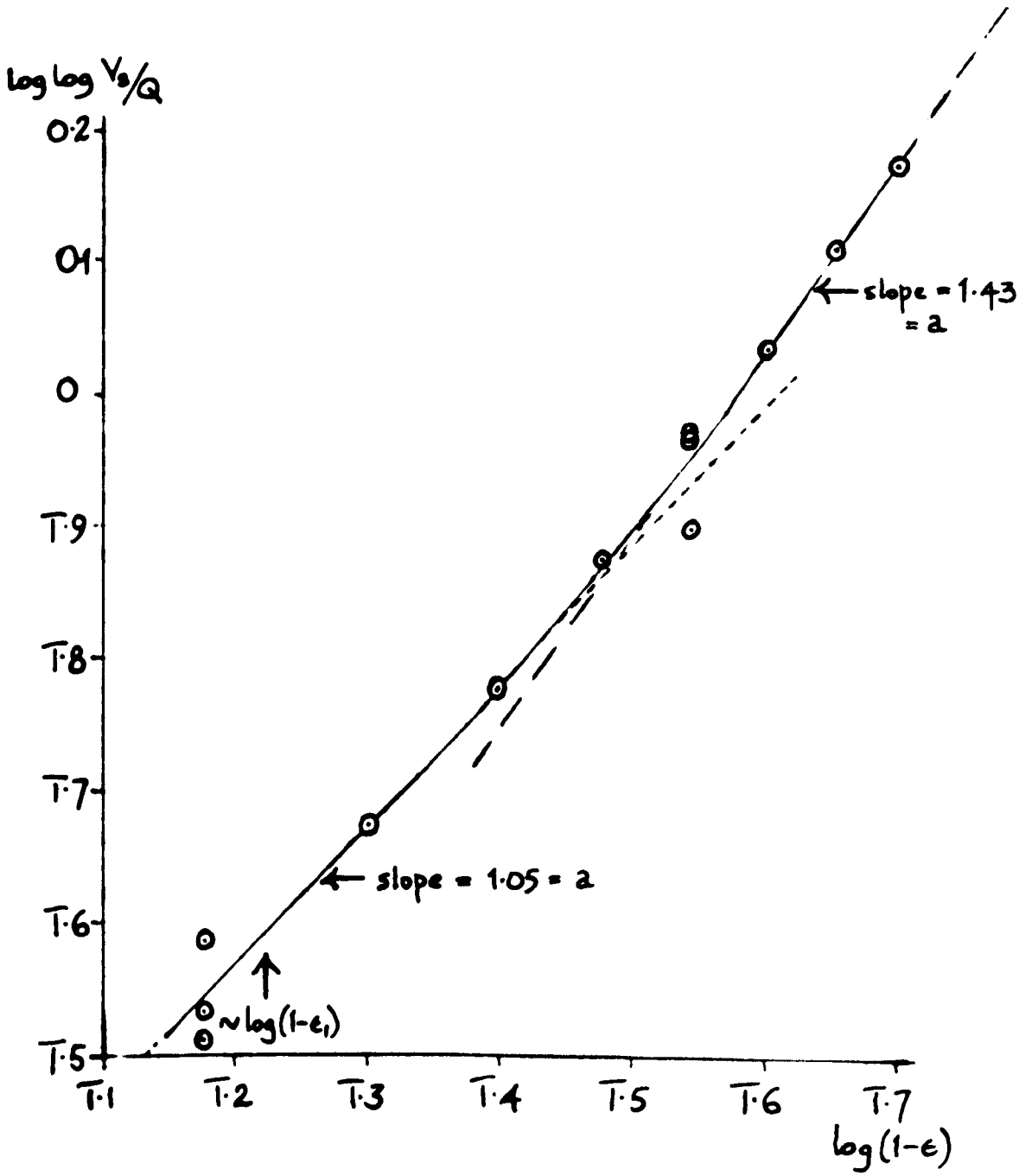

3.6 Factors affecting the dispersion and hindered settling of calcium and other carbonates in a variety of liquids

The literature survey which yielded the data for table 3.2 indicated that few if any workers have examined the effect of numerous different liquids on sedimentation rates for a given solid. Since one of the shortcomings of existing theories is their failure to correlate sedimentation rates with chemical properties, it seemed desirable to conduct such an investigation. The sedimentation behaviour of calcium carbonate has been examined in a variety of liquids, and some qualitative experiments have been carried out with carbonates of copper and nickel. Table 3.14 shows representative experimental data and the results calculated from them by using the methods outlined in section 3.1 (iv) for A, $\bar{r}$, mean $\bar{r}$ and the standard deviation of $\bar{r}$. The value of V_s in the same table was obtained by the method of least squares on the log Q/ϵ^2 and ϵ data. In the same ways, results have been obtained for suspensions of the same sample of calcium carbonate in other liquids (table 3.15) from the experimental data reproduced in section 2.3.

Discussion

The most remarkable effect observed was the considerable ability of methyl, ethyl and isobutyl alcohols to disperse calcium carbonate, relative to its condition in water. Similar behaviour was observed in 1:3, 1:1 and 3:1 $^{v}/_{v}$ mixtures of

Table 3.14

Sedimentation data for dried laboratory-grade calcium carbonate in 0.137 M sodium chloride (aqueous)

E	$Q \times 10^2$ (cm sec^{-1})	log E	log Q	log (Q/E^2)	A	$\bar{r}$ (μ)	mean $\bar{r}$ (μ)	$SD_{\bar{r}}$ (μ)	V_s (cm sec^{-1})
0.9907	8.924	$\bar{1}.9959$	$\bar{2}.9506$	$\bar{2}.9588$	31.62	22.14	22.19	0.25	0.180
0.9874	6.908	$\bar{1}.9945$	$\bar{2}.8393$	$\bar{2}.8503$		22.02			
0.9833	5.387	$\bar{1}.9927$	$\bar{2}.7314$	$\bar{2}.7460$		22.64			
0.9795	3.954	$\bar{1}.9910$	$\bar{2}.5970$	$\bar{2}.6150$		22.34			
0.9760	2.916	$\bar{1}.9894$	$\bar{2}.4648$	$\bar{2}.4860$		21.86			
0.9724	2.285	$\bar{1}.9879$	$\bar{2}.3589$	$\bar{2}.3831$		22.11			

Table 3.15

Sedimentation data for dried laboratory-grade calcium carbonate in various liquids

Liquid	Liquid dielectric constant D	Initial porosity range	A	mean $\bar{r}$ (μ)	$SD_{\bar{r}}$ (μ)
Benzene	2.3	0.9720 - 0.9900	22.5	42.85	1.73
Ether	4.3	0.9722 - 0.9909	15.2	29.01	0.38
Chloroform	5.0	0.9669 - 0.9868	12.5	25.45	0.68
Ethyl acetate	6.4	0.9631 - 0.9851	16.1	10.97	0.29
Expt. 1			16.4	9.75	0.14
Ethyl acetoacetate	15.9	0.9722 - 0.9910			
Expt. 2			16.1	9.84	0.15
Isobutyl alcohol	18.7	0.9631 - 0.9877	Settling times too slow for measurement - Stokes type settling - persistent cloudiness after several days - clear evidence of dispersion compared with situation in water		
Ethyl alcohol	24.3	0.9385 - 0.9877			
Methyl alcohol	32.6	0.9385 - 0.9877			
Water	78.5	0.9519 - 0.9905	26.4	19.69	0.29
0.137 M NaCl	> 78.5	0.9724 - 0.9907	31.6	22.19	0.25
0.216 M NaCl	"	0.9721 - 0.9908	30.2	20.70	0.20
0.263 M NaCl	"	0.9724 - 0.9904	30.0	21.21	0.31
0.458 M NaCl	"	0.9721 - 0.9906	29.2	19.91	0.17
0.756 M NaCl	"	0.9724 - 0.9892	24.7	17.89	0.39
0.915 M NaCl	"	0.9723 - 0.9907	31.8	19.97	0.25

ethylene glycol and water. In each case, a considerable turbidity existed in the fluid (above some settled-out solid) several days after mixing, whereas the other liquids were clear, or virtually so, five to fifteen minutes after commencing sedimentation. Dispersion was also observed, relative to the aqueous suspensions, in ethyl acetate and ethyl acetoacetate, but the effect was less marked than in the alcohols, and hindered settling measurements were possible. Duplicate experiments with ethyl acetoacetate were in good agreement (table 3.15), while triple runs on a single set of suspensions showed that dispersion of chalk in ethyl acetate is a slow continuing process at 20°C (table 3.16).

Table 3.16

Sedimentation data for dried laboratory-grade calcium carbonate in anhydrous ethyl acetate (repeat runs)

Day no.	A	mean $\bar{r}$ (μ)	$SD_{\bar{r}}$ (μ)	V_s (cm sec^{-1})
1	23.0	13.55*	0.52*	0.168
2	20.83	13.30	0.18	0.160
8	18.67	12.76*	0.27*	0.139

*These figures, on the statistical t-test for related means, yield t = 3.25 for 13 degrees of freedom. The difference between the means is highly significant (less than 1% probability of chance occurrence).

It is clear from table 3.15 that there is no simple relationship between the dispersing or flocculating behaviour of the liquids examined and their dielectric constants. For the organic liquids, simple electrostatic considerations would suggest that the tendency to flocculation would be inversely proportional to dielectric constant (Davies, Dollimore and Sharp, 1976) and this was observed with benzene, ether and chloroform, as compared with water. However, with three alcohols, an ester, a β-keto ester, and mixtures of water and a dihydroxy alcohol, the dispersing effect was in each case greater than with water, in spite of dielectric constants smaller than that of water. Thus, dispersing power does not depend solely on the ability of the liquid to function as a dielectric and thus increase the intensity of electrostatic repulsions between the particles. There is some other factor which causes more dispersion than the decrease in dielectric constant causes flocculation.

Alcohols, esters and β-keto esters have one feature in common which may explain the dispersing behaviour: each molecule has one or more oxygen atoms which may co-ordinate to metal ions. This behaviour will be more observable with 'type a' cations, of which calcium ion is a clear example (Ahrland, Chatt and Davies, 1958). Although stability constants have apparently not been reported for the co-ordination of calcium ions by the organic liquids discussed in this paper, evidence is available (Sillén and Martell, 1964) of the markedly greater co-ordinating power of ethyl acetoacetate, as compared with water, and of the relatively great co-ordinating power also possessed by methanol and ethanol (table 3.17).

Table 3.17

Stability constants for water and ethyl acetoacetate as ligands

Cation (M)	Ligand (L)	Approximate stability constant	
H^+	Water in methanol	K_{ML}	$10^{0.7}$
	Water in ethanol		$10^{1.2}$
	Ethyl acetoacetate in ethanol		$10^{13.9}$
Cu^{2+}	Water in ethanol	K_{ML_2}	$10^{-0.8}$
	Ethyl acetoacetate in 1:1 water:dioxan		10^{15}
Ni^{2+}	Water in ethanol	K_{ML_2}	$10^{-0.1}$
	Ethyl acetoacetate in 99:1 ethanol:water		$10^{19.5}$

The stability constants K_{ML_x} are defined by equations such as

$$K_{ML} = \frac{(ML)}{(M)\ (L)}$$

$$K_{ML_2} = \frac{(ML_2)}{(M)\ (L)^2}$$

where (M) = unco-ordinated cation concentration in solution

(L) = unco-ordinated ligand concentration in solution

(ML_X) = concentration of complex ML_X in solution

The simple proton is to all intents and purposes unknown in chemistry (Bell, 1959), and therefore for $M = H^+$, $L = H_2O$, K_{ML} would be extremely large in the absence of any other effective ligand. The fact that $K_{H_3O^+} = 10^{0.7}$ only, for water in methanol, and $10^{1.2}$ only, for water in ethanol, shows that these alcohols are not much weaker proton co-ordinators than water. The fractional stability constants for water ligand with copper (II) and nickel (II) ions show that ethanol is superior to water as a co-ordinator of these ions. The large ethyl acetoacetate constants show the marked superiority of that liquid over ethanol. Finally, it is well known that calcium salts form many complexes with oxygen-donor species (Sidgwick, 1950). Oligo-oxy compounds, such as octa- and deca-carboxylic acids, are used as boiler-water additives, since they have marked dispersing effect on calcium carbonate deposits (Richardson, Jones and Harris, 1970).

It therefore seems reasonable to suggest that the unexpected dispersion, observed for calcium carbonate in certain organic

liquids, is due to the ability to co-ordinate calcium ions through oxygen centres, this co-ordination effect being greater than the tendency to flocculation due to decreased dielectric constant (compared with the situation in aqueous suspensions). The enhanced co-ordinating power would result in increased diffusion of calcium ions from the solid into the liquid, with corresponding increase in particle-particle repulsion. The electrostatic forces thus generated would then tend to produce greater dispersion than in water, as observed.

Since such behaviour would not be specific to calcium carbonate, the study was extended briefly, so as to assess the relative effects of water, methanol and ethyl acetoacetate on nickel carbonate and of water and methanol on basic copper carbonate. Suspensions, each of 40 g solid made up to 200 cm^3, were compared qualitatively for degree of dispersion and appearance of hindered settling. The relevant physical constants for the liquids are shown in table 3.18. It was found that these compounds behave similarly to calcium carbonate.

In methanol, there was slower settling of the interface and finer particle size for both carbonates (compared with the situation in water). This is unexpected from a consideration of Stokes' Law (since methanol is less dense and less viscous than water) and also from the lower dielectric constant of methanol.

With nickel carbonate in ethyl acetoacetate, there was a persistent cloudiness, as compared with a slowly-settling clear

interface in water, and the suspended material was noticeably finer in the ester than in water. It is clear that the ester disperses nickel carbonate in a way which is unexpected from its dielectric constant. It is concluded that for all three carbonates, the dispersing (co-ordinating) effect of the organic liquids is greater than their flocculating (dielectric) effect.

The effect on calcium carbonate of several sodium chloride solutions, up to 0.915 M, was not marked. This is probably not unexpected, since the surface area of the carbonate, as measured by nitrogen absorption, was low ($4.0\ m^2.g^{-1}$). The apparently complex relationship of $\bar{r}$ and ionic strength may be due to a combination of effects such as double-layer suppression and ion-exchange.

Conclusions

The dispersion of calcium carbonate in a liquid is directly related to the co-ordinating power of that liquid for calcium ions. The magnitude of the dispersing effect, due to co-ordination, may be noticeably greater than the flocculating effect of relatively low dielectric constant of the liquid, relative to the situation when the liquid is water.

The enhanced dispersion corresponds to reduced tendency for sedimentation with a clear suspension/supernatant interface - i.e. to less-hindered settling. Thus, hindrance to settling of calcium carbonate is inversely related to the co-ordinating

power of the liquid for the calcium ion. In previous sections (3.2.2, 3.2.7), it has been concluded that hindrance to settling is directly proportional to charge density in the double layer round the particles (d_c), solid density (ρ_s), liquid viscosity (ρ_l), and liquid dielectric constant (D); and inversely proportional to the difference of viscosity ($\Delta\eta$) between suspension and bulk liquid. Now, adding the inverse relationship to the cation-liquid stability constant (K_{ML_x}), one may write schematically:

$$\text{hindrance} \propto f\left(\frac{d_c,\ \rho_s,\ \eta_l,\ D}{\Delta\eta,\ K_{ML_x}}\right) \qquad (3.42)$$

From table 3.15, the effect of liquid dielectric constant appears to have two distinct aspects. There was increase of hindrance (as represented by increase of A) with decrease of dielectric constant in the series chloroform-ether-benzene; this increased hindrance is apparently due to increased flocculation. On the other hand, there was increase of hindrance with increased dielectric constant and decreased flocculation in the series chloroform-water-salt solutions. This second mechanism of hindrance, observed at higher values of dielectric constant and apparently electrostatic in origin, has been discussed in section 3.2.3 on the basis of data from the literature. These two effects are presumably connected with the differences of sedimentation behaviour between calcium carbonate in water and aqueous salt solutions, and calcium carbonate in some organic media

and ballotini in aqueous glycerol, which were discussed in section 3.4.

3.7 Consequences of hexagonal models of the sedimenting 'plug'

To recapitulate from section 1.3.3, Richardson and Zaki (1954 a) developed two versions of a cell-type model for sedimenting spherical particles, in which the particles were assumed to be in 'expanded close-packed' hexagonal arrays horizontally, and lined up vertically above each other, so that the liquid up-flows were parallel, vertical and laminar. In one model, the horizontal layers were assumed actually to touch ('configuration II'), while in the other, the interparticle separation was assumed the same, horizontally and vertically ('configuration I'). Configuration II gave better agreement with their experimental data.

In configuration II, the hexagonal cell is of vertical thickness 2r, for solid spheres of radius r, with a length of hexagonal side (= distance between particle centres in the horizontal plane) $2r_1$, where $r_1 > r$ (figure 3.16 a). Richardson and Zaki assumed that the effective volume occupied by the sedimenting material is composed of vertical cylindrical shapes. The total occupied space per hexagon is made up of one complete cylinder and six one-thirds of such a cylinder, equivalent to three cylinders in all. If the radius of such a cylinder is r_2, the

Figure 3·16 a
Horizontal cross-section of the Richardson and Zaki 'configuration II'

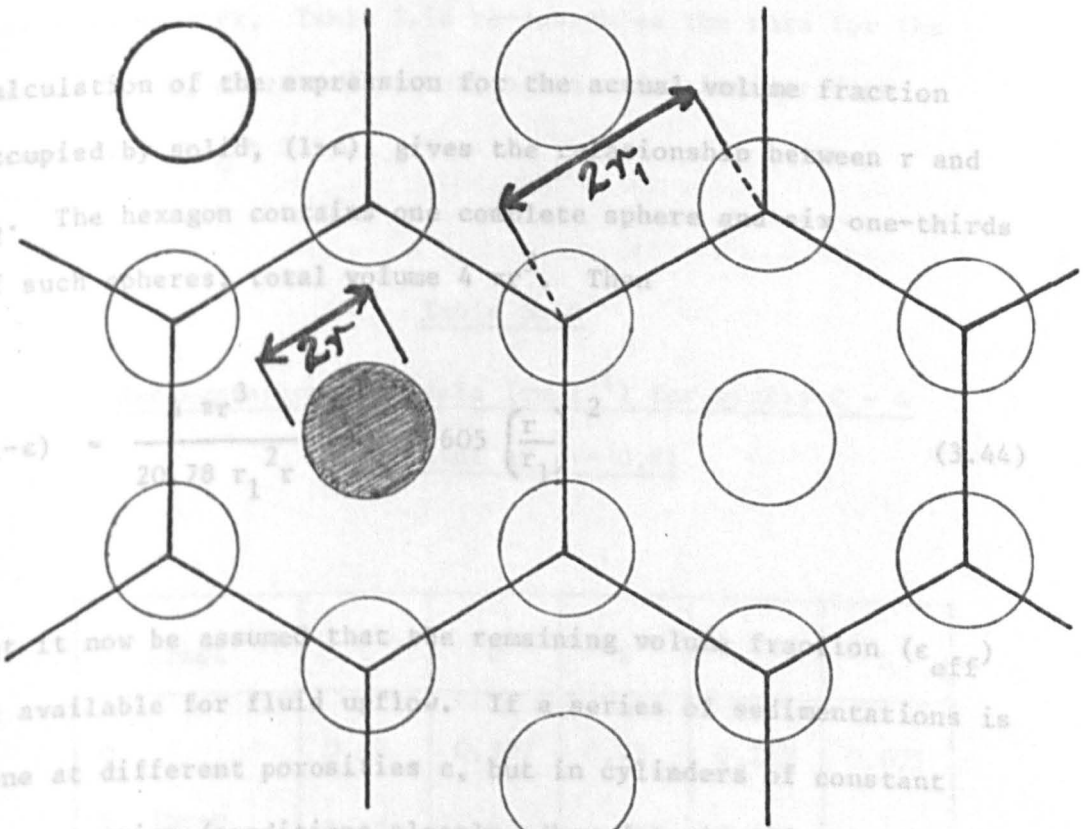

effective solid volume per hexagon is 3 ($\pi r_2^2 . 2r$) = 6 $\pi r_2^2 r$. The cross-sectional area of a hexagon of side $2r_1$ is 10.39 r_1^2, and the total volume in this case will be 20.78 $r_1^2 r$. The effective solid volume fraction ($1-\varepsilon_{eff}$) is therefore given by

$$(1-\varepsilon_{eff}) = \frac{6\ \pi r_2^2 r}{20.78\ r_1^2 r} = 0.907 \left(\frac{r_2}{r_1}\right)^2 \qquad (3.43)$$

Calculation of the expression for the actual volume fraction occupied by solid, ($1-\varepsilon$), gives the relationship between r and r_2. The hexagon contains one complete sphere and six one-thirds of such spheres, total volume 4 πr^3. Then

$$(1-\varepsilon) = \frac{4\ \pi r^3}{20.78\ r_1^2 r} = 0.605 \left(\frac{r}{r_1}\right)^2 \qquad (3.44)$$

Let it now be assumed that the remaining volume fraction (ε_{eff}) is available for fluid upflow. If a series of sedimentations is done at different porosities ε, but in cylinders of constant cross-section (conditions closely adhered to in this study), then the sedimentations occur under uniform hydrostatic head, and the factor varying the rate of fluid upflow is the fraction of total volume available for such flow, ε_{eff}. At infinite dilution, $\varepsilon = \varepsilon_{eff} = 1$ and the sedimentation rate is V_s. At any other porosity, $\varepsilon \neq \varepsilon_{eff}$ if the particles have an effective volume greater than their actual solid volume, and $Q = V_s . \varepsilon_{eff}$. The effective porosity, ε_{eff}, is the generalised correction term in

sedimentation equations, and in Richardson and Zaki's expression, for instance, $\varepsilon_{eff} = \varepsilon^{4.65}$.

From that equation, for $\varepsilon = 0.81$, $\varepsilon_{eff} = 0.81^{4.65} = 0.3754$. One therefore predicts that ballotini, which have $\varepsilon_l = 0.81$, will show $Q\varepsilon_l/V_s = 0.3754$, agreeing to 1% with $Q\varepsilon_l/V_s = \exp^{-1}$, predicted from equations developed in this study. Tables 3.6 and 3.8 show Q and V_s data for grades of ballotini examined in the present work. Table 3.18 re-assembles the data for the grades C - G, where sedimentation was under laminar flow conditions ($Re_m \leqslant 0.2$).

Table 3.18

Sedimentation rate data ($cm.s^{-1}$) for grades C - G ballotini at $\varepsilon = 0.81$

Grade	C	D	E	F	G
Q	0.42	0.307	0.25	0.212	0.077
V_s (mean calculated)	1.125	1.015	0.695	0.55	0.17
Q/V_s	0.373	0.302	0.360	0.385	0.453

Mean $Q/V_s = 0.3746$ $cm.s^{-1}$; standard deviation $= \pm 0.048$

The mean result is in excellent agreement with the predictions,

and the standard deviation indicates 68% confidence that the true mean lies within the range 0.327 - 0.423.

Therefore, ballotini at solid volume fraction $(1-\varepsilon) = 0.19$ behave as if the effective fraction $(1-\varepsilon_{eff})$ is 0.625. This increase of solid volume, due either to flocculation or to associated liquid (or both), means that the effective spherical radius r_{eff} must be related to the solid particle radius r as follows:

$$\frac{\text{effective radius}}{\text{solid radius}} = \frac{r_{eff}}{r} = \frac{(\text{effective solid volume fraction})^{0.33^{\cdot}}}{(\text{actual solid volume fraction})^{0.33^{\cdot}}}$$

$$= \frac{(0.625)^{0.33^{\cdot}}}{(0.19)^{0.33^{\cdot}}} = 1.49$$

This value $r_{eff} = 1.49\ r$ may be interpreted in terms of Richardson and Zaki's configuration II by writing

$$(1-\varepsilon_{eff}) = 0.625 = 0.907 \left(\frac{r_2}{r_1}\right)^2$$

which gives $r_1 = 1.205\ r_2$.

Now, from equation 3.44, for $(1-\varepsilon) = 0.19$,

$$0.19 = 0.605 \left(\frac{r}{r_1}\right)^2$$

which gives $r_1 = 1.79\ r$

and therefore $r_2 = 1.48\ r$.

The cylindrical radius r_2 is therefore closely similar to the effective radius 1.49 r, and this particular condition leads to a cell as in figure 3.16 b. The nearest distance between solid surfaces in the horizontal arrays is found to be 1.6 r.

This situation corresponds to the condition of maximum solids flux, ε_1, where 'breaks' occur in sedimentation curves. The particle-particle distance 1.6 r in the horizontal arrays is in reasonably good agreement with Ramakrishna and Rao's derivation from Steinour's data of 1.2 r (in all three dimensions) for ballotini and 1.4 r (similarly) for tapioca at the 'break' porosities ($\varepsilon_1 \simeq 0.80$ and 0.83 respectively). Steinour (1944 a, figure 8) shows experimental points for the glass spheres which imply a break below $\varepsilon = 0.80$, probably at about 0.78. Interpolation on the graph gives Q/V_s at this porosity (i.e. $Q\varepsilon_1/V_s$) very near indeed to $\exp^{-1}$. His data for tapioca (1944 a, table I) are markedly deficient around ε_1, but the $Q\varepsilon_1/V_s$ value must lie between 0.278 and 0.488, with a high probability of its being approximately symmetrically between these values (i.e. about 0.39). It has been noted earlier that the Q/V_s values for the break points in Ramakrishna and Rao's own graphs (1965, figures 4, 5) correspond to Q/V_s values about 0.35 and 0.42.

It was speculated in section 1.3.4 that Slack's observation of sedimenting simple polygons of spheres might mean that the

Figure 3·16 b

'Configuration II' cross - section corresponding to $\epsilon = 0.81$, $\epsilon_{eff} = 0.375$

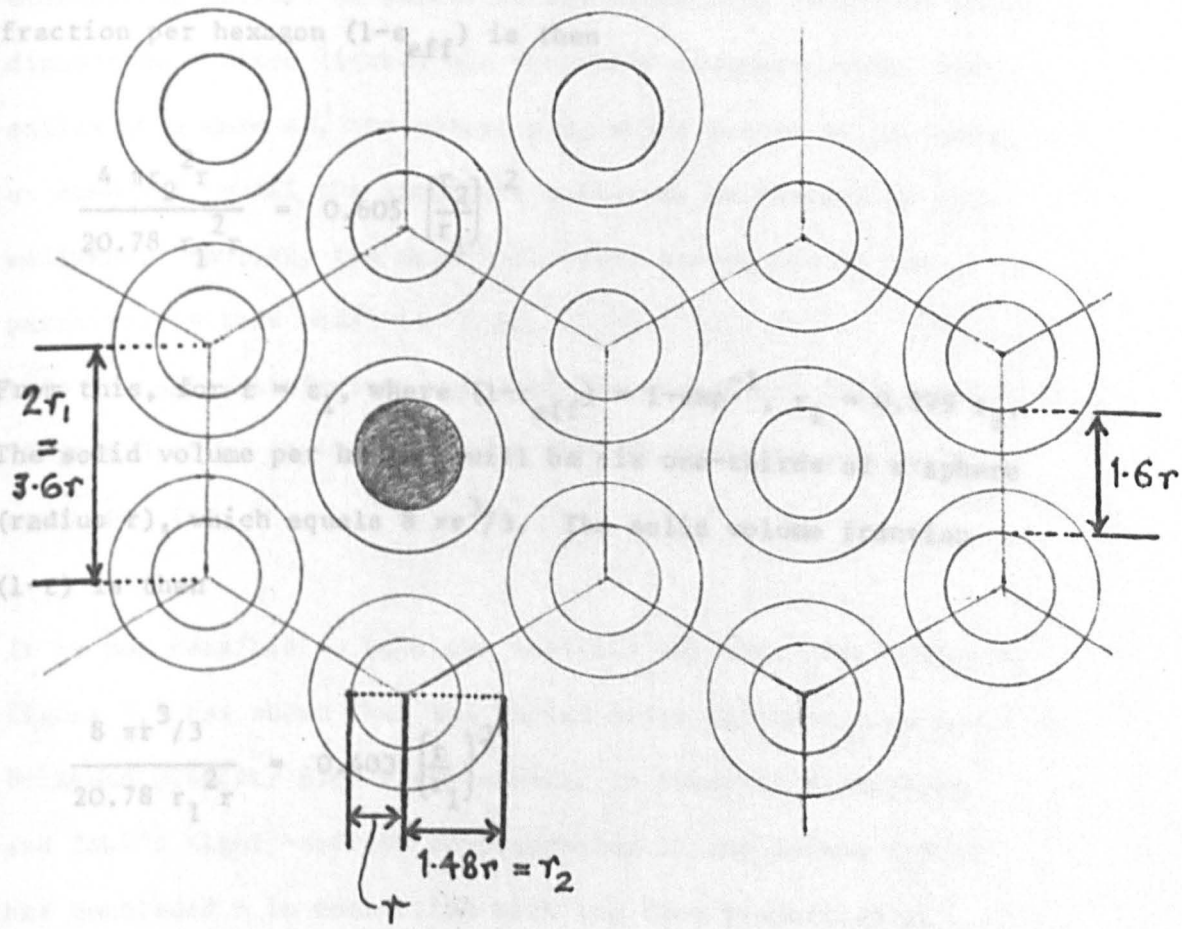

threshold concentration for hindered settling is that porosity at which fusion of such polygons occurs. For a model of the sedimenting 'plug' based on Richardson and Zaki's configuration II, but formed of simple hexagons, each hexagon of particles would have an upflow of fluid at its centre, instead of a particle. The effective solid volume per hexagon would be six one-thirds of a cylinder, depth 2r and radius r_2 (where the particle radius is r), which equals $4\ \pi r_2^2 r$. The effective solid volume fraction per hexagon $(1-\varepsilon_{eff})$ is then

$$\frac{4\ \pi r_2^2 r}{20.78\ r_1^2 r} = 0.605 \left(\frac{r_2}{r_1}\right)^2$$

From this, for $\varepsilon = \varepsilon_1$, where $(1-\varepsilon_{eff}) = 1-\exp^{-1}$, $r_1 = 0.979\ r_2$. The solid volume per hexagon will be six one-thirds of a sphere (radius r), which equals $8\ \pi r^3/3$. The solid volume fraction $(1-\varepsilon)$ is then

$$\frac{8\ \pi r^3/3}{20.78\ r_1^2 r} = 0.403 \left(\frac{r}{r_1}\right)^2$$

For $(1-\varepsilon_1) = 0.19$, as it is with ballotini, this gives $r_1 = 1.456$ r, and therefore $r_2 = 1.49$ r. (The r_2/r value is unchanged because it is the value necessary for $\varepsilon_1 = 0.19$, $\varepsilon_{eff} = \exp^{-1}$.)

The ratio $r_1 = 1.456$ r leads to a theoretical cell of overlapping

occupied volumes (figure 3.16 c). This is an attractive model of spheres interconnected by lenses of stagnant fluid; the overlaps could correspond to a thickening of the lenses as shown by the dotted lines in the diagram. Alternatively the 'overlap' fluid could be between the particles in the vertical direction, as Richardson and Zaki's experimental data indeed suggested. The plug would then consist of a coherent three-dimensional network of particles and associated fluid, in three dimensions. Since liquids are virtually incompressible, and solids even more so, the entire plug would settle as one mass, as observed, until the structure collapses on compaction into sediment. However, the mean horizontal separation of the particles in this model is 2.34r.
This is as satisfactory as the Richardson and Zaki model (figure 3.16 b) in its agreement with Ramakrishna and Rao's estimate, 2r.

It is not sensible to take the analysis further. For instance, figure 3.5 has shown that the random-array sedimentation model of Brinkman predicts flow rates similar to those of Richardson and Zaki's highly-ordered configuration I, and Sutton (1976) has concluded - in connection with the flow properties of powders - that understanding of particle packing is still at a rudimentary level. It seems probable, nonetheless, that some coherent three-dimensional array of particles and associated liquid is set up in hindered settling. The true situation may be a cohesion of polyhedra of various sizes, based on the various possible packings of spheres (Smalley, 1970).

Figure 3.16c

Cross-section of simple-hexagonal configuration corresponding to $\epsilon = 0.81$, $\epsilon_{eff} = \exp^{-1}$

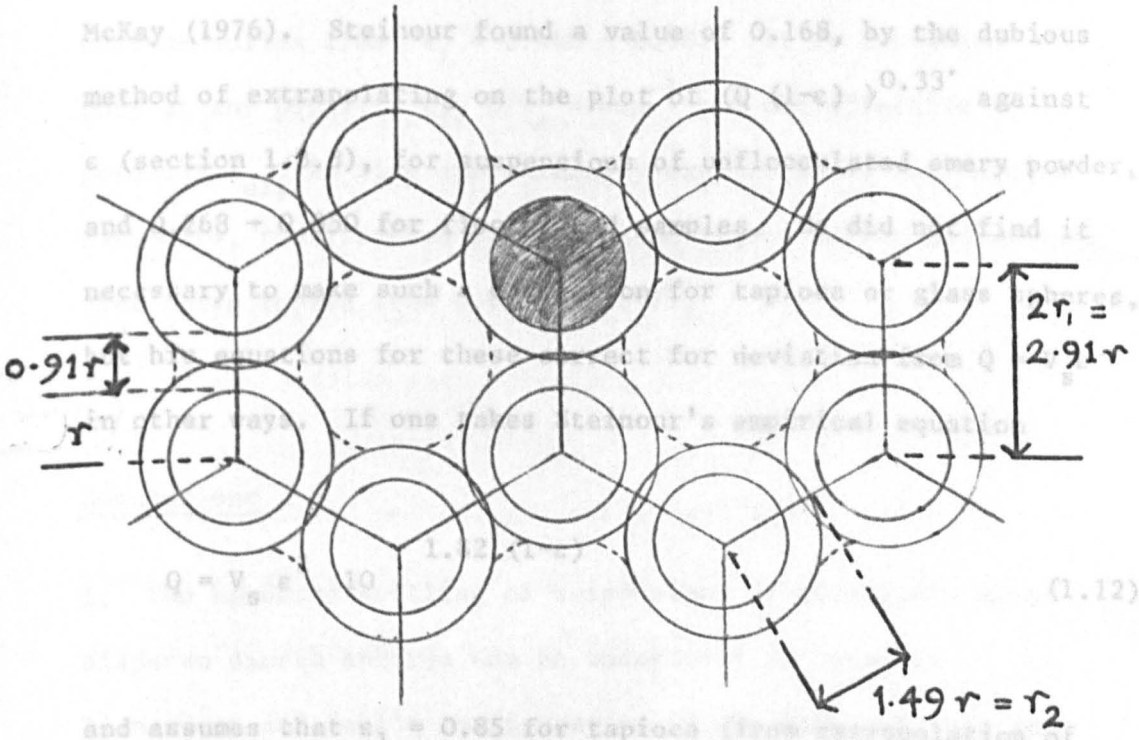

Another way of expressing the results is to derive the fraction of associated fluid in the sedimenting flow units. For ballotini at porosity $\varepsilon = \varepsilon_1 = 0.81$, where $Q\varepsilon_1/V_s = \varepsilon_{eff} = 0.375$,

$$\frac{(1-\varepsilon_{eff}) - (1-\varepsilon)}{(1-\varepsilon_{eff})} = \frac{0.625 - 0.19}{0.625} = 0.70 \qquad (3.45)$$

This quantity has been termed w_i by Steinour (1944 b) and v_i by McKay (1976). Steinour found a value of 0.168, by the dubious method of extrapolating on the plot of $(Q\ (1-\varepsilon)\ )^{0.33'}$ against ε (section 1.3.3), for suspensions of unflocculated emery powder, and 0.268 - 0.350 for flocculated samples. He did not find it necessary to make such a correction for tapioca or glass spheres, but his equations for these correct for deviation from $Q = V_s\varepsilon$ in other ways. If one takes Steinour's empirical equation

$$Q = V_s\ \varepsilon^2\ \ 10^{-\ 1.82\ (1-\varepsilon)} \qquad (1.12)$$

and assumes that $\varepsilon_1 = 0.85$ for tapioca (from extrapolation of lines on his figure 3, 1944 a), one obtains

$$Q\varepsilon_1/V_s = (0.85)^2\ \ 10^{-\ 0.273} = 0.3853$$

in agreement with the value (~ 0.39) just estimated, and not far from $\exp^{-1} = 0.3679$. If $\varepsilon_{eff} = 0.3853$, $(1-\varepsilon_{eff}) = 0.6147$, and with $(1-\varepsilon) = 0.15$, we have

$$v_i = w_i = 0.6147 - 0.15/0.6147 = 0.76$$

The values of w_i in the range 0.168 - 0.350 then correspond to a correction for additional associated liquid with angular emery powder, as compared with the almost spherical tapioca. McKay has reported values of v_i from 0.74 to 0.99 for phthalocyanine pigments and dextran gel in organic media. For calcium carbonate in various liquids, this study has shown initial porosities for maximum solids flux, $\varepsilon_1 = 0.960 - 0.987$. It is concluded that at any porosity ε_1, $Q/V_s \simeq \exp^{-1}$ and the effective porosity ε_{eff} is also approximately $\exp^{-1}$. Thus, for calcium carbonate, the fraction of associated liquid in the sedimenting flow units ranged from 0.937 to 0.979.

Conclusions

1. The hindered settling of suspensions of relatively monodisperse smooth spheres can be understood in terms of Richardson and Zaki's configuration II, by assuming that the spheres have associated liquid sedimenting with them so as to make the effective radius of the spheres about 1.5 times that of the solid particle. This corresponds to the sedimenting flow units containing about 70% of associated liquid by volume. The behaviour can also be interpreted in terms of a simple hexagonal model with the same proportion of associated liquid.

2. At a solid volume fraction $(1-\varepsilon) \simeq 0.2$, for smooth spheres,

there is an effective volume fraction of sedimenting material $(1-\varepsilon_{eff}) \simeq 0.625$, and this corresponds to an interface settling rate $Q \simeq V_s \exp^{-1}$. This degree of crowding of the flow units causes a new form of sedimentation behaviour to occur, compared with the situation at higher porosities. This new form occurs at porosities below the porosity for maximum solids flux, ε_1. ε_1 therefore represents the minimum solids concentration for sigmoidal dependence of sedimentation rate on porosity.

3. The occurrence of maximum solids flux at higher values of porosity than ~ 0.80 (the ε_1 value for ballotini) can be understood on the basis of the same model, on the assumption that the solid is then associated with a larger relative volume of fluid. For calcium carbonate in a variety of fluids, this corresponds to sedimenting flow units which are 94 - 98% fluid by volume. These percentages are surprisingly large, but are similar to values recently reported in the literature for organic pigments and a dextran polymer.

3.8 Studies of settled sediments

From studies on flocculated kaolinite in aqueous media, Michaels and Bolger (1962) adapted the Richardson and Zaki equation to read

$$Q = V_s (1 - k (1-\varepsilon))^{4.65} \qquad (1.30)$$

where k = volume of each floc per unit volume of solids contained in it.

The derived values of k ranged from 35 to 65, which correspond to $v_i = w_i = 0.97 - 0.985$. The authors concluded that sedimentation rates, sediment volume and aggregate size were a function of just two variables, floc volume fraction and the strength of the attractive force between flocs, and Dixon (1977) has concluded that these concepts give a quite satisfactory explanation of high degrees of hindrance: it is due only to flocculation. However, there seems to be difficulty in reconciling data from this study with this hypothesis.

In fitting equation (1.30) to experimental data, k is varied, in place of the variation of n in the generalised Richardson-Zaki equation

$$Q = V_s . \varepsilon^n \qquad (1.53)$$

An increase in n corresponds to an increase in k.

Calculating from experimental data given in section 2.3 gives values of n shown in table 3.19.

Table 3.19

Values of n for calcium carbonate in various liquids

Liquid	Liquid dielectric constant	n	Initial porosity range
Benzene	2.3	48.6	0.972 - 0.990
Diethyl ether	4.3	35.6	0.972 - 0.991
Ethyl acetate	6.4	36.1	0.963 - 0.985
Ethyl acetoacetate	15.9	38.2	0.972 - 0.991
Acetone	21.4	24.4	0.963 - 0.990
Water	78	62.2	0.9519- 0.9905
0.137 M NaCl	> 78	73.9	0.972 - 0.991
0.915 M NaCl	> 78	74.2	0.972 - 0.991

The interpretation of Michaels and Bolger requires larger values of k for the sodium chloride systems than for the cases where organic liquids were used. Dixon states specifically that a large value of k means that the individual entities in the flocculated suspension are not the individual particles but the much larger flocs. It follows that larger values of k mean still larger flocs, and the prediction is that the largest flocs of calcium carbonate in this study would be found in the sodium chloride solutions. But visual inspection of calcium

carbonate suspensions shows that the flocs are considerably bigger in benzene or ether than in sodium chloride solution, and the sedimentation analysis bears this out (table 3.15).

There seem to be two possibilities to explain the larger k values for the suspensions in salt solutions:

(i) the flocs, although relatively small, are more open, and thus trap more stagnant fluid,

and

(ii) the flocs are not more open, but have more associated fluid round them.

The first situation would presumably lead to greater compressibility of the flocs in the salt solutions. Davies, Dollimore and Sharp (1977) therefore attempted to check on this by determining compressibility coefficients (x) under gravity for the settled sediments, writing

$$V = cm^{x} \tag{3.46}$$

where V = final settled volume,

c = a constant, equivalent to the settled volume of one gram of sediment,

m = mass of calcium carbonate

x = compressibility coefficient

Plots of log V against log x gave reasonable fits to this simple theory (figures 3.17 a, b). If the sediment is incompressible under gravity, x = 1. The more a sediment is compressible, the lower is x. Extrapolating back to log m = 0 enables an estimate to be made of the settled volume of a one gram sample of sediment (c). The values obtained are shown in table 3.20.

Table 3.20

Compressibility coefficients (x) and one-gram settled volumes (c) for calcium carbonate sediments in various liquids

Liquid	x	c
Benzene	0.76	10.1
Diethyl ether	0.81	8.03
Ethyl acetate	0.94	2.86
Ethyl acetoacetate	1.00	2.0
Acetone	0.82	6.61
Water	0.82	4.17
0.137 M NaCl	0.93	3.27
0.458 M NaCl	0.95	3.03
0.915 M NaCl	0.97	2.90

It is concluded that the flocs in sodium chloride solution are

Figures 3.1 / 2, b
Logarithmic plots of settled sediment volumes (V) against mass (m) of calcium carbonate in various liquids

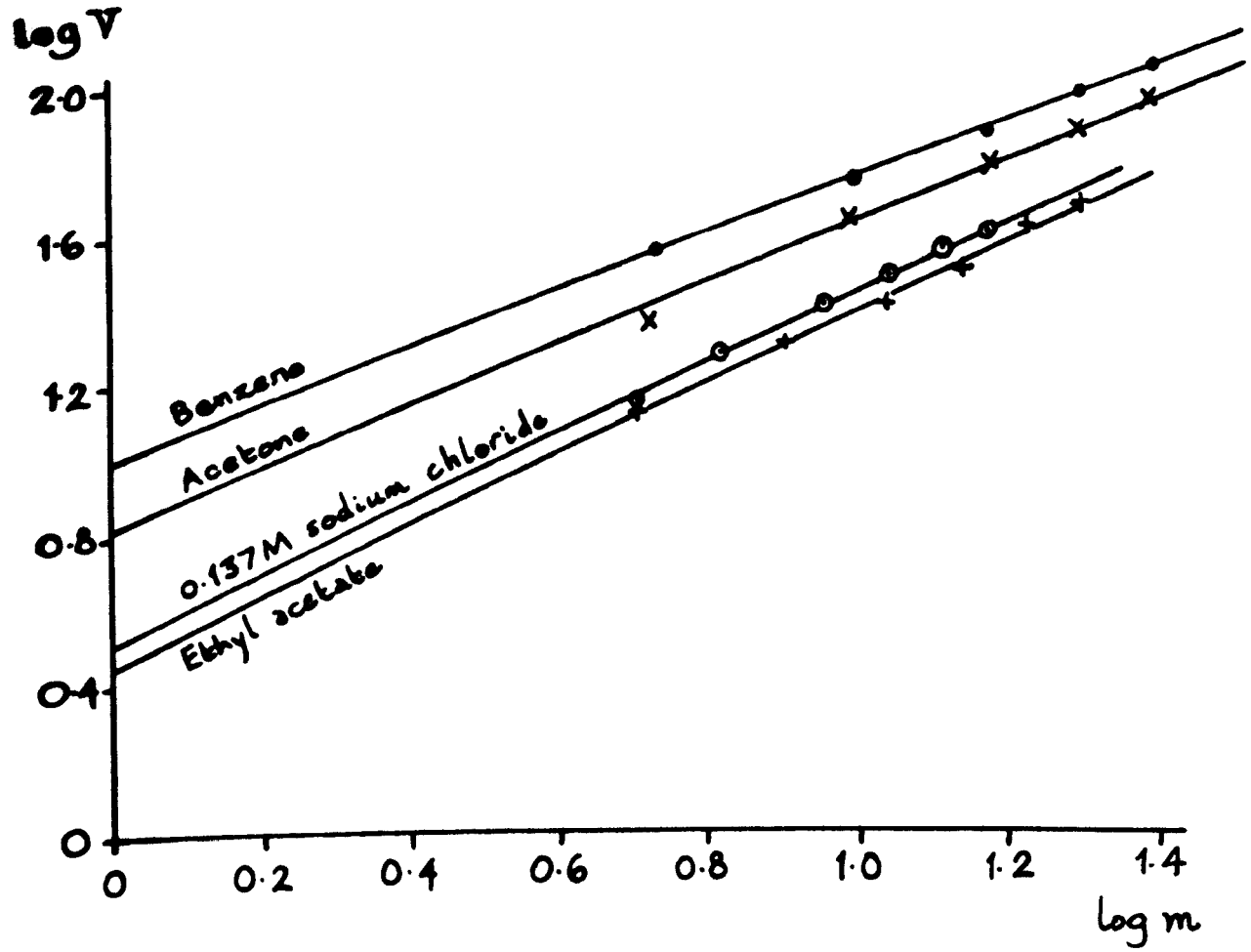

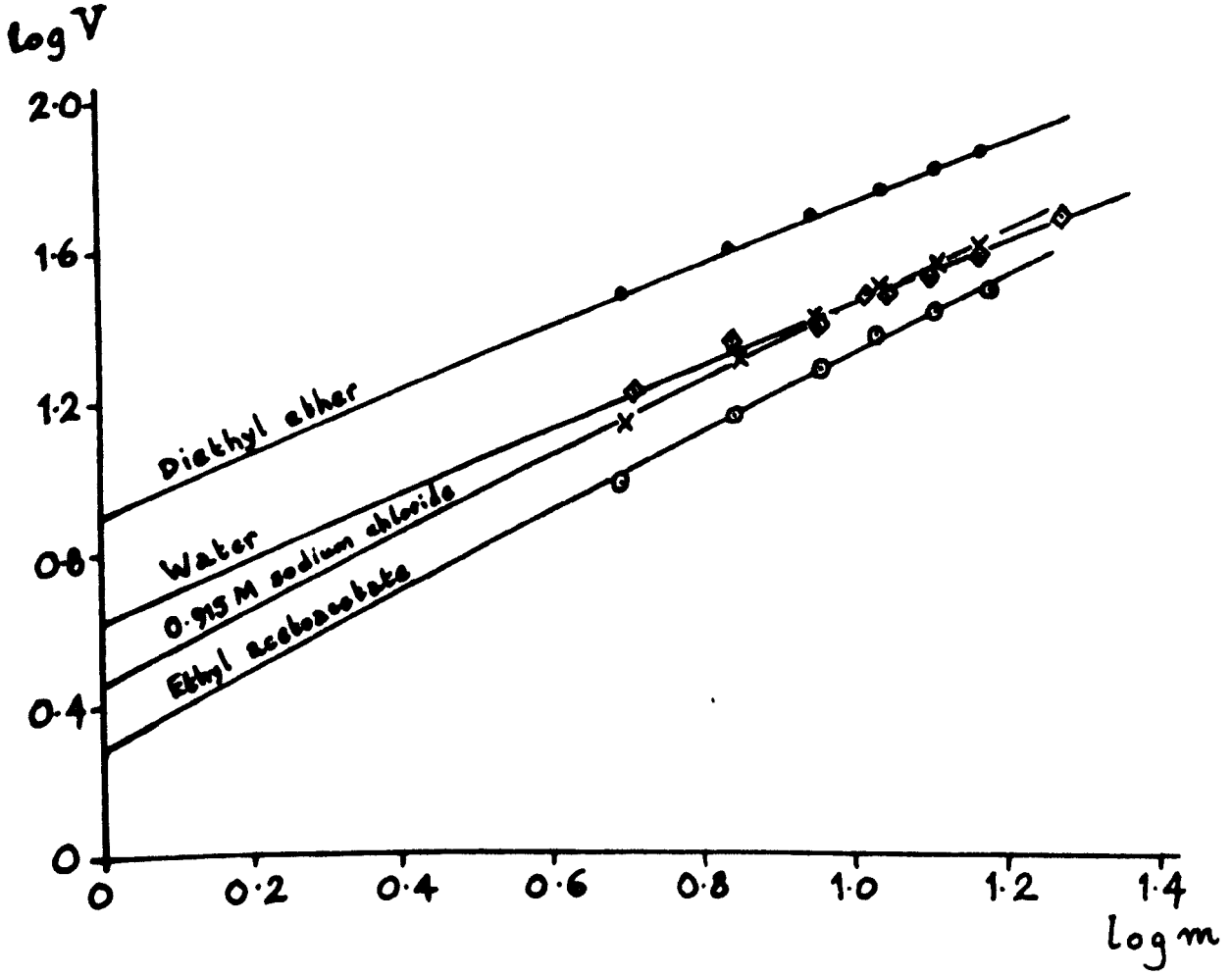

less open than those in acetone, diethyl ether and benzene. Higher values of k in the aqueous system therefore correspond to more associated liquid per unit mass of solid in the flow units. This circumstance, in which the 'stagnant' liquid is apparently around the particles (flocs), rather than within them, is a particle-liquid interaction effect such as was postulated in sections 3.2.2 and 3.2.3.

Ethyl acetate and ethyl acetoacetate, which disperse calcium carbonate more than water does (section 3.6), also give denser, less compressible sediments. This is understandable on the basis of the greater co-ordinating power of the esters, which would give greater diffusion of calcium ions from the solid (compared with the situation in water). The resultant greater negative charge density on the particles would make them less likely to flocculate and more difficult to compress together, and would reduce the likelihood of co-ordination of liquid molecules to calcium ions on the surface. The result would be a less-compressible sediment, with less attached liquid giving greater density, as observed. There should also be less associated liquid in the sedimenting flow units.

McKay (1976 a) has correlated interface settling rates with settled sediment volumes in a way which allows for the estimation of v_i, the volume proportion of associated liquid in the sedimenting flow units. He developed a modification of Steinour's empirical equation

$$Q = V_s \frac{(1-\varepsilon)}{pv} (1-pv)^2 \ 10^{-1.82\ pv} \qquad (3.47)$$

where v = settled sediment volume fraction (i.e. settled volume/total suspension volume)

and pv = volume fraction of the flow units (i.e. volume of solid + associated liquid/total suspension volume)

so that p is the volume ratio between the flow units and the settled sediment.

$$\text{Since} \quad v_i = \frac{pv - (1-\varepsilon)}{pv} \tag{3.48}$$

values of Q, V_s, ε and v can be used to calculate v_i. Evaluation of p is difficult, but mean values have been derived for calcium carbonate suspensions in benzene, ether, ethyl acetate, ethyl acetoacetate, water and two concentrations of sodium chloride. Uncertainty as to the true value of V_s is avoided, and some simplification achieved, by a method of simultaneous equations. For two porosities k and j,

$$Q_i = V_s \frac{(1-\varepsilon_k)}{pv_k} (1-pv_k)^2 . 10^{-1.82\, pv_k}$$

$$\text{and} \quad Q_j = V_s \frac{(1-\varepsilon_j)}{pv_j} (1-pv_j)^2 . 10^{-1.82\, pv_j}$$

$$\text{whence} \quad \frac{Q_i}{Q_j} = \frac{(1-\epsilon_k)}{(1-\epsilon_j)} \cdot \frac{v_j}{v_k} \cdot \frac{(1-pv_k)^2}{(1-pv_j)^2} \cdot 10^{-1.82\,p\,(v_j-v_k)} \qquad (3.49)$$

Extreme values of Q, ϵ and v were taken from the experimental data (section 2.3), and by iteration of likely values of p in equation 3.49, values which gave equality were calculated. These are reproduced in table 3.21, together with values of v_i calculated using equation 3.48, and the compressibility data from table 3.20. The degree of hindrance to sedimentation is indicated by the parameter n.

Table 3.21

Comparison of flow unit/sediment ratios (p), liquid volume fractions in flow units (v_i) and hindrance and compressibility data for calcium carbonate suspensions

Liquid	p	v_i	x	c ($cm^3.g^{-1}$)	n
Benzene	0.775	0.916	0.76	10.1	48.6
Diethyl ether	0.66	0.889	0.81	8.03	35.6
Ethyl acetate	0.90	0.780	0.94	2.86	36.1
Ethyl acetoacetate	0.97	0.810	1.00	2.0	38.2
Water	1.75	0.936	0.82	4.17	62.2
0.458 M NaCl	1.70	0.921	0.95	3.03	68.9
0.915 M NaCl	1.63	0.915	0.97	2.9	74.2

Values $p < 1$ mean that the total volume of flow units is less than the settled sediment volume, corresponding to free liquid in the settled material. It is not surprising that low values are obtained for the bulky and compressible flocculated sediments in benzene and ether. The value $p = 1$ corresponds to equality of flow unit and sediment volumes, and the values $p = 0.90$ and 0.97 for ethyl acetate and acetoacetate imply that little fluid other than associated liquid is present in the sediment. It was predicted earlier that there would be relatively little associated liquid in these cases, and this is corroborated by the low values of v_i in table 3.21. The values $p > 1$ for the suspensions in water and salt solutions imply that associated liquid must be stripped from the flow units during the compaction of the sediment. Such a 'stripping' might be thought of as due to the squeezing out of contained liquid from within flocs, but it occurs with the less-compressible sediments. The stripping must therefore occur predominantly by removal of fluid from around the particles and flocs, rather than by the expression of contained fluid from flocs. It is concluded that this is definite evidence of the existence of 'stagnant' or associated liquid, in considerable volume fractions, on the outer surfaces of particles in sedimenting aqueous suspensions.

The influence of mean flow-unit volume on hindrance to sedimentation may be shown by further use of the parameter p. This quantity does not refer directly to the settled volumes per gram, c, since these are extrapolated values for sediments of different compressibilities. Instead, p relates properly

to the mean sediment volume per gram of contained solid over the experimental range of porosities, since p was calculated as a mean over that range. The original data of section 2.3 give mean sediment volumes per gram of calcium carbonate as shown in table 3.22. Multiplication by the appropriate p values gives mean flow-unit volumes per gram. These values can be compared with one another, and with the corresponding values for the hindrance parameter n.

Table 3.22

Mean sediment and flow-unit volumes per gram of solid for calcium carbonate suspensions, and the hindrance parameter n

Liquid	Sediment volume (cm^3)	Flow-unit volume (cm^3)	n
Benzene	5.95	4.61	48.6
Diethyl ether	5.15	3.40	35.6
Ethyl acetate	2.45	2.21	36.1
Ethyl acetoacetate	2.02	1.96	38.2
Water	2.60	4.55	62.2
0.458 M NaCl	2.67	4.54	68.9
0.915 M NaCl	2.76	4.49	74.2

The table shows that there is increased hindrance (increased n)

from ether to benzene, which may be attributed to increased bulkiness of the flocs (flow units). But this steric hindrance to sedimentation does not apply to the series ether - ethyl acetate - ethyl acetoacetate where a variation of mean flow-unit volume from 3.40 to 1.96 $cm^3.g^{-1}$ gave little variation of hindrance. Indeed, the smaller flow units gave slightly more hindrance. The results also show that the mean flow-unit size decreases in the series benzene - water - 0.458 M and 0.915 M sodium chloride solutions, although there is increase of hindrance to sedimentation in the same direction.

In the latter two series, therefore, floc size is not the factor controlling hindrance; there is another factor which is dominant. From the increase of hindrance with ionic strength in the aqueous suspensions (see also table 3.15 and the general evidence of the influence of polarity in section 3.2.2) it is concluded that this factor is electrostatic in origin. The behaviour of suspensions of calcium carbonate in ethyl acetate and acetoacetate is compatible with the existence of ion-ligand (i.e. ion-liquid dipole) interactions causing hindrance. The additional fluid round the sedimenting particles in aqueous suspensions, which is stripped off during the compaction into sediment, is compatible with the existence of hydrogen bonding in water, causing additional association of liquid molecules together, round the particles.

The evidence indicates that there are two factors causing hindrance to sedimentation. One is flocculation, leading to relative bulkiness of the sedimenting material, and consequent occlusion of

liquid, as postulated by Michaels and Bolger in 1962. The other is a particle-liquid interaction, electrostatic in nature, causing the association of liquid round the particles or flocs, as distinct from liquid retained in an immobile condition within flocs.

3.9 Constancy of the structure of the sedimenting 'plug'

It was speculated at the end of Chapter 1 that the structure of the sedimenting 'plug', as set up at the onset concentration for hindered settling, might undergo a transition, at some lower porosity, to a more closely-packed regime. If this were so, there would presumably be a notable change in the magnitude of the parameter a as a consequence of the transition. However, in figures 3 a - g, after the change of slope (i.e. of a) at or near ϵ_1, there is little or no sign of any major change in the value of a, although it is probably not a true constant. There therefore seems little or no evidence of a major transition from one structure of the 'plug' to another; the geometry of the three-dimensional array of ballotini as set up at or near ϵ_1 is apparently maintained down to porosities in the region $\epsilon = 0.45 - 0.5$. If one regards the ratios of flow rates at these porosities to the corresponding Stokes' limiting velocities as the fractions of free flow space within the suspensions, then such spaces correspond to only 3 - 4% of the suspension volumes. Apart from this small remaining possibility of sedimentation, the whole porosity range for hindered sedimentation was examined.

The conclusion is therefore reached that the 'plug' structure is maintained, once formed, and this is consistent with Harris's (1977) conclusion that the proportion of associated liquid on the solid particles is constant, irrespective of porosity. On the hypothesis of interconnecting 'lenses' of liquid between particles, transition to a closer-packed regime would correspond to an increase in the number of interconnecting liquid volumes, with a corresponding increase in the proportion of associated liquid.

Chapter 4 Summary of conclusions

1. The hindered settling of suspensions of relatively monodisperse smooth spheres can be understood in terms of a model of the sedimenting mass in which the particles are assumed to be in 'expanded close-packed' hexagonal horizontal arrays, and lined up vertically above one another, so that the liquid upflows are parallel, vertical and laminar. This is in agreement with conclusions reached that hindered settling is more likely in suspensions of relatively dense solids in relatively viscous liquids.

   The sedimentation behaviour can also be interpreted in terms of a simple-hexagonal model. Both models involve the assumption that the spheres have associated liquid sedimenting with them so as to make the effective radius of the spheres about 1.5 times that of the solid particle. This corresponds to the sedimenting flow units containing about 70% of associated liquid by volume. At this proportion of associated liquid, the simple-hexagonal model corresponds to a sedimenting 'plug' of particles interconnected by volumes of associated liquid.

2. The existence of a transition (at or near a porosity ϵ_1) from exponential to sigmoidal dependence of sedimentation rate on porosity has been demonstrated by the analysis of experimental data using an equation

$$Q = V_s \exp\left(-\frac{(1-\varepsilon)^a}{1-\varepsilon^*}\right) \qquad (3.31)$$

developed in this study. In the equation, Q is the suspension/supernatant interface settling rate, V_s is the settling rate at infinite dilution, ε is the porosity (liquid volume fraction of uniformly-mixed suspension) corresponding to Q, and ε^* is that porosity for which $a = 1$ precisely, and at which $Q/V_s = \exp^{-1}$.

For suspensions of relatively monodisperse glass spheres in aqueous glycerol, there is a clear transition from an exponential relationship of interface settling rates on porosity ($a < 1$) at porosities above ε_1, to a sigmoidal relationship ($a > 1$) at porosities below ε_1. It has been shown that the calculated values of a are not susceptible to serious error because of uncertainties in V_s or in precise choice of sedimentation equation. That is to say, the changes in the values of a do appear to indicate a true change of sedimentation behaviour, and are not an adventitious error of calculation. Previously-published sedimentation equations, which are only exponential in character, are therefore incomplete representations of the experimental behaviour.

Some data for essentially monodisperse systems from the literature show a similar change of behaviour, as did some

markedly polydisperse calcium carbonate suspensions in organic media in the present study. On the other hand, calcium carbonate in water and in aqueous sodium chloride showed little evidence of transition over the range of porosity which could be studied.

3. For suspensions of smooth spheres, a solid volume fraction $\simeq 0.2$ corresponds to an effective solid volume fraction $\simeq 0.625$, and this corresponds to an interface settling rate $Q \simeq V_s \exp^{-1}$. This degree of crowding of the flow units causes a new form of sedimentation behaviour to occur, compared with the situation at higher porosities. This form of sedimentation, which is known as hindered settling, is characterised by clear suspension/supernatant interfaces which settle at constant rates (Q), and by a sigmoidal dependence of Q on porosity ε. The porosity for onset of this behaviour is at or near ε_1, the porosity for maximum sedimentation mass transfer rate (maximum solids flux). The behaviour corresponds to the existence of a coherent three-dimensional array or 'plug' of particles and associated liquid, as referred to above.

If the experimental behaviour is acceptably represented by the generalised Richardson and Zaki equation

$$Q = V_s \varepsilon^n \qquad (1.53)$$

then one may write

$$\varepsilon_1 = \frac{n}{n+1} \tag{3.8}$$

If it obeys the Dollimore-McBride equation

$$Q = V_s . 10^{-bC} \tag{3.2}$$

in which -b is the slope of the plot of log Q against C, the concentration of solid in the uniformly-mixed suspension, then

$$\varepsilon_1 = 1 - (2.303\, b\rho_s)^{-1} \tag{3.17}$$

4. If one imagines the formation of suspensions by the addition of smooth spheres to a given volume of liquid, then the sedimentation mass transfer rate increases from zero at infinite dilution (i.e. at $\varepsilon = 1$) to its maximum value at ε_1. When further solid is added (i.e. at porosities $< \varepsilon_1$), the transfer rate falls due to the further crowding together of particles while maintaining the basic geometry of the particle-particle packing established at ε_1.

The occurrence of maximum solids flux at lower solid volume fraction than ~ 0.2 can be understood on the basis of the same 'plug' models, if it is assumed that the solid is then associated with a larger relative volume of liquid. For calcium carbonate in a variety of liquids, two methods of

calculation indicate that this corresponds to sedimenting units which are 78 - 98% liquid by volume.

5. The transition from exponential to sigmoidal dependence of settling rate on porosity may be interpreted as a change from essentially tortuous upflow of supernatant liquid, through a relatively random array of sedimenting particles, to essentially linear upflow, through a sedimenting 'plug' of relatively high symmetry. Theory would predict that the plug must always give smoother upflow, and therefore greater settling rates. But the experimental settling rates for the 'plug' (i.e. below ε_1) are less than the theoretical rates for tortuous upflow at the same porosities. The 'plug' is therefore more hindered than the same mass of solid would be in random array. The factor causing the additional hindrance to settling is taken to be the association or 'stagnation' of liquid round and between the particles or flocs in the 'plug'.

6. Correlation of interface settling rates with settled sediment volumes for suspensions of calcium carbonate in water and aqueous salt solutions indicated that associated liquid must be stripped from the flow units during compaction into sediment. Since the sediments are relatively incompressible under gravity, the stripping must occur predominantly from around particles and flocs, rather than by the expression of

contained liquid from within flocs. This is taken as definite evidence of the existence of associated liquid, in considerable volume fractions, on the outer surfaces of particles and flocs, and between such elements of solid, in these suspensions.

7. The dispersion of calcium carbonate, nickel carbonate and basic copper carbonate in a liquid is directly related to the co-ordinating power of that liquid for the cations of the solid. The magnitude of the dispersing effect, due to co-ordination, is greater than the flocculating effect of the relatively low dielectric constants of the liquids, in these cases, compared with the situation in aqueous suspensions. The degree of hindrance to settling of the carbonates is inversely related to the co-ordinating power of the liquid.

8. Two factors have been identified, which cause interface settling rates to be less than those observed for suspensions of uniformly-sized smooth spheres. One is flocculation, as postulated by Michaels and Bolger in 1962. The additional factor, not identified by those authors, is particle-liquid interaction and is electrostatic in origin. In aqueous suspensions of calcium carbonate, this causes a marked association of the liquid round the particles or flocs. With some liquids which are stronger co-ordinating agents than

water, solid cation-liquid dipole interaction leads to an otherwise-unexpected dispersion of the particles, and relatively little associated liquid. The behaviour of smooth spheres has itself been interpreted as involving substantial volumes of liquid associated with the spheres.

The particle-liquid interaction operates by two mechanisms. In the aqueous suspensions, the effect is to reduce the volume of liquid free for upflow, with a corresponding reduction in the possibility of solid sedimentation. With the more-strongly co-ordinating liquids, the effect is one of particle-particle dispersion (compared with the situation in water) so that the sedimenting units have relatively low mass and correspondingly low sedimentation rates.

Data from the literature and from this study indicate that electrostatic interactions are more important than space-filling effects (i.e. flocculation) in causing hindrance to the sedimentation of calcium carbonate and kaolinite in water and in aqueous solutions of electrolytes, and even in causing the dispersion of solids in hydrocarbon media.

9. Sedimentation equations (i.e. equations which relate interface settling rates to the liquid volume fractions in suspensions) are inadequate if they fail to correspond to a maximum of solids flux, which must occur experimentally for all suspensions. Equations which fail in this way include

those identified in this thesis by the numbers 1.10, 1.11, 1.13, 1.14, 1.16, 1.18 and 1.20. The Kozeny-Carman equation 1.27 must also be included unless an experimental 'constant' is allowed to assume increasing values above $\varepsilon = \varepsilon_l$.

Correction terms including the expression $\varepsilon^3/1-\varepsilon$ commonly fail to give the required solids flux maximum. Correction terms named 'shape factors' (which frequently include the expression $\varepsilon^3/1-\varepsilon$) are probably misleadingly named, because particle shape is probably not a major factor affecting sedimentation behaviour.

10. The extrapolation of observed interface settling rates Q to infinite dilution, where $Q = V_s$, the Stokes' limiting settling rate, is a simple method of determining mean equivalent spherical radii $\bar{r}$ of sedimenting particles with acceptable accuracy. The rates are actually sigmoidally related to porosity ε, but such curve-fittings are difficult, and extrapolation by exponential functions does not introduce serious error (at least for relatively monodisperse spheres). The recommended method of calculating $\bar{r}$ (if the plot of log Q against suspension concentration C is acceptably linear) is to plot log Q against C to obtain the slope -b, calculate Steinour's parameter A from

$$A = b\rho_s + \frac{2 \log \varepsilon}{1-\varepsilon} \tag{3.16}$$

(where ρ_s = solid density)

and obtain $\bar{r}$ from

$$\bar{r} = \left(\frac{9Q\eta \, 10^{A(1-\varepsilon)}}{2g \, (\rho_s - \rho_l)} \right)^{0.5} \tag{3.1}$$

(where ρ_l = liquid density)

Appendix: Derivation of the sigmoidal hindered sedimentation equation by analogy from the expression for the normal distribution curve

Equation 3.31 was derived by analogy from the normal distribution equation

$$y = k_1 \exp^{-\frac{x^2}{k_2}} \tag{A1}$$

since one half of that distribution is of sigmoidal form, and more than one half of the distribution has the general form of the schematic sedimentation curve (figure 1.12).

On this model, one would write

$$Q = V_s . \exp^{-\frac{x^a}{k_2}} \tag{A2}$$

The generalized Richardson and Zaki equation may be written as

$$Q = V_s . \exp^{n \ln \varepsilon} \tag{A3}$$

and, from equations A2 and A3,

$$n \ln \varepsilon = - x^a / k_2 \tag{A4}$$

Now, when $\varepsilon = 1$, $n \ln \varepsilon = 0$; i.e. $x = 0$. Hence let $x = (1-\varepsilon)$,

since $(1-\varepsilon) = 0$ when $\varepsilon = 1$.

We may then write

$$Q = V_s \cdot \exp^{-\frac{(1-\varepsilon)^a}{k_2}} \tag{A5}$$

Now it has been shown experimentally that $Q\varepsilon_1 \simeq V_s \exp^{-1}$. Therefore from equation (A5), if $a = 1$ at $\varepsilon = \varepsilon_1$,

$$k_2 = (1-\varepsilon_1) \tag{A6}$$

Since experimentally a does equal unity in the region of ε_1, the assumption just made is justified, and we may write

$$Q = V_s \cdot \exp^{-\frac{(1-\varepsilon)^a}{1-\varepsilon_1}} \tag{3.31}$$

More generally, if $a = 1$ at some porosity $\varepsilon = \varepsilon^*$,

$$Q = V_s \cdot \exp^{\frac{(1-\varepsilon)^a}{1-\varepsilon^*}} \tag{3.32}$$

It may be noted that the plot of log log V_s/Q against log $(1-\varepsilon)$, to yield a value or values of a, does not depend on knowledge of

the magnitude of ε^* (or of ε_1, if this is different).

Figure A1 demonstrates that equation 3.32 leads to an exponential plot if a < 1, while the curve is increasingly sigmoidal as a increases above unity. One might therefore conclude that the equation is capable of representing the sedimentation behaviour for both a < 1 and for a > 1. However, when a < 1, the experimental data yield unexpectedly low values for ε^*. Expected values are obtained from the modified equation

$$Q = V_s \cdot \exp - \left(\frac{1-\varepsilon}{1-\varepsilon^*} \right)^a \qquad (3.35)$$

Equations 3.31 and 3.32 therefore apply only to the range of porosity for which a > 1 (i.e. below ε_1). This range corresponds to the formation of clear interfaces (i.e. to well-developed cases of hindered settling).

Figure A1 : Variation of the function $V_s \exp^{-(1-\epsilon)^2/1-\epsilon^*}$ with the magnitude of the parameter a

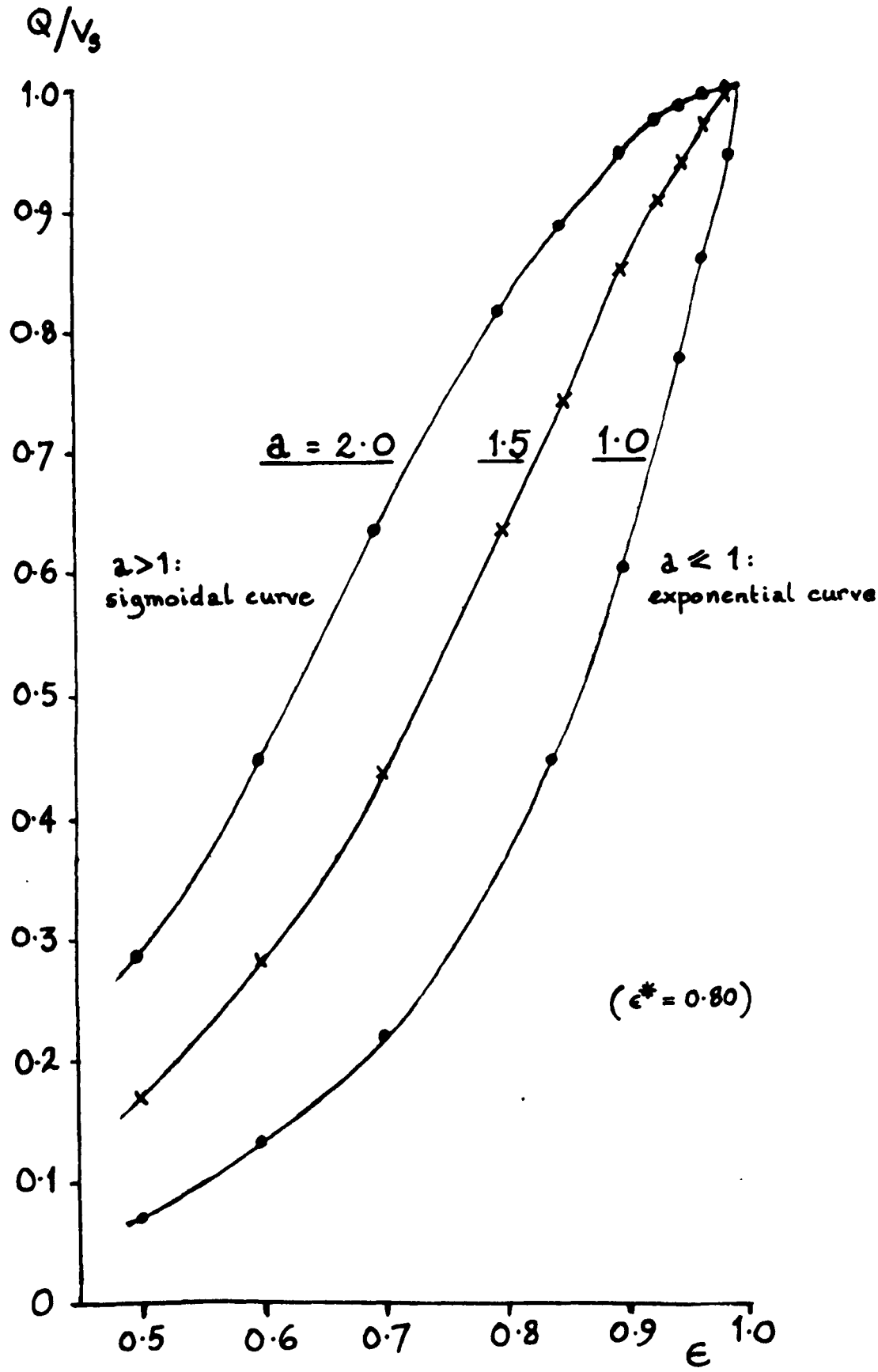

References

S. Ahrland, J. Chatt and N. R. Davies, Quart. Rev., 12 (1958) 265.

T. Allen, 'Particle Size Measurement', 2nd edition, p. 176, Chapman and Hall, 1976.

R. P. Bell, 'The Proton in Chemistry', Cornell Univ. Press, Ithaca, N.Y., 1959.

S. H. Bell and V. T. Crowl in 'Dispersion of Powders in Liquids', G. D. Parfitt (ed.), Elsevier, 1969, Chap. 5.

L. von Bertalanffy, 'General System Theory', George Braziller Inc., New York, 1968 (Allen Lane The Penguin Press, London, 1971).

J. I. Bhatty, L. Davies and D. Dollimore, Chemical Society/ Society for Analytical Chemistry Particle Size Analysis Conference, Salford, 1977.

F. Booth, Proc. Roy. Soc., A203 (1950) 533.

F. Booth, J. Chem. Phys., 22 (1954) 1956.

H. C. Brinkman, Appl. Sci. Res., A1 (1947) 27.

H. C. Brinkman, Appl. Sci. Res., A1 (1948) 81.

H. C. Brinkman, Appl. Sci. Res., A2 (1949) 190.

J. M. Burgers, Proc. Koninkl. Akad. Wetenschap, Amsterdam, 44 (1941) 1045. 1941 a.

J. M. Burgers, Proc. Koninkl. Akad. Wetenschap, Amsterdam, 44 (1941) 1177. 1941 b.

J. M. Burgers, Proc. Koninkl. Akad. Wetenschap, Amsterdam, 45 (1942) 9.

P. C. Carman, Trans. Inst. Chem. Engrs, 15 (1937) 150.

P. C. Carman, J. Soc. Chem. Ind., 57 (1938) 225.

P. C. Carman, J. Soc. Chem. Ind., 58 (1939) 1.

H. S. Coe and G. H. Clavenger, Trans. Amer. Inst. Mining Engrs, 55 (1916) 356.

J. R. Christian and D. Dollimore, Water Res., 5 (1971) 177.

J. M. Dalla Valle, J. P. McBride, V. D. Allred and E. V. Jones, U.S. Atom. Energy Commissn. Report ORNL - 2565 (1958)

H. P. G. D'Arcy, 'Les Fontaines Publiques de la Ville de Dijon', Victor Dalamont, Paris, 1856.

O. L. Davies and P. L. Goldsmith (editors), 'Statistical Methods in Research and Production', 4th edition, Longman, London 1972.

L. Davies and D. Dollimore,(1977 a),Powder Technology, 16 (1977) 59.

L. Davies and D. Dollimore,(1977 b),Powder Technology, in the press, 1977.

L. Davies and D. Dollimore,(1977 c),Powder Technology, in the press, 1977.

L. Davies, D. Dollimore and G. B. McBride, Powder Technology, 16 (1977) 45.

L. Davies, D. Dollimore and J. H. Sharp, Powder Technology, 13 (1976) 123.

L. Davies, D. Dollimore and J. H. Sharp, Powder Technology, 17 (1977) 151.

V. Deryaguin, Trans. Farad. Soc., 36 (1940) 203.

D. C. Dixon, Powder Technology, 17 (1977) 147.

D. C. Dixon, J. E. Buchanan and P. Souter, Powder Technology, in the press, 1977.

D. Dollimore and G. R. Heal, J. Appl. Chem., 12 (1962) 445.

D. Dollimore and T. A. Horridge, Trans. and J. Brit. Ceram. Soc., 70 (1971) 191.

D. Dollimore and G. B. McBride, J. Appl. Chem., 18 (1968) 136.

D. Dollimore and N. F. Owens, Proc. 6th Int. Congr. Surf. Act., Zurich, 1972.

A. Einstein, Ann. Phys., Leipzig, 19 (1906) 286.

A. Einstein, Ann. Phys., Leipzig, 34 (1911) 591.

A. Einstein, Kolloid Zeits., 27 (1920) 137.

F. Eirich and H. Mark, Papier-Fabrik., 27 (1937) 251.

G. M. Fair and L. P. Hatch, J. Amer. Water Wks. Assoc., 25 (1933) 1551.

H. Faxen, Z. angew. Math. and Mech., I (1927) 79.

W. F. Ford and J. White, Trans. Brit. Ceram. Soc., 56 (1957) 309.

A. W. Francis, Physics, 4 (1933) 403.

T. R. Galloway and B. H. Sage, Chem. Eng. Sci., 25 (1970) 495.

A. M. Gaudin, 'Principles of Mineral Dressing', McGraw-Hill, 1939, pp. 175-7.

A. M. Gaudin and M. C. Fuerstenau, Eng. Mining J., 159 (1958) 110.

A. M. Gaudin, M. C. Fuerstenau and S. R. Mitchell, Mining Eng., 11 (1959) 613.

A. M. Gaudin and M. C. Fuerstenau, Intern. Mining Proc. Congr., London, 1960.

W. H. Gauvin and S. Katta, Int. Powder Tech. Conference, Harrogate 1973.

J. A. Goddard and G. Monecelli, private communication, University of Salford, 1973.

E. Guth, I. Gold and R. Simha, Kolloid Zeits., 74 (1936) 226.

E. W. Hall, Ph.D. thesis, University of Birmingham, 1956.

J. Happel, J. Appl. Phys., 28 (1957) 1288.

J. Happel, A. I. Ch. E. Journal, 4 (1958) 197.

C. C. Harris, Powder Technology, 17 (1977) 235.

E. Hatschek, 'Viscosity of Liquids', Bell, London, 1928.

P. G. W. Hawksley in 'Some Aspects of Fluid Flow', Arnold, London (1951), chap. 7.

H. Heywood, 3rd Congr. Eur. Fed^{n}. of Chem. Eng^{g}., London (1962) A1.

R. Johne, Chemie-Eng. Techn., 36 (1966) 428.

B. H. Kaye and R. P. Boardman, 3rd. Congr. Europ. Fed^{n}. of Chem. Eng^{g}., London, 1962, A17.

W. O. Kermack, A. G. McKendrick and E. Ponder, Proc. Roy. Soc., Edinburgh, 44 (1928) 170.

J. A. Kitchener, Brit. Polym. J., 4 (1972) 217.

H. Koelmans and J. Th. G. Overbeek, Disc. Farad. Soc., 18 (1954) 52.

B. Koglin, Dip. Ing. thesis, University of Karlsruhe, 1971.

B. Kopelman and C. C. Gregg, J. Phys. Chem., 55 (1951) 557.

J. Kozeny, Sitzber. Akad. Wiss., Wien., Abh IIa 136 (1927) 271.

S. Kruyer, Trans. Farad. Soc., 54 (1958) 1758.

H. R. Kruyt, Colloid Science, Vol. I., pp. 78, 197 Elsevier, Amsterdam, 1952.

H. R. Kruyt and F. G. van Selms, Rec. trav. chem., 62 (1943) 407.

C. L. Kusik and J. Happel, A. I. Ch. E. J., 1 (1962) 163.

G. J. Kynch, Trans. Farad. Soc., 48 (1952) 166.

W. K. Lewis, E. R. Gilliland and W. C. Bauer, Ind. Eng. Chem., 41 (1949) 1104.

K. E. Lewis and G. D. Parfitt, Trans. Farad. Soc., 62 (1966) 1652.

W. F. Linke and R. B. Booth, Trans. Amer. Inst. Min. Metall. Engrs., 217 (1959) 364.

H. Lumer, Growth, 1 (1937) 140.

G. B. McBride, Ph.D. thesis, University of Salford, 1974.

D. N. L. McGown and G. D. Parfitt, Disc. Farad. Soc., 42 (1966) 225.

D. N. L. McGown and G. D. Parfitt, Kolloid Zeits., 219 (1967) 48.

D. N. L. McGown, G. D. Parfitt and E. Willis, J. Colloid. Sci., 20 (1965) 650.

R. B. McKay (1976 a) J. Appl. Chem. Biotechnol., 26 (1976) 55.

J. J. McNown and P.- N. Lin, Proc. 2nd Midwestern Conf. on Fluid Mech., Ohio State Univ., 1952.

R. B. McKay (1976 b), Fatipec Congress preprint, 13 (1976) 428; British Ink Maker, 19 (1977) 59.

F. C. Micale, Y. K. Lui and A. C. Zettlemoyer, Disc. Farad. Soc., 42 (1966) 238.

A. S. Michaels and J. C. Bolger, Ind. Eng. Chem., Fundamentals, 1 (1962) 25.

D. R. Oliver, Thesis, University of Birmingham, 1954.

C. Orr and J. M. Dalla Valle, in Fine Particle Measurements, Macmillan, New York, 1959.

N. F. Owens, M.Sc. thesis, University of Salford, 1971.

J. M. L. Poiseuille, Mem. Savants Etranges (Paris), 9 (1846) 433 English translation Rheol. Mem., 1 (1940).

T. C. Powers, Bull. Portland Cement Res. Lab., 2 (1939).

R. E. Pavlik and E. B. Sansone, Powder Tech., 8 (1973) 159.

V. Ramakrishna and S. R. Rao, J. Applied Chem., 15 (1965) 473.

I. Reich and R. D. Vold, J. Phys. Chem., 63 (1957) 1497.

J. F. Richardson and W. N. Zaki, (1954 a),Chem. Eng. Sci., 3 (1954) 65.

J. F. Richardson and W. N. Zaki, (1954 b),Trans. Inst. Chem. Engrs., 32 (1954) 35.

N. R. Richardson, T. I. Jones and A. Harris, B.P. 1369429 (1970).

L. A. Romo, Disc. Farad. Soc., 42 (1966) 232.

S. Ross, J. Colloid Interface Sci., 42 (1973) 52.

R. A. Ruehrwein and D. W. Ward, Soil Sci., 73 (1952) 485.

E. B. Sansone and T. M. Civic, Powder Tech., 12 (1975) 11.

M. Sengupta, J. Colloid Interface Sci., 26 (1968) 240.

N. V. Sidgwick, 'The Chemical Elements and their Compounds', Oxford Univ. Press, 1950, pp. 259-260.

L. G. Sillén and A. E. Martell, 'Stability Constants of Metal Ion Complexes', Special Publ. No. 17 (2nd Edition), Chemical Society, London, 1964.

G. W. Slack (1962): D. Dollimore and F. A. Watson, University of Salford, private communications; reported in part by R. E. Pattle, 3rd Congr. Eur. Fedn. Chem. Engg., London, 1962, p. 40.

I. J. Smalley, Powder Technology, 4 (1970) 97.

M. S. von Smoluchowski, Int. Congr. Math., Cambridge, 2 (1912) 192.

M. S. von Smoluchowski, in Graetz: Handbuch der Elektrizitat und Magnetismns, vol. II, p. 385, Leipzig, 1921.

H. H. Steinour, Ind. Eng. Chem., 36 (1944) 618. 1944 a.

H. H. Steinour, Ind. Eng. Chem., 36 (1944) 840. 1944 b.

H. H. Steinour, Ind. Eng. Chem., 36 (1944) 901. 1944 c.

O. Stern, Z. Elektrochem., 30 (1924) 508.

W. L. Stevens, Biometrics, 7 (1951) 247.

G. G. Stokes, Math. and phys. papers, 1901.

H. M. Sutton, in G. D. Parfitt and K. S. W. Sing (editors), 'Characterization of Powder Surfaces', chap. 3, Academic Press, 1976.

D. M. P. Thompson, undergraduate research dissertation, University of Salford, 1972.

D. M. P. Thompson, University of Salford, private communication, 1974.

S. Uchida, Rep. Inst. Sci. Technol., Tokyo, 3 (1949) 97; abstr. Ind. Eng. Chem., 46 (1954) 1194.

V. Vand, J. Phys. and Colloid Chem., 52 (1948) 277.

J. L. van der Minne and P. H. J. Hermanie, J. Colloid Sci., 8 (1953) 38.

E. J. W. Verwey and J. Th. G. Overbeek, 'Theory of the Stability of Lyophobic Colloids', Elsevier, Amsterdam 1948.

S. Vieira and R. Hoffmann, Applied Statistics, 26 (1977) 143.

S. G. Ward, J. Oil and Colour Chemists' Assoc., 38 (1955) 9.

D. T. Wasan, W. Wnek, R. Davies, M. Jackson and B. H. Kaye, Powder Technol., 14 (1976) 209, 229.

R. H. Wilhelm and M. Kwauk, Chem. Eng. Progr., 44 (1948) 201.

S. G. Ward and R. L. Whitmore, Brit. J. Appl. Phys., 1 (1950) 286.

J. Werther, J. Powder and Bulk Solids Technology, 1 (14) 1977.